Agroforestry and Biochar for Climate Change Mitigation: Carbon Storage, Soil Carbon Cycling, and Greenhouse Gas Emissions

by

Cole D. Gross

A thesis submitted in partial fulfillment of the requirements for the degree of

Doctor of Philosophy

in

Soil Science

Department of Renewable Resources
University of Alberta

Abstract

Agroforestry systems (AFS) and the application of organic amendments in croplands can contribute to carbon (C) sequestration and reduction in greenhouse gas (GHG) emissions from agricultural lands. However, previously understudied differences among AFS and organic amendments may underestimate their climate change mitigation potential. Additionally, land use and management practices that increase C inputs to soil may have dual effects on soil C dynamics, in some cases resulting in intensified loss (a.k.a. priming) of soil organic C (SOC) and initially reducing SOC storage. In a 3-year field study, I assessed various C stocks and GHG emissions across two common AFS (hedgerows and shelterbelts) and their component land uses: perennial vegetated areas with and without trees (woodland and grassland, respectively), newly planted saplings in grassland, and adjacent annual cropland in central Alberta, Canada. In the cropland, I also compared one-time additions of manure compost and its biochar derivative to a control to assess their effects on SOC and GHG emissions. Manure compost and biochar were applied at equivalent C rates (7 Mg C ha^{-1}) and tilled into the surface 10 cm of soil. I further conducted a 150-d incubation in a controlled growth chamber to quantify SOC changes due to living roots and their C inputs in soils collected from the component land uses of the AFS, as well as those amended with manure compost and its biochar derivative, using the C stable isotope natural abundance technique. In the field study, nitrous oxide emissions were 89% lower under perennial vegetation relative to the cropland (0.02 and 0.18 g N m^{-2} y^{-1}, respectively) between 2018 and 2020. Heterotrophic respiration in the woodland was 53% lower in shelterbelts relative to hedgerows (279 and 600 g C m^{-2} y^{-1}, respectively) in 2020. Within the woodland, the deadwood C stock was more important in hedgerows (35 Mg C ha^{-1} or 7% of ecosystem C) than shelterbelts (2 Mg C ha^{-1} or < 1% of ecosystem C), and likely affected C cycling in the woodland by enhancing soil labile

C and microbial biomass in hedgerows. Total ecosystem C was 1.90–2.55 times greater within the woodland than in all other land uses. Shelterbelt and hedgerow woodlands contained 2.09 and 3.03 times more C, respectively, than adjacent cropland. In the cropland, biochar led to the sequestration of SOC at a rate of 2.5 Mg C ha^{-1} y^{-1} relative to the control. In 2018 and 2019, manure addition increased total GHG (sum of carbon dioxide, methane, and nitrous oxide as CO_2-equivalents) emissions by 33%, on average, relative to both the control and biochar addition. In contrast, in 2020, biochar addition reduced total GHG emissions by 21% relative to both the control and manure addition. Results from the incubation experiment showed that priming of soil-derived C due to the influence of living roots was limited to the aggregated clay fraction (that is, clay within water-stable silt-size microaggregates), greatest in the surface soil (0.51–1.27 mg C g^{-1} soil), and similar across land uses. However, biochar minimized priming within the aggregated clay fraction. In soils with greater SOC content (that is, surface and woodland soils relative to subsurface and cropland soils, respectively), a larger proportion of clay-protected C was found in silt-size microaggregates. My findings are threefold: (1) AFS are important for fostering C sequestration and reducing GHG emissions and, in particular, retaining hedgerows (legacy woodland) and their associated deadwood across temperate agroecosystems is key to help mitigate climate change; (2) the application of biochar, rather than its manure compost feedstock, increased surface SOC sequestration and had either no effect on or reduced GHG emissions relative to the control; and (3) living roots can destabilize clay-protected C within silt-size microaggregates, leading to rapid and preferential decomposition of clay-protected C; however, biochar can stabilize clay-protected C within silt-size microaggregates under the influence of living roots. Moreover, root-driven stabilization or destabilization of clay-protected C within silt-size microaggregates may mediate SOC sequestration and SOC storage capacity, which has important implications for our

understanding of SOC persistence and the underlying processes used in soil C models. To help meet climate change mitigation goals, I recommend incentivizing the retention and establishment of AFS on agricultural lands, as well as supporting and optimizing biochar application in agriculture.

Preface

This thesis is an original work by Cole D. Gross. I was responsible for conceptualization and methodology, data collection and analysis, synthesis, data visualization, and writing and editing. Coauthors for specific chapters, as detailed below, were also responsible for conceptualization and methodology, reviewing and editing, and/or supervision.

Chapter 2 of this thesis has been published as Gross CD, Bork EW, Carlyle CN, Chang SX (2022) Agroforestry perennials reduce nitrous oxide emissions and their live and dead trees increase ecosystem carbon storage. *Global Change Biology,* 00, 1–17. doi:10.1111/gcb.16322. All authors contributed to conceptualization and methodology. I was responsible for investigation and writing the original draft, while all authors contributed to review and editing. Supervision was provided by Chang SX and Bork EW.

Chapter 3 of this thesis has been published as Gross CD, Bork EW, Carlyle CN, Chang SX (2022) Biochar and its manure-based feedstock have divergent effects on soil organic carbon and greenhouse gas emissions in croplands. *Science of The Total Environment*, 806, 151337. doi:10.1016/j.scitotenv.2021.151337. All authors contributed to conceptualization and methodology. I was responsible for investigation and writing the original draft, while all authors contributed to review and editing. Supervision was provided by Chang SX and Bork EW.

Chapter 4 of this thesis is in preparation for submission to a peer-reviewed journal as Gross CD, Bork EW, Wissel B, Carlyle CN, Chang SX (exp. Sep 2022) Root-driven destabilization of clay-protected carbon within silt-size microaggregates. I was responsible for conceptualization, methodology, investigation, and writing the original draft. Wissel B contributed to methodology, while all authors contributed to review and editing. Supervision was provided by Chang SX and Bork EW. Guidance and feedback at various stages were provided by all coauthors.

Chapter 5 of this thesis is in preparation for submission to a peer-reviewed journal as Gross CD, Bork EW, Wissel B, Carlyle CN, Chang SX (exp. Sep 2022) Biochar stabilizes clay-protected carbon within silt-size microaggregates. I was responsible for conceptualization, methodology, investigation, and writing the original draft. Wissel B contributed to methodology, while all authors contributed to review and editing. Supervision was provided by Chang SX and Bork EW. Guidance and feedback at various stages were provided by all coauthors.

Acknowledgements

Many thanks to my supervisor, Scott Chang, co-supervisor, Edward Bork, committee member, Cameron Carlyle, and collaborator, Björn Wissel, for their guidance, advice, encouragement, and helpful feedback. Thanks also to Sylvie Quideau and Peter Blenis for the thought-provoking conversations and feedback. I am particularly grateful to Scott for his support and the opportunities with which he provided me, which helped further develop me as an independent researcher and instructor, as well as to Edward, for his mentorship. Additionally, the University of Alberta has been a wonderful and supportive community and I am very appreciative to have had the opportunity to study, teach, and work at such an excellent university.

I gratefully acknowledge the financial support provided to me by a Doctoral Vanier Scholarship and a Killam Memorial Graduate Scholarship, which allowed me to expand my doctoral research and, ultimately, its impact. I also gratefully acknowledge a grant (AGGP2-039) from the Agricultural Greenhouse Gas Program from Agriculture and Agri-Food Canada to Scott Chang, Edward Bork, and Cameron Carlyle that supported this research.

A special thank you to my laboratory members over the years and the researchers who have assisted with this work. Specifically, many thanks to Michael Carson, Jonathan Tieu, Mary Villeneuve, Sheetal Patel, Carmen Roman Perez, Guanyu Chen, Maliha Rahman, Jinhyeob Kwak, Prem Pokharel, Runli Yuan, Wendi Yu, Emma Bowman, Ming Cao, Zhengfeng An, Max Menear, Qi Wang, and Danielle Ratcliffe for their help in the field and/or laboratory. I also express my gratitude to the landowners and farmers who worked with me throughout the duration of the field study for their generosity, assistance, and cooperation. It was a pleasure working with everyone.

My heartfelt gratitude to my friends and family for all their encouragement. I am very thankful to have shared this adventure with Tien Weber, Dauren Kaliaskar, Laio Sobrinho, Gleb Kravchinsky, Kiah Leicht, Erin Daly, and Jonathan Tieu. My endless thanks to my parents, as I would not be where or who I am today without their love and encouragement. I cannot express how much their support has meant to me. And finally, my deepest thanks to my partner, Carmen Roman Perez, who inspires me in so many ways. She has made this road possible through her love and support—the beautiful beginning of a journey that I am so happy we get to take together.

~Life of Soil~

where death turns to life
and all things are made anew
beneath our feet

Table of Contents

List of Tables

Page

List of Figures

Page

Chapter 1. Introduction

Soil is the largest terrestrial carbon (C) stock (Lehmann & Kleber, 2015) and acts as a global C sink, sequestering around 20–30% of anthropogenic C emissions annually (Pan *et al.*, 2011; Le Quéré *et al.*, 2018). However, the cultivation of soils leads to the release of large amounts of C to the atmosphere (Guo & Gifford, 2002; Ciais *et al.*, 2013). The growing human population and demand for food and other agricultural products have led to more forests and grasslands being converted to intensively farmed agroecosystems. Agricultural management practices affect greenhouse gas (GHG) emissions from soils by altering the soil environment and, in turn, changing the size and composition of microbial communities and their activities, including the facilitation of nutrient cycling.

Agricultural soils can act as an important source of GHG emissions to the atmosphere and contribute to global climate change (Ciais *et al.*, 2013). Between 2007 and 2016, agriculture contributed 12% of the total global anthropogenic GHG emissions (IPCC, 2019). The three major GHGs contributing to agricultural emissions are carbon dioxide (CO_2), nitrous oxide (N_2O), and methane (CH_4), of which CO_2 is the most abundant GHG emitted from agricultural soils (Ciais *et al.*, 2013). Microbial decomposition of soil organic C (SOC) results in C being released to the atmosphere as CO_2. As a means of mitigation, efforts to increase C sequestration, especially in agricultural soils, have received increasing attention (Minasny *et al.*, 2017; Zomer *et al.*, 2017). Widely recognized strategies to increase SOC across agroecosystems include the use of cover crops, improved crop rotations, reduced tillage, and organic amendments (Lal, 2004; Paustian *et al.*, 2016). Land-use management is another effective means to increase C sequestration both above- and belowground in agroecosystems. Compared with conventional agroecosystems, land-use systems that deliberately incorporate woody perennials into agricultural fields, called agroforestry systems (AFS), facilitate C sequestration and reduce GHG emissions (Lal, 2004; Paustian *et al.*, 2016; Shi *et al.*, 2018).

Utilizing land-use and other management practices to increase SOC storage is considered key to help drawdown atmospheric CO_2 as we reduce fossil fuel emissions to mitigate climate change (IPCC, 2022). Moreover, increasing SOC can enhance the resilience of agricultural land to drought and other climate changes by increasing overall soil health (such as nutrient- and water-holding capacities, soil aggregation and aeration, and microbial diversity) (Amundson & Biardeau, 2018). Therefore, how soils cycle and store new C inputs has important implications for both the

global C cycle and food security (Lorenz & Lal, 2022). Land use and management practices that increase C inputs to soil may have dual effects on soil C dynamics, in some cases resulting in the intensified loss (a.k.a. priming) of SOC and initially reducing SOC storage (Dijkstra *et al.*, 2021).

1.1. Climate change mitigation potential of agroforestry

Although less than 10% of global agricultural land contains a substantial woody vegetation component, trees incorporated into croplands and pastures have been estimated to store 6.93 Pg C (Chapman *et al.*, 2020). Globally, the trees of AFS cover an estimated 960 M ha, with associated soils containing at least 3.6 Pg more C than adjacent cropland and pasture (Shi *et al.*, 2018). Trees in AFS globally are estimated to sequester between 3 and 6 Mg C ha^{-1} y^{-1} up to a tree age of 50 years (Ma *et al.*, 2020), while temperate AFS are estimated to have SOC sequestration rates of about 0.18 Mg C ha^{-1} y^{-1} in the upper 40 cm of soil, not including the litter layer (Mayer *et al.*, 2022). Moreover, well-aerated soils under forested cover act as sinks for CH_4 and release less N_2O than intensively managed cropland soils (Baah-Acheamfour *et al.*, 2016; Paustian *et al.*, 2016). Therefore, converting more conventional agroecosystems to AFS creates substantial mitigation opportunities through C sequestration both above- and belowground, as well as by reducing the emissions of potent GHGs such as N_2O and CH_4.

Globally, the adoption of agroforestry could store ~1–9 Pg more C, which is up to 8% of the total mitigation needed by 2030 to limit global warming to 2 °C (Meinshausen *et al.*, 2009; Chapman *et al.*, 2020). In Canada, over 65 M ha are dedicated to agricultural use, and over 30% of this agricultural land is in Alberta (Statistics Canada Census of Agriculture, 2008). In this province alone, there is a substantial opportunity for converting more intensively farmed agroecosystems to AFS, specifically by planting trees at road/field margins (An *et al.*, 2022), thereby helping to mitigate climate change. For example, the woodlands of AFS in central Alberta were shown to store 2.26 times (or 178.5 Mg ha^{-1}) more C than adjacent cropland and pasture (Ma *et al.*, 2022), emphasizing the importance of AFS in this region for C sequestration. However, current AFS may benefit from active management, enhancement, or expansion, such as the planting of trees in perennial vegetated areas that lack a consistent woody component (for example, gaps in trees along road/field margins) (Shrestha *et al.*, 2018) and tree planting that facilitates niche complementarity (Ma *et al.*, 2022). The total amount of C that can be sequestered and stored by AFS remains dependent on a variety of factors, including the specific agroforestry system type,

time since forest stand establishment, and tree species richness (Kim *et al.*, 2016; Feliciano *et al.*, 2018; Ma *et al.*, 2020).

Common linear agroforestry system types in the temperate climate zone include hedgerows and shelterbelts. Both types of AFS are usually retained or established at agricultural road/field margins, with hedgerows consisting of naturally-occurring legacy perennial vegetation buffers that include a dense woody component, while shelterbelts, also referred to as windbreaks, consist of planted woody perennial vegetation on previously cleared land that was usually under cultivation at one time (Mayrinck *et al.*, 2019; Drexler *et al.*, 2021). Functionally, hedgerows differ from shelterbelts primarily due to having greater tree density, a broader age distribution of trees, and the inclusion of shrubs (Drexler *et al.*, 2021). Shrubs are less commonly planted among the row(s) of trees in shelterbelts but tend to proliferate within hedgerows, allowing hedgerows to play a more valuable ecological role compared with shelterbelts (Drexler *et al.*, 2021). Although hedgerows and shelterbelts have been found to store similar amounts of C in living biomass and soil (Ma *et al.*, 2022), CO_2 fluxes can vary between the two AFS (Baah-Acheamfour *et al.*, 2016, 2020), suggesting underlying differences in C cycling. The perennial vegetation component of AFS captures and stores more CO_2 in biomass (namely woody biomass) and increases C inputs to the soil relative to adjacent cropland, especially as litter and through the extensive and deep rooting systems of woody species (Jandl *et al.*, 2014; Cardinael *et al.*, 2018). Greater protection of SOC, such as through the formation of aggregates due to less soil disturbance, also helps increase C stocks in soils under forested cover (Lorenz & Lal, 2014; Le Bissonnais *et al.*, 2018). Moreover, AFS contribute to enhanced biodiversity and other vital ecosystem services relative to conventional agroecosystems (Kreitzman *et al.*, 2022).

1.2. Climate change mitigation potential of biochar

In addition to the adoption of agroforestry, incorporating organic amendments into agricultural soils could increase SOC storage and decrease GHG emissions (Stavi & Lal, 2013; Gross & Glaser, 2021). Moreover, increasing SOC storage can benefit the soil by increasing soil nutrient- and water-holding capacities, which could enhance crop yield and the ecological goods and services generated by agricultural land. The application of readily available organic amendments such as biowastes to agricultural soils is a common practice. Manure compost application has shown promise for increasing SOC stocks (Tautges *et al.*, 2019; Gross & Glaser,

2021), specifically within the silt and clay fraction of soil macroaggregates (Yu *et al.*, 2012) and particulate organic matter (Sleutel *et al.*, 2006), among other benefits to the soil (Martínez-Blanco *et al.*, 2013). In general, manure compost is more promising than raw manure as a soil amendment for increasing SOC sequestration and reducing GHG emissions from agroecosystems (Ryals *et al.*, 2015; Shrestha *et al.*, 2018). However, there is mounting evidence that biochar (organic material pyrolyzed under low or no oxygen conditions) may be a superior tool for increasing SOC storage and mitigating agricultural GHG emissions from soil (Lehmann *et al.*, 2006; Sohi *et al.*, 2010; Shakoor *et al.*, 2021).

Compared with biowaste amendments, amending soil with biochar has been shown to have a greater potential for increasing SOC stocks (Yousaf *et al.*, 2017) and reducing the emission of GHGs, including N_2O (Cayuela *et al.*, 2014; Shakoor *et al.*, 2021) and CH_4 (Jeffery *et al.*, 2016). Biochar can increase SOC protection and storage (Lehmann *et al.*, 2011; Hernandez-Soriano *et al.*, 2016a; Weng *et al.*, 2017), as well as help reduce microbial activity and metabolism (Hernandez-Soriano *et al.*, 2016b; Yousaf *et al.*, 2017) and decrease the activities of soil enzymes involved in the degradation of organic C compounds (Lehmann *et al.*, 2011; Li *et al.*, 2018; Pokharel *et al.*, 2018). However, applying biochar at large scales is complicated by the additional costs to produce biochar and the lack of pyrolysis facilities used to mass-produce biochar (Roberts *et al.*, 2010; Galinato *et al.*, 2011; Spokas *et al.*, 2012).

1.3. Knowns and unknowns of soil carbon dynamics

Land use and management practices aimed at increasing SOC include conversion of annually cropped land to perennial ecosystems, such as secondary forest or grassland, the adoption of agroforestry systems, or incorporation of perennial or cover crops (Paustian *et al.*, 2016; Schlautman *et al.*, 2021; IPCC, 2022). These practices increase root litter and exudate C inputs (together termed rhizodeposition) to both surface and deeper soil layers. Warming and elevated atmospheric CO_2 concentrations are expected to increase above- and belowground vegetation growth in many regions globally (Jones *et al.*, 2005; Ciais *et al.*, 2013), which would also increase C inputs to the soil via rhizodeposition. In terrestrial ecosystems, living roots can have both stabilizing and destabilizing effects on SOC (Dijkstra *et al.*, 2021). For example, living roots increase microbial turnover and, in turn, microbial necromass that can be stabilized in the soil (Zhu *et al.*, 2020; Dijkstra *et al.*, 2021; Sokol *et al.*, 2022). However, by providing fresh C inputs and

enhancing microbial activity, living roots can also intensify the loss of SOC, a phenomenon referred to as priming (Kuzyakov *et al.*, 2000). Priming effects may lead to initial net decreases in SOC storage despite additional C inputs (Dijkstra & Cheng, 2007; Sulman *et al.*, 2014; Dijkstra *et al.*, 2021).

Mineral sorption is widely considered to play a fundamental role in the protection of SOC from microbial decomposition and occurs mainly within the clay fraction (Angst *et al.*, 2018; Rasmussen *et al.*, 2018). This mineral-associated C is largely composed of microbial products that may be predominantly derived from rhizodeposition (Liang *et al.*, 2017; Sokol & Bradford, 2019; Sokol *et al.*, 2019). However, root exudates can rapidly foster the release of mineral-associated C into the dissolved organic C pool, rendering the C more labile (Clarholm *et al.*, 2015; Keiluweit *et al.*, 2015). Root-exudate mediated C release from mineral-C associations may help explain the greater contribution of root exudates relative to root litter with respect to priming effects (Shahzad *et al.*, 2015; Pierson *et al.*, 2021), as well as the increased vulnerability of finer- rather than coarser-textured soils to rhizosphere priming (Huo *et al.*, 2017). Deeper soil layers, where the SOC is often hundreds to thousands of years old (Fontaine *et al.*, 2007; Schmidt *et al.*, 2011) and storage mainly occurs via sorption to clay particles (Angst *et al.*, 2018), are also susceptible to rhizosphere priming effects (Mobley *et al.*, 2015; Tian *et al.*, 2016; Shahzad *et al.*, 2018).

In addition to mineral sorption, SOC protection from microbial decomposition is provided by soil aggregation. Microaggregates (< 250 μm), which are stabilized within macroaggregates (> 250 μm), are particularly important for providing SOC protection by creating anoxic conditions or making C less physically accessible to microorganisms (Six *et al.*, 2002; Rasse *et al.*, 2005; Totsche *et al.*, 2018). The most stable aggregates are silt-size microaggregates (2–53 μm), which largely exclude bacteria from their micropores, thereby physically protecting C that is not on the periphery (Rasse *et al.*, 2005; Lavallee *et al.*, 2019; Yang *et al.*, 2021). Several studies have observed that a substantial portion of SOC is in the form of C bound to clay within silt-size microaggregates (Virto *et al.*, 2008, 2010; Moni *et al.*, 2010). Because this C is both physically and chemically protected from microorganisms, it may persist longer in soil than C that is unprotected or protected by other abiotic mechanisms (Lehmann *et al.*, 2007; Virto *et al.*, 2010; Totsche *et al.*, 2018). Whether this dual protection mechanism renders this C less susceptible to root-driven priming effects is unknown because most aggregation studies do not consider aggregates at the silt-size scale (Virto *et al.*, 2008; Totsche *et al.*, 2018; Lavallee *et al.*, 2019). A

recent study found that clay-protected C within model silt-size microaggregates can be broken down by extracellular enzymes into smaller fragments that are then released into solution (Yang *et al.*, 2021). However, how clay-protected C within silt-size microaggregates is affected by living roots in natural soils has not been investigated.

1.4. Agroforestry and biochar knowledge gaps

Identifying management practices that increase C storage and reduce GHG emissions in agroecosystems will help to improve our ability to mitigate climate change. Despite a general consensus that agroforestry establishment enhances C sequestration, some gaps in our knowledge remain (Nair, 2012). Moreover, field research comparing common biowaste materials and their biochars as agricultural amendments for the purposes of increasing SOC storage and reducing GHG emissions is needed to help quantify the differential benefits between the two types of amendments. A past bias toward sampling only the surface soil results in limitations in our understanding of deep SOC cycling, which is especially important in AFS due to the incorporation of trees and shrubs with deep rooting habits and the unique complexity of multiple land covers (Nair, 2012; Jandl *et al.*, 2014; Cardinael *et al.*, 2018). This past bias also ignores evidence that subsurface SOC can be affected by changes in management practices (Gross & Harrison, 2019; Tautges *et al.*, 2019). Failing to properly account for changes in bulk density with land-use change or management practices is another confounding issue in many past studies that can have a greater impact on SOC stock estimates relative to actual changes in SOC concentrations (Ellert & Bettany, 1995; Wendt & Hauser, 2013). The recommended approach to calculating SOC stocks to overcome biases associated with changes in bulk density is to compare equivalent soil masses rather than fixed soil depths (von Haden *et al.*, 2020).

In AFS, C contained in belowground biomass, understory vegetation, deadwood, and litter is often overlooked, and these potentially important C sinks are not included in many ecosystem C stock estimates for AFS (Ma *et al.*, 2020; Drexler *et al.*, 2021). As far as I am aware, I am the first to assess the contribution of deadwood to ecosystem C stock and its relationship to soil C stocks and GHG emissions within the woodland component of AFS. Forest deadwood is not only an important C sink globally (Pan *et al.*, 2011), but can also influence SOC and CO_2 emissions (Stutz *et al.*, 2017; Bradford *et al.*, 2021; Seibold *et al.*, 2021), as well as play an essential role in

promoting biodiversity and other ecosystem services (Blaser *et al.*, 2013; Vrška *et al.*, 2015; Sandström *et al.*, 2019).

Soils amended with biochar may experience increased root-derived C retention relative to non-amended soils, as well as negative priming (Lehmann *et al.*, 2011; Hernandez-Soriano *et al.*, 2016a; Weng *et al.*, 2017). Biochar amendment can counteract rhizosphere priming through the sorption of root exudates onto biochar surfaces (Weng *et al.*, 2017), both reducing priming effects and increasing root-derived C retention. Biochar has also been found to promote aggregate formation, particularly microaggregate formation, providing additional physical protection of SOC from microbial decomposition (Hernandez-Soriano *et al.*, 2016a; Weng *et al.*, 2017). If biochar accelerates the formation of these organo-mineral microstructures, SOC in biochar-amended soils may be less susceptible to root-driven priming effects (Weng *et al.*, 2017). However, the effect of biochar on SOC stabilization within silt-size microaggregates is unknown.

1.5. Objectives of this thesis research

In a 3-year field study (Chapter 2), I compared hedgerow and shelterbelt AFS and their component land-use types: perennial vegetated areas with and without trees (woodland and grassland, respectively), newly planted saplings in grassland, and adjacent annual cropland. I assessed the effects of AFS and their component land uses on above- and belowground live biomass C stocks (including trees and herbaceous vegetation), soil GHG emission rates (including the partitioning of autotrophic and heterotrophic respiration), surface (including litter) and subsurface SOC stocks (including labile C and microbial biomass, and using an equivalent soil mass-based approach), and total ecosystem C stocks (including standing and downed deadwood). My objective was to elucidate the interdependence of land use, C cycling, and GHG emissions across the two common linear AFS in the temperate climate zone to aid in the development of climate mitigation policies toward increasing C sequestration and reducing GHG emissions from agroecosystems.

I also directly compared one-time additions of manure compost and its biochar derivative in a 3-year field study (Chapter 3) to assess the effects of these organic amendments on GHG emissions, as well as on both the surface and subsurface storage of SOC (using an equivalent soil mass-based approach) in annually cropped agricultural lands. Manure compost was used as the feedstock for biochar production to directly compare this manure compost to its biochar.

Additionally, compared with raw manure, composted manure can be easily stored until transported to a pyrolysis facility, is less expensive to transport due to large decreases in mass and volume, and has reduced moisture content, which facilitates the pyrolysis process (Michel *et al.*, 2004; Roberts *et al.*, 2010). My objective was to aid in the development of targeted management practices across soil types to increase SOC sequestration and reduce GHG emissions from agroecosystems.

In addition to the field studies, I conducted a 150-d incubation in a controlled growth chamber (Chapter 4). The ^{13}C natural abundance technique was used to quantify root-driven SOC dynamics in soils with varying properties (texture, pH, C and N content, etc.) collected from three different land uses (cropland, grassland, and woodland) and depths (0–10, 10–30, and 30–50 cm) by planting a native perennial C_4 plant species (blue grama, *Bouteloua gracilis* (Willd. ex Kunth.) Lag. Ex Griffiths) in soils derived from C_3 plant systems. My objectives were to 1) elucidate the interplay of physical and chemical protection of C under the influence of living roots by quantifying root C incorporation and priming across different soil fractions, including clay-size particles within silt-size microaggregates, and 2) assess the interdependence of soil properties (including SOC storage within soil fractions) and root-driven SOC dynamics across land uses and soil depths.

Finally, I expanded on my previous study (Chapter 4) by using the ^{13}C natural abundance technique to investigate the effects of manure compost and biochar on root-driven SOC dynamics in a 150-d incubation in a controlled growth chamber (Chapter 5). Soils with varying properties (texture, pH, C and N content, etc.) were collected from annually cropped agricultural land and planted with a native perennial C_4 plant species (blue grama, *Bouteloua gracilis* (Willd. ex Kunth.) Lag. Ex Griffiths). I used soils derived from C_3 plant systems that were either amended (two years prior) or not amended with manure compost or its biochar derivative. My objectives were to 1) elucidate the effect of manure compost and biochar on the interplay of physical and chemical protection of C under the influence of living roots by quantifying root C incorporation and priming across different soil fractions, including clay-size particles within silt-size microaggregates, and 2) assess the interdependence of soil properties (including SOC storage within soil fractions) and root-driven SOC dynamics across non-amended and manure- and biochar-amended agricultural soils.

My overall research objective was to aid in the development of management practices that increase C sequestration and reduce GHG emissions from agroecosystems as a means of climate

change mitigation. Achieving this goal involved an approach that considered 1) land-use management at the whole-system level (Chapter 2, agroforestry field study), 2) management practices that can be implemented specifically within cropped fields (Chapter 3, organic amendment field study), 3) mechanisms responsible for driving SOC dynamics under the influence of living roots across land uses in both surface and deeper soil layers (Chapter 4, agroforestry incubation study), and 4) the effect of management practices specific to cropped fields on root-driven SOC dynamics (Chapter 5, organic amendment incubation study).

1.6. References

Amundson R, Biardeau L (2018) Opinion: Soil carbon sequestration is an elusive climate mitigation tool. *Proceedings of the National Academy of Sciences*, **115**, 11652–11656.

An Z, Bork EW, Duan X, Gross CD, Carlyle CN, Chang SX (2022) Quantifying past, current, and future forest carbon stocks within agroforestry systems in central Alberta, Canada. *GCB Bioenergy*, **14**, 669–680.

Angst G, Messinger J, Greiner M et al. (2018) Soil organic carbon stocks in topsoil and subsoil controlled by parent material, carbon input in the rhizosphere, and microbial-derived compounds. *Soil Biology and Biochemistry*, **122**, 19–30.

Baah-Acheamfour M, Carlyle CN, Lim S, Bork EW, Chang SX (2016) Forest and grassland cover types reduce net greenhouse gas emissions from agricultural soils. *Science of The Total Environment*, **571**, 1115–1127.

Baah-Acheamfour M, Carlyle CN, Bork EW, Chang SX (2020) Forest and perennial herbland cover reduce microbial respiration but increase root respiration in agroforestry systems. *Agricultural and Forest Meteorology*, **280**, 107790.

Le Bissonnais Y, Prieto I, Roumet C et al. (2018) Soil aggregate stability in Mediterranean and tropical agro-ecosystems: effect of plant roots and soil characteristics. *Plant and Soil*, **424**, 303–317.

Blaser S, Prati D, Senn-Irlet B, Fischer M (2013) Effects of forest management on the diversity of deadwood-inhabiting fungi in Central European forests. *Forest Ecology and Management*, **304**, 42–48.

Bradford MA, Maynard DS, Crowther TW et al. (2021) Belowground community turnover accelerates the decomposition of standing dead wood. *Ecology*, **102**, 1–13.

Cardinael R, Guenet B, Chevallier T, Dupraz C, Cozzi T, Chenu C (2018) High organic inputs explain shallow and deep SOC storage in a long-term agroforestry system - Combining experimental and modeling approaches. *Biogeosciences*, **15**, 297–317.

Cayuela ML, van Zwieten L, Singh BP, Jeffery S, Roig A, Sánchez-Monedero MA (2014) Biochar's role in mitigating soil nitrous oxide emissions: A review and meta-analysis. *Agriculture, Ecosystems and Environment*, **191**, 5–16.

Chapman M, Walker WS, Cook-Patton SC, Ellis PW, Farina M, Griscom BW, Baccini A (2020) Large climate mitigation potential from adding trees to agricultural lands. *Global Change Biology*, **26**, 4357–4365.

Ciais P, Sabine C, Bala G et al. (2013) Carbon and other biogeochemical cycles. In: *Climate Change 2013: The Physical Science Basis. Contribution of Working Group I to the Fifth Assessment Report of the Intergovernmental Panel on Climate Change* (eds Stocker TF, Qin D, Plattner G-K, Tignor M, Allen SK, Boschung J, Nauels A, Xia Y, Bex V, Midgley PM), pp. 465–570. Cambridge University Press, Cambridge, United Kingdom and New York, NY, USA.

Clarholm M, Skyllberg U, Rosling A (2015) Organic acid induced release of nutrients from metal-stabilized soil organic matter - The unbutton model. *Soil Biology and Biochemistry*, **84**, 168–176.

Dijkstra FA, Cheng W (2007) Interactions between soil and tree roots accelerate long-term soil carbon decomposition. *Ecology Letters*, **10**, 1046–1053.

Dijkstra FA, Zhu B, Cheng W (2021) Root effects on soil organic carbon: A double-edged sword. *New Phytologist*, **230**, 60–65.

Drexler S, Gensior A, Don A (2021) Carbon sequestration in hedgerow biomass and soil in the temperate climate zone. *Regional Environmental Change*, **21**, 1–14.

Ellert BH, Bettany JR (1995) Calculation of organic matter and nutrients stored in soils under contrasting management regimes. *Canadian Journal of Soil Science*, **75**, 529–538.

Feliciano D, Ledo A, Hillier J, Nayak DR (2018) Which agroforestry options give the greatest soil and above ground carbon benefits in different world regions? *Agriculture, Ecosystems and Environment*, **254**, 117–129.

Fontaine S, Barot S, Barré P, Bdioui N, Mary B, Rumpel C (2007) Stability of organic carbon in deep soil layers controlled by fresh carbon supply. *Nature*, **450**, 277–80.

Galinato SP, Yoder JK, Granatstein D (2011) The economic value of biochar in crop production and carbon sequestration. *Energy Policy*, **39**, 6344–6350.

Gross A, Glaser B (2021) Meta-analysis on how manure application changes soil organic carbon storage. *Scientific Reports*, **11**, 1–13.

Gross CD, Harrison RB (2019) The case for digging deeper: Soil organic carbon storage, dynamics, and controls in our changing world. *Soil Systems*, **3**, 28.

Guo LB, Gifford RM (2002) Soil carbon stocks and land use change: A meta analysis. *Global change biology*, **8**, 345–360.

von Haden AC, Yang WH, DeLucia EH (2020) Soils' dirty little secret: Depth-based comparisons can be inadequate for quantifying changes in soil organic carbon and other mineral soil properties. *Global Change Biology*, **26**, 3759–3770.

Hernandez-Soriano MC, Kerré B, Goos P, Hardy B, Dufey J, Smolders E (2016a) Long-term effect of biochar on the stabilization of recent carbon: Soils with historical inputs of charcoal. *GCB Bioenergy*, **8**, 371–381.

Hernandez-Soriano MC, Kerré B, Kopittke PM, Horemans B, Smolders E (2016b) Biochar affects carbon composition and stability in soil: A combined spectroscopy-microscopy study. *Scientific Reports*, **6**, 1–13.

Huo C, Luo Y, Cheng W (2017) Rhizosphere priming effect: A meta-analysis. *Soil Biology and Biochemistry*, **111**, 78–84.

IPCC (2019) *Climate Change and Land: An IPCC special report on climate change, desertification, land degradation, sustainable land management, food security, and greenhouse gas fluxes in terrestrial ecosystems [P.R. Shukla, J. Skea, E. Calvo Buendia, V. Masson-Delmot*. Geneva, Switzerland, 896 pp.

IPCC (2022) Summary for policymakers. In: *Climate Change 2022: Mitigation of Climate Change. Contribution of Working Group III to the Sixth Assessment Report of the Intergovernmental Panel on Climate Change* (eds Shukla PR, Skea J, Slade R, Khourdajie A Al, Diemen R van, McCollum D, Pathak M, Some S, Vyas P, Fradera R, Belkacemi M, Hasija A, Lisboa G, Luz S, Malley J), p. 63. Cambridge University Press, Cambridge, UK and New York, NY, USA.

Jandl R, Rodeghiero M, Martinez C et al. (2014) Current status, uncertainty and future needs in soil organic carbon monitoring. *Science of the Total Environment*, **468**–**469**, 376–383.

Jeffery S, Verheijen FGA, Kammann C, Abalos D (2016) Biochar effects on methane emissions from soils: A meta-analysis. *Soil Biology and Biochemistry*, **101**, 251–258.

Jones C, McConnell C, Coleman K, Cox P, Falloon P, Jenkinson D, Powlson D (2005) Global climate change and soil carbon stocks; predictions from two contrasting models for the turnover of organic carbon in soil. *Global Change Biology*, **11**, 154–166.

Keiluweit M, Bougoure JJ, Nico PS, Pett-Ridge J, Weber PK, Kleber M (2015) Mineral protection of soil carbon counteracted by root exudates. *Nature Climate Change*, **5**, 588–595.

Kim DG, Kirschbaum MUF, Beedy TL (2016) Carbon sequestration and net emissions of CH4 and N2O under agroforestry: Synthesizing available data and suggestions for future studies. *Agriculture, Ecosystems and Environment*, **226**, 65–78.

Kreitzman M, Eyster H, Mitchell M et al. (2022) Woody perennial polycultures in the U.S. Midwest enhance biodiversity and ecosystem functions. *Ecosphere*, **13**, 1–35.

Kuzyakov Y, Friedelb JK, Stahra K (2000) Review of mechanisms and quantification of priming effects. *Soil Biology & Biochemistry*, **32**, 1485–1498.

Lal R (2004) Soil carbon sequestration impacts on global climate change and food security. *Science*, **304**, 1623–1627.

Lavallee JM, Soong JL, Cotrufo MF (2019) Conceptualizing soil organic matter into particulate and mineral-associated forms to address global change in the 21st century. *Global Change Biology*, 1–13.

Lehmann J, Kleber M (2015) The contentious nature of soil organic matter. *Nature*, **528**, 60–8.

Lehmann J, Gaunt J, Rondon M (2006) Bio-char sequestration in terrestrial ecosystems - A review. *Mitigation and Adaptation Strategies for Global Change*, **11**, 403–427.

Lehmann J, Kinyangi J, Solomon D (2007) Organic matter stabilization in soil microaggregates: Implications from spatial heterogeneity of organic carbon contents and carbon forms. *Biogeochemistry*, **85**, 45–57.

Lehmann J, Rillig MC, Thies J, Masiello CA, Hockaday WC, Crowley D (2011) Biochar effects on soil biota - A review. *Soil Biology and Biochemistry*, **43**, 1812–1836.

Li Y, Li Y, Chang SX, Yang Y, Fu S, Jiang P (2018) Biochar reduces soil heterotrophic respiration in a subtropical plantation through increasing soil organic carbon recalcitrancy and decreasing carbon-degrading microbial activity. *Soil Biology and Biochemistry*, **122**,

173–185.

Liang C, Schimel JP, Jastrow JD (2017) The importance of anabolism in microbial control over soil carbon storage. *Nature Microbiology*, **2**, 1–6.

Lorenz K, Lal R (2014) Soil organic carbon sequestration in agroforestry systems. A review. *Agronomy for Sustainable Development*, **34**, 443–454.

Lorenz K, Lal R (2022) *Soil Organic Carbon Sequestration in Terrestrial Biomes of the United States*, 1st edn. Springer, Cham, Switzerland, 201 pp.

Ma Z, Chen HYH, Bork EW, Carlyle CN, Chang SX (2020) Carbon accumulation in agroforestry systems is affected by tree species diversity, age and regional climate: A global meta-analysis. *Global Ecology and Biogeography*, **29**, 1817–1828.

Ma Z, Bork EW, Carlyle CN, Tieu J, Gross CD, Chang SX (2022) Carbon stocks differ among land-uses in agroforestry systems in western Canada. *Agricultural and Forest Meteorology*, **313**, 108756.

Martínez-Blanco J, Lazcano C, Christensen TH et al. (2013) Compost benefits for agriculture evaluated by life cycle assessment. A review. *Agronomy for Sustainable Development*, **33**, 721–732.

Mayer S, Wiesmeier M, Sakamoto E, Hübner R, Cardinael R, Kühnel A, Kögel-Knabner I (2022) Soil organic carbon sequestration in temperate agroforestry systems – A meta-analysis. *Agriculture, Ecosystems and Environment*, **323**.

Mayrinck RC, Laroque CP, Amichev BY, Van Rees K (2019) Above- and below-ground carbon sequestration in shelterbelt trees in Canada: A review. *Forests*, **10**, 1–17.

Meinshausen M, Meinshausen N, Hare W et al. (2009) Greenhouse-gas emission targets for limiting global warming to 2°C. *Nature*, **458**, 1158–1162.

Michel FC, Pecchia JA, Rigot J, Keener HM (2004) Mass and nutrient losses during the composting of dairy manure amended with sawdust or straw. *Compost Science and Utilization*, **12**, 323–334.

Minasny B, Malone BP, McBratney AB et al. (2017) Soil carbon 4 per mille. *Geoderma*, **292**, 59–86.

Mobley ML, Lajtha K, Kramer MG, Bacon AR, Heine PR, Richter DD (2015) Surficial gains and subsoil losses of soil carbon and nitrogen during secondary forest development. *Global Change Biology*, **21**, 986–996.

Moni C, Rumpel C, Virto I, Chabbi A, Chenu C (2010) Relative importance of sorption versus aggregation for organic matter storage in subsoil horizons of two contrasting soils. *European Journal of Soil Science*, **61**, 958–969.

Nair PKR (2012) Carbon sequestration studies in agroforestry systems: A reality-check. *Agroforestry Systems*, **86**, 243–253.

Pan Y, Birdsey RA, Fang J et al. (2011) A large and persistent carbon sink in the world's forests. *Science*, **333**, 988–993.

Paustian K, Lehmann J, Ogle S, Reay D, Robertson GP, Smith P (2016) Climate-smart soils. *Nature*, **532**, 49–57.

Pierson D, Evans L, Kayhani K, Bowden RD, Nadelhoffer K, Simpson M, Lajtha K (2021) Mineral stabilization of soil carbon is suppressed by live roots, outweighing influences from litter quality or quantity. *Biogeochemistry*, **154**, 433–449.

Pokharel P, Kwak JH, Ok YS, Chang SX (2018) Pine sawdust biochar reduces GHG emission by decreasing microbial and enzyme activities in forest and grassland soils in a laboratory experiment. *Science of the Total Environment*, **625**, 1247–1256.

Le Quéré C, Andrew RM, Friedlingstein P et al. (2018) Global carbon budget 2017. *Earth System Science Data*, **10**, 405–448.

Rasmussen C, Heckman K, Wieder WR et al. (2018) Beyond clay: towards an improved set of variables for predicting soil organic matter content. *Biogeochemistry*, **137**, 297–306.

Rasse DP, Rumpel C, Dignac MF (2005) Is soil carbon mostly root carbon? Mechanisms for a specific stabilisation. *Plant and Soil*, **269**, 341–356.

Roberts KG, Gloy BA, Joseph S, Scott NR, Lehmann J (2010) Life cycle assessment of biochar systems: Estimating the energetic, economic, and climate change potential. *Environmental Science and Technology*, **44**, 827–833.

Ryals R, Hartman MD, Parton WJ, Delonge MS, Silver WL (2015) Long-term climate change mitigation potential with organic matter management on grasslands. *Ecological Applications*, **25**, 531–545.

Sandström J, Bernes C, Junninen K, Lõhmus A, Macdonald E, Müller J, Jonsson BG (2019) Impacts of dead wood manipulation on the biodiversity of temperate and boreal forests. A systematic review. *Journal of Applied Ecology*, **56**, 1770–1781.

Schlautman B, Bartel C, Diaz-Garcia L et al. (2021) Perennial groundcovers: An emerging

technology for soil conservation and the sustainable intensification of agriculture. *Emerging Topics in Life Sciences*, **5**, 337–347.

Schmidt MWI, Torn MS, Abiven S et al. (2011) Persistence of soil organic matter as an ecosystem property. *Nature*, **478**, 49–56.

Seibold S, Rammer W, Hothorn T et al. (2021) The contribution of insects to global forest deadwood decomposition. *Nature*, **597**, 77–81.

Shahzad T, Chenu C, Genet P, Barot S, Perveen N, Mougin C, Fontaine S (2015) Contribution of exudates, arbuscular mycorrhizal fungi and litter depositions to the rhizosphere priming effect induced by grassland species. *Soil Biology and Biochemistry*, **80**, 146–155.

Shahzad T, Rashid MI, Maire V et al. (2018) Root penetration in deep soil layers stimulates mineralization of millennia-old organic carbon. *Soil Biology and Biochemistry*, **124**, 150–160.

Shakoor A, Shahzad SM, Chatterjee N et al. (2021) Nitrous oxide emission from agricultural soils: Application of animal manure or biochar? A global meta-analysis. *Journal of Environmental Management*, **285**, 112170.

Shi L, Feng W, Xu J, Kuzyakov Y (2018) Agroforestry systems: Meta-analysis of soil carbon stocks, sequestration processes, and future potentials. *Land Degradation & Development*, **29**, 1–12.

Shrestha BM, Chang SX, Bork EW, Carlyle CN (2018) Enrichment planting and soil amendments enhance carbon sequestration and reduce greenhouse gas emissions in agroforestry systems: A review. *Forests*, **9**, 1–18.

Six J, Conant RT, Paul E a, Paustian K (2002) Stabilization mechanisms of soil organic matter: Implications for C-saturatin of soils. *Plant and Soil*, **241**, 155–176.

Sleutel S, De Neve S, Németh T, Tóth T, Hofman G (2006) Effect of manure and fertilizer application on the distribution of organic carbon in different soil fractions in long-term field experiments. *European Journal of Agronomy*, **25**, 280–288.

Sohi SP, Krull E, Lopez-Capel E, Bol R (2010) A review of biochar and its use and function in soil. *Advances in Agronomy*, **105**, 47–82.

Sokol NW, Bradford MA (2019) Microbial formation of stable soil carbon is more efficient from belowground than aboveground input. *Nature Geoscience*, **12**, 46–53.

Sokol NW, Kuebbing SE, Karlsen-Ayala E, Bradford MA (2019) Evidence for the primacy of

living root inputs, not root or shoot litter, in forming soil organic carbon. *New Phytologist*, **221**, 233–246.

Sokol NW, Slessarev E, Marschmann GL et al. (2022) Life and death in the soil microbiome: How ecological processes influence biogeochemistry. *Nature Reviews Microbiology*, **0123456789**.

Spokas KA, Cantrell KB, Novak JM et al. (2012) Biochar: A synthesis of its agronomic impact beyond carbon sequestration. *Journal of Environmental Quality*, **41**, 973–989.

Statistics Canada Census of Agriculture (2008) *Census of Agriculture for Alberta, 2006*. 1–13 pp.

Stavi I, Lal R (2013) Agroforestry and biochar to offset climate change: A review. *Agronomy for Sustainable Development*, **33**, 81–96.

Stutz KP, Dann D, Wambsganss J, Scherer-Lorenzen M, Lang F (2017) Phenolic matter from deadwood can impact forest soil properties. *Geoderma*, **288**, 204–212.

Sulman BN, Phillips RP, Oishi AC, Shevliakova E, Pacala SW (2014) Microbe-driven turnover offsets mineral-mediated storage of soil carbon under elevated CO2. *Nature Climate Change*, **4**, 1099–1102.

Tautges NE, Chiartas JL, Gaudin ACM, O'Geen AT, Herrera I, Scow KM (2019) Deep soil inventories reveal that impacts of cover crops and compost on soil carbon sequestration differ in surface and subsurface soils. *Global Change Biology*, **25**, 3753–3766.

Tian Q, Yang X, Wang X et al. (2016) Microbial community mediated response of organic carbon mineralization to labile carbon and nitrogen addition in topsoil and subsoil. *Biogeochemistry*, **128**, 125–139.

Totsche KU, Amelung W, Gerzabek MH et al. (2018) Microaggregates in soils. *Journal of Plant Nutrition and Soil Science*, **181**, 104–136.

Virto I, Barré P, Chenu C (2008) Microaggregation and organic matter storage at the silt-size scale. *Geoderma*, **146**, 326–335.

Virto I, Moni C, Swanston C, Chenu C (2010) Turnover of intra- and extra-aggregate organic matter at the silt-size scale. *Geoderma*, **156**, 1–10.

Vrška T, Přívětivý T, Janík D, Unar P, Šamonil P, Král K (2015) Deadwood residence time in alluvial hardwood temperate forests - A key aspect of biodiversity conservation. *Forest Ecology and Management*, **357**, 33–41.

Wendt JW, Hauser S (2013) An equivalent soil mass procedure for monitoring soil organic carbon in multiple soil layers. *European Journal of Soil Science*, **64**, 58–65.

Weng Z (Han), Van Zwieten L, Singh BP et al. (2017) Biochar built soil carbon over a decade by stabilizing rhizodeposits. *Nature Climate Change*, **7**, 371–376.

Yang JQ, Zhang X, Bourg IC, Stone HA (2021) 4D imaging reveals mechanisms of clay-carbon protection and release. *Nature Communications*, **12**.

Yousaf B, Liu G, Wang R, Abbas Q, Imtiaz M, Liu R (2017) Investigating the biochar effects on C-mineralization and sequestration of carbon in soil compared with conventional amendments using the stable isotope (δ13C) approach. *GCB Bioenergy*, **9**, 1085–1099.

Yu H, Ding W, Luo J, Geng R, Cai Z (2012) Long-term application of organic manure and mineral fertilizers on aggregation and aggregate-associated carbon in a sandy loam soil. *Soil and Tillage Research*, **124**, 170–177.

Zhu X, Jackson RD, DeLucia EH, Tiedje JM, Liang C (2020) The soil microbial carbon pump: From conceptual insights to empirical assessments. *Global Change Biology*, **26**, 6032–6039.

Zomer RJ, Bossio DA, Sommer R, Verchot L V. (2017) Global sequestration potential of increased organic carbon in cropland soils. *Scientific Reports*, **7**, 1–8.

Chapter 2. Agroforestry perennials reduce nitrous oxide emissions and their live and dead trees increase ecosystem carbon storage

Cole D. Gross[1], Edward W. Bork[2], Cameron N. Carlyle[2], Scott X. Chang[1]

[1] Department of Renewable Resources, Faculty of Agricultural, Life and Environmental Sciences, University of Alberta, 442 Earth Sciences Building, Edmonton, AB T6G 2E3, Canada; cgross@ualberta.ca (C.D.G.); sxchang@ualberta.ca (S.X.C.)

[2] Department of Agricultural, Food and Nutritional Science, Faculty of Agricultural, Life and Environmental Sciences, University of Alberta, 410 Agriculture/Forestry Centre, Edmonton, AB T6G 2P5, Canada; ebork@ualberta.ca (E.W.B.); cameron.carlyle@ualberta.ca (C.N.C.)

2.1. Abstract

Agroforestry systems (AFS) contribute to carbon (C) sequestration and reduction in greenhouse gas emissions from agricultural lands. However, previously understudied differences among AFS may underestimate their climate change mitigation potential. In this 3-y field study, I assessed various C stocks and greenhouse gas emissions across two common AFS (hedgerows and shelterbelts) and their component land uses: perennial vegetated areas with and without trees (woodland and grassland, respectively), newly planted saplings in grassland, and adjacent annual cropland in central Alberta, Canada. Between 2018 and 2020 (~April–October), nitrous oxide emissions were 89% lower under perennial vegetation relative to the cropland (0.02 and 0.18 g N m^{-2} y^{-1}, respectively). In 2020, heterotrophic respiration in the woodland was 53% lower in shelterbelts relative to hedgerows (279 and 600 g C m^{-2} y^{-1}, respectively). Within the woodland, deadwood C stock was particularly important in hedgerows (35 Mg C ha^{-1} or 7% of ecosystem C) relative to shelterbelts (2 Mg C ha^{-1} or < 1% of ecosystem C), and likely affected C cycling differences between the woodland types by enhancing soil labile C and microbial biomass in hedgerows. Deadwood C stock was positively correlated with annual heterotrophic respiration and total (to ~100 cm depth) soil organic C, water-soluble organic C, and microbial biomass C. Total ecosystem C was 1.90–2.55 times greater within the woodland than all other land uses, with 176, 234, 237, and 449 Mg C ha^{-1} found in the cropland, grassland, planted saplings treatment, and woodland, respectively. Shelterbelt and hedgerow woodlands contained 2.09 and 3.03 times more C, respectively, than adjacent cropland. My findings emphasize the importance of AFS for fostering C sequestration and reducing greenhouse gas emissions and, in particular, retaining hedgerows (legacy woodland) and their associated deadwood across temperate agroecosystems to help mitigate climate change.

Graphical abstract:

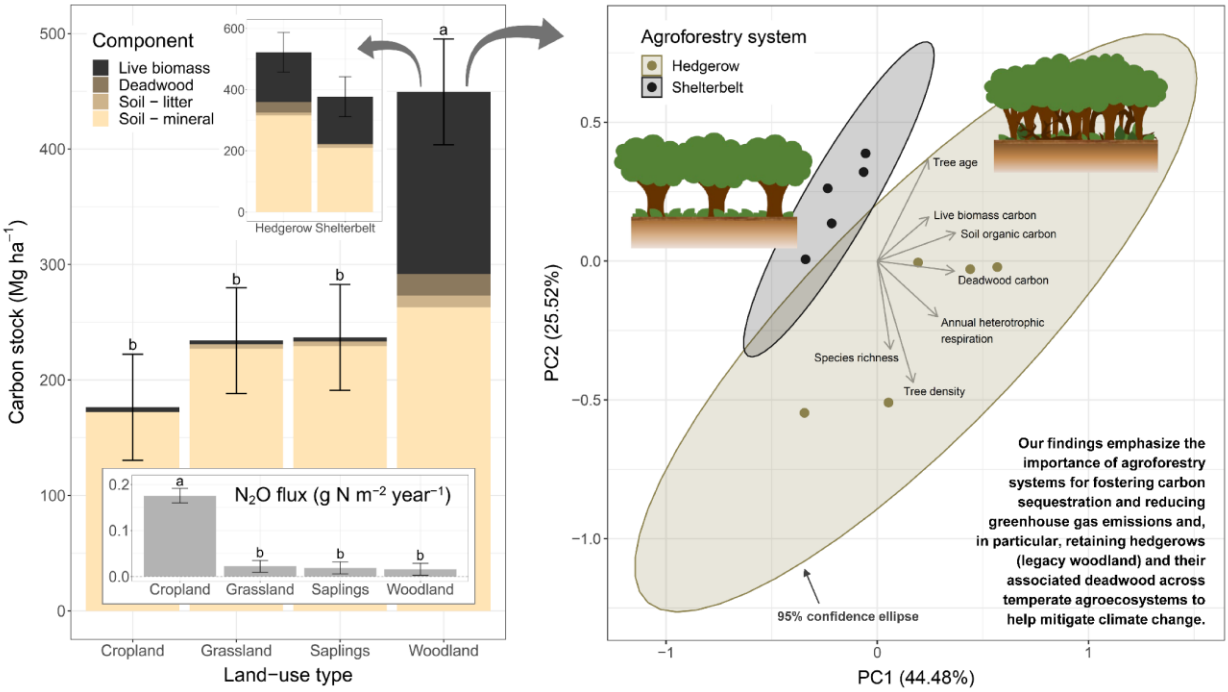

Keywords: agroforestry systems, climate change mitigation, deadwood, ecosystem carbon sequestration, greenhouse gas emissions, soil organic carbon, sustainable agriculture

Highlights:

- Ecosystem carbon (C) was 2+ times greater in the woodland relative to other land uses.
- N_2O emissions were 89% lower under perennial vegetation relative to annual cropland.
- Deadwood was an important C stock in the hedgerow woodland (7% of ecosystem C).
- Deadwood C stock was positively related to soil C stocks and heterotrophic respiration.
- Agroforestry, especially hedgerows and associated deadwood, fosters C sequestration.

2.2. Introduction

Agricultural soils can act as an important source of greenhouse gas (GHG) emissions to the atmosphere and contribute to global climate change (Ciais *et al.*, 2013). Between 2007 and 2016, agriculture contributed 12% of the total global anthropogenic GHG emissions (IPCC, 2019). As a means of mitigation, efforts to increase carbon (C) sequestration, especially in agricultural soils, have received increasing attention (Minasny *et al.*, 2017; Zomer *et al.*, 2017). Widely recognized strategies to increase soil organic C (SOC) across agroecosystems include the use of cover crops, improved crop rotations, reduced tillage, and organic amendments (Lal, 2004; Paustian *et al.*, 2016). Land-use management is another effective means to increase C sequestration both above- and belowground in agroecosystems. Compared with conventional agroecosystems, land-use systems that deliberately incorporate woody perennials into agricultural fields, called agroforestry systems (AFS), facilitate C sequestration and reduce GHG emissions (Lal, 2004; Paustian *et al.*, 2016; Shi *et al.*, 2018).

Common linear agroforestry types in the temperate climate zone include hedgerows and shelterbelts. Both types of AFS are usually at agricultural road/field margins, with hedgerows consisting of naturally-occurring legacy perennial vegetation buffers that include a dense woody component, while shelterbelts, also referred to as windbreaks, consist of planted woody perennial vegetation on previously cleared land that was usually under cultivation at one time (Mayrinck *et al.*, 2019; Drexler *et al.*, 2021). Functionally, hedgerows differ from shelterbelts primarily due to having greater tree density, a broader age distribution of trees, and the inclusion of shrubs (Drexler *et al.*, 2021). Shrubs are less commonly planted among the row(s) of trees in shelterbelts but tend to proliferate within hedgerows, allowing hedgerows to play a more valuable ecological role compared with shelterbelts (Drexler *et al.*, 2021). Although hedgerows and shelterbelts have been found to store similar amounts of C in living biomass and soil (Ma *et al.*, 2022), carbon dioxide (CO_2) fluxes can vary between the two AFS (Baah-Acheamfour *et al.*, 2016, 2020), suggesting underlying differences in C cycling. The perennial vegetation component of AFS captures and stores more CO_2 in biomass (namely woody biomass) and increases C inputs to the soil relative to adjacent cropland, especially as litter and through the extensive and deep rooting systems of woody species (Jandl *et al.*, 2014; Cardinael *et al.*, 2018). Greater protection of SOC, such as through the formation of aggregates due to less soil disturbance, also helps increase C stocks in soils under forested cover (Lorenz & Lal, 2014; Le Bissonnais *et al.*, 2018). Moreover, AFS contribute to

enhanced biodiversity and other vital ecosystem services relative to conventional agroecosystems (Kreitzman *et al.*, 2022).

Although less than 10% of global agricultural land contains a substantial woody vegetation component, trees incorporated into croplands and pastures have been estimated to store 6.93 Pg C (Chapman *et al.*, 2020). The global area of agroforestry tree cover is estimated to be at least 960 M ha, with associated soils containing at least 3.6 Pg more C than adjacent cropland and pasture (Shi *et al.*, 2018). Trees in AFS globally are estimated to sequester between 3 and 6 Mg C ha^{-1} y^{-1} up to a tree age of 50 years (Ma *et al.*, 2020), while temperate AFS are estimated to have SOC sequestration rates of about 0.18 Mg C ha^{-1} y^{-1} in the upper 40 cm of soil, not including the litter layer (Mayer *et al.*, 2022). Moreover, well-aerated soils under forested cover act as sinks for methane (CH_4) and release less nitrous oxide (N_2O) than intensively managed cropland soils (Baah-Acheamfour *et al.*, 2016; Paustian *et al.*, 2016). Therefore, converting more conventional agroecosystems to AFS creates substantial mitigation opportunities through C sequestration both above- and belowground, as well as by reducing the emissions of potent GHGs such as N_2O and CH_4.

Globally, the adoption of agroforestry could store ~1–9 Pg more C, which is up to 8% of the total mitigation needed by 2030 to limit global warming to 2 °C (Meinshausen *et al.*, 2009; Chapman *et al.*, 2020). In Canada, over 65 M ha are dedicated to agricultural use and over 30% of this agricultural land is in Alberta (Statistics Canada Census of Agriculture, 2008). In this province alone, there is substantial opportunity for converting more intensively farmed agroecosystems to AFS, specifically by planting trees at road/field margins (An *et al.*, 2022), thereby helping to mitigate climate change. For example, the woodlands of AFS in central Alberta were shown to store 2.26 times (or 178.5 Mg ha^{-1}) more C than adjacent cropland and pasture (Ma *et al.*, 2022), emphasizing the importance of AFS in this region for C sequestration. However, current AFS may benefit from active management, enhancement, or expansion, such as the planting of trees in perennial vegetated areas that lack a consistent woody component (for example, gaps in trees along road/field margins) (Shrestha *et al.*, 2018) and tree planting that facilitates niche complementarity (Ma *et al.*, 2022). The total amount of C that can be sequestered and stored by AFS remains dependent on a variety of factors, including the specific agroforestry system type, time since forest stand establishment, and tree species richness (Kim *et al.*, 2016; Feliciano *et al.*, 2018; Ma *et al.*, 2020).

Identifying management practices that increase C storage and reduce GHG emissions in agroecosystems will help to improve our ability to mitigate climate change. Despite a general consensus that agroforestry establishment enhances C sequestration, some gaps in our knowledge remain (Nair, 2012). A past bias toward sampling only the surface soil results in limitations in our understanding of deep SOC cycling, which is especially important in AFS due to the incorporation of trees and shrubs with deep rooting habits and the unique complexity of multiple land covers (Nair, 2012; Jandl *et al.*, 2014; Cardinael *et al.*, 2018). Failing to properly account for changes in bulk density with land-use change is another confounding issue in many past studies that can have a greater impact on SOC stock estimates relative to actual changes in SOC concentrations (Ellert & Bettany, 1995; Wendt & Hauser, 2013). The recommended approach to calculate SOC stocks to overcome biases associated with changes in bulk density is to compare equivalent soil masses rather than fixed soil depths (von Haden *et al.*, 2020). Moreover, C contained in belowground biomass, understory vegetation, deadwood, and litter is often overlooked, and these potentially important C sinks are not included in many ecosystem C stock estimates for AFS (Ma *et al.*, 2020; Drexler *et al.*, 2021). As far as I am aware, I am the first to assess the contribution of deadwood to ecosystem C stock and its relationship to soil C stocks and GHG emissions within the woodland component of AFS. Forest deadwood is not only an important C sink globally (Pan *et al.*, 2011), but can also influence SOC and CO_2 emissions (Stutz *et al.*, 2017; Bradford *et al.*, 2021; Seibold *et al.*, 2021), as well as play an essential role in promoting biodiversity and other ecosystem services (Blaser *et al.*, 2013; Vrška *et al.*, 2015; Sandström *et al.*, 2019).

In this 3-y field study, I compare hedgerow and shelterbelt AFS and their component land-use types: perennial vegetated areas with and without trees (woodland and grassland, respectively), newly planted saplings in grassland, and adjacent annual cropland. I assessed the effects of AFS and their component land uses on above- and belowground live biomass C stocks (including trees and herbaceous vegetation), soil GHG emission rates (including the partitioning of autotrophic and heterotrophic respiration), surface (including litter) and subsurface SOC stocks (including labile C and microbial biomass, and using an equivalent soil mass-based approach), and total ecosystem C stocks (including standing and downed deadwood). My objective was to elucidate the interdependence of land use, C cycling, and GHG emissions across the two common linear AFS in the temperate climate zone to aid in the development of climate mitigation policies toward increasing C sequestration and reducing GHG emissions from agroecosystems.

2.3. Materials and methods

2.3.1. Study area and experimental design

I conducted a 3-y (2018–2020) field study at ten producer-operated, annually cropped agroforestry sites in central Alberta, Canada (Fig. A.S1). Five hedgerow and five shelterbelt systems were examined. Agroforestry system type was determined based on site assessment (i.e., there were clear distinctions between the two AFS with respect to tree density and uniformity) and corroborating information provided by the landowners (e.g., whether the perennial vegetation areas at road/field margins had ever been cleared and cultivated with subsequent planting of trees). The historical monocultural annual crop rotation at all ten study sites was primarily wheat (*Triticum aestivum* L.), barley (*Hordeum vulgare* L.), and canola (*Brassica rapa* L.), although pea (*Pisum sativum* L.) and soybean (*Glycine max* L.) were each planted on one site in 2018. More detailed site information is provided in Gross *et al.* (2022). Briefly, cropland was tilled, seeded, fertilized, and harvested by the landowners according to their common practices during the study. In general, soils were typically tilled to ~10 cm depth prior to seeding and fertilizer was applied at the same time as seeding. Standard fertilization rates were 112-28-17-17 kg ha^{-1} N-P-K-S for canola, 78-22-11 kg ha^{-1} N-P-K for wheat, and 56-28-11 kg ha^{-1} N-P-K for barley. In perennial vegetated areas, common grasses were *Bromus inermis* (Leyss.), *Dactylis glomerata* (L.), and *Elymus sp.*, and common forbs were *Taraxacum officinale* (G. H. Weber *ex* Wiggers) and *Cirsium arvense* (L.). Shrubs, which were sparse, were most common in the hedgerow woodland, wherein *Rosa woodsii* (Lindl.) and *Rubus idaeus* (L.) were prevalent. Tree species were deciduous with aspen (*Populus tremuloides* Michx.) in hedgerows, willow (*Salix pentandra* L.) in shelterbelts, and balsam poplar (*Populus balsamifera* L.) in both AFS.

The regional climate at the study sites was humid continental (Köppen climate classification Dfb) and characterized by large seasonal temperature differences, with warm, sometimes humid summers and cold winters. Historical (from 1988 to 2017) mean annual total precipitation and mean annual temperature in Edmonton, Alberta (township T052R24W4) during the May through August growing season (full year in parentheses) were 275 (432) mm and 14.9 (3.7) °C, respectively (Alberta Climate Information Service, 2021). During the experiment, mean annual total precipitation and mean annual temperature were 197 (387) mm and 16.6 (3.7) °C in 2018, 282 (410) mm and 14.5 (3.3) °C in 2019, and 402 (504) mm and 15.4 (3.8) °C in 2020,

respectively (Alberta Climate Information Service, 2021). Study sites ranged from 617 to 797 m above sea level in elevation. Soils at all ten study sites and under each land-use type generally exhibited high levels of surface SOC accumulation (Chernozems in the Canadian soil classification system or Ustic Haplocryolls in the United States soil taxonomy system). All soils were classified by digging an 80-cm+ deep pit next to the plots in 2017 within each land use (Table A.S1).

The study used a split-plot design, comparing hedgerow and shelterbelt AFS (whole plots) and their component land-use types (subplots): perennial vegetated areas with and without trees (hereafter referred to as "woodland" and "grassland," respectively), newly planted saplings in grassland (hereafter referred to as the "saplings" treatment), and adjacent annually cropped land (hereafter referred to as "cropland"). Cropland subplots (5 × 5 m in size) were set up 30 m from trees or road/field margins. Perennial vegetation subplots (3 × 10 m in size) were set up within representative areas with and without trees nearby the cropland subplots. Okanese poplar (*Populus* × 'Okanese') saplings were planted in one of two randomly chosen grassland subplots over a 1-wk duration in early June 2018 at a density of 3333 trees ha^{-1} (10 saplings per subplot). Saplings were two years old and ~1-m tall at the time of planting and were chosen randomly from a batch with consistency in size and vigor. To help saplings establish, each sapling was planted in the center of a 1-m^2 area within which all pre-existing herbaceous vegetation was initially removed by hand, the surface 10 cm of soil was tilled using a shovel, and mulching fabric was applied. Saplings were watered twice monthly for three months following planting to limit mortality. In early June 2019, dead saplings (~10%) were replaced with saplings from the same batch as those planted the previous year, which had been maintained in an outdoor garden.

2.3.2. Data collection and analysis

2.3.2.1. Soil sampling and measurement of soil properties

Soil samples were collected from each subplot at four depth intervals (0–10, 10–30, 30–50, and 50–100 cm) in early May in both 2018 (from the grassland and saplings treatment subplots prior to planting the saplings; Table A.S2) and 2020. In late August 2020, soil samples were collected again from each subplot at only two depth intervals (0–10 and 10–30 cm), as the dryness of the soil prevented me from sampling deeper without causing severe disturbance to the subplots. Soil was collected by augering (3.81-cm diameter) three holes per subplot. Soil was composited by depth, returned to the lab, weighed, and stored at 4 °C until subsequent processing and analysis.

Bulk soil was sieved to 8 mm (Horwath & Paul, 1994; Datta *et al.*, 2014), and plant fragments and rocks (which comprised 0.4% on average by weight of the soil samples) with a diameter > 2 mm were removed from the soil. Apparent bulk density for each depth layer was calculated using the oven-dry mass of soil < 2 mm (von Haden *et al.*, 2020). Basic soil properties are provided in Table A.S1 and more detailed soil property measurement information is provided in Gross *et al.* (2022).

Soil pH was measured with a digital pH meter (Thermo Scientific 710A, Beverly, MA) using a 1:2 ratio (w:v) in ultrapure (MilliporeSigma Milli-Q) water. Soil C and N concentrations were determined by dry combustion on an elemental analyzer (Vario MICRO Cube Elemental Analyzer, Elementar, Hesse, Germany). Prior to analysis, samples with a pH > 6.00 (Walthert *et al.*, 2010) were acid fumigated for 72 h to remove any carbonates (Ramnarine *et al.*, 2011) so that the measured soil C represented organic C. A conversion factor was used to account for the increased weight of acidified soils and not dilute organic C measurements (Ramnarine *et al.*, 2011). Across all soils and depths, inorganic C comprised 5% of total C, most of which (92%) was in the deepest soil layer (50–100 cm) sampled.

The chloroform fumigation-extraction procedure was used to measure soil microbial biomass (Vance *et al.*, 1987; Beck *et al.*, 1997). Briefly, duplicate subsamples of 8 g (oven-dry weight basis) of field-moist soil sieved to < 8 mm were fumigated in a vacuum chamber with ethanol-free chloroform for 48 h in darkness (Jenkinson *et al.*, 2004). Water-soluble organic matter was extracted from both fumigated and non-fumigated samples (Haney *et al.*, 2001; Jenkinson *et al.*, 2004). The supernatant was collected and filtered through a 0.4-µm Whatman Nuclepore polycarbonate filter (Zsolnay, 2003; Chantigny *et al.*, 2007) and then stored at 4 °C prior to analysis with a total organic C (TOC) analyzer (TOC-V and TN unit, Shimadzu Corporation, Kyoto, Japan) using 680 °C combustion catalytic oxidation and the non-purgeable organic C (to remove inorganic C) and total N methods. Microbial biomass C (MBC) and N (MBN) were calculated using an extraction efficiency of 0.45 (Jenkinson *et al.*, 2004). The organic C and total N in the non-fumigated samples were defined as water-soluble organic C (WSOC) and total water-soluble N (WSN).

Soil organic C and total N, microbial biomass C and N, and WSOC and WSN masses were calculated using an equivalent soil mass-based approach (Wendt & Hauser, 2013) and a published R script (von Haden *et al.*, 2020), which uses cubic spline functions to model the relationship between cumulative areal mineral soil mass and cumulative C or N mass. Reference soil masses

were calculated using the hedgerow woodland, which generally had the lowest bulk density within each soil depth layer and was also considered closest to a natural state (Lee *et al.*, 2009). Comparing changes in SOC and N, as well as certain other soil properties, over time using reference soil masses helps overcome biases associated with changes in bulk density due to changes in land use (von Haden *et al.*, 2020).

Soil moisture and temperature values (at a depth of 10 cm) were recorded hourly from ~April through October using a soil monitoring station logger, moisture probe, and temperature sensor (Onset Computer Corporation, Bourne, MA) installed near the center of each subplot. All soil moisture values recorded when the soil temperature was < 0.25 °C (n < 1%) were considered inaccurate (based on the specifications of the instruments) and deleted from the dataset used for statistical analysis.

Soil litter (plant material at various stages of decomposition that overlies the mineral soil; LFH or O horizons in the Canadian or United States soil taxonomy systems, respectively) was collected from three randomly placed quadrats (22 × 31 cm) in each perennial vegetation subplot in late August 2020. Tilling practices prevented accumulation of a litter layer in the cropland. The thickness of the litter layer in perennial vegetation subplots was measured in the field, and samples from the three quadrats were composited for each subplot and returned to the lab. Samples were promptly weighed, thoroughly mixed, and subsamples oven-dried for 72 h at 60 °C and weighed again. Litter layer biomass (Mg ha^{-1}) was calculated using the quadrat area, weight of the composite sample, and a conversion factor based on the subsample moisture content. To obtain litter C and N concentrations, oven-dried subsamples were ground in a blender and a subsample further ground to a fine powder (< 0.1 mm) using a ball mill was analyzed on the elemental analyzer.

2.3.2.2. Gas sampling and measurement of greenhouse gas emission rates

Gas samples were collected every other week between 2018 and 2020 from about April through October from two dark static gas chambers (headspace mean height and volume of 12.2 cm and 0.012 m^3, respectively) equipped with fans (Christiansen *et al.*, 2011) installed in each subplot. In the cropland, chambers were installed between crop rows. More detailed gas sampling and measurement information is provided in Gross *et al.* (2022). Briefly, gas samples were collected from each chamber at 10-min intervals over 30 min (including time zero) usually between

1100 and 1400 h local time (Venterea *et al.*, 2005), stored with a positive pressure in pre-evacuated soda glass Labco Exetainers, and gas concentrations were later measured using a gas chromatograph (Varian CP-3800, Mississauga, Ontario, Canada). Chamber gas concentrations measured by gas chromatograph analysis were converted to mass per volume units using ideal gas relations at standard temperature and pressure corrected for the air temperature during sampling.

Gas flux (g m^{-2} h^{-1}) and cumulative flux (g m^{-2} y^{-1}) values were calculated from the chamber volume (m^3), soil surface area (m^2), and the change in chamber gas concentration (g m^{-3}) over time (h) using the *gasfluxes* R software package (Hüppi *et al.*, 2018) and the *KAPPA.MAX* flux calculation scheme to balance bias and uncertainty related to measurement precision and chamber setup (Hüppi *et al.*, 2018). To convert CH_4 and N_2O to CO_2-equivalents, global warming potentials of 27.2 and 273, respectively, were used, which are based on a 100-y frame and include C cycle responses (Forster *et al.*, 2021). Total GHG flux was calculated as the sum of CO_2, CH_4, and N_2O, with the latter two GHGs assessed as CO_2-equivalents.

2.3.2.3. Partitioning soil respiration into autotrophic and heterotrophic

To partition soil autotrophic (Ra) and heterotrophic (Rh) respiration within the grassland and woodland subplots in 2020, two plastic soil collars (21-cm diameter) were inserted into the soil of each subplot in June 2019, one to ~30 cm and the other to ~5 cm depth. The deeply inserted collars were used to exclude roots, relying on root severance around the perimeters of the collars to reduce Ra within the collars to negligible levels within several months (Kelting *et al.*, 1998; Baah-Acheamfour *et al.*, 2016, 2020). Emergent vegetation within the deeply inserted collars was minimal and was carefully removed prior to gas measurements in 2020, while leaving the litter and mineral soil undisturbed (Arevalo *et al.*, 2011). I did not remove live vegetation from the shallowly inserted collars and static chambers within grassland and woodland subplots, with these gas measurements reflecting total soil respiration (Baah-Acheamfour *et al.*, 2020). Gas measurements from deeply and shallowly inserted collars were made using an infrared gas analyzer equipped with a 20-cm inside diameter soil respiration chamber (LI-8100A, LI-COR Biosciences, Lincoln, Nebraska, USA). Within each subplot, gas measurements from collars were made from May through October 2020 during the same time period as gas sample collection from static chambers.

Autotrophic respiration for the grassland and woodland was calculated as the difference between total soil respiration from the shallowly inserted collars and Rh from the deeply inserted collars. The Ra percentage of total soil respiration for each sampling date and subplot was then used to estimate Rh from the static chamber system. Total GHG flux was calculated as noted previously, except heterotrophic CO_2 rather than total CO_2 emissions were used. For the saplings treatment, only the static chamber system resulting in total soil respiration measurements was used to not damage the root systems by installing deep chambers.

2.3.2.4. Measurement of trees, herbaceous vegetation, and deadwood

All trees within the woodland subplots were identified to the species level and measured for diameter at breast height (DBH) and maximum height (of the tallest stem of a multi-stem tree) in 2020. For multi-stem trees (i.e., *Salix pentandra*), DBH was calculated according to Amichev *et al.* (2016). Wood cores were collected using an increment borer from three dominant trees (and the dominant stem of a multi-stem tree) within the woodland subplots to determine stand age by manually counting the rings. Above- and belowground biomass (Mg ha^{-1}) for the tree species *Populus tremuloides* and *Populus balsamifera* were estimated using allometric equations for Alberta (Xing *et al.*, 2019; Ma *et al.*, 2022). For *Salix pentandra*, aboveground biomass was estimated using an allometric equation from Saskatchewan for the shelterbelt tree species Manitoba maple (*Acer negundo* L.) (Kort & Turnock, 1998; Amichev *et al.*, 2016) and belowground biomass was estimated using an allometric equation for all Canadian hardwood species (Li *et al.*, 2003). Specific plant organ C concentrations for deciduous trees were used to convert biomass to C stocks (Ma *et al.*, 2018).

Aboveground live herbaceous vegetation biomass (consisting of wheat, barley, and canola in the cropland subplots, and grasses and forbs in perennial subplots, all generally under 1 m in height) was destructively sampled ~1–2 weeks prior to swathing/harvest in 2020. Three 50 × 50 cm quadrats were randomly located in each subplot, and all aboveground live herbaceous vegetation was collected and weighed in the field. Subsequently, a randomly selected composite subsample of the herbaceous vegetation for each subplot was returned to the lab, immediately weighed, oven-dried for 72 h at 60 °C, and weighed again. Aboveground live herbaceous vegetation biomass (Mg ha^{-1}) and C stocks were calculated using the quadrat area, the average weight of the three field samples, a conversion factor based on the moisture content of the

composite subsamples, and the C concentrations obtained as described previously for the litter layer. Belowground live herbaceous vegetation biomass (Mg ha^{-1}) and C stocks were estimated using root:shoot ratios (RSR) for soil from 0–100 cm in depth (Thiagarajan *et al.*, 2018) and herbaceous plant root C concentrations (Ma *et al.*, 2018). In my subplots, shrub coverage was minimal (0–2 shrubs per woodland subplot) and therefore I did not sample or include shrub biomass in my estimates. Species richness in perennial subplots was surveyed within two 50 × 50 cm quadrats placed randomly within each third of the subplot (total of six quadrats per subplot) in 2020 and included the over-, mid-, and understory. Additionally, plant percent cover of each species was estimated to the nearest 1% (Fig. A.S2).

Downed deadwood was surveyed within two 1 × 1 m quadrats placed randomly within each third of the woodland subplots (total of six quadrats per subplot) in 2020. Within the quadrats, deadwood with a diameter ≥ 3.0 cm was measured for both diameter and length (Teissier Du Cros & Lopez, 2009). Deadwood with a diameter < 3.0 cm was counted within two size classes (diameter 1–2 and 2–3 cm) and length was averaged (n = 2–13) for each size class. Decay class was determined for coarse (diameter ≥ 7.0 cm) deadwood, while fine deadwood (1 ≤ diameter < 7.0 cm) was designated as either decayed or non-decayed (Harmon *et al.*, 2008; Teissier Du Cros & Lopez, 2009). Downed deadwood mass (Mg ha^{-1}) and C stocks were calculated by multiplying the absolute density (specific for tree species, decay, and size variables) by the volume (using Huber's formula) of each deadwood piece or size class within each quadrat and using decay and size-class specific mass to C conversion factors (Harmon *et al.*, 2008; Teissier Du Cros & Lopez, 2009). All standing dead trees (snags) within the woodland subplots were measured for DBH and height and classified as having primary/secondary or no branches. Snag deadwood mass (Mg ha^{-1}) and C stocks were estimated as described previously for living trees, except foliage was not included in the estimate and branches were included only if applicable (UNFCCC, 2015). All stumps were also measured and their mass and C stocks estimated according to the methods detailed above for downed deadwood (Harmon *et al.*, 2008; Teissier Du Cros & Lopez, 2009).

2.3.3. Statistical analysis

Linear mixed-effect models were used to determine whether AFS and land-use type affected live biomass C stocks, soil GHG emission rates, SOC stocks, and total ecosystem C stocks. A split-plot design model was used for each response variable. The fixed effects were AFS

(whole plot) and land-use type (subplot), while the random effect was site. Repeated measurements were averaged for emissions of GHGs collected within plots (n = 2) and months (n = 2 or 3) and cumulated for annual emissions of GHGs. Autotrophic respiration percentage of total soil respiration data were assessed using the Jenks Natural Breaks Optimization to remove outliers (6% of the data consisting of four negative and ten positive values). Outliers from cumulative CH_4 and N_2O emissions data for 2019 and 2020 were identified using Cook's Distance and removed (1–3 data values). Where necessary for the biomass, GHG, and soil variables, data transformations using the lambda value for the maximum log likelihood for obtaining minimum error sum of squares were conducted to conform data to the assumptions of homogeneous variance and normality of distribution. Non-transformed data were used in the models to calculate least-squares means and standard errors. When significant effects were detected at $p < 0.05$ after using type-III analysis-of-variance (ANOVA), pairwise *post-hoc* comparisons using the Tukey method for p-value adjustment were conducted to compare individual land-use type means. The effect of AFS on tree and deadwood variables was assessed using linear regression and ANOVA. Associations among continuous variables of interest for the woodland were determined using Pearson's parametric correlation and principal components analysis (PCA), the former of which I corrected for the false discovery rate across multiple comparisons using the Benjamini and Hochberg (1995) technique with $\alpha = 0.1$. Specifically, I assessed the relationships among woodland characteristics, soil properties, and various C stocks. All data were analyzed using RStudio Version 1.4.1106 (RStudio Team, 2021).

2.4. Results

2.4.1. Soil properties

Compared with the grassland, the saplings treatment had no effect on any measured soil properties. The cropland had higher soil temperatures than all other land-use types across the three years studied ($p < 0.001$, Fig. A.S5a). In 2018, the cropland had greater soil water content (cm^3 cm^{-3}) relative to the woodland ($p = 0.043$), with a similar but non-significant ($p > 0.05$) trend in 2019 and 2020 (Fig. A.S5c). The cropland also had the greatest bulk density (g cm^{-3}) in all soil depth layers, although these differences were only significant in the 0–10, 10–30, and 50–100 cm mineral soil depth layers ($p \leq 0.001$, Fig. A.S3). The cropland had the lowest pH in soil depth layer 0–10 cm and the highest pH in soil depth layer 50–100 cm ($p \leq 0.007$, Fig. A.S4).

Soil organic C and total N (Mg ha^{-1}) in the litter layer (plant material at various stages of decomposition that overlies the mineral soil, which was absent in the cropland) were almost three times greater in the woodland than the other land-use types ($p = 0.004$, Table 2.1 & Fig. 2.1). The cropland had the lowest SOC and N in all equivalent soil mass (ESM) depth layers, although these differences were only significant in the surface and deep subsoil (ESM depth 0–10 and 50–100 cm, respectively). The woodland contained 1.82 times more SOC than the cropland in the surface soil ($p = 0.045$, Fig. 2.1a) and 1.48 times more N than the cropland in the deep subsoil ($p = 0.017$, Fig. 2.1b). The woodland contained 1.59 and 1.49 times more total SOC and N (to ESM depth 100 cm), respectively, than the cropland, although these differences were not significant ($p = 0.07$).

The woodland and cropland tended to have the highest and lowest WSOC (kg ha^{-1}), respectively, with this pattern reversed for WSN (Fig. 2.2). Total WSN (ESM depth 0–100 cm) was 2.37 times greater in the cropland relative to the woodland ($p = 0.012$, Fig. 2.2b). In contrast, the hedgerow woodland had 2.2 times more total MBC (ESM depth 0–100 cm) than the cropland ($p = 0.011$), and total MBN (ESM depth 0–100 cm) was 1.81–2.15 times greater under perennial vegetation relative to the cropland ($p < 0.001$, Fig. 2.3).

2.4.2. Greenhouse gas emission rates

Trends of annual emissions of GHGs from the soil (~April–October) across land-use types and AFS were generally similar for each year of study (Figs. 4 & S6). Compared with the grassland, the saplings treatment had no effect on emissions of GHGs from the soil (Fig. 2.4). Between 2018 and 2020, CO_2 emissions (total respiration) were 47–57% lower in the cropland and shelterbelt woodland relative to the hedgerow woodland ($p = 0.012$, Fig. 2.4a). Methane uptake was 3.34–5.1 times greater under hedgerow perennial vegetation and shelterbelt grassland relative to the cropland ($p = 0.019$, Fig. 2.4b), while N_2O emissions were 88–91% lower under perennial vegetation relative to the cropland across both AFS ($p < 0.001$, Fig. 2.4c). Cropland N_2O emissions were greatest shortly after fertilizer application during spring seeding, as evidenced by observed emissions in June (Fig. A.S6). Similar to CO_2 emissions, the cropland and shelterbelt woodland had 46–53% lower total GHG emissions (sum of CO_2, CH_4, and N_2O, with the latter two GHGs assessed as CO_2-equivalents) relative to the hedgerow woodland ($p = 0.014$, Fig. 2.4d). Total GHG emissions were largely driven by CO_2, with a minor role of N_2O emissions in the cropland and a negligible role of CH_4 flux.

Autotrophic respiration (measured in 2020) averaged 26% of total respiration and was not affected by land-use type (where only the grassland and woodland were assessed) or AFS (Fig. A.S7). Annual Rh and total GHG emissions (calculated using heterotrophic CO_2) were 53% lower in the shelterbelt woodland relative to the hedgerow woodland ($p \leq 0.015$), while no significant differences ($p > 0.05$) were found between the grassland and woodland land-use types within or across the AFS (Fig. 2.5).

2.4.3. Trees, deadwood, and ecosystem carbon storage

Among sampled woodlands, tree density was greater ($p < 0.001$) in the hedgerows, while DBH was greater ($p < 0.001$) in the shelterbelts (Table 2.2). Total and above- and belowground live tree biomass C (Mg ha^{-1}), tree age, dominant tree height, and vegetation species richness did not differ ($p > 0.05$) between the two AFS (Tables 2.1 & 2.2). Total deadwood C (Mg ha^{-1}) was 17 times greater ($p = 0.044$) in the hedgerow woodland, with the shelterbelt woodland having no coarse downed deadwood and minimal fine downed and snag deadwood (Table 2.1). Within the hedgerow woodland, snag deadwood comprised most of the deadwood C stock (79%), followed by coarse (16%) and fine (4%) downed deadwood (Table 2.1).

Woodlands contained 1.90–2.55 times more total ecosystem C stock (Mg ha^{-1}) than all other land uses ($p < 0.001$), with the shelterbelt and hedgerow woodlands containing 2.09 and 3.03 times more C, respectively, than the adjacent cropland (Table 2.1 & Fig. 2.6). Soil was the largest contributor to total ecosystem C across land uses and AFS (59–99%), and comprised 37% of the difference in total ecosystem C stock between the woodland and cropland. In the hedgerow woodland, soil (to ESM depth 100 cm) comprised 62% of ecosystem C (with 61% in mineral soil and 2% in litter), while live biomass comprised 31% (with 31% in trees and < 1% in herbaceous vegetation) and deadwood comprised 7% (with 5% in snag deadwood and 1% in downed deadwood). In the saplings treatment, sapling biomass contributed negligibly to total ecosystem C (Table 2.1).

2.4.4. Woodland characteristics and carbon stocks and flux

Variation in woodland tree age and density, vegetation species richness, annual Rh, total SOC (to ESM depth 100 cm), live biomass C, and deadwood C stocks among the two AFS was well explained by the first and second principal components axes, which explained 44% and 26%

of the variation among study sites, respectively (Fig. 2.7). The first axis was associated with total SOC and deadwood C stocks, as well as annual Rh, while the second axis was associated with tree density, tree age, and vegetation species richness (Fig. 2.7). Hedgerow and shelterbelt woodlands were clearly separated in the biplot, with minimal overlap of their 95% confidence ellipses (Fig. 2.7). The hedgerow woodland also had far greater variation among study sites than the shelterbelt woodland (Fig. 2.7).

Among the two AFS, tree age in the woodland was positively correlated with aboveground live biomass C stock (Fig. 2.8). Snag deadwood C stock was positively correlated with total SOC stock (to ESM depth 100 cm), total WSOC and MBC stocks (ESM depth 0–100 cm), and annual Rh (Fig. 2.8). Coarse and fine downed deadwood C stocks were positively correlated with surface SOC stock (ESM depth 0–10 cm). Additionally, coarse downed deadwood C stock was positively correlated with total SOC and WSOC stocks, as well as with annual Rh (Fig. 2.8). Total SOC and WSOC stocks were positively correlated, while only the latter was positively correlated with annual Rh (Fig. 2.8).

2.5. Discussion

The substantial amount of additional C stored in woodland relative to cropland and grassland land uses emphasizes the importance of using agroforestry to help meet climate mitigation goals (Shi *et al.*, 2018; Chapman *et al.*, 2020). Nonetheless, the lack of measured effect of the planted saplings relative to the grassland after two years highlights the fact that adding trees to agroecosystems requires a relatively long time frame to increase C stocks (Ma *et al.*, 2020) and could even lead to slight decreases in SOC over the short term (Arevalo *et al.*, 2011), including when trees are added to grassland rather than cropland (Poeplau *et al.*, 2011). Notably, I also found important differences in SOC stocks and C cycling between the two woodland types of the AFS. The rather substantial (albeit non-significant) difference between ecosystem C stocks for the hedgerow and shelterbelt woodlands may reflect a combination of SOC losses following the former cultivation of the now wooded shelterbelts (Poeplau *et al.*, 2011) and, in the hedgerow woodland, both the long-term accumulation of deadwood C and its associated effects on C cycling (Pan *et al.*, 2011; Stokland *et al.*, 2012), as well as the increased protection and storage of SOC over time due to the lack of prior soil disturbance (Lorenz & Lal, 2014; Baah-Acheamfour *et al.*, 2015; Le Bissonnais *et al.*, 2018). The hedgerow woodland also had increased Rh relative to the

shelterbelt woodland, likely reflecting different SOC equilibriums between the two AFS, wherein the hedgerow woodland had greater C inputs (such as from deadwood C) and thus greater C outputs (+321 g C m^{-2} y^{-1} or 10% of the difference in deadwood C stocks between the two AFS) relative to the shelterbelt woodland.

My study is the first to show that deadwood is a potentially important, but previously ignored, component of AFS. Here I show that deadwood C was an important C stock in the hedgerow woodland (35 Mg C ha^{-1} or 7% of ecosystem C) and was positively related to SOC, WSOC, and MBC stocks, as well as annual Rh. Deadwood may enhance soil labile C (such as WSOC), microbial biomass, and, in turn, microbial necromass, potentially explaining its positive relationship with SOC stock and annual Rh (Kaiser & Kalbitz, 2012; Stutz *et al.*, 2017; Liang *et al.*, 2019). For example, dissolved organic C released from decomposing deadwood may become protected through mineral sorption and incorporation into soil aggregates, or it may support soil microbial activity (Stokland *et al.*, 2012; Sandström *et al.*, 2019). I found that the proportion of deadwood C to live biomass C (22%) and total ecosystem C (7%) within the hedgerow woodland was similar to that found in global forests (20% and 8%, respectively) (Pan *et al.*, 2011). Deadwood is not only an important C sink, but also contributes to increased biodiversity in forests (Blaser *et al.*, 2013; Vrška *et al.*, 2015; Sandström *et al.*, 2019), especially concerning fungal communities, which are key to forest C cycling (Lustenhouwer *et al.*, 2020; Seibold *et al.*, 2021; Wang *et al.*, 2021). For instance, the coarse roots of snag deadwood can support substantial microbial communities belowground (Jonsson & Stokland, 2012; Bradford *et al.*, 2021) that also increase SOC stocks (Wang *et al.*, 2021). The contribution of deadwood to total ecosystem C in the hedgerow woodland (particularly snag deadwood, which comprised ~80% of the total deadwood C stock) highlights its potential to affect woodland C cycling and supports the need to include deadwood assessments in future studies of AFS, as does its capacity to enhance biodiversity.

Compared with the cropland, increased mineral surface SOC in the woodland can be attributed to greater above- and belowground C inputs, including through incorporation of C from deadwood and the overlying litter layer, while the tendency for increased deeper SOC may be primarily due to greater root- and microbial-derived C (Gross & Harrison, 2019; Sokol & Bradford, 2019; Sokol *et al.*, 2019). Across all land uses, the subsoil contained nearly half of total SOC (to ~100 cm depth), emphasizing the need to sample deeper soil layers, particularly in AFS (Cardinael *et al.*, 2018). Observed differences in soil bulk density across land uses also underscores

the need to use equivalent soil masses to calculate soil C and N stocks to overcome biases associated with changes in bulk density due to land use activity, such as compaction from agricultural equipment within croplands (von Haden *et al.*, 2020). Soil contributed to over a third of the difference in total ecosystem C stocks between the cropland and woodland, likely due to the combined effect of rapid SOC losses following cultivation and the ongoing accrual of SOC under forest cover (Poeplau *et al.*, 2011; Kim *et al.*, 2016; Ma *et al.*, 2020). However, the small sample size and large variation in SOC among study sites (particularly among hedgerows) prevented me from detecting a significant difference in total SOC stocks across land uses, despite the grassland and woodland containing 1.34 and 1.59 times more SOC than the cropland, respectively. This highlights the importance of using larger sample sizes for field studies examining land use impacts on SOC, particularly for more natural land uses such as hedgerow woodlands, which can vary substantially across a landscape.

Soil was the largest contributor to total ecosystem C stock across land uses and AFS (59–99%), confirming the importance of soils in terrestrial C storage, particularly in Canada (Sothe *et al.*, 2022). Within the woodland, the litter layer (plant material at various stages of decomposition that overlies the mineral soil) contributed only ~2% to total ecosystem C, which is lower than reported in a recent study of AFS in western Canada (Ma *et al.*, 2022), but is similar to a study of shelterbelt AFS in Saskatchewan, Canada (Dhillon & Van Rees, 2017). The amount of C stored in the litter layer is dependent on site-specific variables, such as microenvironmental conditions and tree species (Dhillon & Van Rees, 2017; Joly *et al.*, 2017; Ma *et al.*, 2022), as well as soil macrofauna (Ashton *et al.*, 2005). For example, the Ma *et al.* (2022) study included AFS with evergreen tree species, which may have contributed to decreased litter decomposition rates (Gao *et al.*, 2014; Joly *et al.*, 2017), in turn increasing litter accumulation and associated C stock over time (Dhillon & Van Rees, 2017). Negligible C was stored in the live herbaceous biomass of the woodland (< 1% of total ecosystem C), which is not surprising given the tendency of herbaceous vegetation to produce new growth each year, while about one third of ecosystem C was stored in live tree biomass, similar to the findings of Ma *et al.* (2022). Despite significantly higher tree density in the hedgerow woodland relative to the shelterbelt woodland, live tree biomass C remained similar between the two AFS, probably because larger trees (with greater DBH, like in the shelterbelt woodland) tend to contain the majority of tree biomass C (Mildrexler *et al.*, 2020). I may have underestimated live biomass C in the woodland by not sampling or including shrub

biomass in my estimates, particularly in the hedgerows. However, shrubs contributed to < 1% of woodland ecosystem C stock in the aforementioned study of AFS in western Canada (Ma *et al.*, 2022).

Under perennial vegetation, CH_4 uptake was generally elevated (especially within hedgerows) and N_2O emissions were negligible relative to the cropland. Due to chamber distance from roots (and rhizosphere-stimulated microbial activity) in the cropland, I note that CO_2 emissions (both autotrophic and heterotrophic), CH_4 uptake, and N_2O emissions may have been underestimated (Kelting *et al.*, 1998; Olfs *et al.*, 2018). Nonetheless, installing chambers between crop rows for taller-growing crops is a common practice for gas flux measurements (Olfs *et al.*, 2018). In addition to significantly increased N_2O emissions, the cropland had higher WSN and lower microbial biomass within the subsoil during spring relative to the soils under perennial vegetation, indicating a potential loss of excess N through leaching in the cropland, especially during the spring thaw (Nyborg *et al.*, 1997). The deep-rooting perennial vegetation of AFS can limit cropland N leaching via the uptake of excess N (Wang *et al.*, 2011; Lin *et al.*, 2016), as well as by fostering soil aggregation and the protection of SOC and soil nutrients (Dierks *et al.*, 2021). While the magnitude of impact is dependent on crop distance from perennial vegetation, the retention of additional N and prevention of its leaching within AFS contributes to sustainable agriculture.

Given both the C sequestration and GHG emission mitigation potential of AFS, I recommend the adoption of frameworks that promote the retention and establishment of AFS on agricultural lands across Canada. While AFS establishment increases agroecosystem C storage on decadal timescales, removal of woody vegetation from AFS results in rapid and substantial losses in agroecosystem C storage (Amichev *et al.*, 2020; An *et al.*, 2022). I therefore stress retention of AFS foremost, in accordance with the decision-making framework proposed by Cook-Patton *et al.* (2021). Furthermore, where possible, landowners should be encouraged not to remove deadwood from the woodlands of AFS. As cleared trees and deadwood are usually burned rather than salvaged from agricultural lands (Rudd *et al.*, 2021), thereby releasing the C stored in tree biomass to the atmosphere, retaining deadwood within the woodlands of AFS is essential to avoid reductions in total ecosystem C stocks and help mitigate climate change. Moreover, deadwood enhances biodiversity (Blaser *et al.*, 2013; Vrška *et al.*, 2015; Sandström *et al.*, 2019) and supports healthy soil and ecosystem functions (Stokland *et al.*, 2012; Stutz *et al.*, 2017). Future research

should further explore the relationships between deadwood and both SOC stocks and Rh in forests, including the woodlands of various AFS. For example, the effects of direct manipulations of deadwood within AFS, such as the creation of deadwood on-site from live trees (Sandström *et al.*, 2019), on SOC stocks and Rh would help inform management decisions. Moreover, the benefits of deadwood, such as enhanced biodiversity and soil health, as well as other potential deadwood ecosystem effects, should be quantified in more detail.

2.6. Conclusions

I conclude that AFS are important for fostering C sequestration and reducing GHG emissions. In particular, retaining hedgerows (legacy woodland) and their associated deadwood across temperate agroecosystems is key to help mitigate climate change. I highlight important differences between two common agroforestry woodlands, namely the greater deadwood and soil C stocks, as well as increased Rh, within hedgerows. As such, deadwood C (which contributed substantially to hedgerow woodland ecosystem C stock) should be quantified in future assessments of forest C stocks, including among AFS. Further investigating the ecological importance of deadwood within AFS will enhance our understanding of these systems and the services they provide to society. With the urgent need to address climate change and governments globally committing resources to reduce GHG emissions and increase C sequestration, I recommend incentivizing the retention and establishment of AFS on agricultural lands as an important step to help meet climate change mitigation goals.

Funding: This research was supported by a grant (AGGP2-039) from the Agricultural Greenhouse Gas Program from Agriculture and Agri-Food Canada to S.X.C., E.W.B., and C.N.C., as well as by a Doctoral Vanier Scholarship and a Killam Memorial Graduate Scholarship to C.D.G.

Credit: S.X.C., E.W.B., C.N.C., and C.D.G.: Conceptualization and Methodology. C.D.G.: Investigation and Writing—original draft. C.D.G., S.X.C., E.W.B., and C.N.C.: Writing—review and editing. S.X.C. and E.W.B.: Resources and Supervision.

Acknowledgements: I express my gratitude to the landowners and farmers for their generosity, assistance, and cooperation throughout the duration of the study. A special thank you to the many

researchers who have assisted with this work, especially Michael Carson, Jonathan Tieu, Mary Villeneuve, Sheetal Patel, Guanyu Chen, Maliha Rahman, and Carmen C. Roman-Perez for their help in the field and/or lab.

2.7. References

Alberta Climate Information Service (2021) Alberta Agriculture and Forestry.

Amichev BY, Bentham MJ, Kulshreshtha SN, Laroque CP, Piwowar JM, Van Rees KCJ (2016) Carbon sequestration and growth of six common tree and shrub shelterbelts in Saskatchewan, Canada. *Canadian Journal of Soil Science*, **97**, 368–381.

Amichev BY, Laroque CP, Van Rees KCJ (2020) Shelterbelt removals in Saskatchewan, Canada: implications for long-term carbon sequestration. *Agroforestry Systems*, **94**, 1665–1680.

An Z, Bork EW, Duan X, Gross CD, Carlyle CN, Chang SX (2022) Quantifying past, current, and future forest carbon stocks within agroforestry systems in central Alberta, Canada. *GCB Bioenergy*, **14**, 669–680.

Arevalo CBM, Bhatti JS, Chang SX, Sidders D (2011) Land use change effects on ecosystem carbon balance: From agricultural to hybrid poplar plantation. *Agriculture, Ecosystems and Environment*, **141**, 342–349.

Ashton IW, Hyatt LA, Howe KM, Gurevitch J, Lerdau MT (2005) Invasive species accelerate decomposition and litter nitrogen loss in a mixed deciduous forest. *Ecological Applications*, **15**, 1263–1272.

Baah-Acheamfour M, Chang SX, Carlyle CN, Bork EW (2015) Carbon pool size and stability are affected by trees and grassland cover types within agroforestry systems of western Canada. *Agriculture, Ecosystems and Environment*, **213**, 105–113.

Baah-Acheamfour M, Carlyle CN, Lim S, Bork EW, Chang SX (2016) Forest and grassland cover types reduce net greenhouse gas emissions from agricultural soils. *Science of The Total Environment*, **571**, 1115–1127.

Baah-Acheamfour M, Carlyle CN, Bork EW, Chang SX (2020) Forest and perennial herbland cover reduce microbial respiration but increase root respiration in agroforestry systems. *Agricultural and Forest Meteorology*, **280**, 107790.

Beck T, Joergensen RG, Kandeler E, Makeshin E, Nuss E, Oberholzer HR, Scheu S (1997) An

inter-laboratory comparison of ten different ways of measuring soil microbial biomass C. *Soil Biology & Biochemistry*, **29**, 1023–1032.

Benjamini Y, Hochberg Y (1995) Controlling the false discovery rate: A practical and powerful approach to multiple testing. *Journal of the Royal Statistical Society*, **57**, 289–300.

Le Bissonnais Y, Prieto I, Roumet C et al. (2018) Soil aggregate stability in Mediterranean and tropical agro-ecosystems: effect of plant roots and soil characteristics. *Plant and Soil*, **424**, 303–317.

Blaser S, Prati D, Senn-Irlet B, Fischer M (2013) Effects of forest management on the diversity of deadwood-inhabiting fungi in Central European forests. *Forest Ecology and Management*, **304**, 42–48.

Bradford MA, Maynard DS, Crowther TW et al. (2021) Belowground community turnover accelerates the decomposition of standing dead wood. *Ecology*, **102**, 1–13.

Cardinael R, Guenet B, Chevallier T, Dupraz C, Cozzi T, Chenu C (2018) High organic inputs explain shallow and deep SOC storage in a long-term agroforestry system - Combining experimental and modeling approaches. *Biogeosciences*, **15**, 297–317.

Chantigny MH, Angers DA, Kaiser K, Kalbitz K (2007) Extraction and characterization of dissolved organic matter. In: *Soil Sampling and Methods of Analysis*, 2nd edn (eds Carter MR, Gregorich EG), pp. 617–635. CRC Press, Boca Raton.

Chapman M, Walker WS, Cook-Patton SC, Ellis PW, Farina M, Griscom BW, Baccini A (2020) Large climate mitigation potential from adding trees to agricultural lands. *Global Change Biology*, **26**, 4357–4365.

Christiansen JR, Korhonen JFJ, Juszczak R, Giebels M, Pihlatie M (2011) Assessing the effects of chamber placement, manual sampling and headspace mixing on CH4 fluxes in a laboratory experiment. *Plant and Soil*, **343**, 171–185.

Ciais P, Sabine C, Bala G et al. (2013) Carbon and other biogeochemical cycles. In: *Climate Change 2013: The Physical Science Basis. Contribution of Working Group I to the Fifth Assessment Report of the Intergovernmental Panel on Climate Change* (eds Stocker TF, Qin D, Plattner G-K, Tignor M, Allen SK, Boschung J, Nauels A, Xia Y, Bex V, Midgley PM), pp. 465–570. Cambridge University Press, Cambridge, United Kingdom and New York, NY, USA.

Cook-Patton SC, Drever CR, Griscom BW et al. (2021) Protect, manage and then restore lands

for climate mitigation. *Nature Climate Change*, **11**, 1027–1034.

Datta R, Vranová V, Pavelka M, Rejšek K, Formánek P (2014) Effect of soil sieving on respiration induced by low-molecular-weight substrates. *International Agrophysics*, **28**, 119–124.

Dhillon GS, Van Rees KCJ (2017) Soil organic carbon sequestration by shelterbelt agroforestry systems in Saskatchewan. *Canadian Journal of Soil Science*, **97**, 394–409.

Dierks J, Blaser-Hart WJ, Gamper HA, Nyoka IB, Barrios E, Six J (2021) Trees enhance abundance of arbuscular mycorrhizal fungi, soil structure, and nutrient retention in low-input maize cropping systems. *Agriculture, Ecosystems and Environment*, **318**, 107487.

Drexler S, Gensior A, Don A (2021) Carbon sequestration in hedgerow biomass and soil in the temperate climate zone. *Regional Environmental Change*, **21**, 1–14.

Ellert BH, Bettany JR (1995) Calculation of organic matter and nutrients stored in soils under contrasting management regimes. *Canadian Journal of Soil Science*, **75**, 529–538.

Feliciano D, Ledo A, Hillier J, Nayak DR (2018) Which agroforestry options give the greatest soil and above ground carbon benefits in different world regions? *Agriculture, Ecosystems and Environment*, **254**, 117–129.

Forster P, Storelvmo T, Armour K et al. (2021) The Earth's energy budget, climate feedbacks, and climate sensitivity. In: *Climate Change 2021: The Physical Science Basis. Contribution of Working Group I to the Sixth Assessment Report of the Intergovernmental Panel on Climate Change* (eds Masson-Delmotte V, Zhai P, Pirani A, Connors SL, Péan C, Berger S, Caud N, Chen Y, Goldfarb L, Gomis MI, Huang M, Leitzell K, Lonnoy E, Matthews JBR, Maycock KT, Waterfield T, Yelekçi O, Yu R, Zhou B), p. In Press. Cambridge University Press.

Gao Y, Cheng J, Ma Z, Zhao Y, Su J (2014) Carbon storage in biomass, litter, and soil of different plantations in a semiarid temperate region of northwest China. *Annals of Forest Science*, **71**, 427–435.

Gross CD, Harrison RB (2019) The case for digging deeper: Soil organic carbon storage, dynamics, and controls in our changing world. *Soil Systems*, **3**, 28.

Gross CD, Bork EW, Carlyle CN, Chang SX (2022) Biochar and its manure-based feedstock have divergent effects on soil organic carbon and greenhouse gas emissions in croplands. *Science of The Total Environment*, **806**, 151337.

von Haden AC, Yang WH, DeLucia EH (2020) Soils' dirty little secret: Depth-based comparisons can be inadequate for quantifying changes in soil organic carbon and other mineral soil properties. *Global Change Biology*, **26**, 3759–3770.

Haney RL, Franzluebbers AJ, Hons FM, Hossner LR, Zuberer DA (2001) Molar concentration of K2SO4 and soil pH affect estimation of extractable C with chloroform fumigation-extraction. *Soil Biology and Biochemistry*, **33**, 1501–1507.

Harmon ME, Woodall CW, Fasth B, Sexton J (2008) Woody detritus density and density reduction factors for tree species in the United States: A synthesis. *USDA General Technical Report NRS-29. USDA Forest Service Northern Research Station*, 84.

Horwath WR, Paul EA (1994) Microbial biomass. In: *Methods of Soil Analysis: Part 2—Microbiological and Biochemical Properties, SSSA Book Series no. 5* (eds Bottomley PS, Angle JS, Weaver RW), pp. 753–774. Soil Science Society of America, Madison.

Hüppi R, Felber R, Krauss M, Six J, Leifeld J, Fuß R (2018) Restricting the nonlinearity parameter in soil greenhouse gas flux calculation for more reliable flux estimates. *PLoS ONE*, **13**, 1–17.

IPCC (2019) *Climate Change and Land: An IPCC special report on climate change, desertification, land degradation, sustainable land management, food security, and greenhouse gas fluxes in terrestrial ecosystems [P.R. Shukla, J. Skea, E. Calvo Buendia, V. Masson-Delmot*. Geneva, Switzerland, 896 pp.

Jandl R, Rodeghiero M, Martinez C et al. (2014) Current status, uncertainty and future needs in soil organic carbon monitoring. *Science of the Total Environment*, **468**–**469**, 376–383.

Jenkinson DS, Brookes PC, Powlson DS (2004) Measuring soil microbial biomass. *Soil Biology and Biochemistry*, **36**, 5–7.

Joly FX, Milcu A, Scherer-Lorenzen M et al. (2017) Tree species diversity affects decomposition through modified micro-environmental conditions across European forests. *New Phytologist*, **214**, 1281–1293.

Jonsson BG, Stokland JN (2012) The surrounding environment. In: *Biodiversity in Dead Wood*, pp. 194–217. Cambridge University Press, Cambridge.

Kaiser K, Kalbitz K (2012) Cycling downwards - dissolved organic matter in soils. *Soil Biology and Biochemistry*, **52**, 29–32.

Kelting DL, Burger JA, Edwards GS (1998) Estimating root respiration, microbial respiration in

the rhizosphere, and root-free soil respiration in forest soils. *Soil Biology and Biochemistry*, **30**, 961–968.

Kim DG, Kirschbaum MUF, Beedy TL (2016) Carbon sequestration and net emissions of CH4 and N2O under agroforestry: Synthesizing available data and suggestions for future studies. *Agriculture, Ecosystems and Environment*, **226**, 65–78.

Kort J, Turnock R (1998) Carbon reservoir and biomass in Canadian prairie shelterbelts. *Agroforestry Systems*, **44**, 175–186.

Kreitzman M, Eyster H, Mitchell M et al. (2022) Woody perennial polycultures in the U.S. Midwest enhance biodiversity and ecosystem functions. *Ecosphere*, **13**, 1–35.

Lal R (2004) Soil carbon sequestration impacts on global climate change and food security. *Science*, **304**, 1623–1627.

Lee J, Hopmans JW, Rolston DE, Baer SG, Six J (2009) Determining soil carbon stock changes: Simple bulk density corrections fail. *Agriculture, Ecosystems and Environment*, **134**, 251–256.

Li Z, Kurz WA, Apps MJ, Beukema SJ (2003) Belowground biomass dynamics in the Carbon Budget Model of the Canadian Forest Sector: Recent improvements and implications for the estimation of NPP and NEP. *Canadian Journal of Forest Research*, **33**, 126–136.

Liang C, Amelung W, Lehmann J, Kästner M (2019) Quantitative assessment of microbial necromass contribution to soil organic matter. *Global Change Biology*, **25**, 3578–3590.

Lin HC, Huber JA, Gerl G, Hülsbergen KJ (2016) Nitrogen balances and nitrogen-use efficiency of different organic and conventional farming systems. *Nutrient Cycling in Agroecosystems*, **105**, 1–23.

Lorenz K, Lal R (2014) Soil organic carbon sequestration in agroforestry systems. A review. *Agronomy for Sustainable Development*, **34**, 443–454.

Lustenhouwer N, Maynard DS, Bradford MA, Lindner DL, Oberle B, Zanne AE, Crowther TW (2020) A trait-based understanding of wood decomposition by fungi. *Proceedings of the National Academy of Sciences of the United States of America*, **117**, 11551–11558.

Ma S, He F, Tian D et al. (2018) Variations and determinants of carbon content in plants: A global synthesis. *Biogeosciences*, **15**, 693–702.

Ma Z, Chen HYH, Bork EW, Carlyle CN, Chang SX (2020) Carbon accumulation in agroforestry systems is affected by tree species diversity, age and regional climate: A global

meta-analysis. *Global Ecology and Biogeography*, **29**, 1817–1828.

Ma Z, Bork EW, Carlyle CN, Tieu J, Gross CD, Chang SX (2022) Carbon stocks differ among land-uses in agroforestry systems in western Canada. *Agricultural and Forest Meteorology*, **313**, 108756.

Mayer S, Wiesmeier M, Sakamoto E, Hübner R, Cardinael R, Kühnel A, Kögel-Knabner I (2022) Soil organic carbon sequestration in temperate agroforestry systems – A meta-analysis. *Agriculture, Ecosystems and Environment*, **323**.

Mayrinck RC, Laroque CP, Amichev BY, Van Rees K (2019) Above- and below-ground carbon sequestration in shelterbelt trees in Canada: A review. *Forests*, **10**, 1–17.

Meinshausen M, Meinshausen N, Hare W et al. (2009) Greenhouse-gas emission targets for limiting global warming to 2°C. *Nature*, **458**, 1158–1162.

Mildrexler DJ, Berner LT, Law BE, Birdsey RA, Moomaw WR (2020) Large trees dominate carbon storage in forests east of the Cascade Crest in the United States Pacific Northwest. *Frontiers in Forests and Global Change*, **3**, 1–15.

Minasny B, Malone BP, McBratney AB et al. (2017) Soil carbon 4 per mille. *Geoderma*, **292**, 59–86.

Nair PKR (2012) Carbon sequestration studies in agroforestry systems: A reality-check. *Agroforestry Systems*, **86**, 243–253.

Nyborg M, Laidlaw JW, Solberg ED, Malhi SS (1997) Denitrification and nitrous oxide emissions from a black chernozemic soil during spring thaw in Alberta. *Canadian Journal of Soil Science*, **77**, 153–160.

Olfs HW, Westerschulte M, Ruoss N et al. (2018) A new chamber design for measuring nitrous oxide emissions in maize crops. *Journal of Plant Nutrition and Soil Science*, **181**, 69–77.

Pan Y, Birdsey RA, Fang J et al. (2011) A large and persistent carbon sink in the world's forests. *Science*, **333**, 988–993.

Paustian K, Lehmann J, Ogle S, Reay D, Robertson GP, Smith P (2016) Climate-smart soils. *Nature*, **532**, 49–57.

Poeplau C, Don A, Vesterdal L, Leifeld J, Van Wesemael B, Schumacher J, Gensior A (2011) Temporal dynamics of soil organic carbon after land-use change in the temperate zone - carbon response functions as a model approach. *Global Change Biology*, **17**, 2415–2427.

Ramnarine R, Voroney RP, Wagner-Riddle C, Dunfield KE (2011) Carbonate removal by acid

fumigation for measuring the δ13C of soil organic carbon. *Canadian Journal of Soil Science*, **91**, 247–250.

RStudio Team (2021) *RStudio: Integrated Development Environment for R*. Boston, MA.

Rudd L, Kulshreshtha S, Belcher K, Amichev B (2021) Carbon life cycle assessment of shelterbelts in Saskatchewan, Canada. *Journal of Environmental Management*, **297**, 113400.

Sandström J, Bernes C, Junninen K, Lõhmus A, Macdonald E, Müller J, Jonsson BG (2019) Impacts of dead wood manipulation on the biodiversity of temperate and boreal forests. A systematic review. *Journal of Applied Ecology*, **56**, 1770–1781.

Seibold S, Rammer W, Hothorn T et al. (2021) The contribution of insects to global forest deadwood decomposition. *Nature*, **597**, 77–81.

Shi L, Feng W, Xu J, Kuzyakov Y (2018) Agroforestry systems: Meta-analysis of soil carbon stocks, sequestration processes, and future potentials. *Land Degradation & Development*, **29**, 1–12.

Shrestha BM, Chang SX, Bork EW, Carlyle CN (2018) Enrichment planting and soil amendments enhance carbon sequestration and reduce greenhouse gas emissions in agroforestry systems: A review. *Forests*, **9**, 1–18.

Sokol NW, Bradford MA (2019) Microbial formation of stable soil carbon is more efficient from belowground than aboveground input. *Nature Geoscience*, **12**, 46–53.

Sokol NW, Kuebbing SE, Karlsen-Ayala E, Bradford MA (2019) Evidence for the primacy of living root inputs, not root or shoot litter, in forming soil organic carbon. *New Phytologist*, **221**, 233–246.

Sothe C, Gonsamo A, Arabian J, Kurz WA, Finkelstein SA, Snider J (2022) Large soil carbon storage in terrestrial ecosystems of Canada. *Global Biogeochemical Cycles*, 1–18.

Statistics Canada Census of Agriculture (2008) *Census of Agriculture for Alberta, 2006*. 1–13 pp.

Stokland JN, Siitonen J, Jonsson BG (2012) *Biodiversity in Dead Wood*. Cambridge University Press, Cambridge.

Stutz KP, Dann D, Wambsganss J, Scherer-Lorenzen M, Lang F (2017) Phenolic matter from deadwood can impact forest soil properties. *Geoderma*, **288**, 204–212.

Teissier Du Cros R, Lopez S (2009) Preliminary study on the assessment of deadwood volume

by the French national forest inventory. *Annals of Forest Science*, **66**, 1–10.

Thiagarajan A, Fan J, McConkey BG, Janzen HH, Campbell CA (2018) Dry matter partitioning and residue N content for 11 major field crops in Canada adjusted for rooting depth and yield. *Canadian Journal of Soil Science*, **98**, 574–579.

UNFCCC (2015) *Measurements for Estimation of Carbon Stocks in Afforestation and Reforestation Project Activities under the Clean Development Mechanism: A Field Manual*. 72 pp.

Vance ED, Brookes PC, Jenkinson DS (1987) An extraction method for measuring soil microbial biomass C. *Soil Biology and Biochemistry*, **19**, 703–707.

Venterea RT, Burger M, Spokas KA (2005) Nitrogen oxide and methane emissions under varying tillage and fertilizer management. *Journal of Environment Quality*, **34**, 1467.

Vrška T, Přívětivý T, Janík D, Unar P, Šamonil P, Král K (2015) Deadwood residence time in alluvial hardwood temperate forests - A key aspect of biodiversity conservation. *Forest Ecology and Management*, **357**, 33–41.

Walthert L, Graf U, Kammer A, Luster J, Pezzotta D, Zimmermann S, Hagedorn F (2010) Determination of organic and inorganic carbon, δ13C, and nitrogen in soils containing carbonates after acid fumigation with HCl. *Journal of Plant Nutrition and Soil Science*, **173**, 207–216.

Wang Y, Zhang B, Lin L, Zepp H (2011) Agroforestry system reduces subsurface lateral flow and nitrate loss in Jiangxi Province, China. *Agriculture, Ecosystems and Environment*, **140**, 441–453.

Wang B, An S, Liang C, Liu Y, Kuzyakov Y (2021) Microbial necromass as the source of soil organic carbon in global ecosystems. *Soil Biology and Biochemistry*, **162**, 108422.

Wendt JW, Hauser S (2013) An equivalent soil mass procedure for monitoring soil organic carbon in multiple soil layers. *European Journal of Soil Science*, **64**, 58–65.

Xing D, Bergeron JAC, Solarik KA, Tomm B, Macdonald SE, Spence JR, He F (2019) Challenges in estimating forest biomass: Use of allometric equations for three boreal tree species. *Canadian Journal of Forest Research*, **49**, 1613–1622.

Zomer RJ, Bossio DA, Sommer R, Verchot L V. (2017) Global sequestration potential of increased organic carbon in cropland soils. *Scientific Reports*, **7**, 1–8.

Zsolnay Á (2003) Dissolved organic matter: Artefacts, definitions, and functions. *Geoderma*,

113, 187–209.

2.8. Tables

Table 2.1. Carbon stocks (Mg ha^{-1}) in various components among the different land uses of two agroforestry systems in central Alberta, Canada (n = 10). Least-squares means (one standard error) within each component accompanied by different lowercase letters are significantly different (Tukey-adjusted, $\alpha = 0.05$) among the land-use types and agroforestry systems. Main components are in bold, followed by subcomponents; when subcomponents are further broken down, these sub-subcomponents are in italics.

Component	Hedgerow				Shelterbelt			
	Cropland	Grassland	Saplings*	Woodland	Cropland	Grassland	Saplings*	Woodland
Live biomass†	3.84 (15.85) b	3.16 (15.85) b	4.73 (15.85) b	161.99 (15.85) a	4.53 (15.85) b	3.28 (15.85) b	2.45 (15.85) b	153.61 (15.85) a
Trees	na‡	na	0.13 (0.04)	160.69 (31.59)	na	na	0.13 (0.04)	152.47 (31.59)
Aboveground	na	na	0.01 (0.01)	125.79 (26.03)	na	na	0.01 (0.01)	129.42 (26.03)
Belowground	na	na	0.12 (0.03)	34.90 (6.49)	na	na	0.11 (0.03)	23.05 (6.49)
Herbaceous†	3.84 (0.83) a	3.16 (0.83) a	4.59 (0.83) a	1.30 (0.83) b	4.53 (0.83) a	3.28 (0.83) a	2.32 (0.83) a	1.14 (0.83) b
Aboveground†	3.12 (0.61) a	1.69 (0.61) a	2.47 (0.61) a	0.70 (0.61) b	3.78 (0.61) a	1.77 (0.61) a	1.24 (0.61) a	0.61 (0.61) b
Belowground†	0.73 (0.27) b	1.46 (0.27) a	2.13 (0.27) a	0.61 (0.27) b	0.75 (0.27) b	1.51 (0.27) a	1.08 (0.27) a	0.52 (0.27) b
Deadwood	na	na	na	34.99 (10.22) a	na	na	na	2.06 (10.22) b
Snag	na	na	na	27.77 (8.99)	na	na	na	1.65 (8.99)
Downed	na	na	na	7.22 (1.77) a	na	na	na	0.41 (1.77) b
Coarse	na	na	na	5.67 (1.35)	na	na	na	na
Fine	na	na	na	1.55 (0.52)	na	na	na	0.41 (0.52)
Soil	168.30 (57.01)	276.71 (57.01)	256.17 (57.01)	324.95 (57.01)	175.96 (57.01)	184.99 (57.01)	210.36 (57.01)	221.29 (57.01)
Litter†	na	2.68 (2.74) b	3.21 (2.74) b	9.16 (2.74) a	na	5.28 (2.74) b	4.62 (2.74) b	11.17 (2.74) a
Mineral	168.30 (56.35)	274.03 (56.35)	252.97 (56.35)	315.79 (56.35)	175.96 (56.35)	179.71 (56.35)	205.74 (56.35)	210.11 (56.35)
Total†	172.15 (64.85) b	279.86 (64.85) b	260.90 (64.85) b	521.93 (64.85) a	180.49 (64.85) b	188.27 (64.85) b	212.81 (64.85) b	376.96 (64.85) a

* Saplings were not included in tree biomass tests. † Only land-use type was significant. ‡ na indicates that the component was not present within the given land-use type.

Table 2.2. Characteristics of the woodlands within two agroforestry systems in central Alberta, Canada (n = 10). Least-squares means (one standard error) within each row accompanied by different lowercase letters are significantly different (Tukey-adjusted, $\alpha = 0.05$) between agroforestry systems. DBH, diameter at breast height.

	Hedgerow	Shelterbelt
Tree age (years)*	26.60 (2.77)	28.60 (2.77)
Tree density (tree ha^{-1})	7533 (775) a	1200 (775) b
DBH (cm)	9.57 (2.23) b	29.10 (2.23) a
Tree height (m)*	11.33 (1.72)	10.40 (1.72)
Species richness†	11.40 (2.44)	7.20 (2.44)
Tree species	*Populus tremuloides*, *Populus balsamifera*	*Salix pentandra*, *Populus balsamifera*

* Dominant tree age and height (n = 3). † Includes over-, mid-, and understory.

2.9. Figures

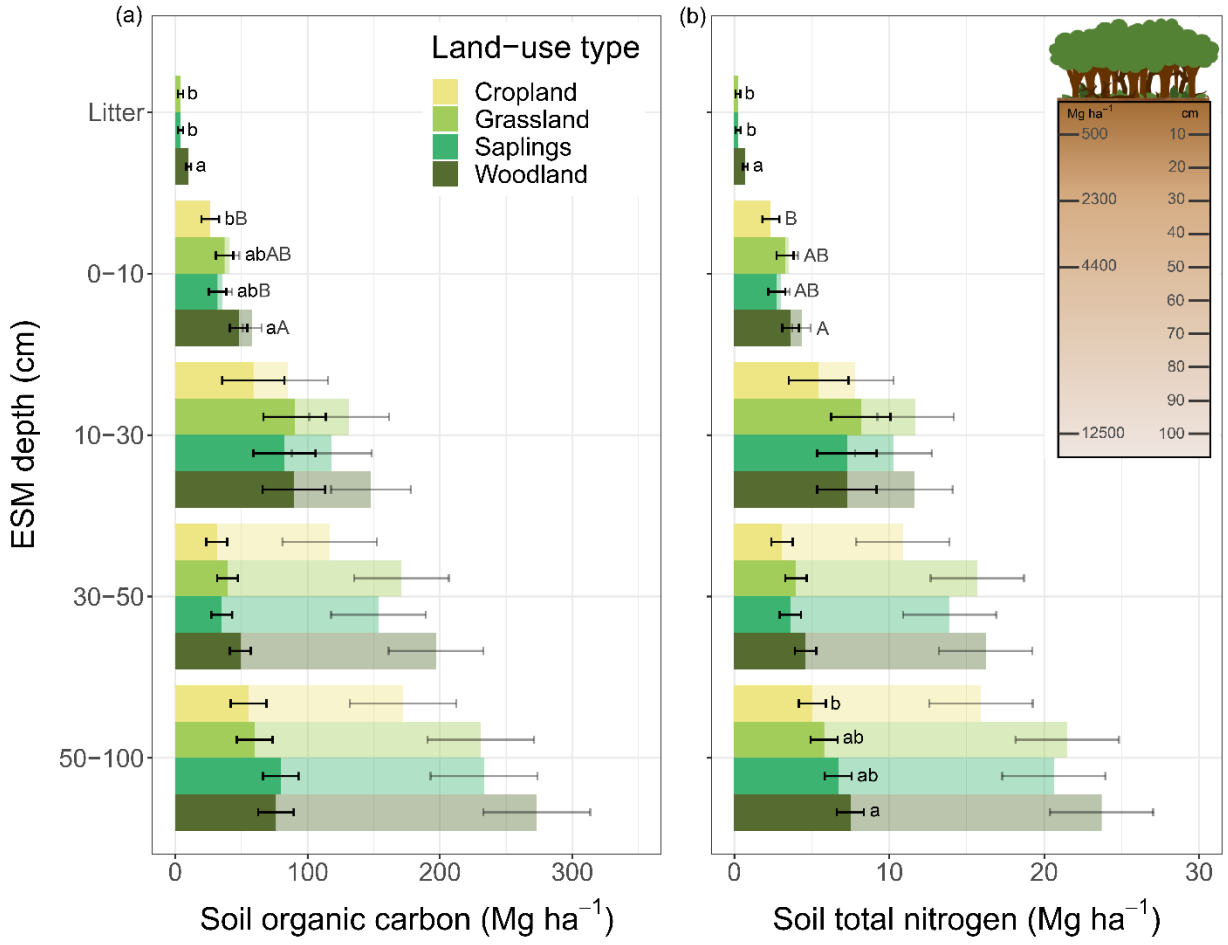

Figure 2.1. Soil (a) organic carbon and (b) total nitrogen stocks among the different land uses of two agroforestry systems in central Alberta, Canada (n = 10). Transparent columns are cumulative stocks based on equivalent soil mass (ESM). Error bars represent ± one standard error. Least-squares means within each ESM depth layer or total cumulative mass accompanied by different lowercase and uppercase letters, respectively, are significantly different (Tukey-adjusted, $\alpha = 0.05$) among the land-use types. The soil profile illustrates the relationship between soil mass and approximate sampling depth within the reference soil (hedgerow woodland).

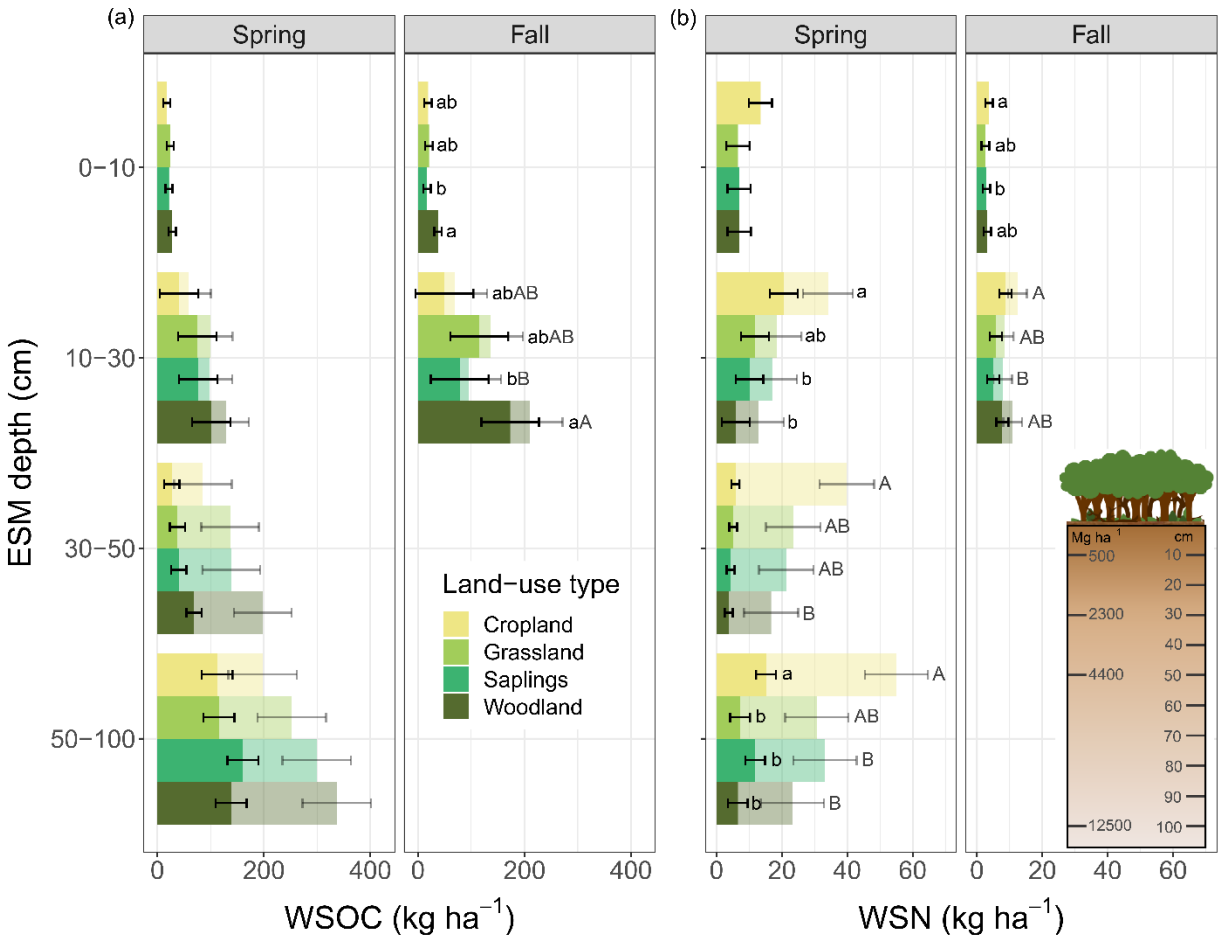

Figure 2.2. Soil water-soluble (a) organic carbon (WSOC) and (b) total nitrogen (WSN) stocks among the different land uses of two agroforestry systems in central Alberta, Canada (n = 10). Transparent columns are cumulative stocks based on equivalent soil mass (ESM). Error bars represent ± one standard error. Least-squares means within each ESM depth layer or total cumulative mass accompanied by different lowercase and uppercase letters, respectively, are significantly different (Tukey-adjusted, $\alpha = 0.05$) among the land-use types. The soil profile illustrates the relationship between soil mass and approximate sampling depth within the reference soil (hedgerow woodland).

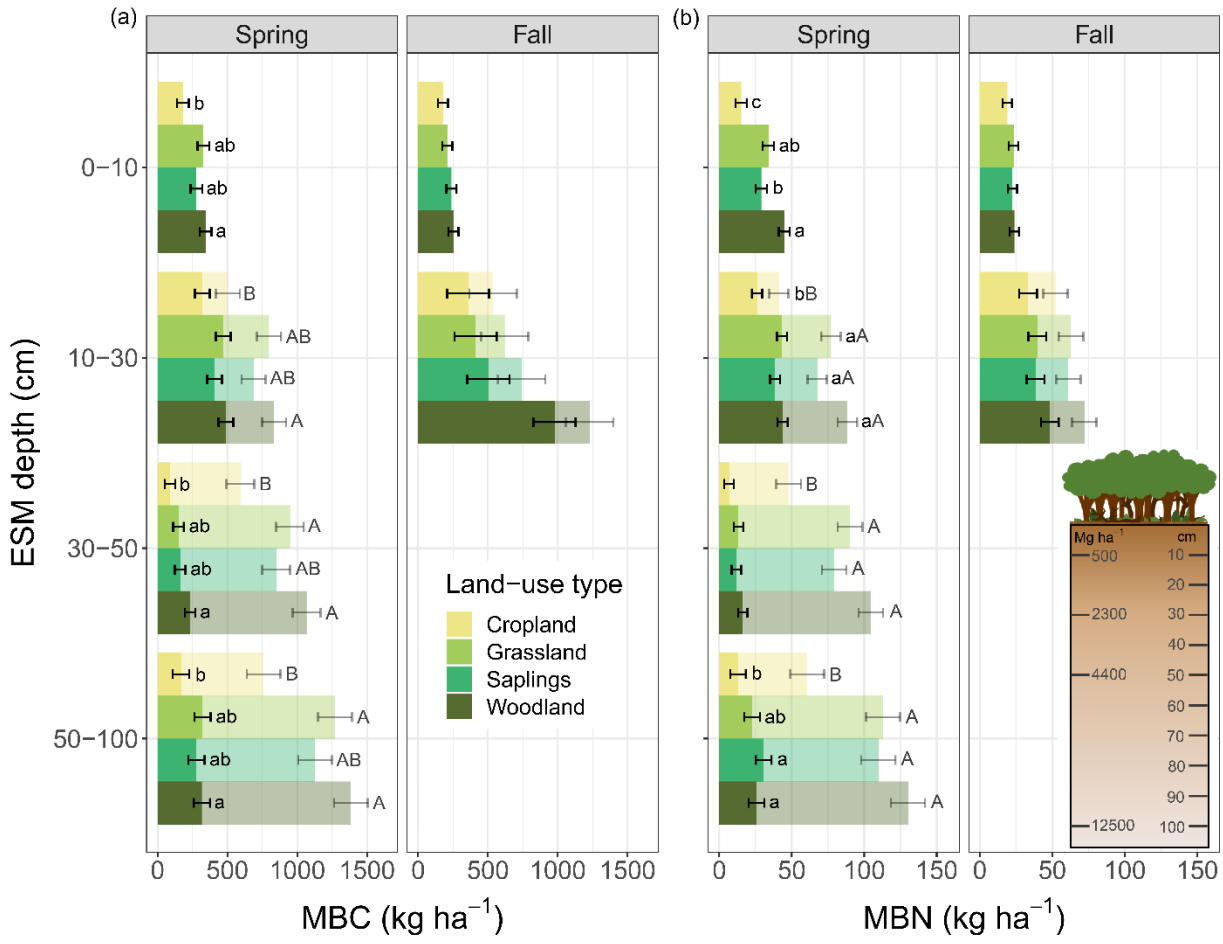

Figure 2.3. Soil microbial biomass (a) carbon (MBC) and (b) nitrogen (MBN) stocks among the different land uses of two agroforestry systems in central Alberta, Canada (n = 10). Transparent columns are cumulative stocks based on equivalent soil mass (ESM). Error bars represent ± one standard error. Least-squares means within each ESM depth layer or total cumulative mass accompanied by different lowercase and uppercase letters, respectively, are significantly different (Tukey-adjusted, α = 0.05) among the land-use types. The soil profile illustrates the relationship between soil mass and approximate sampling depth within the reference soil (hedgerow woodland).

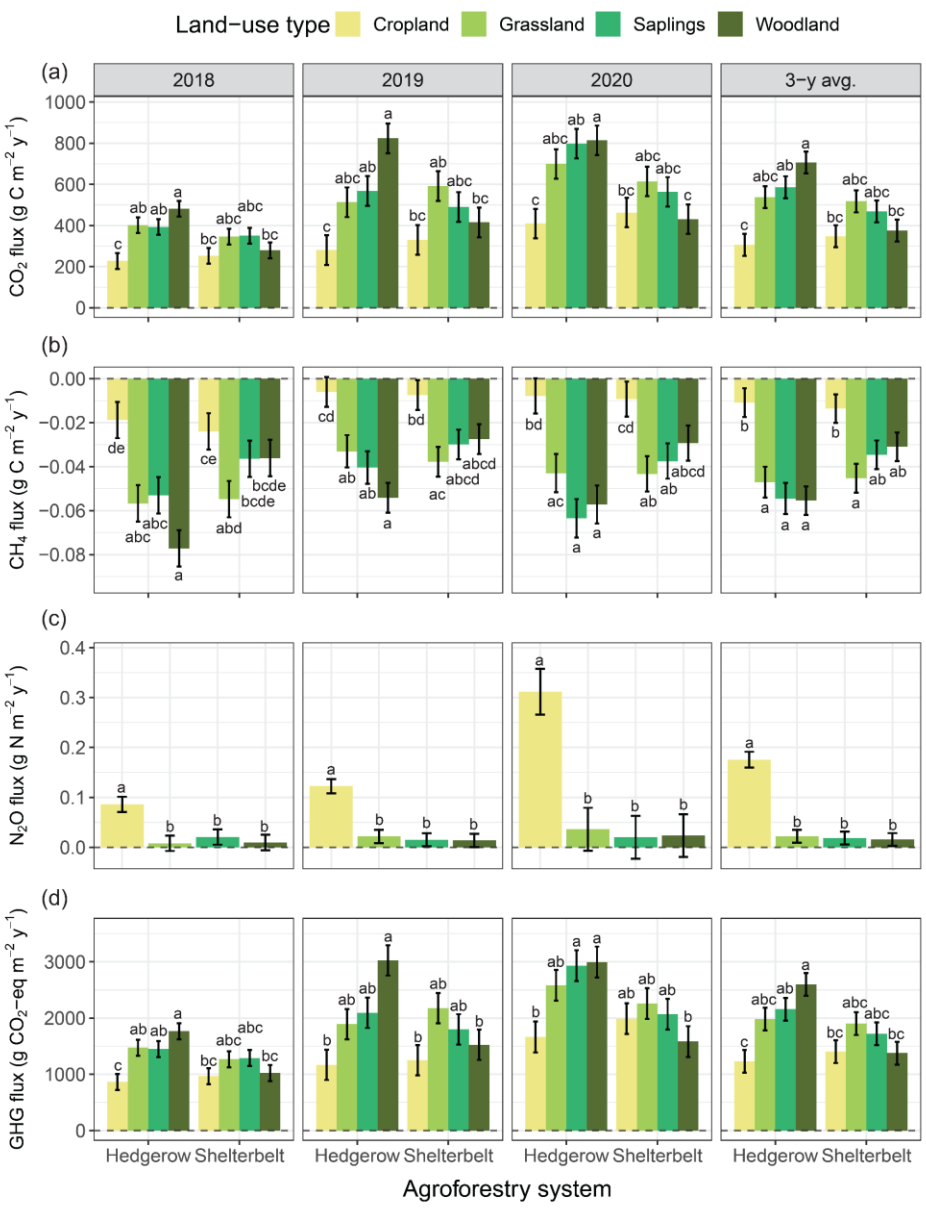

Figure 2.4. Soil (a) carbon dioxide (CO_2), (b) methane (CH_4), (c) nitrous oxide (N_2O), and (d) total greenhouse gas (GHG; sum of CO_2, CH_4, and N_2O) fluxes by year (~April–October) among the different land uses of two agroforestry systems in central Alberta, Canada (n = 10). Error bars represent ± one standard error. Least-squares means within each year accompanied by different lowercase letters are significantly different (Tukey-adjusted, $\alpha = 0.05$) among the land-use types and agroforestry systems. Note that CO_2 (and GHG) flux includes autotrophic respiration.

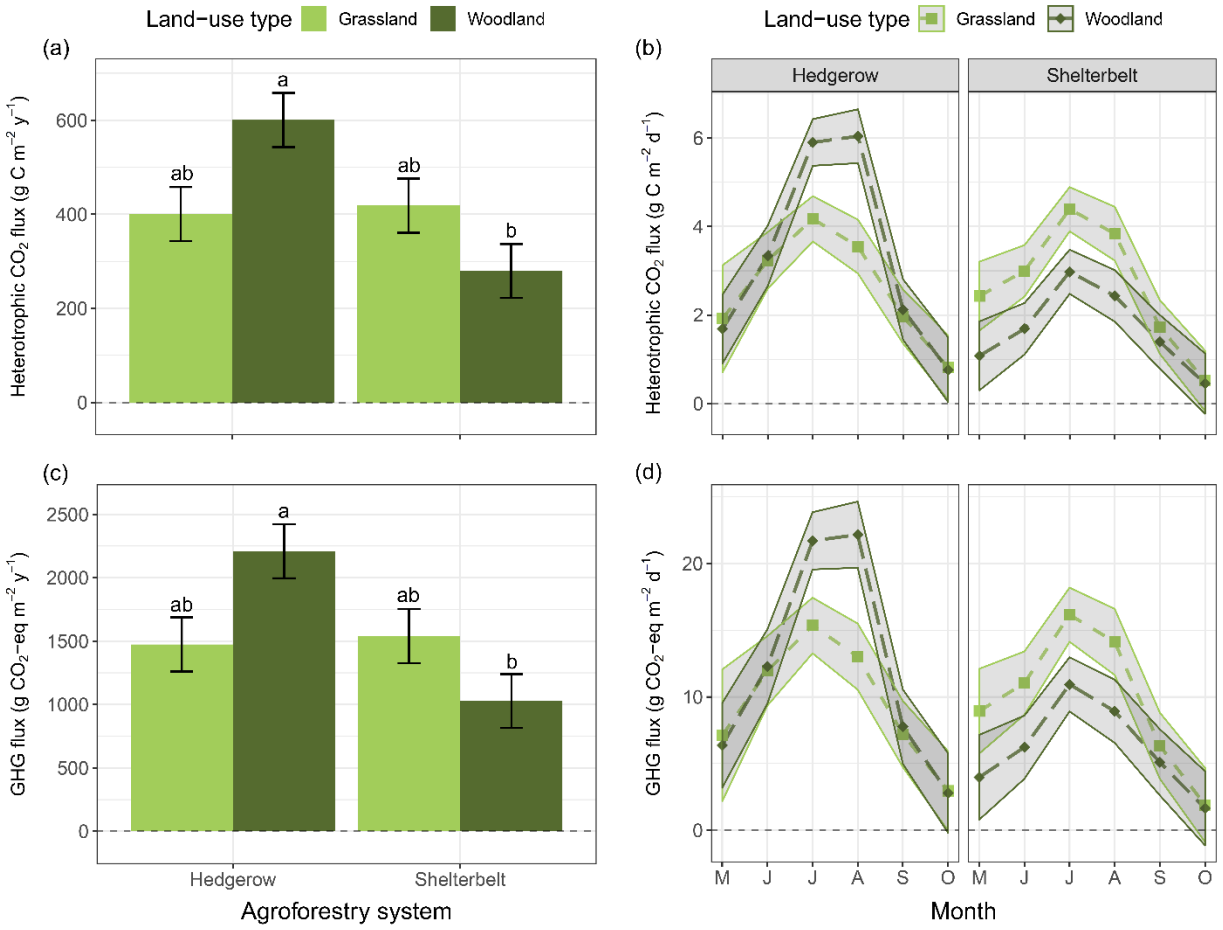

Figure 2.5. Soil heterotrophic carbon dioxide (CO_2) flux (or heterotrophic respiration) by (a) year (2020) and (b) month, and total greenhouse gas (GHG; sum of heterotrophic CO_2, CH_4, and N_2O) flux by (c) year (2020) and (d) month, among the grassland and woodland land uses of two agroforestry systems in central Alberta, Canada (n = 10). Error bars and ribbons represent ± one standard error. Least-squares means by year accompanied by different lowercase letters are significantly different (Tukey-adjusted, α = 0.05) among the land-use types and agroforestry systems.

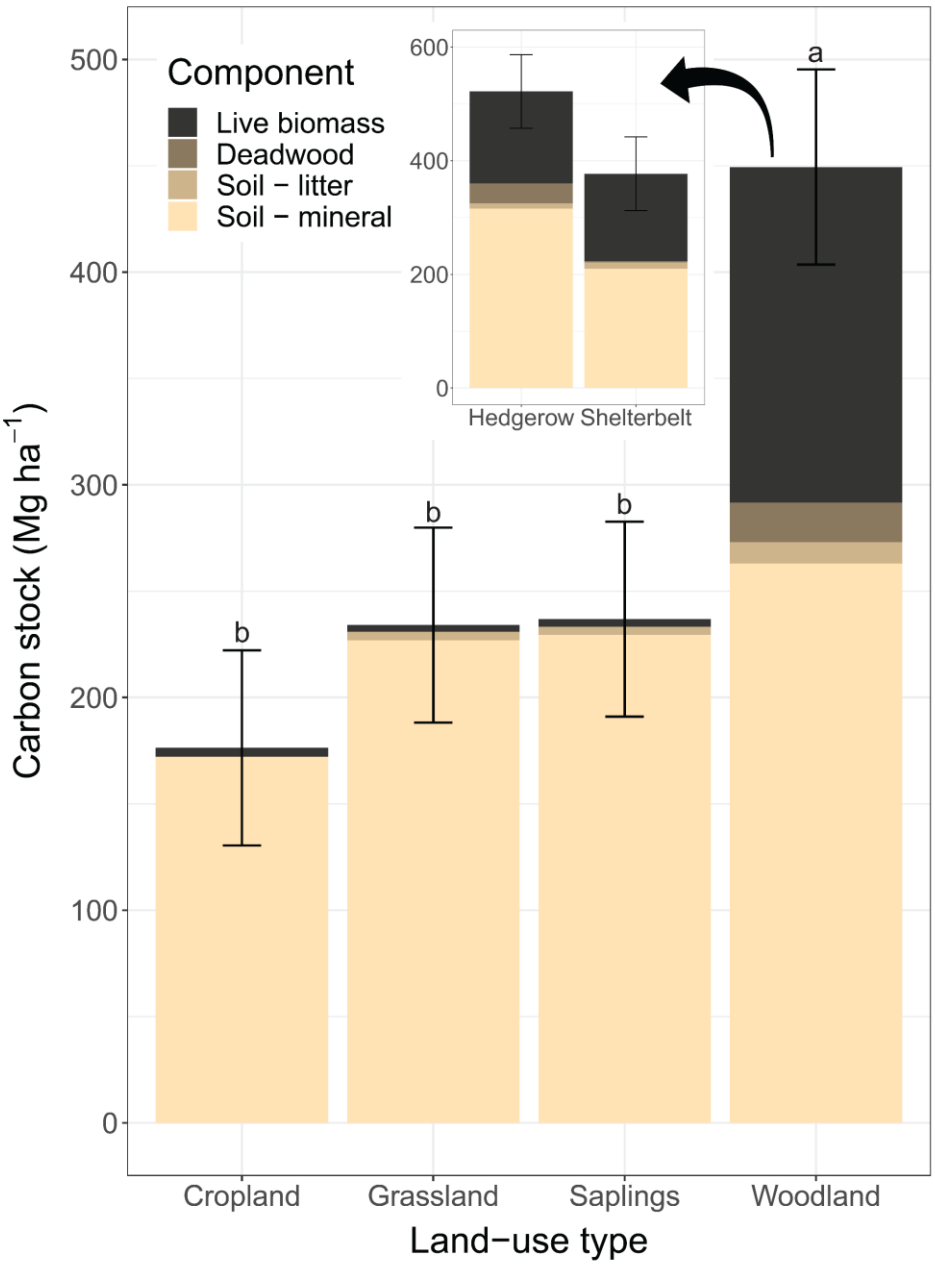

Figure 2.6. Carbon stocks in various components among the different land uses of two agroforestry systems in central Alberta, Canada (n = 10) and (inset) the woodland within each agroforestry system. Error bars represent ± one standard error for total ecosystem carbon stocks. Least-squares means for total ecosystem carbon stocks accompanied by different lowercase letters are significantly different (Tukey-adjusted, $\alpha = 0.05$) among the land-use types and agroforestry systems.

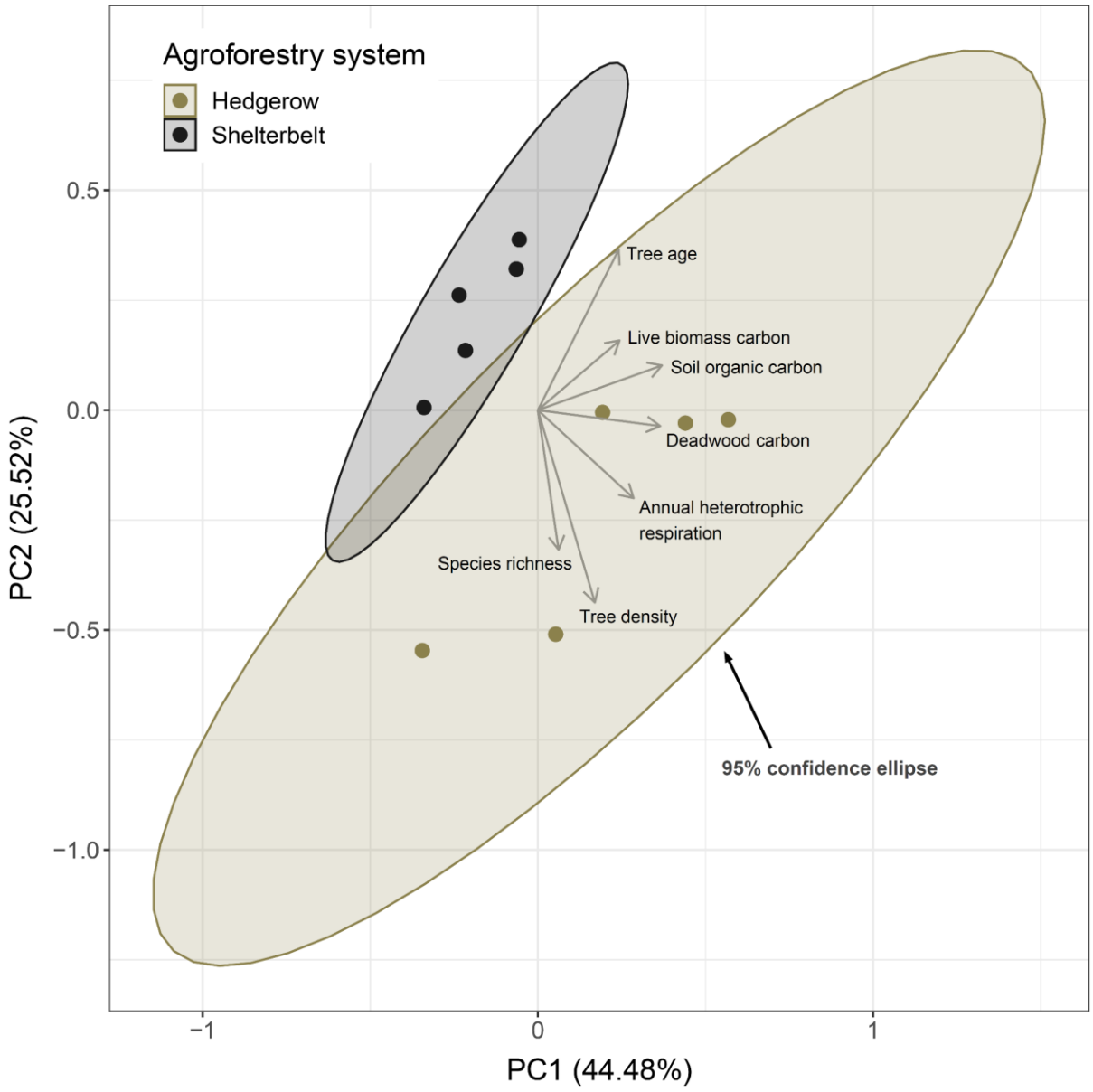

Figure 2.7. Principal components analysis showing associations between woodland characteristics and carbon stocks and flux among two agroforestry systems in central Alberta, Canada (n = 10).

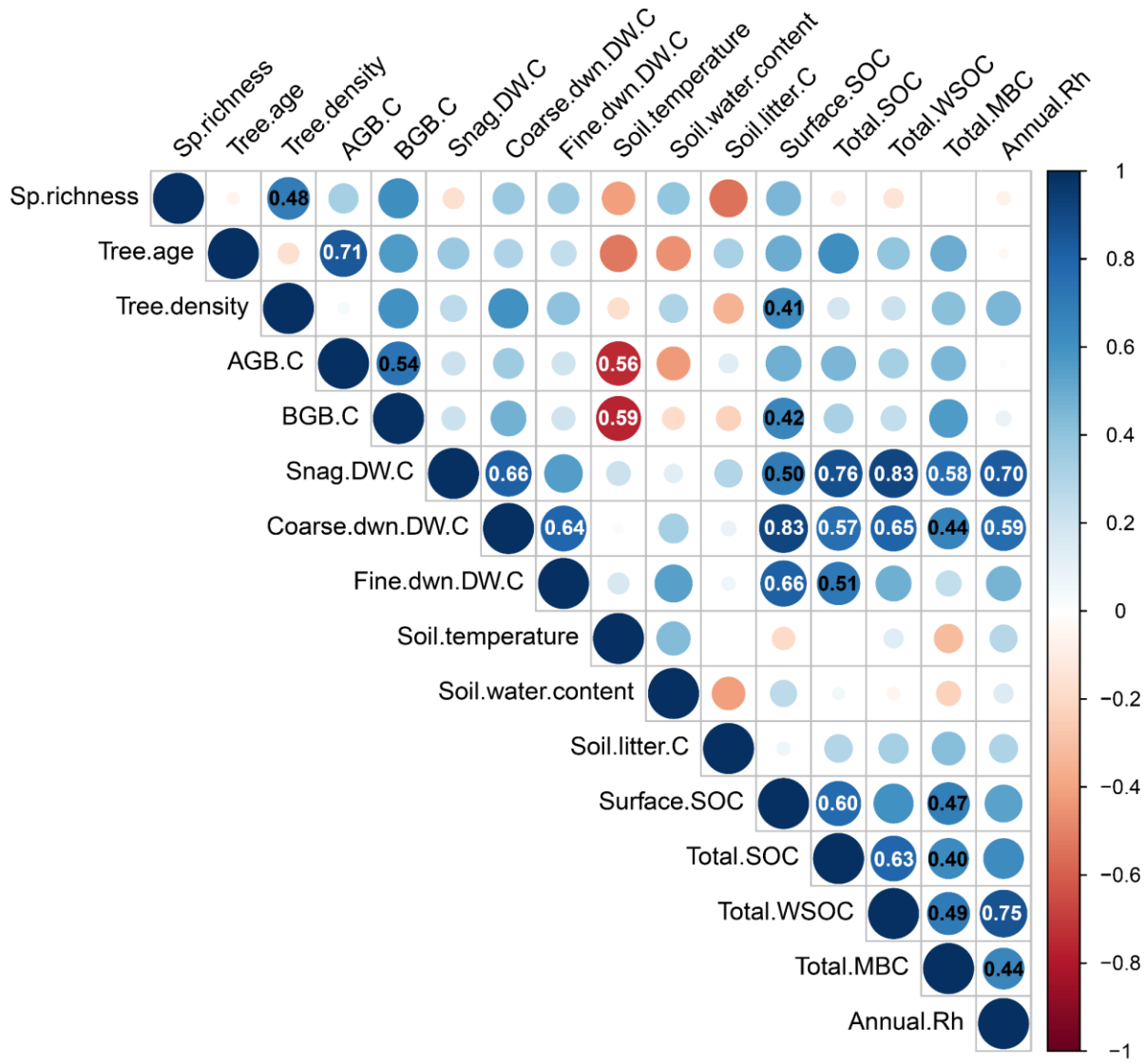

Figure 2.8. Pearson correlations (with R^2 values reported) between woodland characteristics, soil properties, and carbon (C) stocks and flux among two agroforestry systems in central Alberta, Canada (n = 10). Only statistically significant (α = 0.05) correlations are reported. Values in white were significant using the Benjamini and Hochberg (1995) technique (α = 0.1) to correct for the false discovery rate across multiple comparisons. Sp, species; AGB, aboveground live biomass; BGB, belowground live biomass; dwn, downed; DW, deadwood; SOC, soil organic C; WSOC, water-soluble organic C; MBC, microbial biomass C; Rh, heterotrophic respiration.

Chapter 3. Biochar and its manure-based feedstock have divergent effects on soil organic carbon and greenhouse gas emissions in croplands

Cole D. Gross[1], Edward W. Bork[2], Cameron N. Carlyle[2], Scott X. Chang[1]

[1] Department of Renewable Resources, Faculty of Agricultural, Life and Environmental Sciences, University of Alberta, 442 Earth Sciences Building, Edmonton, AB T6G 2E3, Canada; cgross@ualberta.ca (C.D.G.); sxchang@ualberta.ca (S.X.C.)

[2] Department of Agricultural, Food and Nutritional Science, Faculty of Agricultural, Life and Environmental Sciences, University of Alberta, 410 Agriculture/Forestry Centre, Edmonton, AB T6G 2P5, Canada; ebork@ualberta.ca (E.W.B.); cameron.carlyle@ualberta.ca (C.N.C.)

3.1. Abstract

Applying organic amendments to soil can increase soil organic carbon (SOC) storage and reduce greenhouse gas (GHG) emissions generated by agriculture, helping to mitigate climate change. However, it is necessary to determine which type of amendment produces the most desirable results. I conducted a 3-y field study comparing one-time additions of manure compost and its biochar derivative to a control to assess their effects on SOC and GHG emissions at ten annually cropped sites in central Alberta, Canada. Manure compost and biochar were applied at equivalent carbon rates (7 Mg ha^{-1}) and tilled into the surface 10 cm of soil. Two years post-treatment, biochar addition increased surface (0–10 cm) SOC by 12 and 10 Mg ha^{-1} relative to the control and manure addition, respectively. Therefore, the biochar led to the sequestration of SOC at a rate of 2.5 Mg ha^{-1} y^{-1} relative to the control. No treatment effect on deeper (10–100 cm) or cumulative SOC was found. In 2018 and 2019, manure addition increased cumulative GHG (sum of CO_2, CH_4, and N_2O) emissions by 33%, on average, due to greater CO_2 emissions relative to both the control and biochar addition. In contrast, in 2020, biochar addition reduced cumulative GHG emissions by an average of 21% due to lower CO_2 emissions relative to both the control and manure addition. My study shows that the application of biochar, rather than its manure compost feedstock, increased surface SOC sequestration and had either no effect on (first two years) or reduced GHG emissions (year three) relative to the control. I recommend that policy and carbon sequestration initiatives focus on optimizing biochar production-application systems to fully realize the potential of biochar application as a viable climate change mitigation practice in agriculture.

Graphical abstract:

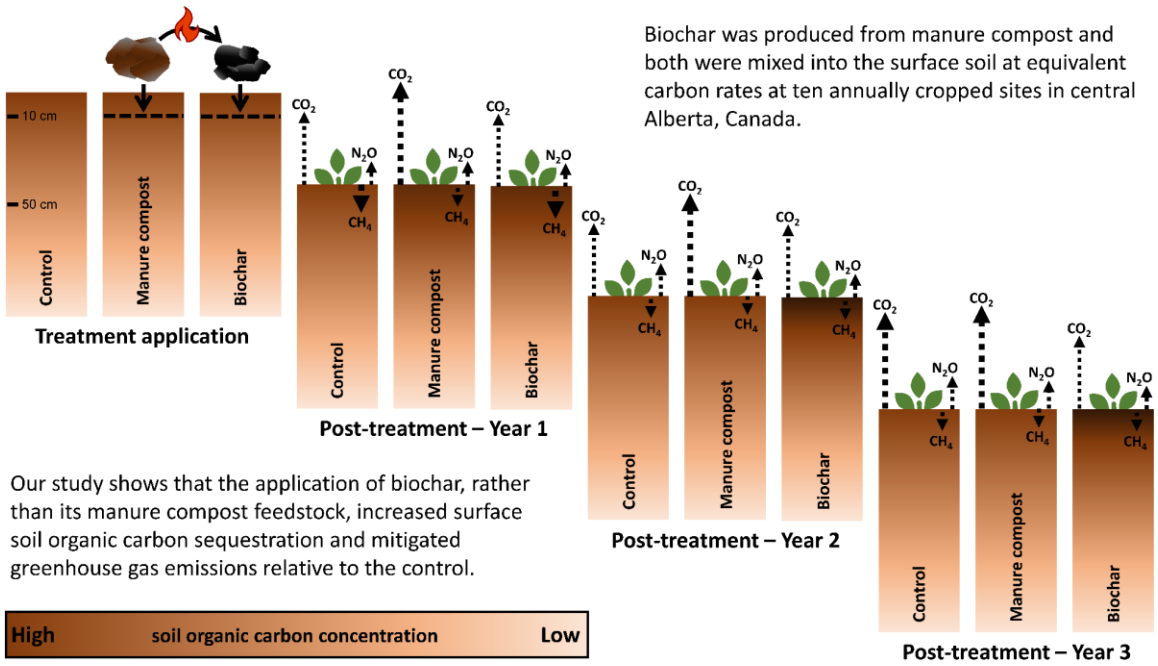

Keywords: biochar, climate change mitigation, greenhouse gas emissions, manure compost, soil organic carbon sequestration, sustainable agriculture

Highlights:

- Biochar (BT) was produced from manure compost (MT) for cropland application.
- BT, MT, and control (CT) treatments were compared during a 3-y field study.
- MT increased annual greenhouse gas (GHG) emissions by 34% relative to BT.
- Annual GHG emissions were 19% lower in BT than in CT in year three.
- BT increased soil organic carbon sequestration by 2.5 Mg ha^{-1} y^{-1} relative to CT.

3.2. Introduction

The ability of soils to sequester and store large amounts of carbon (C) has received increasing attention in our efforts to mitigate the human-mediated flux of greenhouse gases (GHGs) to the atmosphere. The cultivation of soils leads to the release of large amounts of C to the atmosphere (Guo & Gifford, 2002; Ciais *et al.*, 2013). However, the growing human population and demand for food and other agricultural products have led to more forests and grasslands being converted to intensively farmed agroecosystems. Agricultural management practices affect GHG emissions from soils by altering the soil environment and, in turn, changing the size and composition of microbial communities and their activities, including the facilitation of nutrient cycling. Globally, agriculture contributed 14% of the total anthropogenic GHG emissions in 2010 (IPCC, 2014).

Incorporating soil amendments into agricultural soils could increase soil organic C (SOC) storage and decrease GHG emissions (Stavi & Lal, 2013; Gross & Glaser, 2021). In addition to mitigating climate change, increasing SOC storage can benefit the soil by increasing soil nutrient- and water-holding capacities, which could enhance crop yield and the ecological goods and services generated by agricultural land. The application of readily available organic amendments such as biowastes to agricultural soils is a common practice. Manure compost application has shown promise for increasing SOC stocks (Tautges *et al.*, 2019; Gross & Glaser, 2021), specifically within the silt and clay fraction of soil macroaggregates (Yu *et al.*, 2012) and particulate organic matter (Sleutel *et al.*, 2006), among other benefits to the soil (Martínez-Blanco *et al.*, 2013). In general, manure compost is more promising than raw manure as a soil amendment for increasing SOC sequestration and reducing GHG emissions from agroecosystems (Ryals *et al.*, 2015; Shrestha *et al.*, 2018). However, there is mounting evidence that biochar (organic material pyrolyzed under low or no oxygen conditions) may be a superior tool for increasing SOC storage and mitigating agricultural GHG emissions from soil (Lehmann *et al.*, 2006; Sohi *et al.*, 2010; Shakoor *et al.*, 2021).

The three major GHGs contributing to agricultural emissions are carbon dioxide (CO_2), methane (CH_4) and nitrous oxide (N_2O), of which CO_2 is the most abundant GHG emitted from agricultural soils (Ciais *et al.*, 2013). Microbial decomposition of SOC results in C being released to the atmosphere as CO_2. Compared with biowaste amendments, amending soil with biochar has been shown to have a greater potential for increasing SOC stocks (Yousaf *et al.*, 2017) and

reducing the emission of GHGs, including N_2O (Cayuela *et al.*, 2014; Shakoor *et al.*, 2021) and CH_4 (Jeffery *et al.*, 2016). Biochar has been shown to accelerate microaggregate formation and SOC protection, as well as to increase mineral-associated root-derived C retention and the sorption of root exudates to biochar surfaces (Lehmann *et al.*, 2011; Hernandez-Soriano *et al.*, 2016a; Weng *et al.*, 2017). Biochar can also help reduce microbial activity and metabolism (Hernandez-Soriano *et al.*, 2016b; Yousaf *et al.*, 2017) and decrease the activities of soil enzymes involved in the degradation of organic C compounds (Lehmann *et al.*, 2011; Li *et al.*, 2018; Pokharel *et al.*, 2018). However, applying biochar at large scales is complicated by the additional costs to produce biochar and the lack of pyrolysis facilities used to mass produce biochar (Roberts *et al.*, 2010; Galinato *et al.*, 2011; Spokas *et al.*, 2012).

Field research comparing common biowaste materials and their biochars as agricultural amendments for the purposes of increasing SOC storage and reducing GHG emissions is needed to help quantify the differential benefits between the two types of amendments. This information will help inform management practices and policy decisions on reducing GHG emissions generated by agricultural, as well as increasing C sequestration in soils. Additionally, a past bias toward sampling only the surface soil has left knowledge gaps in our understanding of soil C dynamics (Harrison *et al.*, 2011; Stockmann *et al.*, 2013; Jandl *et al.*, 2014) by ignoring evidence that subsurface SOC can be affected by changes in management practices (Gross & Harrison, 2019; Tautges *et al.*, 2019). Another confounding issue in some past studies is not properly accounting for management-related changes in bulk density over time, which can impact SOC stock estimates to a greater degree than actual changes in SOC concentrations (Ellert & Bettany, 1995; Wendt & Hauser, 2013). Comparing equivalent soil masses (rather than fixed depths) is the recommended approach to calculate SOC stocks to overcome biases associated with changes in bulk density due to the application of treatments (von Haden *et al.*, 2020). In this 3-y field study, I directly compared one-time additions of manure compost and its biochar derivative to assess the effects of these organic amendments on GHG emissions, as well as on both the surface and subsurface storage of SOC (using an approach based on equivalent soil masses) in annually cropped agricultural lands. Manure compost was used as the feedstock for biochar production to directly compare this manure compost to its biochar. Additionally, compared with raw manure, composted manure can be easily stored until transport to a pyrolysis facility, is less expensive to

transport due to large decreases in mass and volume, and has reduced moisture content, which facilitates the pyrolysis process (Michel *et al.*, 2004; Roberts *et al.*, 2010).

My objective was to aid in the development of targeted management practices across soil types to increase SOC sequestration and reduce GHG emissions from agroecosystems. I hypothesized that both the manure compost and its biochar would increase SOC, but that biochar would result in lower GHG emissions than its manure compost feedstock due to biochar's relative recalcitrance to microbial decomposition (Lehmann *et al.*, 2011).

3.3. Materials and methods

3.3.1. Study area and experimental design

The 3-y (2018–2020) field study was conducted at ten producer-operated, annually cropped sites in central Alberta, Canada (Fig. B.S1). The historical monocultural annual crop rotation at all ten study sites was wheat (*Triticum aestivum*), barley (*Hordeum vulgare*), and canola (*Brassica rapa*). In 2018, the cereal crops (wheat and barley) were planted on five sites, canola was planted on three sites, and pea (*Pisum sativum*) and soybean (*Glycine max*) were each planted on one site. In 2019 and 2020, the cereal crops were planted on four and seven sites respectively, and canola was planted on the remaining sites following a crop rotation plan for each site. During the study, all sites were tilled, seeded, fertilized, swathed and harvested by the landowners according to their common practices, with all treatments at each site receiving identical management. In general, soils were typically tilled to ~10 cm depth prior to seeding and fertilizer was applied at the same time as seeding. Standard fertilization rates were 112-28-17-17 kg ha^{-1} N-P-K-S for canola, 78-22-11 kg ha^{-1} N-P-K for wheat, and 56-28-11 kg ha^{-1} N-P-K for barley.

The regional climate at the study sites is humid continental (Köppen climate classification Dfb) and characterized by large seasonal temperature differences, with warm, sometimes humid summers and cold winters. Historical (from 1988 to 2017) annual mean total precipitation and annual mean temperature in Edmonton, Alberta (township T052R24W4) during the May through August growing season (full year in parentheses) were 275 (432) mm and 14.9 (3.7) °C, respectively (Alberta Climate Information Service, 2021). During the experiment, mean annual total precipitation and mean annual temperature were 197 (387) mm and 16.6 (3.7) °C in 2018, 282 (410) mm and 14.5 (3.3) °C in 2019, and 402 (504) mm and 15.4 (3.8) °C in 2020, respectively (Alberta Climate Information Service, 2021). The sites ranged from 617–797 m above sea level in

elevation. The soils at all ten study sites exhibited high levels of surface soil organic matter accumulation (Chernozems or Ustic Haplocryolls in the Canadian or United States soil taxonomy systems, respectively). All soils were classified by digging an 80-cm+ deep pit in 2017 next to the treatment plots (Table B.S1).

The study compared one-time additions of manure compost (MT) and its biochar derivative (BT) to a control (CT, no treatment). Cropland plots (7 × 7 m in size, with 2-m buffers between plots and all sampling conducted within the interior 5 × 5 m, leaving a 2-m buffer within each plot) were randomized and set up 30 m from trees or field margins on level ground. Treatment application occurred over a 1-wk duration in early May 2018 prior to seeding (which occurred in mid-May). Manure compost and biochar were applied at equivalent C rates of 7 Mg C ha^{-1}. The manure compost and biochar were applied at 25 and 20 Mg ha^{-1} (dry-weight), respectively, based on the lower C concentration for manure compost (280 mg C g^{-1} manure compost) relative to the biochar (347 mg C g^{-1} biochar). The applied material was tilled into the surface 10 cm of soil using a gas-powered tiller with 2–3 passes. The amount of total nitrogen (N) applied was 185 and 138 kg N ha^{-1} for manure compost and biochar, respectively, due to the lower C:N ratio of the manure compost (37.5) relative to the biochar (50.2). During the application, biochar plots were evenly watered to account for the difference in moisture content between the manure compost and the biochar (52.5% and 0.1%, respectively), as well as to prevent treatment cross-contamination or biochar loss due to the dry biochar being transported by wind. None of the plots or sites were otherwise irrigated for the duration of the study.

The manure (derived from steers fed alfalfa hay, barley straw, lentil pellets, and activated carbon) was composted outdoors for one full year on a farm in south-central Saskatchewan, Canada in a compost pile ~5 × 2 × 60 m (w × h × l), which was turned several times over the course of the year. The manure was composted with livestock bedding material consisting of equal parts barley and wheat straw (~5:1 ratio of manure to straw, mass-basis). A minor component of pine (*Pinus* spp.) and spruce (*Picea* spp.) wood chips was later added to the bulk manure compost prior to biochar production to aid in the pyrolysis process (~10:1 ratio of manure compost to wood chips, mass-basis). Biochar was produced by processing the bulk manure compost at 650 °C for 90 min under low to no oxygen conditions until it was fully pyrolyzed using a retort pyrolysis system.

3.3.2. Data collection and analysis

3.3.2.1. Measurement of soil properties

Soil was collected from each plot at four depth intervals (0–10, 10–30, 30–50, and 50–100 cm) immediately prior to treatment application (early May 2018) and again in early May 2020. In late August 2020, soil samples were collected again from each plot at only two depth intervals (0–10 and 10–30 cm), as the dryness of the soil prevented my ability to sample deeper without severe disturbance to the plot. A hand-rotated auger (3.81 cm diameter) was used to collect the soil samples. Three holes were augered per plot and soil was composited by depth, sealed in pre-weighed plastic bags, and returned to the lab. Composite samples were immediately weighed in the lab and stored at 4 °C until subsequent processing and analysis. Bulk soil was sieved to 8 mm by carefully separating the soil at natural breaks to pass through the sieve openings to minimize disturbance to aggregate structure and soil microbial biomass size and activity (Horwath & Paul, 1994; Datta *et al.*, 2014). Plant fragments and rocks (0.3% on average by weight) with a diameter >2 mm were removed from the soil. Sieved soil was stored at 4 °C until subsequent processing and analysis.

Soil pH was measured with a digital pH meter (Thermo Scientific 710A, Beverly, MA) after mixing oven-dried (40 °C) subsamples with ultrapure (MilliporeSigma Milli-Q) water in a 1:2 ratio (w:v), agitating on a shaker for 30 min at 180 rpm, and standing for 1 h. To obtain total soil C and N concentrations, representative subsamples (oven-dried at 40 °C) were ground to a fine powder with an agate mortar and pestle and analyzed using dry combustion on an elemental analyzer (Vario MICRO Cube Elemental Analyzer, Elementar, Hesse, Germany). For each run of 60 samples on the elemental analyzer, five standards were run to verify accuracy (deviation <2%) and calculate a correction factor.

Total C was equated to organic C for soil with a pH ≤6.00 (Walthert *et al.*, 2010). Soil samples with a pH >6.00 were acid fumigated for 72 h to remove potential carbonates and determine organic C (Ramnarine *et al.*, 2011). Briefly, subsamples of ~300 mg of the fine-ground soil were moistened with 150 µL of ultrapure water, fumigated in a vacuum chamber with 12 M HCl for 72 h, oven-dried at 40 °C to a constant weight, agitated back to a fine powder using a stainless-steel soil scoop, and analyzed on the elemental analyzer as previously described. A conversion factor was used to account for the increased weight of acidified soils that contained carbonates so as not to dilute organic C measurements according to:

$$M_{soil-adj} = M_{soil} \times cf_{acidfum} \quad [3.1]$$

where $M_{soil-adj}$ is the corrected mass of the acidified soil (mg), M_{soil} is the mass of the acidified soil (mg), and $cf_{acidfum}$ is a correction factor equal to the oven-dry pre-fumigated mass divided by the oven-dry post-fumigated mass (Ramnarine *et al.*, 2011). Carbonates were considered to be absent for measurements of low amounts of inorganic C relative to organic C (Hedges & Stern, 1984; Walthert *et al.*, 2010) and the two values (total C and organic C) were averaged to obtain the organic C concentration for the sample. Across all soils, inorganic C in the deepest soil layer sampled (50–100 cm) comprised ~36% of total C, while inorganic C was largely absent from soil above 50 cm.

The chloroform fumigation-extraction procedure was used to measure soil microbial biomass (Vance *et al.*, 1987; Beck *et al.*, 1997). Briefly, duplicate subsamples of 8 g (oven-dry weight basis) of field-moist soil sieved to <8 mm were fumigated in a vacuum chamber with ethanol-free chloroform for 48 h in darkness (Jenkinson *et al.*, 2004). Water-soluble organic matter was extracted from both fumigated and non-fumigated samples by shaking the samples with 0.01 M K_2SO_4 (1:5 w:v) in 50-mL polyethylene tubes for 1 h at 180 rpm (Haney *et al.*, 2001; Jenkinson *et al.*, 2004). Tubes were then centrifuged at 10,000 × g for 10 min, after which 20 mL of the supernatant was collected and filtered through a 0.4-µm Whatman Nuclepore polycarbonate filter (Zsolnay, 2003; Chantigny *et al.*, 2007). The filtrates were stored at 4 °C prior to analysis with a total organic C (TOC) analyzer (TOC-V and TN unit, Shimadzu Corporation, Kyoto, Japan) using 680 °C combustion catalytic oxidation and the non-purgeable organic C (to remove inorganic C) and total N methods. For each run of 60 samples on the TOC analyzer, six standards were run to verify C and N accuracy (deviation <5%), and six blanks were run, averaged, and subsequently subtracted from the raw sample values. Microbial biomass C was calculated according to:

$$MBC = \frac{EC}{k_{EC}} \quad [3.2]$$

where EC is the difference between average organic C in the fumigated and non-fumigated samples, and k_{EC} of 0.45 represents the extraction efficiency of the biomass C (Jenkinson *et al.*,

2004). An equation with the same form as Eq. 3.2, and k_{EN} of 0.45, was used to calculate microbial biomass N. The organic C and total N in the non-fumigated samples were defined as water-soluble organic C (WSOC) and water-soluble total N (WSN).

An equivalent soil mass-based approach (Wendt & Hauser, 2013) was used to calculate SOC and total N, microbial biomass C and N, and WSOC and WSN mass using a web-accessible spreadsheet (Wendt, 2013), which uses a cubic spline function to model the relationship between cumulative areal soil mass and cumulative C or N mass. Reference soil mass layers were calculated using the pretreatment soil mass means for each soil depth layer. Comparing changes in SOC and N, as well as certain other soil properties, over time using reference soil mass layers helps overcome biases associated with changes in bulk density due to the application of treatments or other agricultural management practices (von Haden *et al.*, 2020). Based on the treatment application C rates of 7 Mg C ha^{-1}, only a significant increase in SOC stocks >7 Mg C ha^{-1} was considered as SOC sequestration.

Soil texture was determined using 8–15 g (oven-dry weight basis) of field-moist soil sieved to <8 mm using the protocol and size-separation device described in detail by Virto et al. (2008). Briefly, soil aggregates >53-µm in size were broken up on a shaker (4 h at 180 rpm) using glass beads within a 30-mL plastic bottle sealed with a nylon cloth (Gilson Co. Inc., Columbus, OH) with a 53-µm opening and contained within a 250-mL plastic bottle with 200 mL of ultrapure water. Sand and particulate organic matter collected in the smaller plastic bottle were poured onto a 53-µm sieve, rinsed with ultrapure water until the solution passing through the sieve was clear, backwashed into a pre-weighed aluminum dish, oven-dried at 60 °C to a constant weight, and weighed. The amount of sand was calculated using a correction factor determined by mechanically grinding (ball mill) the sand + particulate organic matter fraction and placing a subsample in a muffle furnace at 500 °C for 4 h (loss-on-ignition method) (Cambardella *et al.*, 2001; Kettler *et al.*, 2001). The silt + clay fraction (collected in the 250-mL bottle after shaking and recovered from the 30-mL bottle after passing through the 53-µm sieve) was subjected to the sequential application of a total of 1500 J cm^{-3} ultrasonic energy to achieve complete dispersion (Kaiser & Berhe, 2014). The silt fraction was separated from the clay fraction by sieving (>20 µm) and through sedimentation and centrifuging according to Stoke's Law (Virto *et al.*, 2008). The silt and clay fractions were collected in pre-weighed aluminum dishes, oven-dried at 40 °C to a constant weight, and weighed to determine their respective amounts.

Soil moisture and temperature values were recorded hourly from ~April through October using a soil monitoring station logger, moisture probe, and temperature sensor (Onset Computer Corporation, Bourne, MA) installed near the center of each plot. Probes and sensors were installed horizontally in undisturbed soil at a depth of 10 cm and the soil excavated to place the probes was carefully refilled. Care was taken not to disturb this area throughout the sampling period. All soil moisture values recorded when the soil temperature was <0.25 °C were considered inaccurate (based on the specifications of the instruments) and deleted from the dataset used for statistical analysis.

3.3.2.2. Measurement of greenhouse gas emission rates

Gas samples were collected every other week from ~April through October from two dark static gas chambers (headspace mean height and volume of 11.1 cm and 0.011 m^3, respectively) equipped with fans (Christiansen *et al.*, 2011) installed in each plot between crop rows to exclude roots. Living vegetation within chambers was largely absent due to herbicides applied at the same time as seeding, greatly minimizing the contribution of soil autotrophic respiration to measured total respiration. Any emergent vegetation was carefully removed from within each chamber prior to gas collection, while leaving the mineral soil and any crop litter undisturbed. Gas collection chambers were carefully installed to avoid soil disturbance inside the chambers and were inserted ~4 cm into the soil to create a seal between the soil and the chamber. Soil chamber headspace height was averaged from post-installation and pre-removal measurements at four points within each chamber. Collection of gas samples from each chamber occurred at 10-min intervals over 30 min (including time zero) and gases were stored with positive pressure in pre-evacuated soda glass Labco Exetainers until subsequent analysis. Gas collection generally occurred between 1100 and 1400 h local time and the order of grouped sites visited in a single day was reversed each trip to avoid potential impact of diurnal temperature changes on soil respiration measurements (Venterea *et al.*, 2005). All sites were generally sampled over a 3-d period.

Concentrations of gasses sampled from dark static chambers were measured using a gas chromatograph (Varian CP-3800, Mississauga, Ontario, Canada) equipped with a thermal conductivity detector, a flame ionization detector, and an electron capture detector to measure the concentrations of CO_2, CH_4, and N_2O, respectively. Six standards of a known concentration for each gas were run for every 100 samples to verify accuracy (deviation <5%). Chamber gas

concentrations measured by gas chromatograph analysis were converted to mass per volume units using ideal gas relations at standard temperature and pressure corrected for the air temperature during sampling according to:

$$\text{Chamber}_{G_{conc}} = \left(G_{conc} \times 44.6 \times \frac{273.15}{T_a} \times M_u\right) \div 10^6 \quad [3.3]$$

where $\text{Chamber}_{G_{conc}}$ is the gas concentration in the chamber at a given time (g m^{-3}), G_{conc} is the gas concentration determined by gas chromatograph analysis (µmol mol^{-1}), 44.6 is moles of gas at standard temperature (273.15 K) and pressure (1.00 atm) (mol m^{-3}), T_a is the measured air temperature during sampling (K), and M_u is the molar mass of the gas (g mol^{-1}).

Gas flux (g m^{-2} h^{-1}) and cumulative flux (g m^{-2} y^{-1}) values were calculated from the chamber volume (m^3), soil surface area (m^2), and the change in chamber gas concentration (g m^{-3}) over time (h) using the *gasfluxes* R software package (Hüppi *et al.*, 2018), which uses linear interpolation to calculate cumulative gas fluxes. The *KAPPA.MAX* flux calculation scheme was used to determine linear or nonlinear (i.e., Hutchinson-Mosier regression model, *HMR* (Pedersen *et al.*, 2010)) flux estimates. The *KAPPA.MAX* method balances bias and uncertainty related to measurement precision and chamber setup (Hüppi *et al.*, 2018). The minimum detectable flux was calculated for CO_2, CH_4, and N_2O using ambient concentration (401, 1.82, and 0.328 µmol mol^{-1}, respectively) and gas chromatograph measurement uncertainty (5, 0.01, and 0.001 µmol mol^{-1}, respectively), as well as the mean chamber volume (m^3) and air temperature (K) at the standard pressure. To convert CH_4 and N_2O to CO_2-equivalents, global warming potentials of 34 and 298, respectively, were used, which are based on a 100-y frame and include climate-carbon feedbacks (IPCC, 2014). Total GHG flux was calculated as the sum of CO_2, CH_4, and N_2O, with the latter two GHGs assessed as CO_2-equivalents.

3.3.2.3. Crop standing biomass

Total aboveground crop biomass samples were collected annually ~1–2 wk prior to swathing or harvest. Three 50 × 50 cm quadrats were randomly located in each plot, and all aboveground biomass was collected and weighed in the field. A composite subsample of the three samples was stored in a pre-weighed bag, returned to the lab, immediately weighed, oven-dried for 72 h at 60 °C, and weighed again. Total aboveground biomass (Mg ha^{-1}) was calculated using

the quadrat area, the average weight of the three field samples, and a conversion factor based on the moisture content of the composite subsamples.

3.3.3. Statistical analysis

Linear mixed-effect models were used to determine whether the treatments affected GHG emissions, soil properties, or crop biomass. The fixed effect was treatment and the random effect was site. Pretreatment values for soil properties were included in the model as a covariate. Repeated measurements were averaged for emissions of GHGs collected within plots (n = 2) and months (n = 2 or 3) and cumulated for annual emissions of GHGs. Where necessary for the GHG and soil variables, data transformations using the lambda value for the maximum log likelihood for obtaining minimum error sum of squares were conducted to conform data to the assumptions of homogeneous variance and normality of distribution. Non-transformed data were used in the models to calculate least-squares means and standard errors. A randomized complete block design model was used for each response variable. When significant effects were detected at $p < 0.05$ after using type-III analysis-of-variance (ANOVA), pairwise *post-hoc* comparisons using the Tukey method for *p*-value adjustment were conducted to compare individual treatment means. Associations between continuous variables of interest were determined using Pearson's parametric correlation to assess the relationships between GHG emissions and soil properties among the treatments and within a given treatment. All data were analyzed using RStudio Version 1.4.1106 (RStudio Team, 2021).

3.4. Results

3.4.1. Soil properties and crop standing biomass

In the surface soil (0–10 cm), BT increased soil pH by 0.30 to 6.04 ($p = 0.030$) relative to the CT and increased OC:N ratios relative to both the CT and MT ($p < 0.001$) (Table 3.1). Additionally, BT increased WSOC:WSN ratios relative to the CT in spring 2020 ($p = 0.030$) and relative to both the CT and MT in fall 2020 ($p < 0.001$ and $p = 0.005$, respectively) (Table 3.2). On a mass basis, differences in SOC and total N between the treatments were similar to the comparisons made for concentrations within soil depth layers (Table 3.1 & 3.2). In the surface soil (~0–10 cm, or the 0–1050 Mg ha^{-1} soil mass layer), BT increased SOC relative to the CT ($p < 0.001$) and MT ($p < 0.001$) (43.46 ± 1.15, 45.65 ± 1.15, and 55.75 ± 1.15 Mg C ha^{-1}, for the CT,

MT, and BT, respectively) and increased total N relative to the CT (p = 0.003) (3.88 ± 0.06, 4.02 ± 0.06, and 4.22 ± 0.06 Mg N ha^{-1}, for the CT, MT, and BT, respectively) (Fig. 3.1). However, these surface SOC and N mass increases were not large enough to lead to overall SOC or N mass differences among treatments at ~100 cm soil depth (i.e., soil cumulative mass of 13950 Mg ha^{-1}). Compared with CT, the MT increased WSOC (p = 0.025) in the subsurface soil (~10–30 cm, or the 1050–3650 Mg ha^{-1} soil mass layer) in spring 2020 (41.26 ± 3.36, 48.99 ± 3.35, 44.65 ± 3.35 kg C ha^{-1}, for the CT, MT, and BT, respectively) and the BT decreased WSN (p < 0.001) in the surface soil in fall 2020 (6.40 ± 1.14, 6.32 ± 1.14, and 4.24 ± 1.14 kg N ha^{-1}, for the CT, MT, and BT, respectively) (Fig. 3.2). Microbial biomass C (MBC) and N (MBN) masses were not affected by the treatments, except in the deepest soil layer (~50–100 cm, or the 6300–13950 Mg ha^{-1} soil mass layer), wherein BT increased MBC relative to the CT (p = 0.032) in spring 2020 (104.95 ± 17.33, 124.81 ± 16.74, and 144.87 ± 17.20 kg ha^{-1}, for the CT, MT, and BT, respectively) (Fig. B.S2).

Differences in soil temperature and water content (measured at 10 cm depth) across treatments were limited to the year in which treatments were applied (2018). Compared with BT, soil temperatures within the MT were lower (p = 0.029) in 2018 (15.29 ± 0.56, 14.64 ± 0.56, and 15.51 ± 0.56 °C, for the CT, MT, and BT, respectively), primarily due to an immediate treatment response in May 2018 (Fig. B.S3a–b). Soil water content was reduced by BT relative to both the CT (p = 0.009) and MT (p = 0.011) in 2018 (30.03 ± 1.55, 29.89 ± 1.55, and 25.33 ± 1.55%, for the CT, MT, and BT, respectively) (Fig. B.S3c–d).

The treatments did not affect total aboveground crop biomass for either the cereal crops (wheat and barley) or canola across the years (Fig. B.S4).

3.4.2. Greenhouse gas emissions

Annual GHG emissions from the soil were largely driven by CO_2 emissions, with a minor role of N_2O emissions (primarily in June, immediately after fertilizer application) and a negligible role of CH_4 fluxes (Fig. 3.3 & 3.4). Compared with both the CT and BT, MT increased cumulative CO_2 emissions by 32 (p < 0.001) and 44% (p < 0.001), respectively, in 2018, and by 37 (p < 0.001) and 28% (p = 0.001), respectively, in 2019. Similarly, MT increased cumulative GHG emissions relative to both the CT and BT by 32 (p < 0.001) and 43% (p < 0.001), respectively, in 2018, and by 32 (p = 0.002) and 29% (p = 0.003), respectively, in 2019. In 2020, BT reduced cumulative

CO_2 and GHG emissions by 17 ($p = 0.013$) and 19% ($p = 0.022$), respectively, relative to the CT, and by 24 ($p < 0.001$) and 23% ($p = 0.004$), respectively, relative to the MT. Methane flux was significantly affected by the treatments only in 2018, wherein BT increased cumulative CH_4 uptake by 37% ($p = 0.026$) relative to the MT. Nitrous oxide emissions were not affected by treatment ($p \geq 0.05$). However, BT tended to have the lowest cumulative N_2O emissions during both 2019 and 2020, an average of 42% lower than the CT, while the MT had an average of 25% lower cumulative N_2O emissions over the same two years relative to the CT.

Monthly CO_2 and GHG emissions averaged across treatments were positively correlated with surface soil temperature ($r = 0.67$, $p < 0.001$; $r = 0.62$, $p < 0.001$, respectively), while monthly CH_4 flux was negatively correlated with surface soil temperature ($r = -0.17$, $p = 0.032$) (Fig. B.S5). Monthly CO_2, N_2O, and GHG emissions were generally positively correlated with surface soil water content ($r = 0.27$, $p < 0.001$; $r = 0.21$, $p = 0.009$; $r = 0.30$, $p < 0.001$, respectively), while monthly CH_4 flux exhibited a stronger positive correlation with surface soil water content ($r = 0.52$, $p < 0.001$). Within BT, average cumulative CO_2, N_2O, and GHG emissions over the three years of the study were not significantly correlated with pretreatment surface soil properties (i.e., % clay, pH, OC:N ratio, or SOC mass) or the change in surface SOC mass (two years post-treatment minus pretreatment) (Fig. B.S6). The change in surface SOC mass also was not significantly correlated with pretreatment surface soil properties. Average cumulative CH_4 emissions were positively correlated only with pretreatment surface soil pH ($r = 0.66$, $p = 0.039$).

3.5. Discussion

3.5.1. Carbon sequestration, dynamics, and flux

The biochar led to surface SOC sequestration at a rate of 2.5 Mg C ha^{-1} y^{-1} relative to the CT (Fig. 3.1a). Although I did not find a significant decrease in cumulative CO_2 emissions or a significant increase in aboveground crop biomass for the BT relative to the CT over the same two years, other (non-exclusive) factors may account for the increased SOC sequestration rate (Fig. 3.3a & B.S4). One possibility is that I missed differences in CO_2 emissions across treatments in 2018 and 2019, owing to the inability to collect gas samples between November and March (inclusive) or in October 2019 (Fig. 3.4). For example, the spring thaw can lead to substantial GHG emissions (Nyborg *et al.*, 1997), during which time the BT may have emitted less CO_2 relative to the CT if the biochar in fact helped slow SOC decomposition, as some studies have found

(Lehmann *et al.*, 2011). Another possibility is that biochar addition enhanced root activity and exudation (Weng *et al.*, 2017), as well as increased sorption and protection of dissolved organic C (DOC) in the surface soil that otherwise would have been transported with water to deeper soil layers. Specifically, the sorption of root-derived C, including root exudates, on biochar surfaces may have contributed to the sequestration of surface SOC (Weng *et al.*, 2017). Biochar surfaces potentially sorbed DOC derived from other sources as well, such as litter incorporated during tillage and microbial-derived C residues. The increase in spring and fall WSOC:WSN ratios and decrease in fall WSN for the BT relative to the CT in the surface soil (~0–10 cm) may have resulted from biochar sorbing and protecting nitrogenous, proteinaceous microbial-derived C residues (Kleber *et al.*, 2007), particularly during the growing season (Table 3.2 & Fig. 3.2b). If biochar addition resulted in less DOC being transported vertically down the soil profile, which is the primary mechanism contributing to deep SOC accumulation (Gross & Harrison, 2019), this also may help explain the (non-significant) trend of the BT having the lowest SOC mass in all soil layers below ~10 cm (Fig. 3.1a). Nonetheless, increased MBC in the BT relative to the CT in the deepest soil layer in the spring, along with a slight (non-significant) increase in WSOC, suggests that DOC transport (and subsequent microbial processing) was not reduced in the BT, at least during peak periods such as during the spring thaw (Fig 2a & S2a). Over time, biochar may have contributed to increased SOC protection mechanisms in the surface soil, as evidenced by the 17% reduction in cumulative CO_2 emissions from the BT relative to the CT in the third year post-treatment (Fig. 3.3a). For example, in addition to SOC protection via direct sorption of C to biochar surfaces, biochar may have fostered the formation of physically-protective aggregates (Hernandez-Soriano *et al.*, 2016b, 2016a; Weng *et al.*, 2017) and reduced microbial activity and metabolism, including the activity of C-degrading enzymes (Lehmann *et al.*, 2011).

Compared with the BT, the C contained in the manure compost was highly available to microorganisms and therefore more readily decomposed, as evidenced by increased (35% on average) cumulative CO_2 emissions for the MT relative to the BT for all three years of study (Fig. 3.3a). Organic matter contained in composting materials generally stabilizes after ~100 days (as indicated by reduced and negligible CO_2 emissions from windrows by this time) (Hao *et al.*, 2004; Michel *et al.*, 2004), suggesting that the manure compost used in this study was relatively stable, having been composted for one year. Nonetheless, when used as an amendment and exposed to the soil microbiome, organic matter in compost is still much more biodegradable than the organic

matter in its biochar derivative (Bolan *et al.*, 2012), with the latter persisting from years to millennia (Lehmann *et al.*, 2006; Gurwick *et al.*, 2013). The greater total N in the manure compost relative to the biochar may have also hastened the decomposition of the organic matter in the manure compost by more readily providing soil microbes with the needed N for metabolic processes. However, due to the annual application of inorganic N fertilizer at the study sites, the effect of the difference in added total N between treatments was likely suppressed.

Given the similar SOC masses in the surface soil of the MT and CT, as well as the similar cumulative CO_2 emissions between the MT and CT during the third year following treatment, a substantial portion of the C contained in the manure compost was likely lost via microbial respiration over the first two years when cumulative CO_2 emissions for the MT were, on average, 35% higher than the CT (Fig. 3.1a & 3.3a). However, some portion of the manure-compost and subsequent microbially-processed C may have been transported to deeper soil layers (Tautges *et al.*, 2019), as evidenced by increased WSOC mass in the subsurface soil (~10–30 cm) during spring 2020 in the MT relative to the CT (Fig. 3.2a). This increased WSOC mass in the subsurface soil of the MT indicates the presence of fresher, less-oxidized and thus less-strongly-sorbed organic C compounds (Lehmann & Kleber, 2015), potentially transported from the surface soil during precipitation events and the spring thaw (Neff & Asner, 2001; Sanderman *et al.*, 2008).

Although the contribution of CH_4 uptake on cumulative GHG emissions was negligible, cumulative CH_4 uptake was increased (more negative) by the BT relative to the MT during the first year (Fig. 3.3b). This increase in CH_4 uptake corresponded to a decrease in surface soil water content for BT relative to MT, with monthly surface soil water content being positively correlated with CH_4 flux and explaining 27% of the variation (Fig. B.S3c & B.S5). Reduced soil water would have decreased microsites in the soil with the anaerobic conditions required for CH_4 production, thereby reducing CH_4 emissions (Oertel *et al.*, 2016). Lower soil water content immediately following biochar application may have been related to hydrophobic aliphatic compounds on the biochar surfaces and in pores, resulting in the biochar-amended soil becoming water repellent, thereby interrupting infiltration (Mao *et al.*, 2019). However, soil water was similar across treatments in the second and third years of the study, potentially due to the oxidation of biochar surfaces or biofilm formation allowing the biochar to become hydrophilic over time (Ojeda *et al.*, 2015).

3.5.2. Nitrous oxide flux

Emissions of N_2O from soils were highest following fertilizer application and followed a trend of CT>MT>BT in the second and third year post-treatment (Fig. 3.3c & 3.4c), consistent with the recent literature (Cayuela *et al.*, 2014; Shrestha *et al.*, 2018; Shakoor *et al.*, 2021). However, N_2O emissions were not significantly affected by treatment and played only a minor role in cumulative GHG emissions. Limited soil-surface coverage and alternate-week measurements likely limited my ability to detect statistical differences across treatments by not accounting for the spatial heterogeneity or the precise contribution of fluxes during periods of high N_2O emissions, such as following fertilizer application (Butterbach-Bahl *et al.*, 2013). As noted previously, I was also unable to collect gas samples during the spring thaw, which can be another peak emission period for N_2O (Nyborg *et al.*, 1997; Butterbach-Bahl *et al.*, 2013). Moreover, the response of soil N_2O emissions to organic amendments (including the magnitude and direction of change) is highly dependent on numerous soil properties such as texture, pH, and C:N ratios (Cayuela *et al.*, 2014; Shakoor *et al.*, 2021). The soils of the agricultural lands studied herein differed drastically, including varied surface soil texture (% sand: 10.05–62.41; % clay: 23.21–35.86), pH (5.06–8.04), and C:N ratios (9.97–12.13), and this high variation may have reduced the consistency in treatment responses and thus my ability to detect statistical differences across treatments (Table B.S1).

3.5.3. Implications for climate change mitigation

My results, alongside decades of literature elucidating the benefits of biochar as a soil amendment, support that biochar application can act as a climate change mitigation strategy by enhancing surface SOC sequestration, thereby reducing GHG emissions resulting from agricultural practices. While changes in surface SOC due to organic amendments should not be viewed independently of potential effects on C-cycling processes occurring deeper in the soil, the latter effects may require longer-term assessments of treated soils, including across different amendment rates and frequencies. Ultimately, effects such as increased SOC, N, and pH in the surface soil due to biochar addition are expected to promote increased soil nutrient- and water-holding capacities and enhance nutrient availability for crop uptake (Atkinson *et al.*, 2010; Major *et al.*, 2010; Spokas *et al.*, 2012).

To fully realize the potential of biochar to mitigate climate change when used as an organic amendment in croplands, lifecycle assessments should be considered. Lifecycle assessments of biomass-pyrolysis systems, wherein the biochar was used as an agricultural soil amendment, have shown promise as far as avoiding net GHG emissions (Roberts *et al.*, 2010; Galinato *et al.*, 2011). However, optimizing biochar production-application systems is necessary to both reduce GHG emissions and support economic viability (Roberts *et al.*, 2010; Galinato *et al.*, 2011; Spokas *et al.*, 2012). The selection of appropriate feedstocks is one way in which to optimize biochar production-application systems. For example, biowaste feedstocks, including livestock manures, were identified as key resources for biochar production that have the potential for economic viability and renewable energy generation, as well as for increasing C sequestration and reducing GHG emissions (Roberts *et al.*, 2010), the latter of which my results have also shown. Indeed, further efforts should be made to assess and optimize biochar production-application systems, especially for processing biowaste feedstocks such as manure compost, the direct application of which only increased GHG emissions and did not increase SOC storage in my study.

3.6. Conclusions

My 3-y field study supports the use of biochar as a soil amendment for the purposes of sequestering SOC and mitigating GHG emissions from annually cropped agricultural lands. Ultimately, the effects of biochar application on surface soil properties, evidenced here by increased SOC, N, and pH, are expected to help foster sustainable agriculture. Although the production of biochar necessitates additional processing and therefore costs relative to more easily available organic feedstocks such as manure, I show that manure compost application had none of the benefits of biochar, namely increasing surface SOC sequestration (2.5 Mg C ha^{-1} y^{-1}, based on equivalent soil masses to overcome biases associated with changes in bulk density) and reducing GHG emissions (19%) from agroecosystems across a range of soil types. By using ten sites with different baseline soil properties, I was able to assess the performance of manure compost and its biochar on a broad scale as far as their differential abilities to mitigate climate change when amended into the soil of agroecosystems. Although I found no correlation between baseline soil properties and SOC sequestration due to biochar amendment, future studies should investigate the performance of biochar across specific soil properties to help prioritize application. Additionally, ongoing and future biochar-amendment studies should sample subsoil as well as surface soil to

continue to monitor and determine treatment effects on deeper SOC-cycling processes over time. I further recommend that policy and carbon sequestration initiatives focus on optimizing biochar production-application systems to fully realize the potential of biochar application as a viable climate change mitigation practice in agriculture.

Funding: This research was supported by a grant (AGGP2-039) from the Agricultural Greenhouse Gas Program from Agriculture and Agri-Food Canada to S.X.C., E.W.B., and C.N.C., as well as by a Doctoral Vanier Scholarship and a Killam Memorial Graduate Scholarship to C.D.G.

Credit: S.X.C., E.W.B., C.N.C., and C.D.G.: Conceptualization and Methodology. C.D.G.: Investigation and Writing—original draft. C.D.G., S.X.C., E.W.B., and C.N.C.: Writing—review and editing. S.X.C. and E.W.B.: Resources and Supervision.

Acknowledgements: I express my gratitude to the landowners and farmers for their generosity, assistance, and cooperation throughout the duration of the study. A special thank you to the many researchers who have assisted with this work, especially Michael Carson, Jonathan Tieu, Guanyu Chen, Maliha Rahman, Mary Villeneuve, Sheetal Patel, and Carmen C. Roman-Perez for their help in the field and/or lab.

3.7. References

Alberta Climate Information Service (2021) Alberta Agriculture and Forestry.

Atkinson CJ, Fitzgerald JD, Hipps NA (2010) Potential mechanisms for achieving agricultural benefits from biochar application to temperate soils: A review. *Plant and Soil*, **337**, 1–18.

Beck T, Joergensen RG, Kandeler E, Makeshin E, Nuss E, Oberholzer HR, Scheu S (1997) An inter-laboratory comparison of ten different ways of measuring soil microbial biomass C. *Soil Biology & Biochemistry*, **29**, 1023–1032.

Bolan NS, Kunhikrishnan A, Choppala GK, Thangarajan R, Chung JW (2012) Stabilization of carbon in composts and biochars in relation to carbon sequestration and soil fertility. *Science of the Total Environment*, **424**, 264–270.

Butterbach-Bahl K, Baggs EM, Dannenmann M, Kiese R, Zechmeister-Boltenstern S (2013) Nitrous oxide emissions from soils: How well do we understand the processes and their

controls? *Philosophical Transactions of the Royal Society B: Biological Sciences*, **368**.

Cambardella CA, Gajda AM, Doran JW, Wienhold BJ, Kettler TA (2001) Estimation of particulate and total organic matter by weight loss-on-ignition. In: *Assessment Methods for Soil Carbon* (eds Lal R, Kimble JM, Follett RJ, Stewart BA), pp. 349–359. Lewis Publishers/CRC Press, Boca Raton, FL.

Cayuela ML, van Zwieten L, Singh BP, Jeffery S, Roig A, Sánchez-Monedero MA (2014) Biochar's role in mitigating soil nitrous oxide emissions: A review and meta-analysis. *Agriculture, Ecosystems and Environment*, **191**, 5–16.

Chantigny MH, Angers DA, Kaiser K, Kalbitz K (2007) Extraction and characterization of dissolved organic matter. In: *Soil Sampling and Methods of Analysis*, 2nd edn (eds Carter MR, Gregorich EG), pp. 617–635. CRC Press, Boca Raton.

Christiansen JR, Korhonen JFJ, Juszczak R, Giebels M, Pihlatie M (2011) Assessing the effects of chamber placement, manual sampling and headspace mixing on CH4 fluxes in a laboratory experiment. *Plant and Soil*, **343**, 171–185.

Ciais P, Sabine C, Bala G et al. (2013) Carbon and other biogeochemical cycles. In: *Climate Change 2013: The Physical Science Basis. Contribution of Working Group I to the Fifth Assessment Report of the Intergovernmental Panel on Climate Change* (eds Stocker TF, Qin D, Plattner G-K, Tignor M, Allen SK, Boschung J, Nauels A, Xia Y, Bex V, Midgley PM), pp. 465–570. Cambridge University Press, Cambridge, United Kingdom and New York, NY, USA.

Datta R, Vranová V, Pavelka M, Rejšek K, Formánek P (2014) Effect of soil sieving on respiration induced by low-molecular-weight substrates. *International Agrophysics*, **28**, 119–124.

Ellert BH, Bettany JR (1995) Calculation of organic matter and nutrients stored in soils under contrasting management regimes. *Canadian Journal of Soil Science*, **75**, 529–538.

Galinato SP, Yoder JK, Granatstein D (2011) The economic value of biochar in crop production and carbon sequestration. *Energy Policy*, **39**, 6344–6350.

Gross A, Glaser B (2021) Meta-analysis on how manure application changes soil organic carbon storage. *Scientific Reports*, **11**, 1–13.

Gross CD, Harrison RB (2019) The case for digging deeper: Soil organic carbon storage, dynamics, and controls in our changing world. *Soil Systems*, **3**, 28.

Guo LB, Gifford RM (2002) Soil carbon stocks and land use change: A meta analysis. *Global change biology*, **8**, 345–360.

Gurwick NP, Moore LA, Kelly C, Elias P (2013) A systematic review of biochar research, with a focus on its stability in situ and its promise as a climate mitigation strategy. *PLoS ONE*, **8**.

von Haden AC, Yang WH, DeLucia EH (2020) Soils' dirty little secret: Depth-based comparisons can be inadequate for quantifying changes in soil organic carbon and other mineral soil properties. *Global Change Biology*, **26**, 3759–3770.

Haney RL, Franzluebbers AJ, Hons FM, Hossner LR, Zuberer DA (2001) Molar concentration of K2SO4 and soil pH affect estimation of extractable C with chloroform fumigation-extraction. *Soil Biology and Biochemistry*, **33**, 1501–1507.

Hao X, Chang C, Larney FJ (2004) Carbon, nitrogen balances and greenhouse gas emission during cattle feedlot manure composting. *Journal of Environmental Quality*, **33**, 37–44.

Harrison RB, Footen PW, Strahm BD (2011) Deep soil horizons: Contribution and importance to soil carbon pools and in assessing whole-ecosystem response to management and global change. *Forest Science*, **57**, 67–76.

Hedges J, Stern J (1984) Carbon and nitrogen determinations of carbonate-containing solids. *Limnology and Oceanography*, **29**, 657–663.

Hernandez-Soriano MC, Kerré B, Goos P, Hardy B, Dufey J, Smolders E (2016a) Long-term effect of biochar on the stabilization of recent carbon: Soils with historical inputs of charcoal. *GCB Bioenergy*, **8**, 371–381.

Hernandez-Soriano MC, Kerré B, Kopittke PM, Horemans B, Smolders E (2016b) Biochar affects carbon composition and stability in soil: A combined spectroscopy-microscopy study. *Scientific Reports*, **6**, 1–13.

Horwath WR, Paul EA (1994) Microbial biomass. In: *Methods of Soil Analysis: Part 2—Microbiological and Biochemical Properties, SSSA Book Series no. 5* (eds Bottomley PS, Angle JS, Weaver RW), pp. 753–774. Soil Science Society of America, Madison.

Hüppi R, Felber R, Krauss M, Six J, Leifeld J, Fuß R (2018) Restricting the nonlinearity parameter in soil greenhouse gas flux calculation for more reliable flux estimates. *PLoS ONE*, **13**, 1–17.

IPCC (2014) *Climate Change 2014: Synthesis Report. Contribution of Working Groups I, II and III to the Fifth Assessment Report of the Intergovernmental Panel on Climate Change [Core*

Writing Team, R.K. Pachauri and L.A. Meyer (eds.)]. Geneva, Switzerland, 151 pp.

Jandl R, Rodeghiero M, Martinez C et al. (2014) Current status, uncertainty and future needs in soil organic carbon monitoring. *Science of the Total Environment*, **468**–**469**, 376–383.

Jeffery S, Verheijen FGA, Kammann C, Abalos D (2016) Biochar effects on methane emissions from soils: A meta-analysis. *Soil Biology and Biochemistry*, **101**, 251–258.

Jenkinson DS, Brookes PC, Powlson DS (2004) Measuring soil microbial biomass. *Soil Biology and Biochemistry*, **36**, 5–7.

Kaiser M, Berhe AA (2014) How does sonication affect the mineral and organic constituents of soil aggregates? - A review. *Journal of Plant Nutrition and Soil Science*, **177**, 479–495.

Kettler TA, Doran JW, Gilbert TL (2001) Simplified method for soil particle-size determination to accompany soil-quality analyses. *Soil Science Society of America Journal*, **65**, 849–852.

Kleber M, Sollins P, Sutton R (2007) A conceptual model of organo-mineral interactions in soils: Self-assembly of organic molecular fragments into zonal structures on mineral surfaces. *Biogeochemistry*, **85**, 9–24.

Lehmann J, Kleber M (2015) The contentious nature of soil organic matter. *Nature*, **528**, 60–8.

Lehmann J, Gaunt J, Rondon M (2006) Bio-char sequestration in terrestrial ecosystems - A review. *Mitigation and Adaptation Strategies for Global Change*, **11**, 403–427.

Lehmann J, Rillig MC, Thies J, Masiello CA, Hockaday WC, Crowley D (2011) Biochar effects on soil biota - A review. *Soil Biology and Biochemistry*, **43**, 1812–1836.

Li Y, Li Y, Chang SX, Yang Y, Fu S, Jiang P (2018) Biochar reduces soil heterotrophic respiration in a subtropical plantation through increasing soil organic carbon recalcitrancy and decreasing carbon-degrading microbial activity. *Soil Biology and Biochemistry*, **122**, 173–185.

Major J, Rondon M, Molina D, Riha SJ, Lehmann J (2010) Maize yield and nutrition during 4 years after biochar application to a Colombian savanna oxisol. *Plant and Soil*, **333**, 117–128.

Mao J, Zhang K, Chen B (2019) Linking hydrophobicity of biochar to the water repellency and water holding capacity of biochar-amended soil. *Environmental Pollution*, **253**, 779–789.

Martínez-Blanco J, Lazcano C, Christensen TH et al. (2013) Compost benefits for agriculture evaluated by life cycle assessment. A review. *Agronomy for Sustainable Development*, **33**, 721–732.

Michel FC, Pecchia JA, Rigot J, Keener HM (2004) Mass and nutrient losses during the composting of dairy manure amended with sawdust or straw. *Compost Science and Utilization*, **12**, 323–334.

Neff JC, Asner GP (2001) Dissolved organic carbon in terrestrial ecosystems: Synthesis and a model. *Ecosystems*, **4**, 29–48.

Nyborg M, Laidlaw JW, Solberg ED, Malhi SS (1997) Denitrification and nitrous oxide emissions from a black chernozemic soil during spring thaw in Alberta. *Canadian Journal of Soil Science*, **77**, 153–160.

Oertel C, Matschullat J, Zurba K, Zimmermann F, Erasmi S (2016) Greenhouse gas emissions from soils—A review. *Chemie der Erde*, **76**, 327–352.

Ojeda G, Mattana S, Àvila A, Alcañiz JM, Volkmann M, Bachmann J (2015) Are soil-water functions affected by biochar application? *Geoderma*, **249**–**250**, 1–11.

Pedersen AR, Petersen S. O., Schelde K. (2010) A comprehensive approach to soil-atmosphere trace-gas flux estimation with static chambers. *European Journal of Soil Science*, **61**, 888–902.

Pokharel P, Kwak JH, Ok YS, Chang SX (2018) Pine sawdust biochar reduces GHG emission by decreasing microbial and enzyme activities in forest and grassland soils in a laboratory experiment. *Science of the Total Environment*, **625**, 1247–1256.

Ramnarine R, Voroney RP, Wagner-Riddle C, Dunfield KE (2011) Carbonate removal by acid fumigation for measuring the δ13C of soil organic carbon. *Canadian Journal of Soil Science*, **91**, 247–250.

Roberts KG, Gloy BA, Joseph S, Scott NR, Lehmann J (2010) Life cycle assessment of biochar systems: Estimating the energetic, economic, and climate change potential. *Environmental Science and Technology*, **44**, 827–833.

RStudio Team (2021) *RStudio: Integrated Development Environment for R*. Boston, MA.

Ryals R, Hartman MD, Parton WJ, Delonge MS, Silver WL (2015) Long-term climate change mitigation potential with organic matter management on grasslands. *Ecological Applications*, **25**, 531–545.

Sanderman J, Baldock JA, Amundson R, Baldock JA (2008) Dissolved organic carbon chemistry and dynamics in contrasting forest and grassland soils. *Biogeochemistry*, **89**, 181–198.

Shakoor A, Shahzad SM, Chatterjee N et al. (2021) Nitrous oxide emission from agricultural

soils: Application of animal manure or biochar? A global meta-analysis. *Journal of Environmental Management*, **285**, 112170.

Shrestha BM, Chang SX, Bork EW, Carlyle CN (2018) Enrichment planting and soil amendments enhance carbon sequestration and reduce greenhouse gas emissions in agroforestry systems: A review. *Forests*, **9**, 1–18.

Sleutel S, De Neve S, Németh T, Tóth T, Hofman G (2006) Effect of manure and fertilizer application on the distribution of organic carbon in different soil fractions in long-term field experiments. *European Journal of Agronomy*, **25**, 280–288.

Sohi SP, Krull E, Lopez-Capel E, Bol R (2010) A review of biochar and its use and function in soil. *Advances in Agronomy*, **105**, 47–82.

Spokas KA, Cantrell KB, Novak JM et al. (2012) Biochar: A synthesis of its agronomic impact beyond carbon sequestration. *Journal of Environmental Quality*, **41**, 973–989.

Stavi I, Lal R (2013) Agroforestry and biochar to offset climate change: A review. *Agronomy for Sustainable Development*, **33**, 81–96.

Stockmann U, Adams MA, Crawford JW et al. (2013) The knowns, known unknowns and unknowns of sequestration of soil organic carbon. *Agriculture, Ecosystems and Environment*, **164**, 80–99.

Tautges NE, Chiartas JL, Gaudin ACM, O'Geen AT, Herrera I, Scow KM (2019) Deep soil inventories reveal that impacts of cover crops and compost on soil carbon sequestration differ in surface and subsurface soils. *Global Change Biology*, **25**, 3753–3766.

Vance ED, Brookes PC, Jenkinson DS (1987) An extraction method for measuring soil microbial biomass C. *Soil Biology and Biochemistry*, **19**, 703–707.

Venterea RT, Burger M, Spokas KA (2005) Nitrogen oxide and methane emissions under varying tillage and fertilizer management. *Journal of Environment Quality*, **34**, 1467.

Virto I, Barré P, Chenu C (2008) Microaggregation and organic matter storage at the silt-size scale. *Geoderma*, **146**, 326–335.

Walthert L, Graf U, Kammer A, Luster J, Pezzotta D, Zimmermann S, Hagedorn F (2010) Determination of organic and inorganic carbon, δ13C, and nitrogen in soils containing carbonates after acid fumigation with HCl. *Journal of Plant Nutrition and Soil Science*, **173**, 207–216.

Wendt JW (2013) ESM sample spreadsheets.

Wendt JW, Hauser S (2013) An equivalent soil mass procedure for monitoring soil organic carbon in multiple soil layers. *European Journal of Soil Science*, **64**, 58–65.

Weng Z (Han), Van Zwieten L, Singh BP et al. (2017) Biochar built soil carbon over a decade by stabilizing rhizodeposits. *Nature Climate Change*, **7**, 371–376.

Yousaf B, Liu G, Wang R, Abbas Q, Imtiaz M, Liu R (2017) Investigating the biochar effects on C-mineralization and sequestration of carbon in soil compared with conventional amendments using the stable isotope (δ13C) approach. *GCB Bioenergy*, **9**, 1085–1099.

Yu H, Ding W, Luo J, Geng R, Cai Z (2012) Long-term application of organic manure and mineral fertilizers on aggregation and aggregate-associated carbon in a sandy loam soil. *Soil and Tillage Research*, **124**, 170–177.

Zsolnay Á (2003) Dissolved organic matter: Artefacts, definitions, and functions. *Geoderma*, **113**, 187–209.

3.8. Tables

Table 3.1. Soil properties among three soil amendment treatments sampled across ten agricultural sites in central Alberta, Canada, as measured in spring 2020 (spring 2018 pretreatment values were used as a covariate for statistical analysis). Least-squares means (one standard error) within each depth layer accompanied by different lowercase letters are significantly different (Tukey-adjusted, $\alpha = 0.05$) among the treatments. BD, bulk density; OC, organic carbon; N, total nitrogen; Conc., concentration.

Soil depth & treatment	BD ($g\ cm^{-3}$)	pH	OC Conc. ($mg\ g^{-1}$ soil)	N Conc. ($mg\ g^{-1}$ soil)	OC:N
0–10 cm					
Control	1.30 (0.04)	5.74 (0.20) b	40.24 (1.10) b	3.60 (0.07) b	11.10 (0.21) b
Manure compost	1.34 (0.04)	5.92 (0.20) ab	42.29 (1.10) b	3.72 (0.07) b	11.31 (0.21) b
Biochar	1.27 (0.04)	6.04 (0.20) a	51.90 (1.10) a	3.95 (0.07) a	13.11 (0.21) a
10–30 cm					
Control	1.32 (0.04)	6.43 (0.08)	21.09 (1.91)	1.99 (0.16)	10.42 (0.24)
Manure compost	1.30 (0.04)	6.39 (0.08)	23.57 (1.92)	2.16 (0.16)	10.49 (0.25)
Biochar	1.29 (0.04)	6.48 (0.08)	19.49 (1.94)	1.86 (0.16)	10.47 (0.24)
30–50 cm[†]					
Control	1.30 (0.07)	6.97 (0.09)	10.17 (0.81)	0.99 (0.07)	10.16 (0.44)
Manure compost	1.30 (0.07)	7.06 (0.09)	9.28 (0.82)	0.98 (0.07)	9.34 (0.44)
Biochar	1.32 (0.07)	7.06 (0.09)	9.27 (0.81)	1.03 (0.07)	9.00 (0.44)
50–100 cm[†]					
Control	1.62 (0.06)	8.10 (0.11)	7.04 (0.86)	0.58 (0.05)	11.65 (0.68)
Manure compost	1.52 (0.06)	8.10 (0.11)	6.91 (0.86)	0.61 (0.05)	11.25 (0.68)
Biochar	1.51 (0.06)	8.07 (0.11)	6.39 (0.86)	0.60 (0.05)	10.94 (0.68)

[†] Each soil layer was tested for *post-hoc* statistical differences only if the overlying layer showed a main effect of treatment for the respective soil property.

Table 3.2. Soil water soluble and microbial carbon and nitrogen among three soil amendment treatments sampled across ten agricultural sites in central Alberta, Canada, as measured in (a) spring 2020 (spring 2018 pretreatment values were used as a covariate for statistical analysis) and (b) fall 2020. Least-squares means (one standard error) within each depth layer accompanied by different lowercase letters are significantly different (Tukey-adjusted, $\alpha = 0.05$) among the treatments. WSOC, water-soluble organic carbon; WSN, water-soluble total nitrogen; MBC, microbial biomass carbon; MBN, microbial biomass nitrogen; Conc., concentration.

Soil depth & treatment	WSOC Conc. (μg OC g^{-1} soil)	WSN Conc. (μg N g^{-1} soil)	WSOC:WSN	MBC Conc. (μg OC g^{-1} soil)	MBN Conc. (μg N g^{-1} soil)
(a) Soils collected in spring 2020					
0–10 cm					
Control	27.86 (2.66)	19.99 (2.90)	2.35 (0.39) b	271.46 (25.38)	22.55 (2.57)
Manure compost	30.43 (2.66)	16.87 (2.90)	2.70 (0.39) ab	262.42 (25.24)	24.69 (2.54)
Biochar	29.45 (2.66)	16.06 (2.90)	3.71 (0.39) a	233.91 (25.49)	22.50 (2.58)
10–30 cm					
Control	14.71 (1.16) b	4.80 (0.68)	3.55 (0.31)	81.30 (6.96)	6.29 (0.64)
Manure compost	17.26 (1.16) a	5.26 (0.68)	3.82 (0.31)	77.44 (6.90)	6.06 (0.63)
Biochar	16.20 (1.16) ab	5.82 (0.68)	3.81 (0.31)	76.48 (7.10)	5.83 (0.65)
30–50 cm[†]					
Control	11.69 (2.43)	2.42 (0.29)	5.08 (0.53)	37.41 (4.76)	2.88 (0.33)
Manure compost	11.78 (2.43)	2.35 (0.29)	5.15 (0.53)	40.94 (4.72)	2.84 (0.32)
Biochar	16.64 (2.42)	2.76 (0.29)	6.56 (0.53)	40.22 (4.76)	3.37 (0.35)
50–100 cm[†]					
Control	17.36 (3.22)	1.81 (0.18)	9.90 (1.24)	12.66 (2.38)	1.15 (0.14)
Manure compost	14.11 (3.24)	1.67 (0.18)	9.57 (1.22)	14.25 (2.31)	1.19 (0.14)
Biochar	22.34 (3.20)	1.90 (0.18)	11.41 (1.21)	18.54 (2.35)	1.39 (0.14)
(b) Soils collected in fall 2020					
0–10 cm					
Control	31.15 (3.12)	5.91 (1.04) a	5.71 (0.78) b	275.98 (39.81)	28.39 (4.12)
Manure compost	31.92 (3.12)	5.81 (1.04) a	6.56 (0.78) b	241.92 (39.81)	26.42 (4.12)
Biochar	28.70 (3.12)	3.95 (1.04) b	8.23 (0.78) a	249.20 (39.81)	28.09 (4.12)
10–30 cm					
Control	18.21 (2.52)	2.50 (0.45)	7.88 (0.95)	84.82 (9.26)	6.53 (0.96)
Manure compost	19.67 (2.52)	2.48 (0.45)	8.90 (0.95)	80.34 (9.26)	6.62 (0.96)
Biochar	20.66 (2.52)	2.53 (0.45)	8.59 (0.95)	96.28 (9.26)	7.64 (0.96)

[†] Each soil layer was tested for *post-hoc* statistical differences only if the overlying layer showed a main effect of treatment for the respective soil property.

3.9. Figures

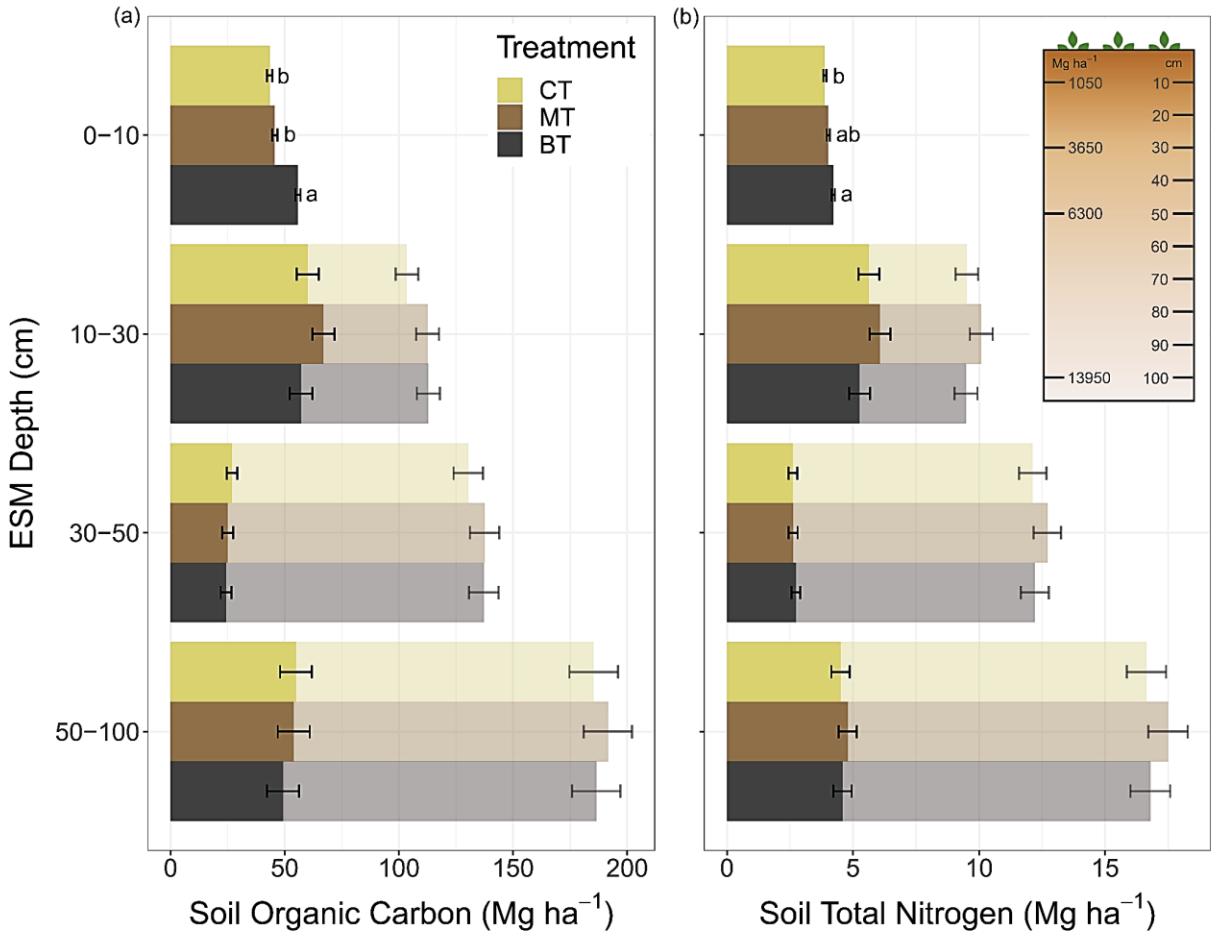

Figure 3.1. (a) Soil organic carbon (SOC) and (b) total nitrogen (N) stocks among three soil amendment treatments sampled across ten agricultural sites in central Alberta, Canada, as measured in spring 2020 (spring 2018 pretreatment values were used as a covariate for statistical analysis). Transparent columns are cumulative stocks based on equivalent soil mass (ESM). Error bars represent ± one standard error. Least-squares means within each ESM depth layer or total cumulative mass accompanied by different lowercase letters are significantly different (Tukey-adjusted, $\alpha = 0.05$) among the treatments. The soil profile illustrates the relationship between soil mass and approximate sampling depth. CT, control treatment; MT, manure compost treatment; BT, biochar treatment.

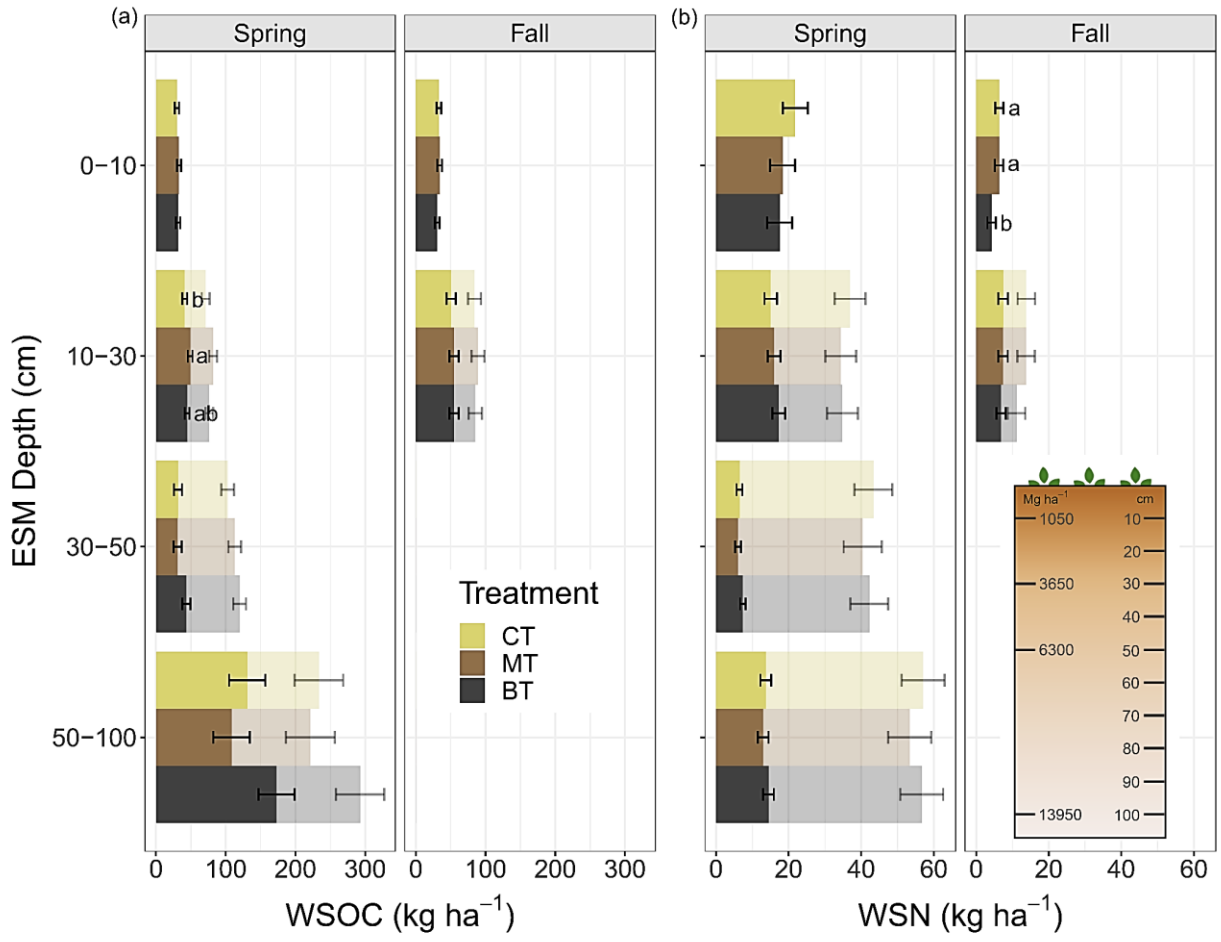

Figure 3.2. (a) Soil water-soluble organic carbon (WSOC) and (b) soil water-soluble total nitrogen (WSN) stocks among three soil amendment treatments sampled across ten agricultural sites in central Alberta, Canada, as measured in spring 2020 (spring 2018 pretreatment values were used as a covariate for statistical analysis) and fall 2020. Transparent columns are cumulative stocks based on equivalent soil mass (ESM). Error bars represent ± one standard error. Least-squares means within each ESM depth layer or total cumulative mass accompanied by different lowercase letters are significantly different (Tukey-adjusted, $\alpha = 0.05$) among the treatments. The soil profile illustrates the relationship between soil mass and approximate sampling depth. CT, control treatment; MT, manure compost treatment; BT, biochar treatment.

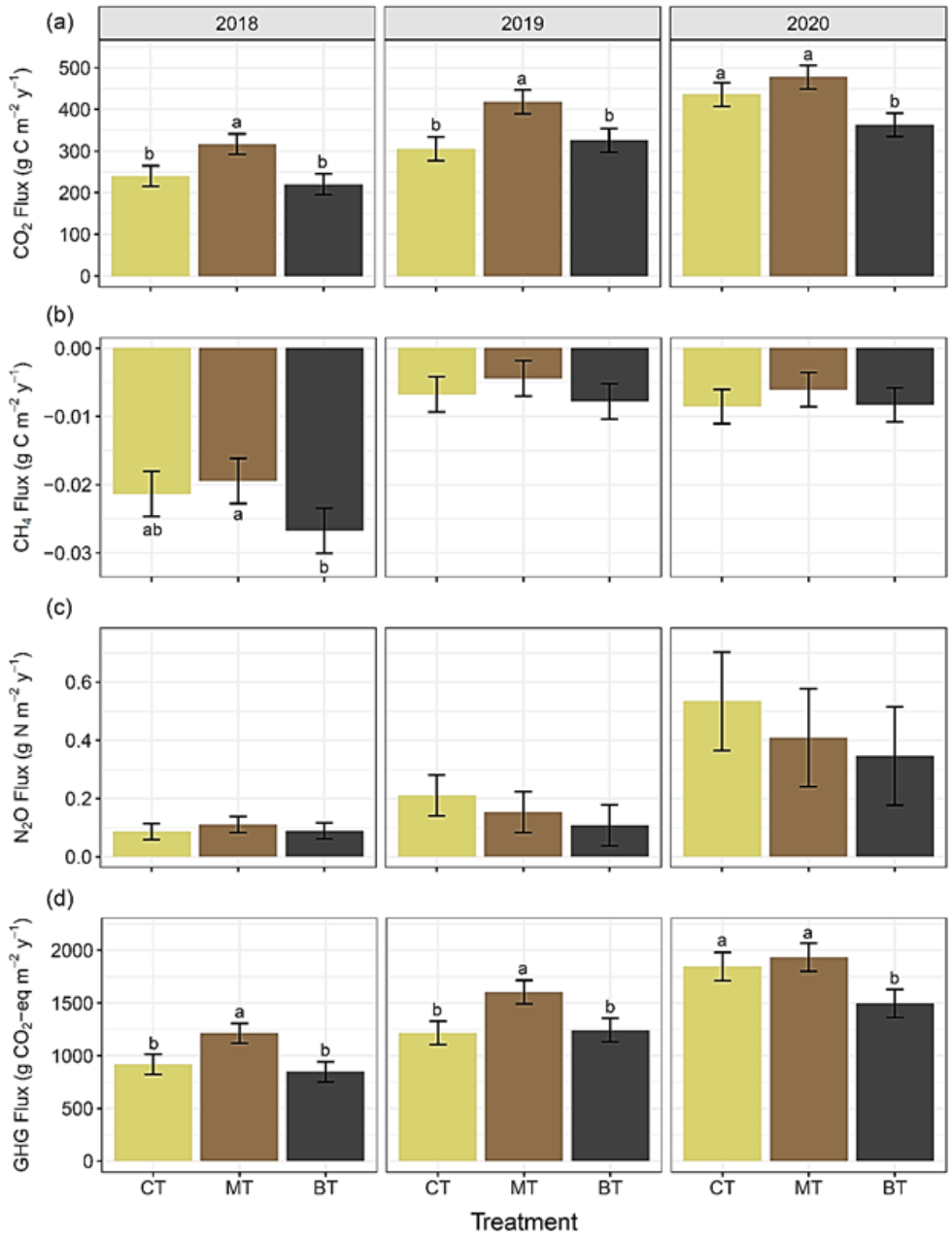

Figure 3.3. Soil (a) carbon dioxide (CO_2), (b) methane (CH_4), (c) nitrous oxide (N_2O), and (d) total greenhouse gas (GHG; sum of CO_2, CH_4, and N_2O) fluxes by year among three soil amendment treatments sampled across ten agricultural sites in central Alberta, Canada. Error bars represent ± one standard error. Least-squares means within each year accompanied by different lowercase letters are significantly different (Tukey-adjusted, $\alpha = 0.05$) among the treatments. CT, control treatment; MT, manure compost treatment; BT, biochar treatment.

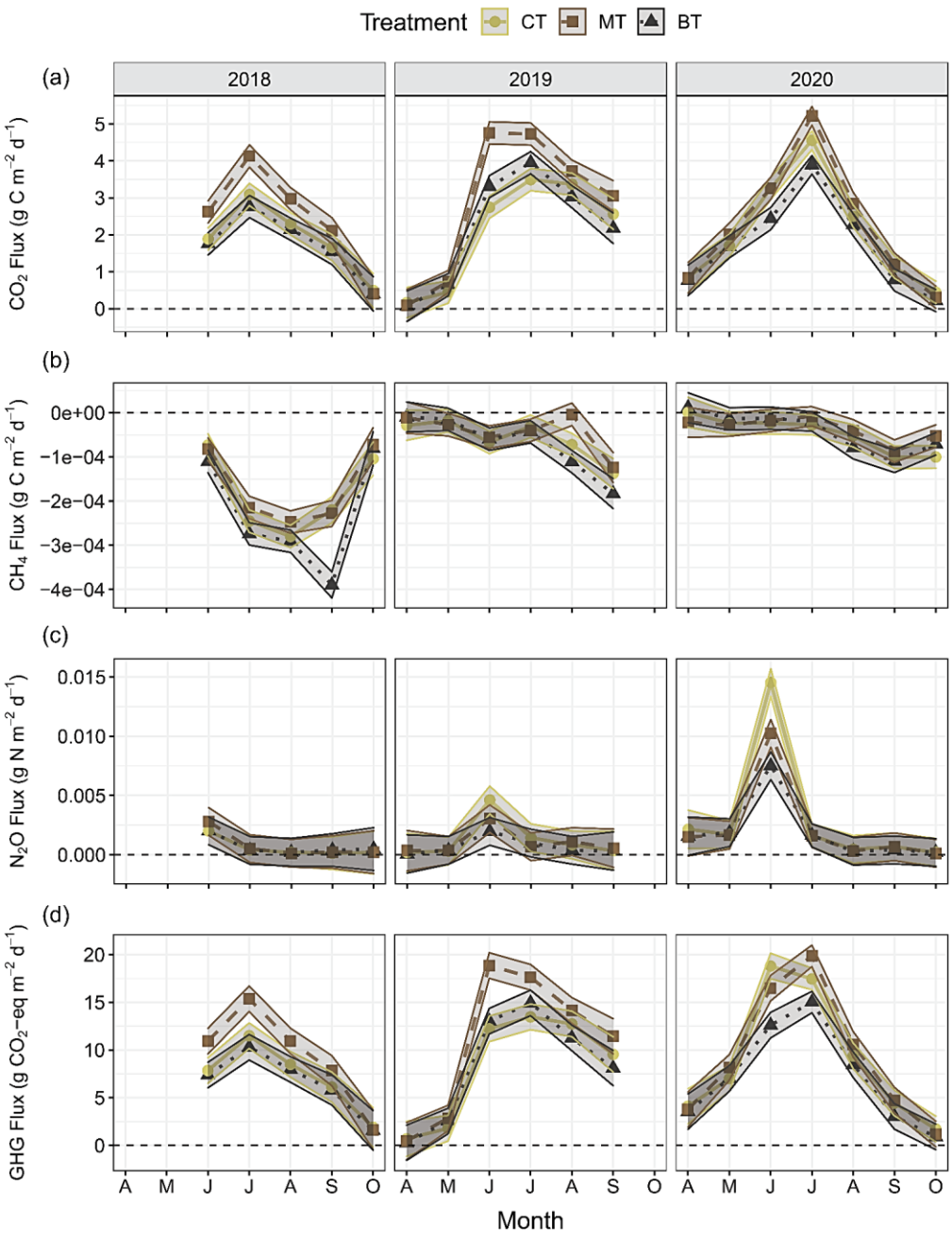

Figure 3.4. Soil (a) carbon dioxide (CO_2), (b) methane (CH_4), (c) nitrous oxide (N_2O), and (d) greenhouse gas (GHG; sum of CO_2, CH_4, and N_2O) fluxes by month and year among three soil amendment treatments sampled across ten agricultural sites in central Alberta, Canada. Error ribbons represent least-squares means ± one standard error. CT, control treatment; MT, manure compost treatment; BT, biochar treatment.

Chapter 4. Root-driven destabilization of clay-protected carbon within silt-size microaggregates

Cole D. Gross[1], Edward W. Bork[2], Björn Wissel[3], Cameron N. Carlyle[2], Scott X. Chang[1]

[1] Department of Renewable Resources, Faculty of Agricultural, Life and Environmental Sciences, University of Alberta, 442 Earth Sciences Building, Edmonton, AB T6G 2E3, Canada; cgross@ualberta.ca (C.D.G.); sxchang@ualberta.ca (S.X.C.)

[2] Department of Agricultural, Food and Nutritional Science, Faculty of Agricultural, Life and Environmental Sciences, University of Alberta, 410 Agriculture/Forestry Centre, Edmonton, AB T6G 2P5, Canada; ebork@ualberta.ca (E.W.B.); cameron.carlyle@ualberta.ca (C.N.C.)

[3] LEHNA, Université Claude Bernard Lyon 1, 69622 Villeurbanne, France; bjoern.wissel@univ-lyon1.fr (B.W.)

4.1. Abstract

Living roots and their fresh carbon (C) inputs can initially result in intensified loss (a.k.a. priming) of soil organic C (SOC), which has important implications for C-capture initiatives. Protection of SOC occurs through mineral sorption and soil aggregation. How sorption of C to clay within silt-size microaggregates may protect SOC from microbial decomposition and play a role in root-driven SOC dynamics is not well understood. Here I quantified SOC changes due to the influence of living roots in soils with varying properties collected from three different land uses (cropland, grassland, and woodland) and soil depths (0–10, 10–30, and 30–50 cm) using the C stable isotope natural abundance technique. Following a 150-d incubation in a controlled growth chamber, paired non-planted and planted (*Bouteloua gracilis*) soils were fractioned into particulate organic matter, silt, non-aggregated clay, and clay within water-stable silt-size microaggregates (aggregated clay). Nearly a third of total SOC was associated with the aggregated clay fraction. In soils with greater SOC content (that is, surface and woodland soils relative to subsurface and cropland soils, respectively), a larger proportion of clay-protected C was within silt-size microaggregates. Priming of soil-derived C was limited to the aggregated clay fraction, greatest in the surface soil (0.51–1.27 mg C g^{-1} soil), and similar across land uses. Microbial growth, root-derived C incorporation into the aggregated clay fraction, and reductions in the mass of the aggregated clay fraction, were positively correlated with priming. Root-derived C comprised 7–13% of the C associated with the aggregated clay fraction, indicating rapid incorporation of root-derived C into silt-size microaggregates. I show that living roots can destabilize clay-protected C within silt-size microaggregates, leading to rapid and preferential decomposition of clay-protected C. This has important implications for our understanding of SOC persistence and the underlying processes used in soil C models.

Graphical abstract:

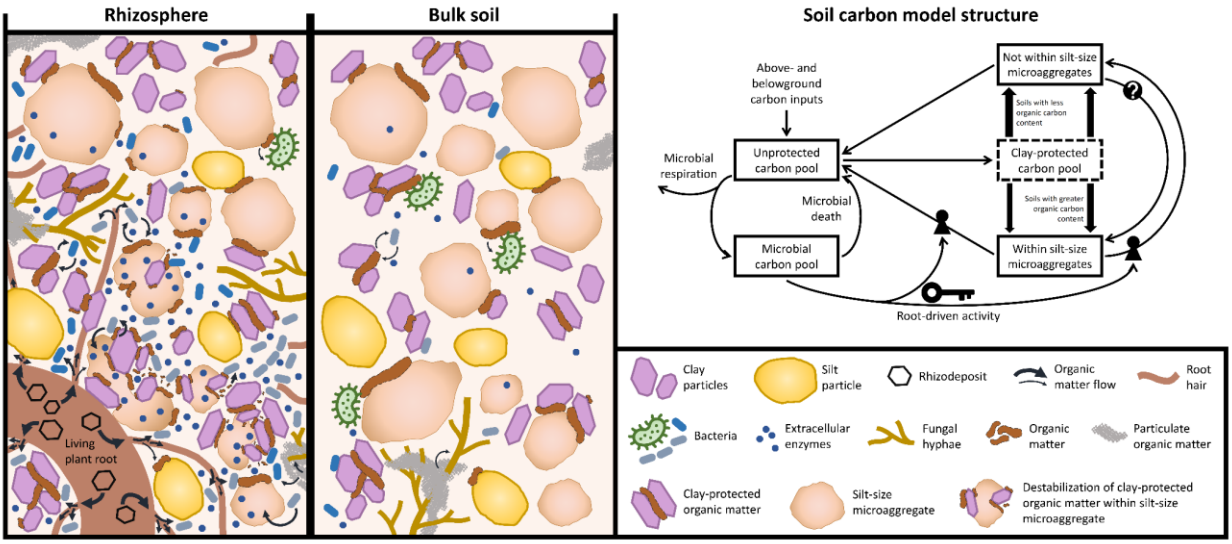

We show that living roots can destabilize clay-protected carbon within silt-size microaggregates, leading to rapid and preferential decomposition of clay-protected carbon. This has important implications for our understanding of soil organic carbon persistence and the underlying processes used in soil carbon models.

Keywords: labile carbon, microbial biomass, mineral-associated organic carbon, particulate organic matter, rhizosphere priming, soil aggregation, stable isotopes

Highlights:

- The aggregated clay fraction stored nearly a third of total soil organic carbon.
- Priming was limited to the aggregated clay fraction and greatest in the surface soil.
- Priming increased with microbial growth and root-derived carbon in aggregated clay.
- Priming increased with reductions in the mass of the aggregated clay fraction.
- Living roots can destabilize clay-protected carbon within silt-size microaggregates.

4.2. Introduction

Soil is the largest terrestrial carbon (C) stock (Lehmann & Kleber, 2015) and acts as a global C sink, sequestering around 20–30% of anthropogenic C emissions annually (Pan *et al.*, 2011; Le Quéré *et al.*, 2018). Utilizing land use and management practices to increase soil organic C (SOC) storage is considered key to helping drawdown atmospheric CO_2 as we reduce fossil fuel emissions to mitigate climate change (IPCC, 2022). Moreover, increasing SOC can enhance the resilience of agricultural land to drought and other climate changes by increasing overall soil health (such as nutrient- and water-holding capacities, soil aggregation and aeration, and microbial diversity) (Amundson & Biardeau, 2018). Therefore, how soils cycle and store new C inputs has important implications for both the global C cycle and food security (Lorenz & Lal, 2022). Land use and management practices that increase C inputs to soil may have dual effects on soil C dynamics, in some cases resulting in intensified loss (a.k.a. priming) of SOC and initially reducing SOC storage (Dijkstra *et al.*, 2021).

Land use and management practices aimed at increasing SOC include conversion of annually cropped land to perennial ecosystems, such as secondary forest or grassland, the adoption of agroforestry systems, or incorporation of perennial or cover crops (Paustian *et al.*, 2016; Schlautman *et al.*, 2021; IPCC, 2022). These practices increase root litter and exudate C inputs (together termed rhizodeposition) to both surface and deeper soil layers. Warming and elevated atmospheric CO_2 concentrations are expected to increase above- and belowground vegetation growth in many regions globally (Jones *et al.*, 2005; Ciais *et al.*, 2013), which would also increase C inputs to soil via rhizodeposition. In terrestrial ecosystems, living roots can have both stabilizing and destabilizing effects on SOC (Dijkstra *et al.*, 2021). For example, living roots increase microbial turnover and, in turn, microbial necromass that can be stabilized in the soil (Zhu *et al.*, 2020; Dijkstra *et al.*, 2021; Sokol *et al.*, 2022). However, by providing fresh C inputs and enhancing microbial activity, living roots can also intensify the loss of SOC, a phenomenon referred to as priming (Kuzyakov *et al.*, 2000). Priming effects may lead to initial net decreases in SOC storage despite additional C inputs (Dijkstra & Cheng, 2007; Sulman *et al.*, 2014; Dijkstra *et al.*, 2021).

Mineral sorption is widely considered to play a fundamental role in the protection of SOC from microbial decomposition and occurs mainly within the clay fraction (Angst *et al.*, 2018; Rasmussen *et al.*, 2018). This mineral-associated C is largely composed of microbial products that

may be predominantly derived from rhizodeposition (Liang *et al.*, 2017; Sokol & Bradford, 2019; Sokol *et al.*, 2019). However, root exudates can rapidly foster the release of mineral-associated C into the dissolved organic C pool, rendering the C more labile (Clarholm *et al.*, 2015; Keiluweit *et al.*, 2015). Root-exudate mediated C release from mineral-C associations may help explain the greater contribution of root exudates relative to root litter with respect to priming effects (Shahzad *et al.*, 2015; Pierson *et al.*, 2021), as well as the increased vulnerability of finer- rather than coarser-textured soils to rhizosphere priming (Huo *et al.*, 2017). Deeper soil layers, where the SOC is often hundreds to thousands of years old (Fontaine *et al.*, 2007; Schmidt *et al.*, 2011) and storage mainly occurs via sorption to clay particles (Angst *et al.*, 2018), are also susceptible to rhizosphere priming effects (Mobley *et al.*, 2015; Tian *et al.*, 2016; Shahzad *et al.*, 2018).

In addition to mineral sorption, SOC protection from microbial decomposition is provided by soil aggregation. Microaggregates (< 250 μm), which are stabilized within macroaggregates (> 250 μm), are particularly important for providing SOC protection by creating anoxic conditions or making C less physically accessible to microorganisms (Six *et al.*, 2002; Rasse *et al.*, 2005; Totsche *et al.*, 2018). The most stable aggregates are silt-size microaggregates (2–53 μm), which largely exclude bacteria from their micropores, thereby physically protecting C that is not on the periphery (Rasse *et al.*, 2005; Lavallee *et al.*, 2019; Yang *et al.*, 2021). Several studies have observed that a substantial portion of SOC is in the form of C bound to clay within silt-size microaggregates (Virto *et al.*, 2008, 2010; Moni *et al.*, 2010). Because this C is both physically and chemically protected from microorganisms, it may persist longer in soil than C that is unprotected or protected by other abiotic mechanisms (Lehmann *et al.*, 2007; Virto *et al.*, 2010; Totsche *et al.*, 2018). Whether this dual protection mechanism renders this C less susceptible to root-driven priming effects is unknown because most aggregation studies do not consider aggregates at the silt-size scale (Virto *et al.*, 2008; Totsche *et al.*, 2018; Lavallee *et al.*, 2019). A recent study found that clay-protected C within model silt-size microaggregates can be broken down by extracellular enzymes (exoenzymes) into smaller fragments that are then released into solution (Yang *et al.*, 2021). However, how clay-protected C within silt-size microaggregates is affected by living roots in natural soils has not been investigated.

Here I used the ^{13}C natural abundance technique to quantify root-driven SOC dynamics in soils with varying properties (texture, pH, C and N content, etc.) collected from three different land uses (cropland, grassland, and woodland) and depths (0–10, 10–30, and 30–50 cm) by

planting a native perennial C_4 plant species (blue grama, *Bouteloua gracilis* (Willd. ex Kunth.) Lag. Ex Griffiths) in soils derived from C_3 plant systems. My objectives were to 1) elucidate the interplay of physical and chemical protection of C under the influence of living roots by quantifying root C incorporation and priming across different soil fractions, including clay-size particles within silt-size microaggregates, and 2) assess the interdependence of soil properties (including SOC storage within soil fractions) and root-driven SOC dynamics across land uses and soil depths.

4.3. Materials and methods

4.3.1. Soils used in incubation

I collected soils from three different land uses (cropland, grassland, and woodland) and depths (0–10, 10–30, and 30–50 cm) in May 2020 at ten producer-operated, annually cropped agroforestry sites in central Alberta, Canada. Soil was collected by augering (3.81-cm diameter) three holes per land-use type, and the soil was composited by depth. The historical monocultural annual crop rotation at all ten study sites was typically a combination of wheat (*Triticum aestivum* L.), barley (*Hordeum vulgare* L.), and canola (*Brassica rapa* L.). Perennial vegetated areas with and without trees (woodland and grassland, respectively) were usually at agricultural road/field margins. Common grasses were *Bromus inermis* (Leyss.), *Dactylis glomerata* (L.), and *Elymus sp.*, and common forbs were *Taraxacum officinale* (G. H. Weber *ex* Wiggers) and *Cirsium arvense* (L.). Tree species were deciduous and consisted of aspen (*Populus tremuloides* Michx.), willow (*Salix pentandra* L.), and balsam poplar (*Populus balsamifera* L.). The soils at all ten study sites and under each land-use type generally exhibited high levels of surface soil organic matter accumulation (Chernozems in the Canadian soil classification system or Ustic Haplocryolls in the United States soil taxonomy system). Basic soil properties are provided in Table C.S1. More detailed site and soil property information is provided in Gross *et al.* (2022).

After the soil samples were returned to the laboratory, field-moist soil was sieved to 8 mm by carefully separating the soil at natural breaks to minimize disturbance of the existing aggregate structure and disruption of soil microbial activity (Horwath & Paul, 1994; Datta *et al.*, 2014). Plant residues and coarse fragments (diameter > 2 mm) were removed from the soil. All soil samples were stored at 4 °C prior to the incubation.

4.3.2. Experimental design and incubation

The incubation experiment used a randomized complete block design. Pre-weighed polypropylene jars (64-mm diameter × 70-mm height) were filled with 60 g (oven-dry weight basis) of sieved (< 8 mm) field-moist soil. To minimize aggregate disruption, bulk density was controlled by repeatedly tapping the base of the jars, attaining a similar bulk density between duplicates. Soil moisture content was adjusted to 60% water-holding capacity by either air-drying or slowly and evenly adding ultrapure (MilliporeSigma Milli-Q) water. Soils were preincubated for 10 days in a growth chamber (Conviron CMP6050, Winnipeg, Manitoba, Canada) with 100% relative humidity, a 17-h photoperiod with 400 μmol m^{-2} s^{-1} light intensity, and temperatures of 26 and 13 °C in the day and night, respectively. To maintain the moisture content at 60% maximal water-holding capacity, soils were moistened with ultrapure water at 3-d intervals (see below for more details).

After the preincubation period, one set of the duplicate soils was planted with 0.3 g of blue grama seeds (Ontario Seed Co., Limited) (hereafter referred to as planted treatment), which were spread evenly over the soil surface. The paired planted and non-planted (bare soil) treatments were then incubated for 150 days under the same conditions as the preincubation period. An additional subset of the soils was planted with blue grama seeds and simultaneously incubated as a reference to determine the amount of water to be added to soils in the planted treatment. Soil in reference jars was destructively sampled weekly during the first half of the incubation to quantify and account for the mass of the fresh grass biomass (both above- and belowground) at various stages of phenological development.

After 150 days, the soil from both planted and non-planted treatments was gently removed from the jars and carefully separated at natural breaks to pass through an 8 mm sieve. Grass blades, stems, and roots were removed from the planted treatment, thoroughly washed with water on a 250-μm sieve, dried at 60 °C for 48 h, and weighed. Most roots were removed with tweezers, although some very fine roots remained embedded in aggregates. Planted and non-planted treatments were processed similarly to avoid any differential processing effect on the pairs. Subsequently, bulk soils were adjusted to 50% water-holding capacity and stored at 4 °C to minimize microbial biomass effects, as well as limit increases in the quantity or strength of organic C interactions with minerals or interactions between minerals, which can affect aggregate stability, labile organic C concentrations, and mineral-associated organic C (Kaiser *et al.*, 2015).

4.3.3. Roots, bulk soil, microbial biomass, and labile carbon analyses

Roots were ground to a fine powder using a stainless-steel ball mill and a composite subsample was analyzed (n = 4) on an Elemental Combustion System (Costech EA; ECSD 4010) that led into a Thermo-Finnigan Delta V isotope ratio mass spectrometer (IRMS). To obtain bulk soil C and nitrogen (N) concentrations, as well as $\delta^{13}C$ values ($\delta^{15}N$ values were generated but not used in this paper), subsamples were dried at 40 °C, ground to a fine powder with an agate mortar and pestle, and analyzed on the EA-IRMS. Prior to analysis, soils that contained carbonates (n = 9) were subject to acid fumigation for 72 h to remove carbonates so that measured soil C represented only organic C (Ramnarine *et al.*, 2011). A conversion factor was used to account for the increased weight of acidified soils so as to not dilute any organic C (Ramnarine *et al.*, 2011). Soils containing carbonates were confirmed prior to the incubation experiment by analyzing subsamples of all the soils with pH > 6.00 on an elemental analyzer (Vario MICRO Cube Elemental Analyzer, Elementar, Hesse, Germany) before and after acid fumigation. For analyses on the EA-IRMS, bovine liver and wheat flour were used as internal laboratory standards. Carbon isotopes are reported in the conventional δ notation (‰) relative to Vienna Pee-Dee-Belemnite for C stable isotopes (Cooper & Wissel, 2012). Samples that were analyzed as laboratory duplicates (9% of the samples) gave isotopic compositions that agreed within 0.2‰ for $\delta^{13}C$.

The chloroform fumigation-extraction procedure was used to measure soil microbial biomass (Vance *et al.*, 1987; Beck *et al.*, 1997). Duplicate subsamples of 5 g (oven-dry weight basis) of soil were fumigated in a vacuum chamber with ethanol-free chloroform for 48 h in darkness (Jenkinson *et al.*, 2004). Water-soluble organic matter was extracted from both fumigated and non-fumigated samples by shaking the samples with 0.01 M K_2SO_4 (1:5 w:v) for 1 h at 180 rpm (Haney *et al.*, 2001; Werth & Kuzyakov, 2010). After centrifuging at 10,000 × g for 10 min, 20 mL of the supernatant was collected and filtered through a 0.4-µm Whatman Nuclepore polycarbonate filter (Zsolnay, 2003; Chantigny *et al.*, 2007). Filtrates were stored at 4 °C prior to analysis with a total organic C (TOC) analyzer (TOC-V and TN unit, Shimadzu Corporation, Kyoto, Japan) using 680 °C combustion catalytic oxidation and the non-purgeable organic C (to remove inorganic C) and total N methods. Microbial biomass C (MBC) was calculated using an extraction efficiency of 0.45 (Jenkinson *et al.*, 2004). The organic C and total N in the non-fumigated samples were defined as water-soluble organic C (WSOC) and N (WSN). To obtain

$\delta^{13}C$ values, 10 mL aliquots of the filtrates were dried at 40 °C, and precipitates were agitated to a fine powder using a stainless-steel soil scoop and analyzed on the EA-IRMS. Prior to drying, 0.4 mL of 1 M HCl was added to the filtrate aliquots from soils that contained carbonates to remove inorganic C.

4.3.4. Physical soil fractionation and soil fraction analyses

Eight grams (oven-dry weight basis) of soil was fractioned into the following: coarse and fine particulate organic matter (POM), coarse and fine silt, non-aggregated clay, and clay within silt-size microaggregates. To protect water-stable silt-size microaggregates from being destroyed while breaking down larger aggregates (> 53 µm), the size-separation device described in detail by Virto *et al.* (2008) was used. Briefly, soil aggregates > 53 µm in size were broken up on a shaker (4 h at 180 rpm) using five glass beads (5-mm diameter) within a 30-mL plastic bottle sealed with a 53-µm-opening nylon cloth (Gilson Co. Inc., Columbus, OH) and contained within a 250-mL plastic bottle with 200 mL of ultrapure water (Virto *et al.*, 2008). This device allowed for the separation of materials < 53 µm in size from the abrasive effects within the small bottle, including water-stable silt-size microaggregates, which passed into the large bottle and remained in suspension during shaking (Virto *et al.*, 2008).

The sand + POM fraction collected in the small bottle was poured onto a 53-µm sieve and rinsed over a beaker with ultrapure water until the solution passing through the sieve was clear. The silt + clay fraction in the large bottle was added to the suspension in the beaker. The sand + POM fraction was backwashed into a 250-µm sieve over a larger 53-µm sieve and rinsed for an additional minute. For the fraction remaining on the 250-µm sieve (hereafter referred to as coarse POM), remaining roots in the planted treatment were removed with tweezers, oven-dried, and weighed. No roots were visible in the fraction collected on the 53-µm sieve (hereafter referred to as fine POM). The dry mass of recovered roots was added to the total root mass for a given planted treatment using a multiple that assumed uniformity in the remaining mass of roots in the bulk soil after initial root removal.

Sedimentation and centrifuging (until the supernatant was clear) according to Stoke's Law were used to separate the dispersed clay-size fraction (< 2 µm; hereafter referred to as non-aggregated clay) from the silt + clay fraction (Virto *et al.*, 2008). The remaining silt-size fraction (consisting of free silt-size particles and water-stable silt-size microaggregates) was subjected to

500 J cm^{-3} ultrasonic energy after transferring this fraction into a 100-mL glass beaker (45-mm diameter, 80-mm height) and adding ultrapure water to result in an 80-mL soil suspension (Kaiser & Berhe, 2014). The ultrasonic probe (Qsonica Q700, Newton, Connecticut, USA) was calibrated as described by Schmidt *et al.* (1999) and the probe tip (12-mm diameter) was immersed 18 mm into the suspension. Samples underwent sonification using 50% amplitude and a pulse:non-pulse ratio of 1:1 to avoid mass losses and prevent overheating of the probe and soil suspension (Yang *et al.*, 2009). To maintain soil suspension temperatures below 30 °C, the base of the beaker was cooled by the continuous circulation of compressed air during sonification.

Following the application of 500 J cm^{-3} ultrasonic energy to break up larger silt-size microaggregates (20–53 μm) (Kaiser & Berhe, 2014), the soil suspension was poured over a 20-μm sieve and rinsed over a beaker with ultrapure water until the solution passing through the sieve was clear. The silt-size fraction remaining on the 20-μm sieve is hereafter referred to as coarse silt. Sedimentation was used to separate most of the clay-size fraction (< 2 μm) dispersed after sonication (hereafter referred to as aggregated clay) from the soil suspension. The remaining soil suspension, which was stored at 4 °C for a maximum of 24 h before further fractionation (Virto *et al.*, 2008; Kaiser *et al.*, 2015), was subjected to an additional 1000 J cm^{-3} ultrasonic energy to achieve complete dispersion (Kaiser & Berhe, 2014). Sedimentation and centrifuging (until the supernatant was clear) were used to separate the remaining clay-size fraction (< 2 μm; included in the aggregated clay) and silt-size fraction (hereafter referred to as fine silt).

All soil fractions were transferred into pre-weighed aluminum dishes, oven-dried at 40 °C, and weighed. The soil fractions (except coarse POM) were ground to a fine powder with an agate mortar and pestle and analyzed on the EA-IRMS to determine their C and N concentrations and $\delta^{13}C$ values. Prior to analysis, soils that contained carbonates were subjected to acid fumigation as previously described. Coarse POM was not analyzed on the EA-IRMS, as this fraction is the least homogeneous and was also contaminated with very fine root fragments in the planted treatment. The amount of C in coarse POM was calculated as the difference between bulk soil C and the sum of C across the other soil fractions for a given sample. Across all samples, the soil mass recovery ratio (sum of soil fractions to total sample used) was 1.01 ± 0.00 (standard error). The C recovery ratio (sum of soil fractions to bulk soil, not including coarse POM) was 0.92, 0.97, and 1.01 ± 0.01 in the 0–10, 10–30, and 30–50 cm soil depths, respectively, wherein the 30–50 cm soil depth had no visible coarse POM in most samples. Differences between the planted and non-planted

treatments in % clay of the < 20 μm fraction and % fine silt of total silt were 0.06 ± 0.11 and −0.02 ± 0.11, respectively.

4.3.5. Calculations

The $\delta^{13}C$ values of microbial biomass were calculated as

$$\delta^{13}C_{mic} = \left[\left(C_{fum} \times \delta^{13}C_{fum}\right) - \left(C_{nfum} \times \delta^{13}C_{nfum}\right)\right] / \left(C_{fum} - C_{nfum}\right) \quad [4.1]$$

where C_{fum} and C_{nfum} are the amounts of water-soluble C (μg C g^{-1} soil) in the fumigated and non-fumigated soils, respectively, and $\delta^{13}C_{fum}$ and $\delta^{13}C_{nfum}$ are the $\delta^{13}C$ values of the fumigated and non-fumigated samples, respectively (Marx *et al.*, 2007; Werth & Kuzyakov, 2008; Vogel *et al.*, 2014).

The contribution of root-derived C (rhizodeposit-C) to total C in MBC, WSOC, soil fractions, or bulk soil in the planted treatment was calculated as

$$C_{rhizodeposit} = f_{rhizodeposit} \times C_{planted} \quad [4.2]$$

where $C_{planted}$ is the amount of C (μg or mg C g^{-1} soil) in MBC, WSOC, soil fractions, or bulk soil in the planted treatment and $f_{rhizodeposit}$ is the fraction of C attributable to root-derived C, calculated as

$$f_{rhizodeposit} = \left(\delta^{13}C_{planted} - \delta^{13}C_{non-planted}\right) / \left(\delta^{13}C_{root} - \delta^{13}C_{non-planted}\right) \quad [4.3]$$

where $\delta^{13}C_{planted}$ is the $\delta^{13}C$ value of C in MBC, WSOC, soil fractions, or bulk soil in the planted treatment, $\delta^{13}C_{non-planted}$ is the $\delta^{13}C$ value of C in MBC, WSOC, soil fractions, or bulk soil in the non-planted treatment, and $\delta^{13}C_{root}$ is the mean $\delta^{13}C$ value of the roots (−15.37 ± 0.02‰) (Marx *et al.*, 2007; Werth & Kuzyakov, 2008). For the $\delta^{13}C$ value of the roots, I accounted for the magnitude of isotopic fractionation between rhizodeposits and microbial biomass, which was assumed to be the same as between the bulk soil and microbial biomass (Werth & Kuzyakov,

2008). Microbial biomass was ^{13}C enriched by an average of 1.25 ± 0.12‰ relative to the bulk soil in the non-planted treatment, consistent with the findings in Werth & Kuzyakov (2010).

Priming of C (mg C g^{-1} soil), i.e., the intensified loss of soil-derived C due to the presence of living roots over the duration of the incubation (150 days), was calculated as

$$C_{primed} = C_{non-planted} - C_{planted}\left(1 - f_{rhizodeposit}\right) \quad [4.4]$$

where $C_{non-planted}$ is the amount of C (mg C g^{-1} soil) in soil fractions or bulk soil in the non-planted treatment.

4.3.6. Statistical analyses

Linear mixed-effect models were used to determine whether priming or soil property differences between treatments were significantly different from zero and whether they differed across land-use types and soil depths. A randomized complete block design model was used for the statistical analyses. Land-use type and soil depth were fixed effects, and site and plot were random effects. Root mass was included in the models as a covariate. All data points with Cook's distance > 4/*n* were examined as potential outliers. Four samples that were consistent outliers across soil fractions were removed from all soil fraction analyses, while additional outliers were removed only when required for the model fit. Where necessary for the soil variables, data transformations using the lambda value for the maximum log likelihood for obtaining minimum error sum of squares were conducted to conform data to the assumptions of homogeneous variance and normality of distribution. Back-transformed data were used to calculate least-squares means and 95% confidence intervals (CIs). For determining differences in soil properties across land-use types and soil depths for the non-planted treatment, similar linear mixed-effect models were used (less the covariate), but non-transformed data were used in the models to calculate least-squares means and standard errors. When significant effects were detected at $p < 0.05$ after using type-III analysis-of-variance (ANOVA), pairwise *post-hoc* comparisons using the Tukey method for *p*-value adjustment were conducted to compare differences among land-use types or soil depths. Associations among continuous variables of interest were determined using Pearson's parametric correlation. Specifically, I assessed the relationships between soil properties in the non-planted

treatment and root-driven soil effects. All data were analyzed using RStudio Version 1.4.1106 and the "lme4" package for the linear mixed-effect models (RStudio Team, 2021).

4.4. Results

4.4.1. Properties of soil fractions in the non-planted treatment

In the non-planted treatment, aggregated clay contained 28% of total SOC across land uses and soil depths (Fig. 4.1a). In contrast, the proportion of total SOC associated with non-aggregated clay increased ($p < 0.001$) with soil depth, with 27, 39, and 44% in the 0–10, 10–30, and 30–50 cm layers, respectively, and was also greater ($p = 0.008$) in the cropland (41%) than the woodland (31%; Fig. 4.1a, c). The proportion of total SOC associated with coarse POM was minimal (≤ 4%) except in the 0–10 cm layer in the woodland (12%).

The mean $\delta^{13}C$ values in the non-planted treatment were −27.37‰ for fine POM, −26.48‰ for coarse silt, −26.37‰ for fine silt, −25.77‰ for non-aggregated clay, −26.17‰ for aggregated clay, and −26.10‰ for the bulk soil (Table C.S2). In general, $\delta^{13}C$ values increased with soil depth. These trends, as well as C:N ratio differences among fractions by soil depth and land-use type (Fig. 4.1b, d), are consistent with expected increases in the extent of microbial processing of organic matter from POM to mineral-associated C and with depth (Sollins *et al.*, 2006).

In the non-planted treatment, aggregated clay comprised a greater ($p < 0.001$) proportion of total clay mass in the 0–10 cm layer (41%) than in the 10–30 and 30–50 cm layers (32 and 31%, respectively; Fig. 4.2a). Similarly, aggregated clay comprised a greater ($p < 0.001$) proportion of total clay-protected C in the 0–10 cm layer (50%) than in the 10–30 and 30–50 cm layers (41 and 39%, respectively; Fig. 4.2a), as well as the woodland relative to the cropland (48 and 41%, respectively; $p = 0.043$; Fig. 4.2b). Across land uses and soil depths, aggregated clay was 1.53 times more enriched in C than non-aggregated clay (Fig. C.S1).

4.4.2. Microbial biomass and labile carbon

In the non-planted treatment, mean $\delta^{13}C$ values for MBC and WSOC were −25.34 and −26.71‰, respectively (Table C.S2). Compared with the non-planted treatment, $\delta^{13}C$ values for MBC and WSOC in the planted treatment increased by an average of 7.03 and 2.27‰, respectively (Table 4.1). The amount of rhizodeposit-C in the MBC was similar across land uses and soil depths (280 μg C g^{-1} soil), as was the increase in MBC within the planted treatment relative to the non-

planted treatment (287 μg C g^{-1} soil; Fig. 4.3a–b). The proportion of MBC comprised of rhizodeposit-C increased ($p < 0.001$) with soil depth and was also greater ($p = 0.007$) in the cropland than the woodland, a reflection of the initial size of the MBC pools (Fig. 4.3c). The amount of rhizodeposit-C in the WSOC was negligible (4–5 μg C g^{-1} soil), as was the increase in WSOC within the planted treatment relative to the non-planted treatment (< 5 μg C g^{-1} soil; Fig. 4.3a–b). Across land uses and soil depths, 50–74% of MBC was comprised of rhizodeposit-C, while only 16–27% of WSOC was comprised of rhizodeposit-C.

4.4.3. Rhizodeposit carbon incorporation and priming

Compared with the non-planted treatment, $\delta^{13}C$ values in the planted treatment increased by 3.06‰ for fine POM, 0.82‰ for coarse silt, 0.54‰ for fine silt, 0.77‰ for non-aggregated clay, 1.16‰ for aggregated clay, and 1.42‰ for the bulk soil (Table 4.1). Across all soil fractions and the bulk soil, the proportion of C comprised of rhizodeposit-C increased ($p < 0.05$) with soil depth and was also typically greater in the cropland than the woodland, a reflection of the initial size of the C pools (Fig. 4.4). Across land uses and soil depths, rhizodeposit-C comprised 7–13% of the C associated with aggregated clay, which represented an overall higher proportion relative to non-aggregated clay and the silt fractions (Fig. 4).

Priming (i.e., the intensified loss of C) within the soil fractions was limited to aggregated clay (Fig. 4.5a). Root-driven soil-derived C losses within aggregated clay were greatest ($p = 0.012$) in the surface soil (1.27, 0.60, and 0.51 mg C g^{-1} soil in the 0–10, 10–30, and 30–50 cm layers, respectively) and similar across land uses (0.78 mg C g^{-1} soil; Fig. 4.5a). Within the bulk soil, priming was similar in magnitude (0.99 mg C g^{-1} soil) and followed a trend of decreasing with soil depth (Fig. 4.5a).

The amount of rhizodeposit-C incorporated into the soil fractions was minimal for the silt fractions relative to the clay fractions and fine POM (Fig. 4.5b). A similar amount of rhizodeposit-C was incorporated into the clay fractions across land uses (0.66 and 0.68 mg C g^{-1} soil for non-aggregated and aggregated clay, respectively; Fig. 4.5b). In contrast to non-aggregated clay, the amount of rhizodeposit-C incorporated into aggregated clay was greater ($p = 0.011$) in the 0–10 than 30–50 cm layer (0.88 and 0.56 mg C g^{-1} soil, respectively; Fig. 4.5b). Rhizodeposit-C incorporation into the bulk soil was an average of 0.99 mg C g^{-1} soil greater than the sum of the measured soil fractions (Fig. 4.5b). This additional rhizodeposit-C was attributable to the amount

of C in the roots remaining in the bulk soil that were removed from coarse POM after physical soil fractionation (0.96 ± 0.06 mg C g^{-1} soil).

Net C changes within the soil fractions were substantial and consistent for fine POM and non-aggregated clay, which both had net C gains (0.76 and 0.61 mg C g^{-1} soil, respectively) across land uses and soil depths (Fig. 4.5c). Aggregated clay had no net C change across land uses or soil depths (Fig. 4.5c). The net C gain for the bulk soil was an average of 0.87 mg C g^{-1} soil greater than the sum of the measured soil fractions, a difference again attributable to the amount of C in the roots remaining in the bulk soil (Fig. 4.5c).

Across land uses and soil depths, priming within aggregated clay was positively correlated with the bulk soil C, the proportion of clay-protected C within aggregated clay, MBC, WSOC, and WSN in the non-planted treatment ($p < 0.003$; Fig. C.S2). All these variables were also positively correlated with each other ($p < 0.012$; Fig. C.S2). The bulk soil C explained 62% of the variation in the proportion of clay-protected C within aggregated clay, while the latter variable explained 41% of the variation in priming within aggregated clay (Fig. C.S2). Root mass (Table C.S3), MBC growth (difference between planted and non-planted treatments), and rhizodeposit-C incorporation into aggregated clay were all positively correlated with priming within aggregated clay and each other ($p < 0.03$; Fig. C.S2). Rhizodeposit-C incorporation into non-aggregated clay was also positively correlated with root mass and MBC growth ($p < 0.001$; Fig. C.S2). The loss of aggregated clay mass in the planted treatment (difference between the aggregated clay to total clay mass proportions in the planted and non-planted treatments), which averaged 2.29% and was similar across land uses and soil depths (Fig. C.S3), was positively correlated with priming within aggregated clay ($p < 0.001$), explaining 37% of the variation (Fig. C.S2). Additionally, the proportion of clay-protected C within aggregated clay in the non-planted treatment was positively correlated with rhizodeposit-C incorporation into aggregated clay and the loss of aggregated clay mass ($p < 0.001$), explaining 17 and 12% of the variation, respectively (Fig. C.S2).

4.5. Discussion

I show that living roots can destabilize clay-protected C within silt-size microaggregates, leading to rapid and preferential decomposition of clay-protected C and further challenging the assumption that C associated with clay or silt-size microaggregates is stable (Keiluweit *et al.*, 2015; Yang *et al.*, 2021). Additionally, my results illustrate an interplay between physical and

chemical protection of SOC, while representative soil C models and most studies consider SOC protection within aggregates and on mineral surfaces as distinct processes (Lehmann & Kleber, 2015; Lavallee *et al.*, 2019). Priming of soil-derived C (i.e., the intensified loss of C) despite overall net C gains in soils subject to plant inputs in my experiment emphasizes the complex effect that living roots have on SOC dynamics. This effect has been referred to as a double-edged sword, wherein roots result in both desirable (stabilization or net gain) and undesirable (destabilization or net loss) effects on SOC (Dijkstra *et al.*, 2021). While the replacement of clay-protected C within silt-size microaggregates with root-derived C resulted in no net C change for the aggregated clay fraction, an overall reduction in the mass of aggregated clay suggests that living roots resulted in SOC destabilization within the parameters of my experiment.

A root-driven reduction in the mass of aggregated clay is important because my study showed that soils with greater SOC content (i.e., surface and woodland soils relative to subsurface and cropland soils, respectively) have higher proportions of clay-protected C within silt-size microaggregates. This indicates that aggregated clay is pivotal in SOC sequestration and stabilization (Chenu & Plante, 2006; Vogel *et al.*, 2014). In fact, aggregated clay was about 1.5 times more enriched in C than non-aggregated clay, potentially due to mineralogy (Virto *et al.*, 2008), preferential attachment of C to aggregated clay (Chenu & Plante, 2006; Vogel *et al.*, 2014; Asano *et al.*, 2018), or the physical protection of C bound to clay-size particles within silt-size microaggregates (Rasse *et al.*, 2005; Yang *et al.*, 2021). Clay-protected C within silt-size microaggregates also comprised nearly a third of total SOC across land uses and soil depths, highlighting the important role that aggregated clay plays in overall SOC storage (Virto *et al.*, 2008; Moni *et al.*, 2010).

In my experiment, root-driven disruption of silt-size microaggregates appeared to outpace any stabilization, as evidenced by a reduction in the mass of aggregated clay. Root-derived C comprised a relatively large proportion of the C associated with aggregated clay, indicating rapid incorporation of root-derived C into silt-size microaggregates and consistent with the findings of Virto *et al.* (2010). Preferential sorption of root-derived C to aggregated clay relative to non-aggregated clay was evident in my experiment because both fractions incorporated relatively similar amounts of root-derived C despite a lower proportion of total clay mass associated with aggregated clay. These results are in agreement with observations of preferential C sorption to surfaces of submicron structures (Vogel *et al.*, 2014; Asano *et al.*, 2018). Exchange reactions,

wherein mineral-associated C is released in favor of new C (Marx *et al.*, 2007; Sanderman *et al.*, 2008), may have been responsible for some of the priming within aggregated clay and help explain the positive relationship between root-derived C incorporation and priming in this fraction. Moreover, root exudates can act as ligands and mediate the release of mineral-associated C (Clarholm *et al.*, 2015; Keiluweit *et al.*, 2015), which can enhance aggregate disruption and turnover. Mechanical disruption of aggregates by living roots can also enhance aggregate turnover and priming effects (He *et al.*, 2020; Wang *et al.*, 2020).

On the other hand, clay-protected C within silt-size microaggregates may be quasi-irreversibly sorbed (Yang *et al.*, 2021) and therefore more resistant to exchange reactions and exudate-mediated release relative to other mineral-associated C. Moreover, silt-size microaggregates are likely more resistant to mechanical disruption than larger aggregates (Totsche *et al.*, 2018). Not only are higher energy levels required to disperse progressively smaller aggregates (Kaiser & Berhe, 2014), but the micropores of silt-size microaggregates are also largely impenetrable (e.g., by root hairs and microorganisms) (Rasse *et al.*, 2005; Yang *et al.*, 2021). However, exoenzymes produced by active microorganisms in response to an influx of simple sugars (Shahzad *et al.*, 2015), such as those within root exudates, are able to diffuse into silt-size microaggregates and break down clay-protected C (Yang *et al.*, 2021). Therefore, priming may have occurred primarily due to exoenzyme-mediated breakdown of organic compounds bound to clay within silt-size microaggregates, which were then released into soil solution and made available for microbial use (Yang *et al.*, 2021). This process could have created a positive feedback loop, particularly in the more C-saturated surface soil, wherein microorganisms produced even more exoenzymes after metabolizing the released organic compounds. Because organic compounds help stabilize microaggregates (Rasse *et al.*, 2005; Lehmann *et al.*, 2007; Totsche *et al.*, 2018), their breakdown and release would have resulted in the destabilization of silt-size microaggregates in my experiment, thereby reducing the mass of aggregated clay (Fig. 4.6). Factors controlling exoenzyme activity, which is not necessarily related to microbial growth (Shahzad *et al.*, 2015; Nannipieri *et al.*, 2018), and the interactions of exoenzymes with clay minerals and aggregates at the silt-size scale or smaller, should be investigated in future studies.

The minimal amount of root-derived C in the dissolved organic C pool suggests that exudates were either rapidly processed by microorganisms or sorbed to mineral surfaces, as found in other studies (Marx *et al.*, 2007; Keiluweit *et al.*, 2015). Consistent with observations that root

exudates increase with root mass (Eisenhauer *et al.*, 2017), microbial growth (suggestive of microorganisms feeding on root exudates) and root mass were positively related in my experiment. Root hairs, which are abundantly produced by grass roots (Rasse *et al.*, 2005), can especially increase exudation and the spatial footprint of roots, enhancing root-driven effects (Holz *et al.*, 2018). This could be partially responsible for the increased priming in more C saturated soils in my experiment, which also had increased root mass. Microorganisms appeared to preferentially use rhizodeposits for growth, as evidenced by the dominance of root-derived C within microbial biomass and similar to findings in other studies (Liang *et al.*, 2002; Wang *et al.*, 2020). An increase in microbial turnover and community changes in conjunction with a decrease in diversity probably occurred due to the influx of easily available root-derived C (Dijkstra *et al.*, 2021; Sokol *et al.*, 2022). Additionally, these microorganisms would have been driven to produce exoenzymes to mineralize soil organic matter after metabolizing energy-rich but nutrient-poor exudates (Shahzad *et al.*, 2015; Gunina & Kuzyakov, 2022). This could explain the rapid and preferential decomposition of clay-protected soil-derived organic matter in my experiment, which had consistent and relatively low C:N ratios (i.e., was nutrient-rich), likely owing to the strong affinity of proteinaceous microbial residues for mineral surfaces (Kleber *et al.*, 2007).

Rates of soil-derived C loss in my experiment were comparable to those reported in other priming studies (Keiluweit *et al.*, 2015; He *et al.*, 2020; Wang *et al.*, 2020). In general, the priming effect is positively related with the size of the initial SOC stock (Kuzyakov *et al.*, 2000). My results are consistent with that relationship. More C-saturated soils may experience increased root-driven replacement of protected C with unprotected C (Dijkstra *et al.*, 2021) as activated microorganisms mine for nutrients (Gunina & Kuzyakov, 2022). In my experiment, soils that were more C saturated also had higher proportions of clay-protected C within silt-size microaggregates, potentially fostering microenvironments that enhanced both priming and new C incorporation. For example, silt-size microaggregates may create more 30-150 μm pores, which are microenvironments that effectively increase the microbial spatial footprint and are associated with higher exoenzyme activities (Kravchenko *et al.*, 2019). While such microenvironments would have enhanced the breakdown of clay-protected C within silt-size microaggregates, causing destabilization, they also would have created more opportunities for protection of microbial products and necromass via sorption onto mineral surfaces (Kravchenko *et al.*, 2019). Most rhizodeposits undergo microbial assimilation, biosynthesis, and turnover (Sokol *et al.*, 2018). Therefore, increased microbial

turnover fueled by the living roots (Dijkstra *et al.*, 2021) and associated necromass may have been a key source of root-derived C that was incorporated into non-aggregated and aggregated clay (Gross & Harrison, 2019; Sokol & Bradford, 2019; Sokol *et al.*, 2019), explaining the positive relationship with microbial growth.

The relatively large amount of root-derived C incorporated into fine POM in my experiment was likely attributable to root hairs and other water-insoluble root debris (Rasse *et al.*, 2005). I note that coarse silt appeared to be primarily composed of C in the form of POM- rather than mineral-associated C, while fine silt also potentially contained a minor component of light POM (Virto *et al.*, 2008). Root-derived C incorporation into non-aggregated clay may have occurred primarily via sorption onto clay-size surfaces without sorbed C, which likely comprised a greater proportion of surface area relative to aggregated clay (Vogel *et al.*, 2014). A reduced effect of exchange reactions and exudate- or exoenzyme-mediated release or breakdown, respectively, of clay-protected C within non-aggregated clay may explain the lack of priming within this fraction. Additionally, transference of formerly aggregated clay (and any still bound soil-derived C) to non-aggregated clay would have muted my ability to measure priming within this fraction. Net C gains within non-aggregated clay due to living roots may lead to a positive feedback loop, wherein dissolved organic C is more likely to be associated with the rough organo-mineral surfaces created (Vogel *et al.*, 2014). Under what conditions (or at what stage) the incorporation of this recent C into non-aggregated clay will foster the formation of clay-size particles into silt-size microaggregates at a rate that surpasses any destabilization is an important question for future research.

4.6. Conclusions

I conclude that clay-protected C within silt-size microaggregates is an important SOC pool across land uses and soil depths in a range of soils with varying properties. While most studies focus on aggregation at scales larger than silt-size, as well as combine silt- and clay-associated C into a single SOC pool, I show that clay-size particles within silt-size microaggregates are functionally different than other clay- and silt-size particles in terms of C storage and cycling. Critically, my study demonstrates that living roots can destabilize clay-protected C within silt-size microaggregates, leading to rapid and preferential decomposition of clay-protected C. Based on my results, I suggest an integrated soil C model that considers the interplay of physical (within

silt-size microaggregates) and chemical (sorption) protection of clay-associated C (Fig. 4.6). I highlight that root-driven stabilization or destabilization of clay-protected C within silt-size microaggregates may mediate SOC sequestration and SOC storage capacity. This has important implications for our understanding of SOC persistence and the underlying processes used in soil C models.

Funding: This research was supported by a Doctoral Vanier Scholarship and a Killam Memorial Graduate Scholarship to C.D.G., as well as a grant (AGGP2-039) from the Agricultural Greenhouse Gas Program from Agriculture and Agri-Food Canada to S.X.C., E.W.B., and C.N.C.

Credit: C.D.G.: Conceptualization. C.D.G. and B.W.: Methodology. C.D.G.: Investigation and Writing—original draft. C.D.G., S.X.C., E.W.B., B.W., and C.N.C.: Writing—review and editing. S.X.C. and E.W.B.: Resources and Supervision. S.X.C., E.W.B., B.W., and C.N.C.: Guidance and Feedback at various stages.

Acknowledgements: Thank you to Mary Villeneuve, Sheetal Patel, and Carmen C. Roman-Perez for their help in the lab.

4.7. References

Amundson R, Biardeau L (2018) Opinion: Soil carbon sequestration is an elusive climate mitigation tool. *Proceedings of the National Academy of Sciences*, **115**, 11652–11656.

Angst G, Messinger J, Greiner M et al. (2018) Soil organic carbon stocks in topsoil and subsoil controlled by parent material, carbon input in the rhizosphere, and microbial-derived compounds. *Soil Biology and Biochemistry*, **122**, 19–30.

Asano M, Wagai R, Yamaguchi N, Takeichi Y, Maeda M, Suga H, Takahashi Y (2018) In search of a binding agent: Nano-scale evidence of preferential carbon associations with poorly-crystalline mineral phases in physically-stable, clay-sized aggregates. *Soil Systems*, **2**, 32.

Beck T, Joergensen RG, Kandeler E, Makeshin E, Nuss E, Oberholzer HR, Scheu S (1997) An inter-laboratory comparison of ten different ways of measuring soil microbial biomass C. *Soil Biology & Biochemistry*, **29**, 1023–1032.

Chantigny MH, Angers DA, Kaiser K, Kalbitz K (2007) Extraction and characterization of

dissolved organic matter. In: *Soil Sampling and Methods of Analysis*, 2nd edn (eds Carter MR, Gregorich EG), pp. 617–635. CRC Press, Boca Raton.

Chenu C, Plante AT (2006) Clay-sized organo-mineral complexes in a cultivation chronosequence: Revisiting the concept of the "primary organo-mineral complex." *European Journal of Soil Science*, **57**, 596–607.

Ciais P, Sabine C, Bala G et al. (2013) Carbon and other biogeochemical cycles. In: *Climate Change 2013: The Physical Science Basis. Contribution of Working Group I to the Fifth Assessment Report of the Intergovernmental Panel on Climate Change* (eds Stocker TF, Qin D, Plattner G-K, Tignor M, Allen SK, Boschung J, Nauels A, Xia Y, Bex V, Midgley PM), pp. 465–570. Cambridge University Press, Cambridge, United Kingdom and New York, NY, USA.

Clarholm M, Skyllberg U, Rosling A (2015) Organic acid induced release of nutrients from metal-stabilized soil organic matter - The unbutton model. *Soil Biology and Biochemistry*, **84**, 168–176.

Cooper RN, Wissel B (2012) Loss of trophic complexity in saline prairie lakes as indicated by stable-isotope based community-metrics. *Aquatic Biosystems*, **8**, 6.

Datta R, Vranová V, Pavelka M, Rejšek K, Formánek P (2014) Effect of soil sieving on respiration induced by low-molecular-weight substrates. *International Agrophysics*, **28**, 119–124.

Dijkstra FA, Cheng W (2007) Interactions between soil and tree roots accelerate long-term soil carbon decomposition. *Ecology Letters*, **10**, 1046–1053.

Dijkstra FA, Zhu B, Cheng W (2021) Root effects on soil organic carbon: A double-edged sword. *New Phytologist*, **230**, 60–65.

Eisenhauer N, Lanoue A, Strecker T, Scheu S, Steinauer K, Thakur MP, Mommer L (2017) Root biomass and exudates link plant diversity with soil bacterial and fungal biomass. *Scientific Reports*, **7**, 1–8.

Fontaine S, Barot S, Barré P, Bdioui N, Mary B, Rumpel C (2007) Stability of organic carbon in deep soil layers controlled by fresh carbon supply. *Nature*, **450**, 277–80.

Gross CD, Harrison RB (2019) The case for digging deeper: Soil organic carbon storage, dynamics, and controls in our changing world. *Soil Systems*, **3**, 28.

Gross CD, Bork EW, Carlyle CN, Chang SX (2022) Biochar and its manure-based feedstock

have divergent effects on soil organic carbon and greenhouse gas emissions in croplands. *Science of The Total Environment*, **806**, 151337.

Gunina A, Kuzyakov Y (2022) From energy to (soil organic) matter. *Global Change Biology*, **28**, 2169–2182.

Haney RL, Franzluebbers AJ, Hons FM, Hossner LR, Zuberer DA (2001) Molar concentration of K2SO4 and soil pH affect estimation of extractable C with chloroform fumigation-extraction. *Soil Biology and Biochemistry*, **33**, 1501–1507.

He Y, Cheng W, Zhou L et al. (2020) Soil DOC release and aggregate disruption mediate rhizosphere priming effect on soil C decomposition. *Soil Biology and Biochemistry*, **144**, 107787.

Holz M, Zarebanadkouki M, Kuzyakov Y, Pausch J, Carminati A (2018) Root hairs increase rhizosphere extension and carbon input to soil. *Annals of Botany*, **121**, 61–69.

Horwath WR, Paul EA (1994) Microbial biomass. In: *Methods of Soil Analysis: Part 2—Microbiological and Biochemical Properties, SSSA Book Series no. 5* (eds Bottomley PS, Angle JS, Weaver RW), pp. 753–774. Soil Science Society of America, Madison.

Huo C, Luo Y, Cheng W (2017) Rhizosphere priming effect: A meta-analysis. *Soil Biology and Biochemistry*, **111**, 78–84.

IPCC (2022) Summary for policymakers. In: *Climate Change 2022: Mitigation of Climate Change. Contribution of Working Group III to the Sixth Assessment Report of the Intergovernmental Panel on Climate Change* (eds Shukla PR, Skea J, Slade R, Khourdajie A Al, Diemen R van, McCollum D, Pathak M, Some S, Vyas P, Fradera R, Belkacemi M, Hasija A, Lisboa G, Luz S, Malley J), p. 63. Cambridge University Press, Cambridge, UK and New York, NY, USA.

Jenkinson DS, Brookes PC, Powlson DS (2004) Measuring soil microbial biomass. *Soil Biology and Biochemistry*, **36**, 5–7.

Jones C, McConnell C, Coleman K, Cox P, Falloon P, Jenkinson D, Powlson D (2005) Global climate change and soil carbon stocks; predictions from two contrasting models for the turnover of organic carbon in soil. *Global Change Biology*, **11**, 154–166.

Kaiser M, Berhe AA (2014) How does sonication affect the mineral and organic constituents of soil aggregates? - A review. *Journal of Plant Nutrition and Soil Science*, **177**, 479–495.

Kaiser M, Kleber M, Berhe AA (2015) How air-drying and rewetting modify soil organic matter

characteristics: An assessment to improve data interpretation and inference. *Soil Biology and Biochemistry*, **80**, 324–340.

Keiluweit M, Bougoure JJ, Nico PS, Pett-Ridge J, Weber PK, Kleber M (2015) Mineral protection of soil carbon counteracted by root exudates. *Nature Climate Change*, **5**, 588–595.

Kleber M, Sollins P, Sutton R (2007) A conceptual model of organo-mineral interactions in soils: Self-assembly of organic molecular fragments into zonal structures on mineral surfaces. *Biogeochemistry*, **85**, 9–24.

Kravchenko AN, Guber AK, Razavi BS, Koestel J, Quigley MY, Robertson GP, Kuzyakov Y (2019) Microbial spatial footprint as a driver of soil carbon stabilization. *Nature Communications*, **10**, 1–10.

Kuzyakov Y, Friedelb JK, Stahra K (2000) Review of mechanisms and quantification of priming effects. *Soil Biology & Biochemistry*, **32**, 1485–1498.

Lavallee JM, Soong JL, Cotrufo MF (2019) Conceptualizing soil organic matter into particulate and mineral-associated forms to address global change in the 21st century. *Global Change Biology*, 1–13.

Lehmann J, Kleber M (2015) The contentious nature of soil organic matter. *Nature*, **528**, 60–8.

Lehmann J, Kinyangi J, Solomon D (2007) Organic matter stabilization in soil microaggregates: Implications from spatial heterogeneity of organic carbon contents and carbon forms. *Biogeochemistry*, **85**, 45–57.

Liang BC, Wang XL, Ma BL (2002) Maize root-induced change in soil organic carbon pools. *Soil Science Society of America Journal*, **66**, 845–847.

Liang C, Schimel JP, Jastrow JD (2017) The importance of anabolism in microbial control over soil carbon storage. *Nature Microbiology*, **2**, 1–6.

Lorenz K, Lal R (2022) *Soil Organic Carbon Sequestration in Terrestrial Biomes of the United States*, 1st edn. Springer, Cham, Switzerland, 201 pp.

Marx M, Buegger F, Gattinger A, Marschner B, Zsolnay Á, Munch JC (2007) Determination of the fate of 13C labelled maize and wheat rhizodeposit-C in two agricultural soils in a greenhouse experiment under 13C-CO2-enriched atmosphere. *Soil Biology and Biochemistry*, **39**, 3043–3055.

Mobley ML, Lajtha K, Kramer MG, Bacon AR, Heine PR, Richter DD (2015) Surficial gains

and subsoil losses of soil carbon and nitrogen during secondary forest development. *Global Change Biology*, **21**, 986–996.

Moni C, Rumpel C, Virto I, Chabbi A, Chenu C (2010) Relative importance of sorption versus aggregation for organic matter storage in subsoil horizons of two contrasting soils. *European Journal of Soil Science*, **61**, 958–969.

Nannipieri P, Trasar-Cepeda C, Dick RP (2018) Soil enzyme activity: a brief history and biochemistry as a basis for appropriate interpretations and meta-analysis. *Biology and Fertility of Soils*, **54**, 11–19.

Pan Y, Birdsey RA, Fang J et al. (2011) A large and persistent carbon sink in the world's forests. *Science*, **333**, 988–993.

Paustian K, Lehmann J, Ogle S, Reay D, Robertson GP, Smith P (2016) Climate-smart soils. *Nature*, **532**, 49–57.

Pierson D, Evans L, Kayhani K, Bowden RD, Nadelhoffer K, Simpson M, Lajtha K (2021) Mineral stabilization of soil carbon is suppressed by live roots, outweighing influences from litter quality or quantity. *Biogeochemistry*, **154**, 433–449.

Le Quéré C, Andrew RM, Friedlingstein P et al. (2018) Global carbon budget 2017. *Earth System Science Data*, **10**, 405–448.

Ramnarine R, Voroney RP, Wagner-Riddle C, Dunfield KE (2011) Carbonate removal by acid fumigation for measuring the δ13C of soil organic carbon. *Canadian Journal of Soil Science*, **91**, 247–250.

Rasmussen C, Heckman K, Wieder WR et al. (2018) Beyond clay: towards an improved set of variables for predicting soil organic matter content. *Biogeochemistry*, **137**, 297–306.

Rasse DP, Rumpel C, Dignac MF (2005) Is soil carbon mostly root carbon? Mechanisms for a specific stabilisation. *Plant and Soil*, **269**, 341–356.

RStudio Team (2021) *RStudio: Integrated Development Environment for R*. Boston, MA.

Sanderman J, Baldock JA, Amundson R, Baldock JA (2008) Dissolved organic carbon chemistry and dynamics in contrasting forest and grassland soils. *Biogeochemistry*, **89**, 181–198.

Schlautman B, Bartel C, Diaz-Garcia L et al. (2021) Perennial groundcovers: An emerging technology for soil conservation and the sustainable intensification of agriculture. *Emerging Topics in Life Sciences*, **5**, 337–347.

Schmidt MWI, Rumpel C, Kögel-Knabner I (1999) Evaluation of an ultrasonic dispersion

procedure to isolate primary organomineral complexes from soils. *European Journal of Soil Science*, **50**, 87–94.

Schmidt MWI, Torn MS, Abiven S et al. (2011) Persistence of soil organic matter as an ecosystem property. *Nature*, **478**, 49–56.

Shahzad T, Chenu C, Genet P, Barot S, Perveen N, Mougin C, Fontaine S (2015) Contribution of exudates, arbuscular mycorrhizal fungi and litter depositions to the rhizosphere priming effect induced by grassland species. *Soil Biology and Biochemistry*, **80**, 146–155.

Shahzad T, Rashid MI, Maire V et al. (2018) Root penetration in deep soil layers stimulates mineralization of millennia-old organic carbon. *Soil Biology and Biochemistry*, **124**, 150–160.

Six J, Conant RT, Paul E a, Paustian K (2002) Stabilization mechanisms of soil organic matter: Implications for C-saturatin of soils. *Plant and Soil*, **241**, 155–176.

Sokol NW, Bradford MA (2019) Microbial formation of stable soil carbon is more efficient from belowground than aboveground input. *Nature Geoscience*, **12**, 46–53.

Sokol NW, Sanderman J, Bradford MA (2018) Pathways of mineral-associated soil organic matter formation: Integrating the role of plant carbon source, chemistry, and point of entry. *Global Change Biology*, 12–24.

Sokol NW, Kuebbing SE, Karlsen-Ayala E, Bradford MA (2019) Evidence for the primacy of living root inputs, not root or shoot litter, in forming soil organic carbon. *New Phytologist*, **221**, 233–246.

Sokol NW, Slessarev E, Marschmann GL et al. (2022) Life and death in the soil microbiome: How ecological processes influence biogeochemistry. *Nature Reviews Microbiology*, **0123456789**.

Sollins P, Swanston C, Kleber M et al. (2006) Organic C and N stabilization in a forest soil: Evidence from sequential density fractionation. *Soil Biology and Biochemistry*, **38**, 3313–3324.

Sulman BN, Phillips RP, Oishi AC, Shevliakova E, Pacala SW (2014) Microbe-driven turnover offsets mineral-mediated storage of soil carbon under elevated CO2. *Nature Climate Change*, **4**, 1099–1102.

Tian Q, Yang X, Wang X et al. (2016) Microbial community mediated response of organic carbon mineralization to labile carbon and nitrogen addition in topsoil and subsoil.

Biogeochemistry, **128**, 125–139.

Totsche KU, Amelung W, Gerzabek MH et al. (2018) Microaggregates in soils. *Journal of Plant Nutrition and Soil Science*, **181**, 104–136.

Vance ED, Brookes PC, Jenkinson DS (1987) An extraction method for measuring soil microbial biomass C. *Soil Biology and Biochemistry*, **19**, 703–707.

Virto I, Barré P, Chenu C (2008) Microaggregation and organic matter storage at the silt-size scale. *Geoderma*, **146**, 326–335.

Virto I, Moni C, Swanston C, Chenu C (2010) Turnover of intra- and extra-aggregate organic matter at the silt-size scale. *Geoderma*, **156**, 1–10.

Vogel C, Mueller CW, Höschen C et al. (2014) Submicron structures provide preferential spots for carbon and nitrogen sequestration in soils. *Nature Communications*, **5**, 1–7.

Wang X, Yin L, Dijkstra FA, Lu J, Wang P, Cheng W (2020) Rhizosphere priming is tightly associated with root-driven aggregate turnover. *Soil Biology and Biochemistry*, **149**, 107964.

Werth M, Kuzyakov Y (2008) Root-derived carbon in soil respiration and microbial biomass determined by 14C and 13C. *Soil Biology and Biochemistry*, **40**, 625–637.

Werth M, Kuzyakov Y (2010) 13C fractionation at the root-microorganisms-soil interface: A review and outlook for partitioning studies. *Soil Biology and Biochemistry*, **42**, 1372–1384.

Yang XM, Drury CF, Reynolds WD, MacTavish DC (2009) Use of sonication to determine the size distributions of soil particles and organic matter. *Canadian Journal of Soil Science*, **89**, 413–419.

Yang JQ, Zhang X, Bourg IC, Stone HA (2021) 4D imaging reveals mechanisms of clay-carbon protection and release. *Nature Communications*, **12**.

Zhu X, Jackson RD, DeLucia EH, Tiedje JM, Liang C (2020) The soil microbial carbon pump: From conceptual insights to empirical assessments. *Global Change Biology*, **26**, 6032–6039.

Zsolnay Á (2003) Dissolved organic matter: Artefacts, definitions, and functions. *Geoderma*, **113**, 187–209.

4.8. Tables

Table 4.1. Change (difference between planted and non-planted treatments) in $\delta^{13}C$ values (least-squares means and 95% confidence intervals) of soil fractions by soil depth and land-use type across ten agroforestry sites in central Alberta, Canada. POM, particulate organic matter; MBC, microbial biomass carbon; WSOC, water-soluble organic carbon.

Soil depth (cm)	0–10	10–30	30–50
Fine POM (*n* = 85)	1.50 (1.13, 1.91)	3.49 (2.92, 4.14)	4.39 (3.70, 5.19)
Coarse silt (*n* = 83)	0.34 (0.13, 0.56)	0.82 (0.58, 1.06)	1.35 (1.09, 1.63)
Fine silt (*n* = 84)	0.23 (0.08, 0.38)	0.45 (0.30, 0.62)	0.94 (0.76, 1.13)
Non-aggregated clay (*n* = 85)	0.54 (0.40, 0.68)	0.66 (0.53, 0.81)	1.13 (0.97, 1.29)
Aggregated clay (*n* = 85)	0.97 (0.60, 1.37)	1.01 (0.65, 1.41)	1.48 (1.08, 1.94)
Bulk soil (*n* = 87)	0.80 (0.51, 1.11)	1.32 (1.00, 1.68)	2.11 (1.71, 2.55)
MBC (*n* = 87)	5.67 (4.82, 6.48)	7.17 (6.37, 7.95)	8.24 (7.46, 8.99)
WSOC (*n* = 89)	1.81 (1.40, 2.27)	2.04 (1.62, 2.52)	2.97 (2.45, 3.55)
Land-use type	Cropland	Grassland	Woodland
Fine POM (*n* = 85)	3.81 (3.09, 4.67)	2.90 (2.27, 3.63)	2.27 (1.75, 2.87)
Coarse silt (*n* = 83)	1.04 (0.80, 1.31)	0.76 (0.52, 1.02)	0.63 (0.41, 0.87)
Fine silt (*n* = 84)	0.67 (0.47, 0.90)	0.58 (0.37, 0.81)	0.34 (0.15, 0.54)
Non-aggregated clay (*n* = 85)	0.91 (0.73, 1.11)	0.70 (0.51, 0.89)	0.70 (0.52, 0.88)
Aggregated clay (*n* = 85)	1.42 (1.00, 1.89)	1.22 (0.81, 1.68)	0.83 (0.46, 1.24)
Bulk soil (*n* = 87)	1.65 (1.26, 2.09)	1.37 (1.00, 1.78)	1.12 (0.77, 1.50)
MBC (*n* = 87)	8.27 (7.36, 9.17)	6.60 (5.64, 7.53)	6.22 (5.23, 7.17)
WSOC (*n* = 89)	2.74 (2.17, 3.38)	2.02 (1.54, 2.57)	2.02 (1.53, 2.58)

4.9. Figures

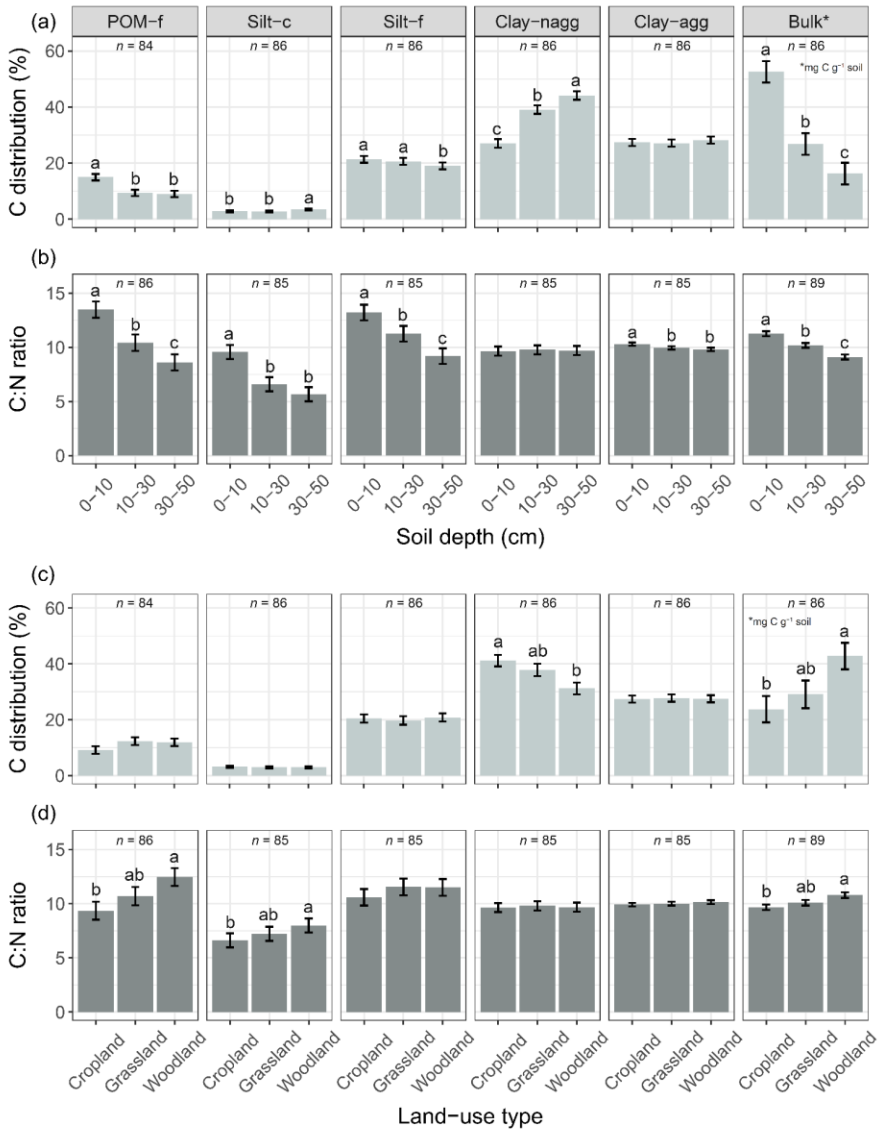

Figure 4.1. Non-planted treatment (a, c) carbon (C) distributions and (b, d) C to nitrogen (N) ratios of soil fractions by (a, b) soil depth and (c, d) land-use type across ten agroforestry sites in central Alberta, Canada. Bulk soil shows C concentration (mg C g^{-1} soil) rather than C distribution (%). Error bars represent ± one standard error. Least-squares means within each soil fraction accompanied by different lowercase letters are significantly different (Tukey-adjusted, $\alpha = 0.05$) among the soil depths or land-use types. POM-f, fine particulate organic matter; silt-c, coarse silt; silt-f, fine silt; clay-nagg, non-aggregated clay; clay-agg, aggregated clay.

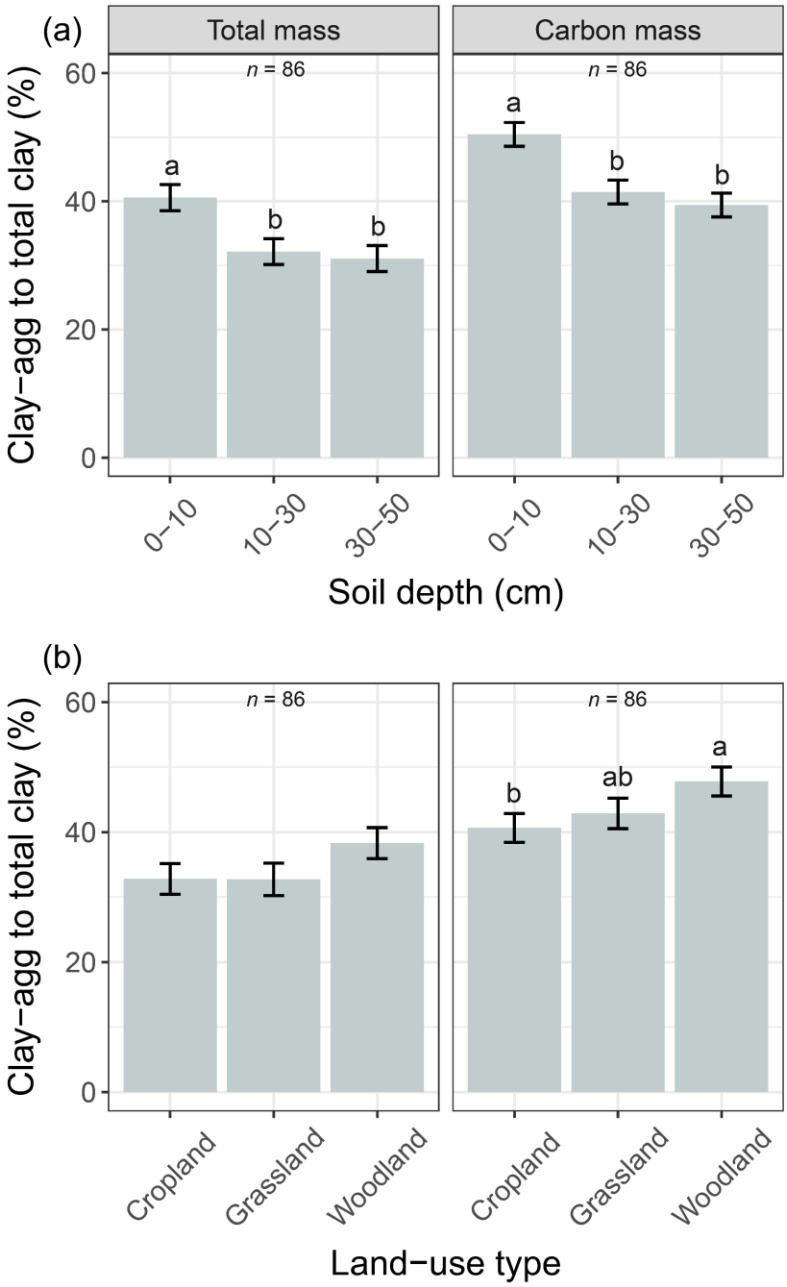

Figure 4.2. Non-planted treatment aggregated clay fraction (clay-agg) to total clay (total mass or carbon mass) proportions by (a) soil depth and (b) land-use type across ten agroforestry sites in central Alberta, Canada. Error bars represent ± one standard error. Least-squares means within each component accompanied by different lowercase letters are significantly different (Tukey-adjusted, $\alpha = 0.05$) among the soil depths or land-use types.

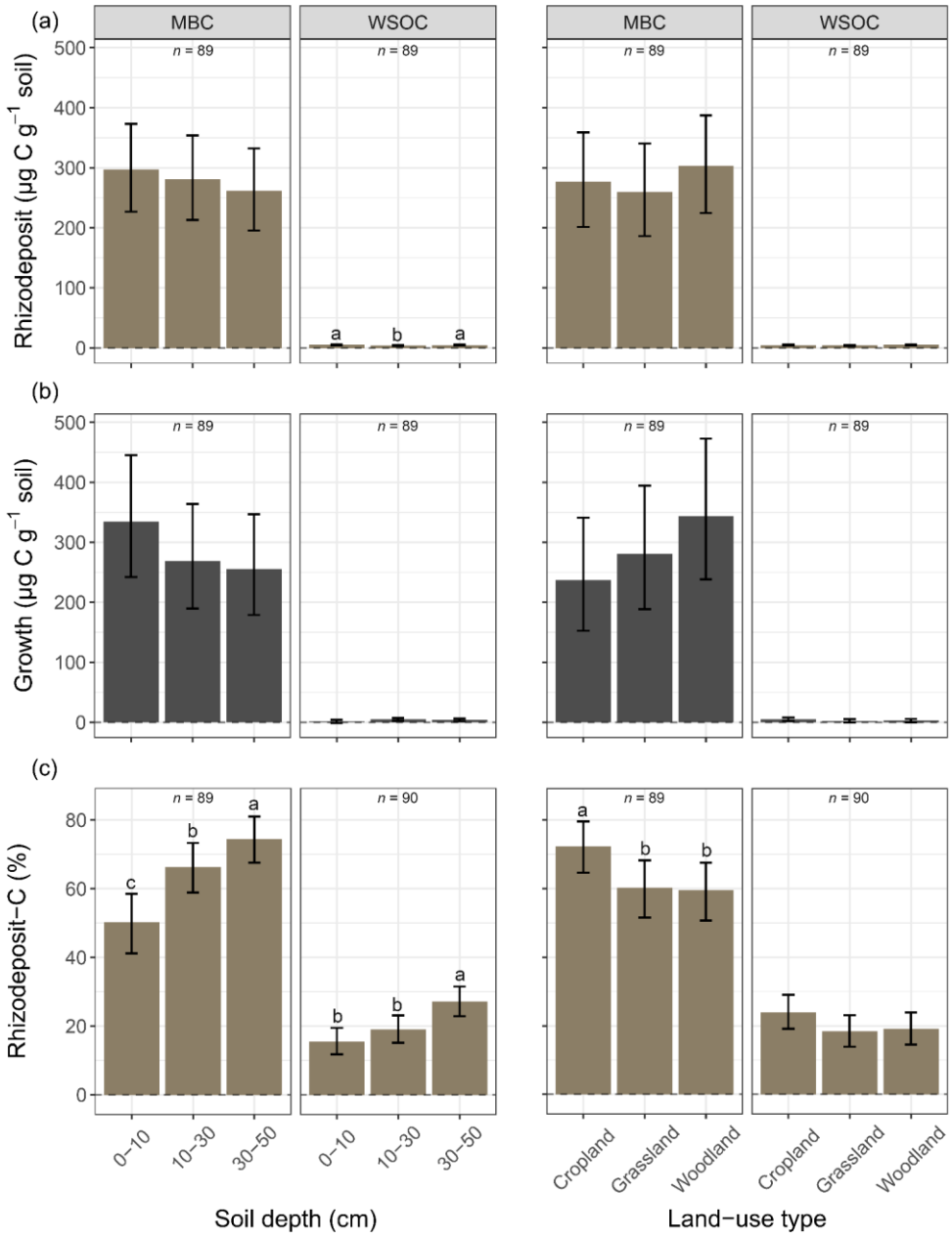

Figure 4.3. Microbial biomass carbon (MBC) and water-soluble organic carbon (WSOC) (a) rhizodeposit carbon (C) incorporation, (b) growth (difference between planted and non-planted treatments), and (c) rhizodeposit-C proportions by soil depth and land-use type across ten agroforestry sites in central Alberta, Canada. Error bars represent ± 95% confidence intervals. Least-squares means within MBC or WSOC accompanied by different lowercase letters are significantly different (Tukey-adjusted, $\alpha = 0.05$) among the soil depths or land-use types.

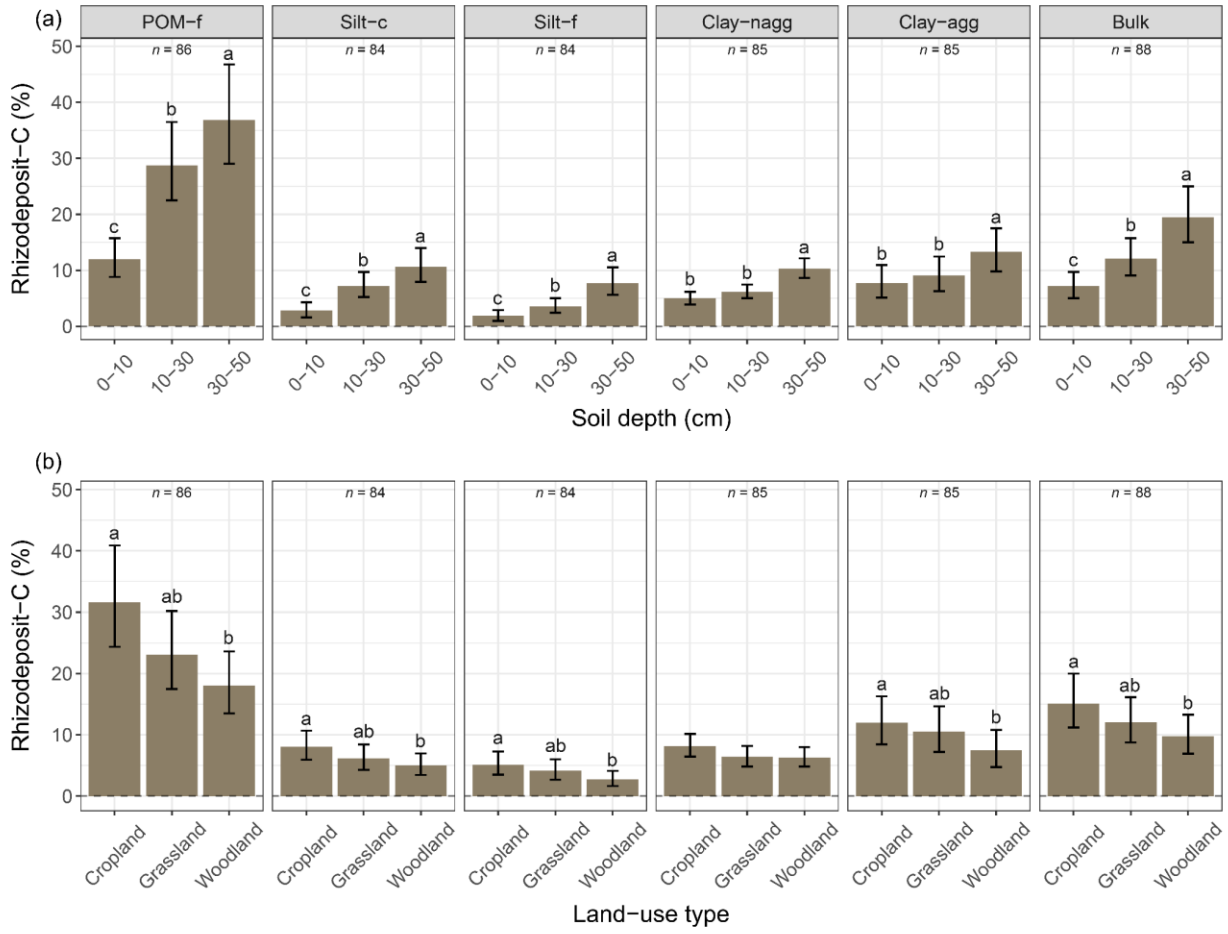

Figure 4.4. Rhizodeposit-carbon (C) proportions of soil fractions by (a) soil depth and (b) land-use type across ten agroforestry sites in central Alberta, Canada. Error bars represent ± 95% confidence intervals. Least-squares means within each soil fraction accompanied by different lowercase letters are significantly different (Tukey-adjusted, $\alpha = 0.05$) among the soil depths or land-use types. POM-f, fine particulate organic matter; silt-c, coarse silt; silt-f, fine silt; clay-nagg, non-aggregated clay; clay-agg, aggregated clay.

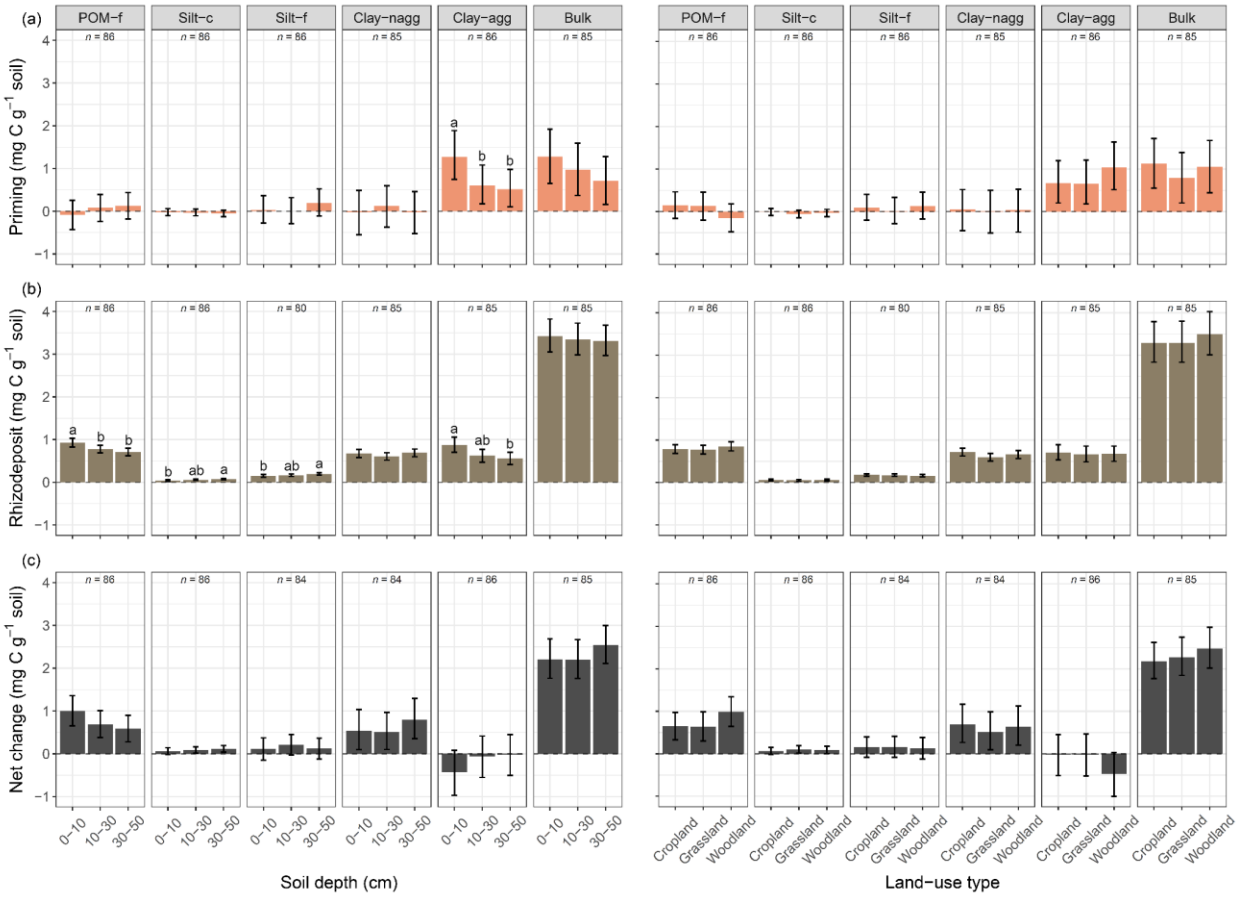

Figure 4.5. (a) Priming, i.e., the intensified loss of carbon (C), (b) rhizodeposit C incorporation, and (c) net C change (difference between planted and non-planted treatments) of soil fractions by soil depth and land-use type across ten agroforestry sites in central Alberta, Canada. Error bars represent ± 95% confidence intervals. Least-squares means within each soil fraction accompanied by different lowercase letters are significantly different (Tukey-adjusted, $\alpha = 0.05$) among the soil depths. POM-f, fine particulate organic matter; silt-c, coarse silt; silt-f, fine silt; clay-nagg, non-aggregated clay; clay-agg, aggregated clay.

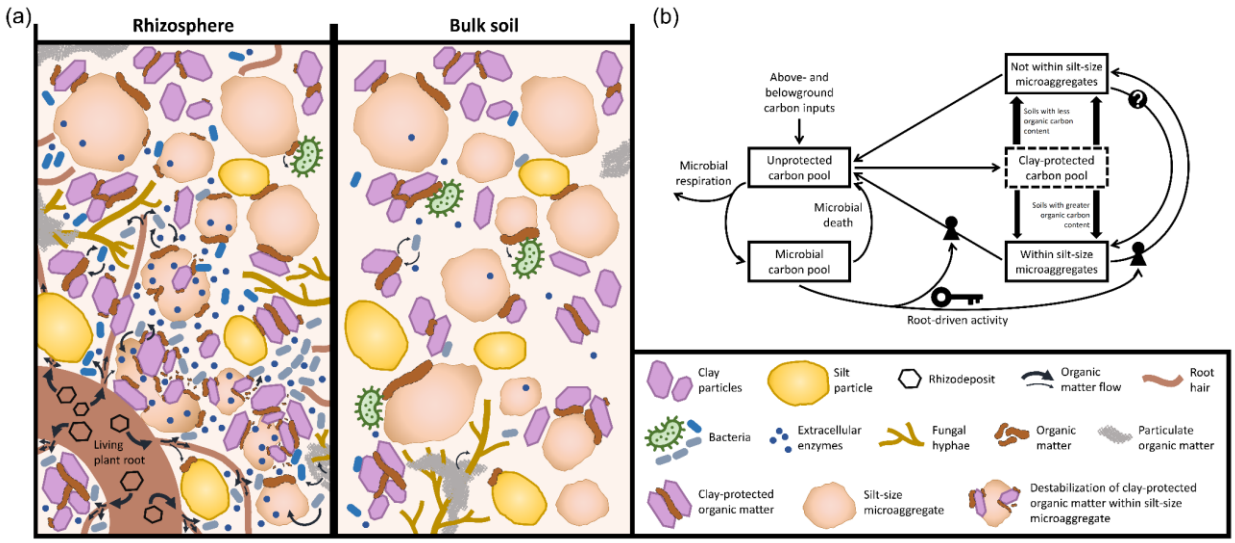

Figure 4.6. (a) Proposed conceptual model for root-driven destabilization of clay-protected organic matter within water-stable silt-size microaggregates (adapted from Sokol *et al.,* 2022) and (b) a soil carbon model structure that implements the interplay of physical (within silt-size microaggregates) and chemical (sorption) protection of clay-associated carbon (expanded from Yang *et al.,* 2021). Thicker arrows indicate greater rates of flow.

Chapter 5. Biochar stabilizes clay-protected carbon within silt-size microaggregates

Cole D. Gross[1], Edward W. Bork[2], Björn Wissel[3], Cameron N. Carlyle[2], Scott X. Chang[1]

[1] Department of Renewable Resources, Faculty of Agricultural, Life and Environmental Sciences, University of Alberta, 442 Earth Sciences Building, Edmonton, AB T6G 2E3, Canada; cgross@ualberta.ca (C.D.G.); sxchang@ualberta.ca (S.X.C.)

[2] Department of Agricultural, Food and Nutritional Science, Faculty of Agricultural, Life and Environmental Sciences, University of Alberta, 410 Agriculture/Forestry Centre, Edmonton, AB T6G 2P5, Canada; ebork@ualberta.ca (E.W.B.); cameron.carlyle@ualberta.ca (C.N.C.)

[3] LEHNA, Université Claude Bernard Lyon 1, 69622 Villeurbanne, France; bjoern.wissel@univ-lyon1.fr (B.W.)

5.1. Abstract

Carbon (C) sequestration initiatives may be impeded by root-driven intensified loss (a.k.a. priming) of soil organic C (SOC). Protection of SOC from microbial decomposition occurs through soil aggregation and mineral sorption, which may be enhanced by organic amendments such as biochar. How sorption of C to clay within silt-size microaggregates is affected by the interaction between root-driven dynamics and organic amendments is unknown. Here I quantified SOC changes due to the influence of living roots in soils—either non-amended or amended (two years prior) with manure compost or its biochar derivative—collected from annually cropped agricultural land using the C stable isotope natural abundance technique. Following a 150-d incubation in a controlled growth chamber, paired non-planted and planted (*Bouteloua gracilis*) soils were fractioned into particulate organic matter, silt, non-aggregated clay, and clay within water-stable silt-size microaggregates (aggregated clay). Priming of soil-derived C was limited to the aggregated clay fraction and was only significantly different from zero in non- and manure-amended soils (1.30 and 1.25 mg C g^{-1} soil, respectively). Microbial growth, root-derived C incorporation into the aggregated clay fraction, and reductions in the mass of the aggregated clay fraction, were positively correlated with priming. Biochar minimized the effect that living roots had on reducing the mass of the aggregated clay fraction, potentially due to the presence of fine-silt-size biochar and its sorption of root exudates or interactions with microorganisms and exoenzymes. I conclude that biochar can stabilize clay-protected C within silt-size microaggregates under the influence of living roots, which may foster long-term SOC sequestration and stabilization across agricultural lands in soils with varying properties.

Graphical abstract:

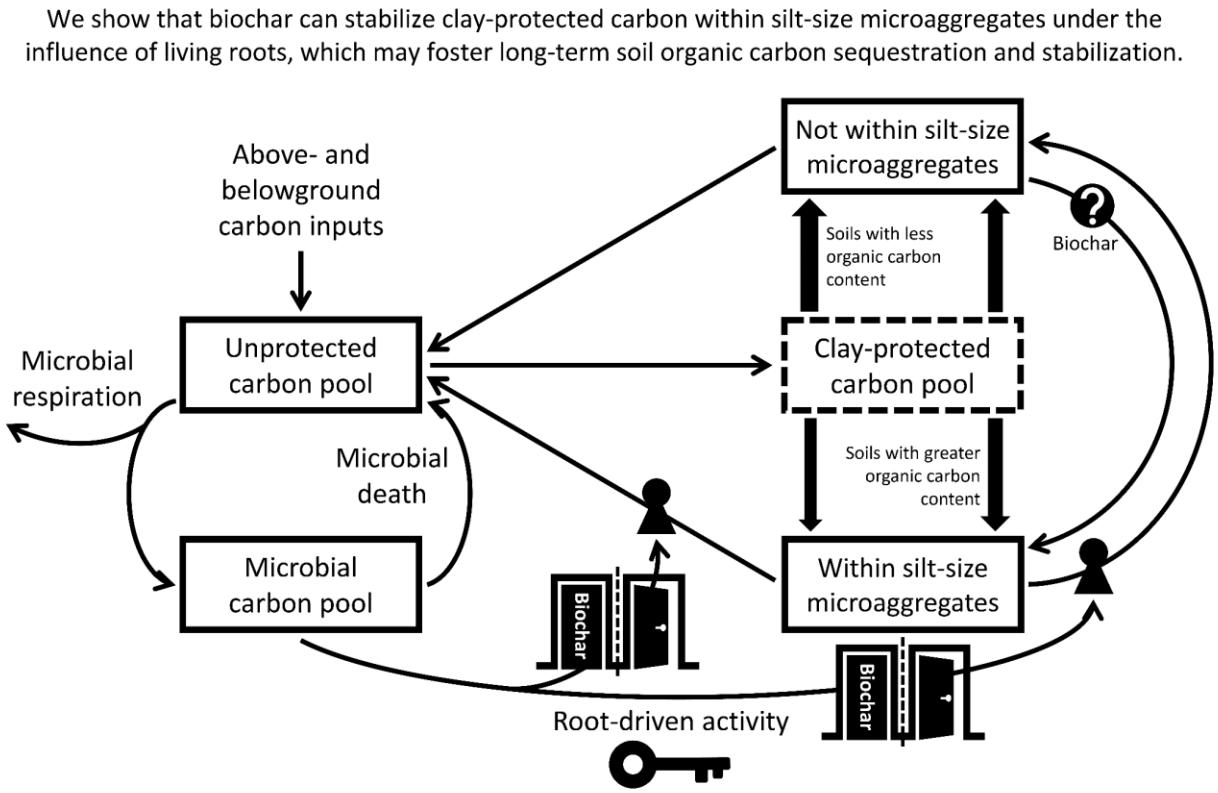

Keywords: biochar, labile carbon, microbial biomass, mineral-associated organic carbon, particulate organic matter, rhizosphere priming, soil aggregation, stable isotopes

Highlights:

- Priming was limited to the aggregated clay fraction.
- Priming increased with microbial growth and root-derived carbon in aggregated clay.
- Priming increased with reductions in the mass of the aggregated clay fraction.
- Biochar minimized mass reductions and priming within the aggregated clay fraction.
- Biochar can stabilize clay-protected carbon within silt-size microaggregates.

5.2. Introduction

Cultivation results in the loss of large amounts of carbon (C) from the soil (Guo & Gifford, 2002). This C is released to the atmosphere, exacerbating global climate change (Ciais *et al.*, 2013). Increasing soil organic C (SOC) storage is key to help mitigate climate change (IPCC, 2022) and can also increase soil health (e.g., increased nutrient- and water-holding capacities, microbial diversity, aeration, and soil aggregation), enhancing the resilience of agricultural land to climate changes such as drought (Amundson & Biardeau, 2018). However, increasing C inputs to soil can result in intensified loss (a.k.a. priming) of SOC, initially reducing SOC storage (Dijkstra *et al.*, 2021). Understanding how agricultural soils under different management regimes store and cycle new C inputs will allow for the development of targeted management practices to increase C sequestration and, in turn, food security (Lorenz & Lal, 2022).

Incorporating organic amendments into agricultural soils is a common management practice used to increase SOC (Lal, 2004; Paustian *et al.*, 2016) by adding organic C to the soil in relatively large amounts, usually at infrequent intervals. Additional practices aimed at increasing SOC, such as the use of perennial or cover crops (Paustian *et al.*, 2016; Schlautman *et al.*, 2021; IPCC, 2022), increase C inputs to the soil more gradually and over longer periods by increasing root litter and exudate C inputs (together termed rhizodeposition). Fresh C inputs enhance microbial activity, which can intensify the loss of SOC, a phenomenon referred to as priming (Kuzyakov *et al.*, 2000). In particular, living roots can have both stabilizing and destabilizing effects on SOC (Dijkstra *et al.*, 2021), with rhizosphere priming effects sometimes resulting in initial net decreases in SOC storage despite additional C inputs (Dijkstra & Cheng, 2007; Sulman *et al.*, 2014; Dijkstra *et al.*, 2021).

Chemically and physically protected SOC may persist longer in soil than C that is more readily accessible to microorganisms (Lehmann *et al.*, 2007; Virto *et al.*, 2010; Totsche *et al.*, 2018). Sorption of organic C to soil minerals, particularly to the clay fraction, is considered to provide protection from microbial decomposition (Angst *et al.*, 2018; Rasmussen *et al.*, 2018). This mineral-associated C may be primarily comprised of microbial residues (Kleber *et al.*, 2007; Liang *et al.*, 2019). Because living roots increase microbial turnover, they also increase microbial products and necromass that can be stabilized in the soil (Zhu *et al.*, 2020; Dijkstra *et al.*, 2021; Sokol *et al.*, 2022). However, root exudates can cause priming by mediating the release of mineral-associated C into the dissolved organic C pool, which is readily available to microorganisms

(Clarholm *et al.*, 2015; Keiluweit *et al.*, 2015). Living roots can also foster the formation of aggregates (Rasse *et al.*, 2005; Totsche *et al.*, 2018), which physically protect SOC from microbial decomposition, as well as enhance aggregate turnover and therefore priming effects (He *et al.*, 2020; Wang *et al.*, 2020).

Soils amended with biochar (organic material pyrolyzed under low or no oxygen conditions) may experience increased root-derived C retention relative to non-amended soils, as well as negative priming (Lehmann *et al.*, 2011; Hernandez-Soriano *et al.*, 2016a; Weng *et al.*, 2017). Biochar amendment can counteract rhizosphere priming through the sorption of root exudates onto biochar surfaces (Weng *et al.*, 2017), both reducing priming effects and increasing root-derived C retention. Biochar has also been found to promote aggregate formation, particularly microaggregate formation, providing additional physical protection of SOC from microbial decomposition (Hernandez-Soriano *et al.*, 2016a; Weng *et al.*, 2017). Silt-size microaggregates (2–53 μm) are especially important for providing SOC protection by largely excluding bacteria from their micropores (Rasse *et al.*, 2005; Lavallee *et al.*, 2019; Yang *et al.*, 2021). If biochar accelerates the formation of these organo-mineral microstructures, SOC in biochar-amended soils may be less susceptible to root-driven priming effects (Weng *et al.*, 2017). However, little is known about SOC stabilization within silt-size microaggregates because most aggregation studies do not consider aggregates at this size scale (Virto *et al.*, 2008; Totsche *et al.*, 2018; Lavallee *et al.*, 2019).

My previous study showed that living roots can destabilize clay-protected C within silt-size microaggregates, leading to rapid and preferential decomposition of clay-protected C (Chapter 4). Here I expand on my previous study by using the ^{13}C natural abundance technique to investigate the effects of manure compost and biochar on root-driven SOC dynamics in soils with varying properties (texture, pH, C and N content, etc.) collected from annually cropped agricultural land and planted with a native perennial C_4 plant species (blue grama, *Bouteloua gracilis* (Willd. ex Kunth.) Lag. Ex Griffiths). I used soils derived from C_3 plant systems that were either amended (two years prior) or not amended with manure compost or its biochar derivative. My objectives were to 1) elucidate the effect of manure compost and biochar on the interplay of physical and chemical protection of C under the influence of living roots by quantifying root C incorporation and priming across different soil fractions, including clay-size particles within silt-size microaggregates, and 2) assess the interdependence of soil properties (including SOC storage

within soil fractions) and root-driven SOC dynamics across non-amended and manure- and biochar-amended agricultural soils.

5.3. Materials and methods

5.3.1. Soils used in incubation

I collected surface soils (0–10 cm) in May 2020 from ten producer-operated, annually cropped sites in central Alberta, Canada. Soil was collected by augering (3.81-cm diameter) three holes per treatment (non-amended or amended with manure compost or its biochar derivative) and soil was composited by site. The historical monocultural annual crop rotation at all ten study sites was typically a combination of wheat (*Triticum aestivum* L.), barley (*Hordeum vulgare* L.), and canola (*Brassica rapa* L.). The soils at all ten study sites exhibited high levels of surface soil organic matter accumulation (Chernozems in the Canadian soil classification system or Ustic Haplocryolls in the United States soil taxonomy system). More detailed site and soil property information is provided in Gross *et al.* (2022).

Manure compost and biochar were applied (to plots 7 × 7 m in size) at equivalent C rates of 7 Mg C ha^{-1} in early May 2018 and tilled into the surface 10 cm of soil. The manure compost and biochar were applied at 25 and 20 Mg ha^{-1} (dry-weight), respectively, based on the C concentration for manure compost (280 mg C g^{-1} manure compost) and biochar (347 mg C g^{-1} biochar). The amount of nitrogen (N) applied was 185 and 138 kg N ha^{-1} for manure compost and biochar, respectively, due to the lower C:N ratio of the manure compost (37.5) relative to the biochar (50.2). The manure (derived from steers fed alfalfa hay, barley straw, lentil pellets, and activated carbon) was composted outdoors for one full year. The manure was composted with livestock bedding material consisting of equal parts barley and wheat straw (~5:1 ratio of manure to straw, mass-basis). A minor component of pine (*Pinus* spp.) and spruce (*Picea* spp.) wood chips was later added to the bulk manure compost prior to biochar production to aid in the pyrolysis process (~10:1 ratio of manure compost to wood chips, mass-basis). Biochar was produced by processing the bulk manure compost at 650 °C for 90 min under low to no oxygen conditions until it was fully pyrolyzed using a retort pyrolysis system. The mean $\delta^{13}C$ values of the manure compost (n = 3) and biochar (n = 3), respectively, were −25.50 and −26.44 ± 0.05‰. More detailed information with respect to the field experiment is provided in Gross *et al.* (2022).

After the soil samples were returned to the laboratory, field-moist soil was sieved to 8 mm by carefully separating the soil at natural breaks to minimize disturbance of the existing aggregate structure and disruption of soil microbial activity (Horwath & Paul, 1994; Datta *et al.*, 2014). Plant residues and coarse fragments (diameter > 2 mm) were removed from the soil. All soil samples were stored at 4 °C prior to the incubation.

5.3.2. Experimental design and incubation

The incubation experiment used a randomized complete block design. Pre-weighed polypropylene jars (64-mm diameter × 70-mm height) were filled with 60 g (oven-dry weight basis) of sieved (< 8 mm) field-moist soil. To minimize aggregate disruption, bulk density was controlled by repeatedly tapping the base of the jars, attaining a similar bulk density between duplicates. Soil moisture content was adjusted to 60% water-holding capacity by either air-drying or slowly and evenly adding ultrapure (MilliporeSigma Milli-Q) water. Soils were preincubated for 10 days in a growth chamber (Conviron CMP6050, Winnipeg, Manitoba, Canada) with 100% relative humidity, a 17-h photoperiod with 400 μmol m^{-2} s^{-1} light intensity, and temperatures of 26 and 13 °C in the day and night, respectively. To maintain the moisture content at 60% maximal water-holding capacity, soils were moistened with ultrapure water at 3-d intervals (see below for more details).

After the preincubation period, one set of the duplicate soils was planted with 0.3 g of blue grama seeds (Ontario Seed Co., Limited) (hereafter referred to as planted treatment), which were spread evenly over the soil surface. The paired planted and non-planted (bare soil) treatments were then incubated for 150 days under the same conditions as the preincubation period. An additional subset of the soils was planted with blue grama seeds and simultaneously incubated as a reference to determine the amount of water to be added to soils in the planted treatment. Soil in reference jars was destructively sampled weekly during the first half of the incubation to quantify and account for the mass of the fresh grass biomass (both above- and belowground) at various stages of phenological development.

After 150 days, the soil from both planted and non-planted treatments was gently removed from the jars and carefully separated at natural breaks to pass through an 8 mm sieve. Grass blades, stems, and roots were removed from the planted treatment, thoroughly washed with water on a 250-μm sieve, dried at 60 °C for 48 h, and weighed. Most roots were removed with tweezers,

although some very fine roots remained embedded in aggregates. Planted and non-planted treatments were processed similarly to avoid any differential processing effect on the pairs. Subsequently, bulk soils were adjusted to 50% water-holding capacity and stored at 4 °C to minimize microbial biomass effects, as well as limit increases in the quantity or strength of organic C interactions with minerals or interactions between minerals, which can affect aggregate stability, labile organic C concentrations, and mineral-associated organic C (Kaiser *et al.*, 2015).

5.3.3. Roots, bulk soil, microbial biomass, and labile carbon analyses

Roots were ground to a fine powder using a stainless-steel ball mill and a composite subsample was analyzed ($n = 4$) on an Elemental Combustion System (Costech EA; ECSD 4010) that led into a Thermo-Finnigan Delta V isotope ratio mass spectrometer (IRMS). To obtain bulk soil C and nitrogen (N) concentrations, as well as $\delta^{13}C$ values ($\delta^{15}N$ values were generated but not used in this paper), subsamples were dried at 40 °C, ground to a fine powder with an agate mortar and pestle, and analyzed on the EA-IRMS. Prior to analysis, soils that contained carbonates ($n = 3$) were subject to acid fumigation for 72 h to remove carbonates so that measured soil C represented only organic C (Ramnarine *et al.*, 2011). A conversion factor was used to account for the increased weight of acidified soils so as to not dilute any organic C (Ramnarine *et al.*, 2011). Soils containing carbonates were confirmed prior to the incubation experiment by analyzing subsamples of all the soils with pH > 6.00 on an elemental analyzer (Vario MICRO Cube Elemental Analyzer, Elementar, Hesse, Germany) before and after acid fumigation. For analyses on the EA-IRMS, bovine liver and wheat flour were used as internal laboratory standards. Carbon isotopes are reported in the conventional δ notation (‰) relative to Vienna Pee-Dee-Belemnite for C stable isotopes (Cooper & Wissel, 2012). Samples that were analyzed as laboratory duplicates (9% of the samples) gave isotopic compositions that agreed within 0.2‰ for $\delta^{13}C$.

The chloroform fumigation-extraction procedure was used to measure soil microbial biomass (Vance *et al.*, 1987; Beck *et al.*, 1997). Duplicate subsamples of 5 g (oven-dry weight basis) of soil were fumigated in a vacuum chamber with ethanol-free chloroform for 48 h in darkness (Jenkinson *et al.*, 2004). Water-soluble organic matter was extracted from both fumigated and non-fumigated samples by shaking the samples with 0.01 M K_2SO_4 (1:5 w:v) for 1 h at 180 rpm (Haney *et al.*, 2001; Werth & Kuzyakov, 2010). After centrifuging at 10,000 × g for 10 min, 20 mL of the supernatant was collected and filtered through a 0.4-µm Whatman Nuclepore

polycarbonate filter (Zsolnay, 2003; Chantigny *et al.*, 2007). Filtrates were stored at 4 °C prior to analysis with a total organic C (TOC) analyzer (TOC-V and TN unit, Shimadzu Corporation, Kyoto, Japan) using 680 °C combustion catalytic oxidation and the non-purgeable organic C (to remove inorganic C) and total N methods. Microbial biomass C (MBC) was calculated using an extraction efficiency of 0.45 (Jenkinson *et al.*, 2004). The organic C and total N in the non-fumigated samples were defined as water-soluble organic C (WSOC) and N (WSN). To obtain $\delta^{13}C$ values, 10 mL aliquots of the filtrates were dried at 40 °C, and precipitates were agitated to a fine powder using a stainless-steel soil scoop and analyzed on the EA-IRMS. Prior to drying, 0.4 mL of 1 M HCl was added to the filtrate aliquots from soils that contained carbonates to remove inorganic C.

5.3.4. Physical soil fractionation and soil fraction analyses

Eight grams (oven-dry weight basis) of soil was fractioned into the following: coarse and fine particulate organic matter (POM), coarse and fine silt, non-aggregated clay, and clay within silt-size microaggregates. To protect water-stable silt-size microaggregates from being destroyed while breaking down larger aggregates (> 53 µm), the size-separation device described in detail by Virto *et al.* (2008) was used. Briefly, soil aggregates > 53 µm in size were broken up on a shaker (4 h at 180 rpm) using five glass beads (5-mm diameter) within a 30-mL plastic bottle sealed with a 53-µm-opening nylon cloth (Gilson Co. Inc., Columbus, OH) and contained within a 250-mL plastic bottle with 200 mL of ultrapure water (Virto *et al.*, 2008). This device allowed for the separation of materials < 53 µm in size from the abrasive effects within the small bottle, including water-stable silt-size microaggregates, which passed into the large bottle and remained in suspension during shaking (Virto *et al.*, 2008).

The sand + POM fraction collected in the small bottle was poured onto a 53-µm sieve and rinsed over a beaker with ultrapure water until the solution passing through the sieve was clear. The silt + clay fraction in the large bottle was added to the suspension in the beaker. The sand + POM fraction was backwashed into a 250-µm sieve over a larger 53-µm sieve and rinsed for an additional minute. For the fraction remaining on the 250-µm sieve (hereafter referred to as coarse POM), remaining roots in the planted treatment were removed with tweezers, oven-dried, and weighed. No roots were visible in the fraction collected on the 53-µm sieve (hereafter referred to as fine POM). The dry mass of recovered roots was added to the total root mass for a given planted

treatment using a multiple that assumed uniformity in the remaining mass of roots in the bulk soil after initial root removal.

Sedimentation and centrifuging (until the supernatant was clear) according to Stoke's Law were used to separate the dispersed clay-size fraction (< 2 μm; hereafter referred to as non-aggregated clay) from the silt + clay fraction (Virto *et al.*, 2008). The remaining silt-size fraction (consisting of free silt-size particles and water-stable silt-size microaggregates) was subjected to 500 J cm^{-3} ultrasonic energy after transferring this fraction into a 100-mL glass beaker (45-mm diameter, 80-mm height) and adding ultrapure water to result in an 80-mL soil suspension (Kaiser & Berhe, 2014). The ultrasonic probe (Qsonica Q700, Newton, Connecticut, USA) was calibrated as described by Schmidt *et al.* (1999) and the probe tip (12-mm diameter) was immersed 18 mm into the suspension. Samples underwent sonification using 50% amplitude and a pulse:non-pulse ratio of 1:1 to avoid mass losses and prevent overheating of the probe and soil suspension (Yang *et al.*, 2009). To maintain soil suspension temperatures below 30 °C, the base of the beaker was cooled by the continuous circulation of compressed air during sonification.

Following the application of 500 J cm^{-3} ultrasonic energy to break up larger silt-size microaggregates (20–53 μm) (Kaiser & Berhe, 2014), the soil suspension was poured over a 20-μm sieve and rinsed over a beaker with ultrapure water until the solution passing through the sieve was clear. The silt-size fraction remaining on the 20-μm sieve is hereafter referred to as coarse silt. Sedimentation was used to separate most of the clay-size fraction (< 2 μm) dispersed after sonication (hereafter referred to as aggregated clay) from the soil suspension. The remaining soil suspension, which was stored at 4 °C for a maximum of 24 h before further fractionation (Virto *et al.*, 2008; Kaiser *et al.*, 2015), was subjected to an additional 1000 J cm^{-3} ultrasonic energy to achieve complete dispersion (Kaiser & Berhe, 2014). Sedimentation and centrifuging (until the supernatant was clear) were used to separate the remaining clay-size fraction (< 2 μm; included in the aggregated clay) and silt-size fraction (hereafter referred to as fine silt).

All soil fractions were transferred into pre-weighed aluminum dishes, oven-dried at 40 °C, and weighed. The soil fractions (except coarse POM) were ground to a fine powder with an agate mortar and pestle and analyzed on the EA-IRMS to determine their C and N concentrations and $\delta^{13}C$ values. Prior to analysis, soils that contained carbonates were subjected to acid fumigation as previously described. Coarse POM was not analyzed on the EA-IRMS, as this fraction is the least homogeneous and was also contaminated with very fine root fragments in the planted treatment.

The amount of C in coarse POM was calculated as the difference between bulk soil C and the sum of C across the other soil fractions for a given sample. Across all samples, the soil mass recovery ratio (sum of soil fractions to total sample used) was 1.00 ± 0.00 (standard error). The C recovery ratio (sum of soil fractions to bulk soil, not including coarse POM) was 0.95 ± 0.01, 0.95 ± 0.02, and 0.90 ± 0.02 for the control, manure compost, and biochar treatments, respectively, wherein biochar-amended soil contained visible biochar particles in coarse POM in most samples. Differences between the planted and non-planted treatments in % clay of the < 20 μm fraction and % fine silt of total silt were 0.00 ± 0.15 and 0.15 ± 0.15, respectively.

5.3.5. Calculations

The $\delta^{13}C$ values of microbial biomass were calculated as

$$\delta^{13}C_{mic} = \left[\left(C_{fum} \times \delta^{13}C_{fum}\right) - \left(C_{nfum} \times \delta^{13}C_{nfum}\right)\right] / \left(C_{fum} - C_{nfum}\right) \quad [5.1]$$

where C_{fum} and C_{nfum} are the amounts of water-soluble C (μg C g^{-1} soil) in the fumigated and non-fumigated soils, respectively, and $\delta^{13}C_{fum}$ and $\delta^{13}C_{nfum}$ are the $\delta^{13}C$ values of the fumigated and non-fumigated samples, respectively (Marx *et al.*, 2007; Werth & Kuzyakov, 2008; Vogel *et al.*, 2014).

The contribution of root-derived C (rhizodeposit-C) to total C in MBC, WSOC, soil fractions, or bulk soil in the planted treatment was calculated as

$$C_{rhizodeposit} = f_{rhizodeposit} \times C_{planted} \quad [5.2]$$

where $C_{planted}$ is the amount of C (μg or mg C g^{-1} soil) in MBC, WSOC, soil fractions, or bulk soil in the planted treatment and $f_{rhizodeposit}$ is the fraction of C attributable to root-derived C, calculated as

$$f_{rhizodeposit} = \left(\delta^{13}C_{planted} - \delta^{13}C_{non-planted}\right) / \left(\delta^{13}C_{root} - \delta^{13}C_{non-planted}\right) \quad [5.3]$$

where $\delta^{13}C_{planted}$ is the δ^{13}C value of C in MBC, WSOC, soil fractions, or bulk soil in the planted treatment, $\delta^{13}C_{non-planted}$ is the δ^{13}C value of C in MBC, WSOC, soil fractions, or bulk soil in the non-planted treatment, and $\delta^{13}C_{root}$ is the mean δ^{13}C value of the roots (−15.37 ± 0.02‰) (Marx *et al.*, 2007; Werth & Kuzyakov, 2008). For the δ^{13}C value of the roots, I accounted for the magnitude of isotopic fractionation between rhizodeposits and microbial biomass, which was assumed to be the same as between the bulk soil and microbial biomass (Werth & Kuzyakov, 2008). Microbial biomass was ^{13}C enriched by an average of 1.25 ± 0.15‰ relative to the bulk soil in the non-planted treatment, consistent with the findings in Werth & Kuzyakov (2010).

Priming of C (mg C g^{-1} soil), i.e., the intensified loss of soil-derived C due to the presence of living roots over the duration of the incubation (150 days), was calculated as

$$C_{primed} = C_{non-planted} - C_{planted}\left(1 - f_{rhizodeposit}\right) \quad [5.4]$$

where $C_{non-planted}$ is the amount of C (mg C g^{-1} soil) in soil fractions or bulk soil in the non-planted treatment.

5.3.6. Statistical analyses

Linear mixed-effect models were used to determine whether priming or soil property differences between the planted and non-planted treatments were significantly different from zero and whether they differed among the agricultural treatments: control (non-amended), manure compost (hereafter referred to as manure for brevity), and biochar. A randomized complete block design model was used for the statistical analyses. Agricultural treatment was the fixed effect and site was the random effect. Root mass was included in the models as a covariate. All data points with Cook's distance > 4/*n* were examined as potential outliers and removed when required for the model fit. Where necessary for the soil variables, data transformations using the lambda value for the maximum log likelihood for obtaining minimum error sum of squares were conducted to conform data to the assumptions of homogeneous variance and normality of distribution. Back-transformed data were used to calculate least-squares means and 95% confidence intervals (CIs). For determining differences in soil properties across the agricultural treatments for the non-planted treatment, similar linear mixed-effect models were used (less the covariate), but non-transformed data were used in the models to calculate least-squares means and standard errors. When

significant effects were detected at $p < 0.05$ after using type-III analysis-of-variance (ANOVA), pairwise *post-hoc* comparisons using the Tukey method for *p*-value adjustment were conducted to compare differences among agricultural treatments. Associations among continuous variables of interest were determined using Pearson's parametric correlation. Specifically, I assessed the relationships between soil properties in the non-planted treatment and root-driven soil effects. All data were analyzed using RStudio Version 1.4.1106 and the "lme4" package for the linear mixed-effect models (RStudio Team, 2021).

5.4. Results

5.4.1. Properties of soil fractions in the non-planted treatment

In the non-planted treatment, aggregated and non-aggregated clay had similar C concentrations across agricultural treatments, with 11.72 and 12.29 mg C g^{-1} soil, respectively (Fig. 5.1a). In contrast, biochar-amended soil had greater ($p < 0.001$) C concentrations than non- and manure-amended soils in fine silt, fine POM, and the bulk soil (Fig. 5.1a). Coarse POM C concentrations were also greater ($p < 0.001$) in biochar-amended soil than in non- and manure-amended soils, with 3.96, 1.72, and 1.80 mg C g^{-1} soil, respectively. Similar to the differences found among agricultural treatments for C concentrations, the C:N ratio was greater ($p < 0.001$) in biochar-amended soil than in non- and manure-amended soils in fine silt, fine POM, and the bulk soil (Fig. 5.1b).

In the non-planted treatment, $\delta^{13}C$ values were −27.67‰ for fine POM, −26.83‰ for coarse silt, −26.73‰ for fine silt, −26.00‰ for non-aggregated clay, −26.67‰ for aggregated clay, and −26.37‰ for the bulk soil (Table D.S1). No differences across agricultural treatments were found. Aggregated clay comprised a similar proportion of total clay mass (39%) and clay-protected C (48%) across agricultural treatments, with biochar-amended soil having slightly (but non-significant) greater amounts (Fig. D.S1). Aggregated clay was 1.46 times more enriched in C than non-aggregated clay across agricultural treatments (Fig. D.S2).

5.4.2. Microbial biomass and labile carbon

In the non-planted treatment, $\delta^{13}C$ values for MBC and WSOC were −25.25 and −26.80‰, respectively (Table D.S1), with no difference found across agricultural treatments. Compared with the non-planted treatment, $\delta^{13}C$ values for MBC and WSOC in the planted treatment increased by

an average of 6.77 and 1.72‰, respectively (Table 5.1). The amount of rhizodeposit-C in the MBC was similar across agricultural treatments (353–408 μg C g^{-1} soil). The increase in MBC within the planted treatment relative to the non-planted treatment (i.e., microbial growth) was also similar across agricultural treatments (307–429 μg C g^{-1} soil). The majority of MBC was comprised of rhizodeposit-C (61%), while a much smaller proportion of WSOC was comprised of rhizodeposit-C (14–16%; Fig. 5.2). The amount of rhizodeposit-C in the WSOC was negligible across agricultural treatments (4–5 μg C g^{-1} soil), as was the increase in WSOC within the planted treatment relative to the non-planted treatment (1–6 μg C g^{-1} soil).

5.4.3. Rhizodeposit carbon incorporation and priming

Compared with the non-planted treatment, $\delta^{13}C$ values in the planted treatment increased by 0.44‰ for coarse silt, 0.30‰ for fine silt, 0.56‰ for non-aggregated clay, 0.98‰ for aggregated clay, and 0.99‰ for the bulk soil (Table 5.1). For fine POM, the increase was greater ($p < 0.001$) in non- and manure-amended soils (2.36 and 2.31‰, respectively) relative to biochar-amended soil (1.68‰; Table 5.1). Similarly, the proportion of C comprised of rhizodeposit-C within fine POM was greater ($p < 0.001$) in non- and manure-amended soils than in biochar-amended soil, a reflection of the initial size of the C pools (Fig. 5.3). Across agricultural treatments, rhizodeposit-C comprised 7% of the C associated with aggregated clay, which represented an overall higher proportion relative to non-aggregated clay (5%) and the silt fractions (2–3%; Fig. 5.3).

Priming (i.e., the intensified loss of C) within the soil fractions was limited to aggregated clay (Fig. 5.4a). Root-driven soil-derived C losses within aggregated clay were only significantly different from zero in non- and manure-amended soils (1.30 and 1.25 mg C g^{-1} soil, respectively; Fig. 5.4a). Within the bulk soil, priming was similar in magnitude across agricultural treatments (1.08–1.54 mg C g^{-1} soil; Fig. 5.4a). A similar amount of rhizodeposit-C was incorporated into all soil fractions and the bulk soil across agricultural treatments (Fig. 5.4b). The amount of rhizodeposit-C incorporated into the soil fractions was minimal for the silt fractions relative to the clay fractions and fine POM (Fig. 5.4b). Rhizodeposit-C incorporation into the bulk soil was an average of 1.09 mg C g^{-1} soil greater than the sum of the measured soil fractions (Fig. 5.4b). This additional rhizodeposit-C was attributable to the amount of C in the roots remaining in the bulk soil that were removed from coarse POM after physical soil fractionation (0.98 ± 0.12 mg C g^{-1}

soil). Net C changes within the soil fractions were limited to fine POM (except for a minimal net C gain within coarse silt for biochar-amended soil) and were similar across agricultural treatments (0.73–0.87 mg C g^{-1} soil; Fig. 5.4c). The net C gain for the bulk soil was an average of 1.25 mg C g^{-1} soil greater than the sum of the measured soil fractions, a difference again attributable to the amount of C in the roots remaining in the bulk soil (Fig. 5.4c).

Across agricultural treatments, priming within aggregated clay was positively correlated with the proportion of clay-protected C within aggregated clay and WSN in the non-planted treatment ($p < 0.01$; Fig. D.S3). Priming within aggregated clay was also positively correlated with MBC growth (difference between planted and non-planted treatments), rhizodeposit-C incorporation into aggregated clay, and the loss of aggregated clay mass in the planted treatment (difference between the aggregated clay to total clay mass proportions in the planted and non-planted treatments), with the latter two variables explaining 50 and 45% of the variation, respectively, in priming within aggregated clay ($p < 0.03$; Fig. D.S3). Specifically, living roots had a more neutral effect on the mass of aggregated clay in biochar-amended soil (+0.21%) relative to non- and manure-amended soils, wherein the mass of aggregated clay tended to be reduced by living roots (−1.72 and 0.60%, respectively; Fig. D.S4). The loss of aggregated clay mass was positively correlated with MBC growth, as well as the proportion of clay-protected C within aggregated clay and MBC in the non-planted treatment ($p < 0.03$; Fig. D.S3). Root mass (Table D.S2) and MBC growth were positively correlated ($p = 0.01$; Fig. D.S3). In the non-planted treatment, bulk soil C was positively correlated with the proportion of clay-protected C within aggregated clay ($p < 0.001$; Fig. D.S3).

5.5. Discussion

I show that biochar can stabilize clay-protected C within silt-size microaggregates under the influence of living roots. My results highlight an interplay between physical (within silt-size microaggregates) and chemical (sorption) protection of SOC as affected by biochar (Weng *et al.*, 2017), as well as the dual effects (stabilizing and destabilizing) of living roots on SOC dynamics (Dijkstra *et al.*, 2021). In my experiment, overall net C gains occurred despite priming of soil-derived C. These net C gains resulted largely from root-derived C in the form of fine POM, which is a relatively labile form of SOC (Lavallee *et al.*, 2019) and likely originated from water-insoluble root debris such as root hairs (Rasse *et al.*, 2005). Priming was driven by rapid and preferential

decomposition of clay-protected C, further challenging the assumption that C associated with clay is stable (Keiluweit *et al.*, 2015; Yang *et al.*, 2021). Therefore, the stabilizing effect of biochar on clay-protected C within silt-size microaggregates has important implications for the long-term stabilization and accumulation of SOC in agricultural soils.

A higher proportion of clay-protected C within silt-size microaggregates was positively related to greater total SOC content, underscoring the importance of this SOC pool. Additionally, aggregated clay was more enriched in C than non-aggregated clay, indicating that aggregation at the silt-size scale is a critical component in enhancing SOC storage. These results are consistent with the findings of my study that assessed the same SOC pools across land uses and soil depths (Chapter 4), as well as others that studied microaggregates at the silt-size scale or smaller (Virto *et al.*, 2010; Vogel *et al.*, 2014; Asano *et al.*, 2018). Indeed, aggregated clay can play a pivotal role in SOC sequestration and stabilization (Chenu & Plante, 2006; Vogel *et al.*, 2014). While living roots destabilized aggregated clay and associated C in non- and manure-amended soils, the presence of biochar reduced this effect. Incorporation of root-derived C into aggregated clay occurred rapidly in non- and manure-amended soils, but was also diminished in biochar-amended soil, suggesting that biochar reduced the extent of root-driven disruption of silt-size microaggregates and associated C turnover rates.

Root-derived C was preferentially sorbed to aggregated clay relative to non-aggregated clay in my experiment (given the lower proportion of total clay mass associated with aggregated clay), similar to my previous observations (Chapter 4) and other studies (Vogel *et al.*, 2014; Asano *et al.*, 2018). However, this preferential sorption was more evident in non- and manure-amended soils than biochar-amended soil, potentially resulting from a shift in root-derived C incorporation into fine silt in biochar-amended soil. This shift may have occurred if some of the fine silt was comprised of fine-silt-size biochar, especially if this fine-silt-size biochar was incorporated into silt-size microaggregates (Virto *et al.*, 2008; Weng *et al.*, 2017). Indeed, biochar particles generally have high porosity and surface area for sorbing C (Lin *et al.*, 2012; Hernandez-Soriano *et al.*, 2016b). The higher C content and C:N ratio in fine silt in biochar-amended soil is suggestive of the presence of biochar particles in this fraction (as opposed to, for example, greater SOC storage in fine silt resulting only from an indirect effect of biochar amendment).

A shift in root-derived C incorporation into fine silt in biochar-amended soil may be responsible for the diminished priming within aggregated clay and enhanced priming within fine

silt in biochar-amended soil relative to non- and manure-amended soils. The strong positive relationship between root-derived C incorporation into aggregated clay and priming in this fraction supports this scenario. For example, root exudates, which can mediate the release of mineral-associated C (Clarholm *et al.*, 2015; Keiluweit *et al.*, 2015) and enhance aggregate disruption, may have been sorbed on the surfaces of fine-silt-size biochar (Weng *et al.*, 2017), reducing the destabilizing effects of the living roots. Exchange reactions, wherein mineral-associated C is released in favor of new C (Marx *et al.*, 2007; Sanderman *et al.*, 2008), likely enhanced priming within fine silt in biochar-amended soil. Future studies should investigate if biochar at the fine-silt-size scale and associated root-derived C retention can directly foster the formation of clay-size particles into silt-size microaggregates, as this could lead to a positive feedback loop (Vogel *et al.*, 2014; Weng *et al.*, 2017).

Another potential mechanism by which biochar may have minimized priming within aggregated clay is by reducing microbial activity and metabolism (Hernandez-Soriano *et al.*, 2016b; Yousaf *et al.*, 2017). Specifically, biochar may have limited priming within aggregated clay by decreasing the activities of exoenzymes (Lehmann *et al.*, 2011), which can diffuse into silt-size microaggregates (with micropores too small for microorganisms to penetrate) and break down associated clay-protected C (Yang *et al.*, 2021). Sorption of exoenzymes to biochar can reduce exoenzyme activity through immobilization (Lehmann *et al.*, 2011). Additionally, co-localization of microorganisms and organic C on biochar surfaces (such as within fine silt in my experiment) can decrease the need for exoenzyme production (Lehmann *et al.*, 2011). The strong positive relationship between root-driven reduction in the mass of aggregated clay and priming in this fraction supports this scenario. That is, biochar may have reduced the diffusion of exoenzymes into silt-size microaggregates and therefore limited the subsequent break down of the organic compounds helping to stabilize them (Rasse *et al.*, 2005; Lehmann *et al.*, 2007; Totsche *et al.*, 2018). The ability of biochar to stabilize clay-protected C within silt-size microaggregates under the influence of living roots (e.g., through interactions with microorganisms and exoenzymes) may depend on a number of factors, such as its age (Lin *et al.*, 2012) and feedstock (Hernandez-Soriano *et al.*, 2016b), the effects of which are important questions for future research.

In biochar-amended soil, a shift in priming from within aggregated to non-aggregated clay was evident and was potentially an indirect effect of reduced transference of formerly aggregated clay (and any remaining bound soil-derived C) to non-aggregated clay. Across agricultural

treatments, the preferential use of rhizodeposits by microorganisms for growth (as evidenced by the dominance of root-derived C within microbial biomass) likely resulted in increased nutrient mining by microorganisms (Shahzad *et al.*, 2015; Gunina & Kuzyakov, 2022). This could explain the rapid and preferential root-driven decomposition of clay-protected soil-derived organic matter, which was nutrient-rich (low C:N ratio) and abundant relative to other forms of organic matter. These results are consistent with my previous study (Chapter 4) and underscore the complex effect that living roots have on SOC dynamics, such as increased nutrient mining by activated microorganisms and increased microbial turnover (Dijkstra *et al.*, 2021; Sokol *et al.*, 2022), the latter of which creates opportunities for protection of microbial necromass via sorption onto mineral surfaces (Gross & Harrison, 2019; Sokol & Bradford, 2019; Sokol *et al.*, 2019). The stabilizing effect of biochar on silt-size microaggregates may increase root-derived C retention in the long-term (Weng *et al.*, 2017), including the retention of microbial products and necromass.

5.6. Conclusions

I conclude that clay-protected C within silt-size microaggregates is an important SOC pool that can be affected rapidly by management practices. Critically, my study demonstrates that biochar can stabilize clay-protected C within silt-size microaggregates under the influence of living roots, which may foster long-term SOC sequestration and stabilization. This evident interplay between the physical and chemical protection of SOC supports my proposal of an integrated soil C model (Chapter 4). Here I suggest expanding this model to consider the mitigating effect of biochar on root-driven SOC destabilization (Fig. 5.5). Finally, my results support the use of biochar, rather than its manure compost feedstock, as an amendment across agricultural lands in soils with varying properties to help meet climate change mitigation goals by enhancing SOC storage and stability.

Funding: This research was supported by a Doctoral Vanier Scholarship and a Killam Memorial Graduate Scholarship to C.D.G., as well as a grant (AGGP2-039) from the Agricultural Greenhouse Gas Program from Agriculture and Agri-Food Canada to S.X.C., E.W.B., and C.N.C.

Credit: C.D.G.: Conceptualization. C.D.G. and B.W.: Methodology. C.D.G.: Investigation and Writing—original draft. C.D.G., S.X.C., E.W.B., B.W., and C.N.C.: Writing—review and editing.

S.X.C. and E.W.B.: Resources and Supervision. S.X.C., E.W.B., B.W., and C.N.C.: Guidance and Feedback at various stages.

Acknowledgements: Thank you to Mary Villeneuve, Sheetal Patel, and Carmen C. Roman-Perez for their help in the lab.

5.7. References

Amundson R, Biardeau L (2018) Opinion: Soil carbon sequestration is an elusive climate mitigation tool. *Proceedings of the National Academy of Sciences*, **115**, 11652–11656.

Angst G, Messinger J, Greiner M et al. (2018) Soil organic carbon stocks in topsoil and subsoil controlled by parent material, carbon input in the rhizosphere, and microbial-derived compounds. *Soil Biology and Biochemistry*, **122**, 19–30.

Asano M, Wagai R, Yamaguchi N, Takeichi Y, Maeda M, Suga H, Takahashi Y (2018) In search of a binding agent: Nano-scale evidence of preferential carbon associations with poorly-crystalline mineral phases in physically-stable, clay-sized aggregates. *Soil Systems*, **2**, 32.

Beck T, Joergensen RG, Kandeler E, Makeshin E, Nuss E, Oberholzer HR, Scheu S (1997) An inter-laboratory comparison of ten different ways of measuring soil microbial biomass C. *Soil Biology & Biochemistry*, **29**, 1023–1032.

Chantigny MH, Angers DA, Kaiser K, Kalbitz K (2007) Extraction and characterization of dissolved organic matter. In: *Soil Sampling and Methods of Analysis*, 2nd edn (eds Carter MR, Gregorich EG), pp. 617–635. CRC Press, Boca Raton.

Chenu C, Plante AT (2006) Clay-sized organo-mineral complexes in a cultivation chronosequence: Revisiting the concept of the "primary organo-mineral complex." *European Journal of Soil Science*, **57**, 596–607.

Ciais P, Sabine C, Bala G et al. (2013) Carbon and other biogeochemical cycles. In: *Climate Change 2013: The Physical Science Basis. Contribution of Working Group I to the Fifth Assessment Report of the Intergovernmental Panel on Climate Change* (eds Stocker TF, Qin D, Plattner G-K, Tignor M, Allen SK, Boschung J, Nauels A, Xia Y, Bex V, Midgley PM), pp. 465–570. Cambridge University Press, Cambridge, United Kingdom and New York, NY, USA.

Clarholm M, Skyllberg U, Rosling A (2015) Organic acid induced release of nutrients from

metal-stabilized soil organic matter - The unbutton model. *Soil Biology and Biochemistry*, **84**, 168–176.

Cooper RN, Wissel B (2012) Loss of trophic complexity in saline prairie lakes as indicated by stable-isotope based community-metrics. *Aquatic Biosystems*, **8**, 6.

Datta R, Vranová V, Pavelka M, Rejšek K, Formánek P (2014) Effect of soil sieving on respiration induced by low-molecular-weight substrates. *International Agrophysics*, **28**, 119–124.

Dijkstra FA, Cheng W (2007) Interactions between soil and tree roots accelerate long-term soil carbon decomposition. *Ecology Letters*, **10**, 1046–1053.

Dijkstra FA, Zhu B, Cheng W (2021) Root effects on soil organic carbon: A double-edged sword. *New Phytologist*, **230**, 60–65.

Gross CD, Harrison RB (2019) The case for digging deeper: Soil organic carbon storage, dynamics, and controls in our changing world. *Soil Systems*, **3**, 28.

Gross CD, Bork EW, Carlyle CN, Chang SX (2022) Biochar and its manure-based feedstock have divergent effects on soil organic carbon and greenhouse gas emissions in croplands. *Science of The Total Environment*, **806**, 151337.

Gunina A, Kuzyakov Y (2022) From energy to (soil organic) matter. *Global Change Biology*, **28**, 2169–2182.

Guo LB, Gifford RM (2002) Soil carbon stocks and land use change: A meta analysis. *Global change biology*, **8**, 345–360.

Haney RL, Franzluebbers AJ, Hons FM, Hossner LR, Zuberer DA (2001) Molar concentration of K2SO4 and soil pH affect estimation of extractable C with chloroform fumigation-extraction. *Soil Biology and Biochemistry*, **33**, 1501–1507.

He Y, Cheng W, Zhou L et al. (2020) Soil DOC release and aggregate disruption mediate rhizosphere priming effect on soil C decomposition. *Soil Biology and Biochemistry*, **144**, 107787.

Hernandez-Soriano MC, Kerré B, Goos P, Hardy B, Dufey J, Smolders E (2016a) Long-term effect of biochar on the stabilization of recent carbon: Soils with historical inputs of charcoal. *GCB Bioenergy*, **8**, 371–381.

Hernandez-Soriano MC, Kerré B, Kopittke PM, Horemans B, Smolders E (2016b) Biochar affects carbon composition and stability in soil: A combined spectroscopy-microscopy

study. *Scientific Reports*, **6**, 1–13.

Horwath WR, Paul EA (1994) Microbial biomass. In: *Methods of Soil Analysis: Part 2—Microbiological and Biochemical Properties, SSSA Book Series no. 5* (eds Bottomley PS, Angle JS, Weaver RW), pp. 753–774. Soil Science Society of America, Madison.

IPCC (2022) Summary for policymakers. In: *Climate Change 2022: Mitigation of Climate Change. Contribution of Working Group III to the Sixth Assessment Report of the Intergovernmental Panel on Climate Change* (eds Shukla PR, Skea J, Slade R, Khourdajie A Al, Diemen R van, McCollum D, Pathak M, Some S, Vyas P, Fradera R, Belkacemi M, Hasija A, Lisboa G, Luz S, Malley J), p. 63. Cambridge University Press, Cambridge, UK and New York, NY, USA.

Jenkinson DS, Brookes PC, Powlson DS (2004) Measuring soil microbial biomass. *Soil Biology and Biochemistry*, **36**, 5–7.

Kaiser M, Berhe AA (2014) How does sonication affect the mineral and organic constituents of soil aggregates? - A review. *Journal of Plant Nutrition and Soil Science*, **177**, 479–495.

Kaiser M, Kleber M, Berhe AA (2015) How air-drying and rewetting modify soil organic matter characteristics: An assessment to improve data interpretation and inference. *Soil Biology and Biochemistry*, **80**, 324–340.

Keiluweit M, Bougoure JJ, Nico PS, Pett-Ridge J, Weber PK, Kleber M (2015) Mineral protection of soil carbon counteracted by root exudates. *Nature Climate Change*, **5**, 588–595.

Kleber M, Sollins P, Sutton R (2007) A conceptual model of organo-mineral interactions in soils: Self-assembly of organic molecular fragments into zonal structures on mineral surfaces. *Biogeochemistry*, **85**, 9–24.

Kuzyakov Y, Friedelb JK, Stahra K (2000) Review of mechanisms and quantification of priming effects. *Soil Biology & Biochemistry*, **32**, 1485–1498.

Lal R (2004) Soil carbon sequestration impacts on global climate change and food security. *Science*, **304**, 1623–1627.

Lavallee JM, Soong JL, Cotrufo MF (2019) Conceptualizing soil organic matter into particulate and mineral-associated forms to address global change in the 21st century. *Global Change Biology*, 1–13.

Lehmann J, Kinyangi J, Solomon D (2007) Organic matter stabilization in soil microaggregates:

Implications from spatial heterogeneity of organic carbon contents and carbon forms. *Biogeochemistry*, **85**, 45–57.

Lehmann J, Rillig MC, Thies J, Masiello CA, Hockaday WC, Crowley D (2011) Biochar effects on soil biota - A review. *Soil Biology and Biochemistry*, **43**, 1812–1836.

Liang C, Amelung W, Lehmann J, Kästner M (2019) Quantitative assessment of microbial necromass contribution to soil organic matter. *Global Change Biology*, **25**, 3578–3590.

Lin Y, Munroe P, Joseph S, Kimber S, Van Zwieten L (2012) Nanoscale organo-mineral reactions of biochars in ferrosol: An investigation using microscopy. *Plant and Soil*, **357**, 369–380.

Lorenz K, Lal R (2022) *Soil Organic Carbon Sequestration in Terrestrial Biomes of the United States*, 1st edn. Springer, Cham, Switzerland, 201 pp.

Marx M, Buegger F, Gattinger A, Marschner B, Zsolnay Á, Munch JC (2007) Determination of the fate of 13C labelled maize and wheat rhizodeposit-C in two agricultural soils in a greenhouse experiment under 13C-CO2-enriched atmosphere. *Soil Biology and Biochemistry*, **39**, 3043–3055.

Paustian K, Lehmann J, Ogle S, Reay D, Robertson GP, Smith P (2016) Climate-smart soils. *Nature*, **532**, 49–57.

Ramnarine R, Voroney RP, Wagner-Riddle C, Dunfield KE (2011) Carbonate removal by acid fumigation for measuring the δ13C of soil organic carbon. *Canadian Journal of Soil Science*, **91**, 247–250.

Rasmussen C, Heckman K, Wieder WR et al. (2018) Beyond clay: towards an improved set of variables for predicting soil organic matter content. *Biogeochemistry*, **137**, 297–306.

Rasse DP, Rumpel C, Dignac MF (2005) Is soil carbon mostly root carbon? Mechanisms for a specific stabilisation. *Plant and Soil*, **269**, 341–356.

RStudio Team (2021) *RStudio: Integrated Development Environment for R*. Boston, MA.

Sanderman J, Baldock JA, Amundson R, Baldock JA (2008) Dissolved organic carbon chemistry and dynamics in contrasting forest and grassland soils. *Biogeochemistry*, **89**, 181–198.

Schlautman B, Bartel C, Diaz-Garcia L et al. (2021) Perennial groundcovers: An emerging technology for soil conservation and the sustainable intensification of agriculture. *Emerging Topics in Life Sciences*, **5**, 337–347.

Schmidt MWI, Rumpel C, Kögel-Knabner I (1999) Evaluation of an ultrasonic dispersion

procedure to isolate primary organomineral complexes from soils. *European Journal of Soil Science*, **50**, 87–94.

Shahzad T, Chenu C, Genet P, Barot S, Perveen N, Mougin C, Fontaine S (2015) Contribution of exudates, arbuscular mycorrhizal fungi and litter depositions to the rhizosphere priming effect induced by grassland species. *Soil Biology and Biochemistry*, **80**, 146–155.

Sokol NW, Bradford MA (2019) Microbial formation of stable soil carbon is more efficient from belowground than aboveground input. *Nature Geoscience*, **12**, 46–53.

Sokol NW, Kuebbing SE, Karlsen-Ayala E, Bradford MA (2019) Evidence for the primacy of living root inputs, not root or shoot litter, in forming soil organic carbon. *New Phytologist*, **221**, 233–246.

Sokol NW, Slessarev E, Marschmann GL et al. (2022) Life and death in the soil microbiome: How ecological processes influence biogeochemistry. *Nature Reviews Microbiology*, **0123456789**.

Sulman BN, Phillips RP, Oishi AC, Shevliakova E, Pacala SW (2014) Microbe-driven turnover offsets mineral-mediated storage of soil carbon under elevated CO2. *Nature Climate Change*, **4**, 1099–1102.

Totsche KU, Amelung W, Gerzabek MH et al. (2018) Microaggregates in soils. *Journal of Plant Nutrition and Soil Science*, **181**, 104–136.

Vance ED, Brookes PC, Jenkinson DS (1987) An extraction method for measuring soil microbial biomass C. *Soil Biology and Biochemistry*, **19**, 703–707.

Virto I, Barré P, Chenu C (2008) Microaggregation and organic matter storage at the silt-size scale. *Geoderma*, **146**, 326–335.

Virto I, Moni C, Swanston C, Chenu C (2010) Turnover of intra- and extra-aggregate organic matter at the silt-size scale. *Geoderma*, **156**, 1–10.

Vogel C, Mueller CW, Höschen C et al. (2014) Submicron structures provide preferential spots for carbon and nitrogen sequestration in soils. *Nature Communications*, **5**, 1–7.

Wang X, Yin L, Dijkstra FA, Lu J, Wang P, Cheng W (2020) Rhizosphere priming is tightly associated with root-driven aggregate turnover. *Soil Biology and Biochemistry*, **149**, 107964.

Weng Z (Han), Van Zwieten L, Singh BP et al. (2017) Biochar built soil carbon over a decade by stabilizing rhizodeposits. *Nature Climate Change*, **7**, 371–376.

Werth M, Kuzyakov Y (2008) Root-derived carbon in soil respiration and microbial biomass determined by 14C and 13C. *Soil Biology and Biochemistry*, **40**, 625–637.

Werth M, Kuzyakov Y (2010) 13C fractionation at the root-microorganisms-soil interface: A review and outlook for partitioning studies. *Soil Biology and Biochemistry*, **42**, 1372–1384.

Yang XM, Drury CF, Reynolds WD, MacTavish DC (2009) Use of sonication to determine the size distributions of soil particles and organic matter. *Canadian Journal of Soil Science*, **89**, 413–419.

Yang JQ, Zhang X, Bourg IC, Stone HA (2021) 4D imaging reveals mechanisms of clay-carbon protection and release. *Nature Communications*, **12**.

Yousaf B, Liu G, Wang R, Abbas Q, Imtiaz M, Liu R (2017) Investigating the biochar effects on C-mineralization and sequestration of carbon in soil compared with conventional amendments using the stable isotope (δ13C) approach. *GCB Bioenergy*, **9**, 1085–1099.

Zhu X, Jackson RD, DeLucia EH, Tiedje JM, Liang C (2020) The soil microbial carbon pump: From conceptual insights to empirical assessments. *Global Change Biology*, **26**, 6032–6039.

Zsolnay Á (2003) Dissolved organic matter: Artefacts, definitions, and functions. *Geoderma*, **113**, 187–209.

5.8. Tables

Table 5.1. Agricultural treatment effects on changes (difference between planted and non-planted treatments) in $\delta^{13}C$ values of soil fractions across ten agricultural sites in central Alberta, Canada. Least-squares means (95% confidence intervals) within each soil fraction accompanied by different lowercase letters are significantly different (Tukey-adjusted, $\alpha = 0.05$) among the agricultural treatments. POM, particulate organic matter; MBC, microbial biomass carbon; WSOC, water-soluble organic carbon.

Treatment	Control	Manure	Biochar
Fine POM (*n* = 30)	2.36 (2.12, 2.59) a	2.31 (2.07, 2.54) a	1.68 (1.43, 1.92) b
Coarse silt (*n* = 29)	0.49 (0.24, 0.76)	0.41 (0.15, 0.68)	0.41 (0.16, 0.67)
Fine silt (*n* = 28)	0.27 (0.11, 0.43)	0.27 (0.12, 0.44)	0.35 (0.20, 0.51)
Non-aggregated clay (*n* = 29)	0.57 (0.44, 0.71)	0.55 (0.41, 0.69)	0.57 (0.43, 0.71)
Aggregated clay (*n* = 29)	1.15 (0.69, 1.68)	1.15 (0.67, 1.70)	0.63 (0.23, 1.08)
Bulk soil (*n* = 29)	1.02 (0.85, 1.20)	0.94 (0.77, 1.11)	1.00 (0.84, 1.18)
MBC (*n* = 29)	6.65 (5.97, 7.32)	6.57 (5.86, 7.24)	7.08 (6.41, 7.73)
WSOC (*n* = 29)	1.96 (1.72, 2.21)	1.68 (1.46, 1.91)	1.53 (1.30, 1.77)

5.9. Figures

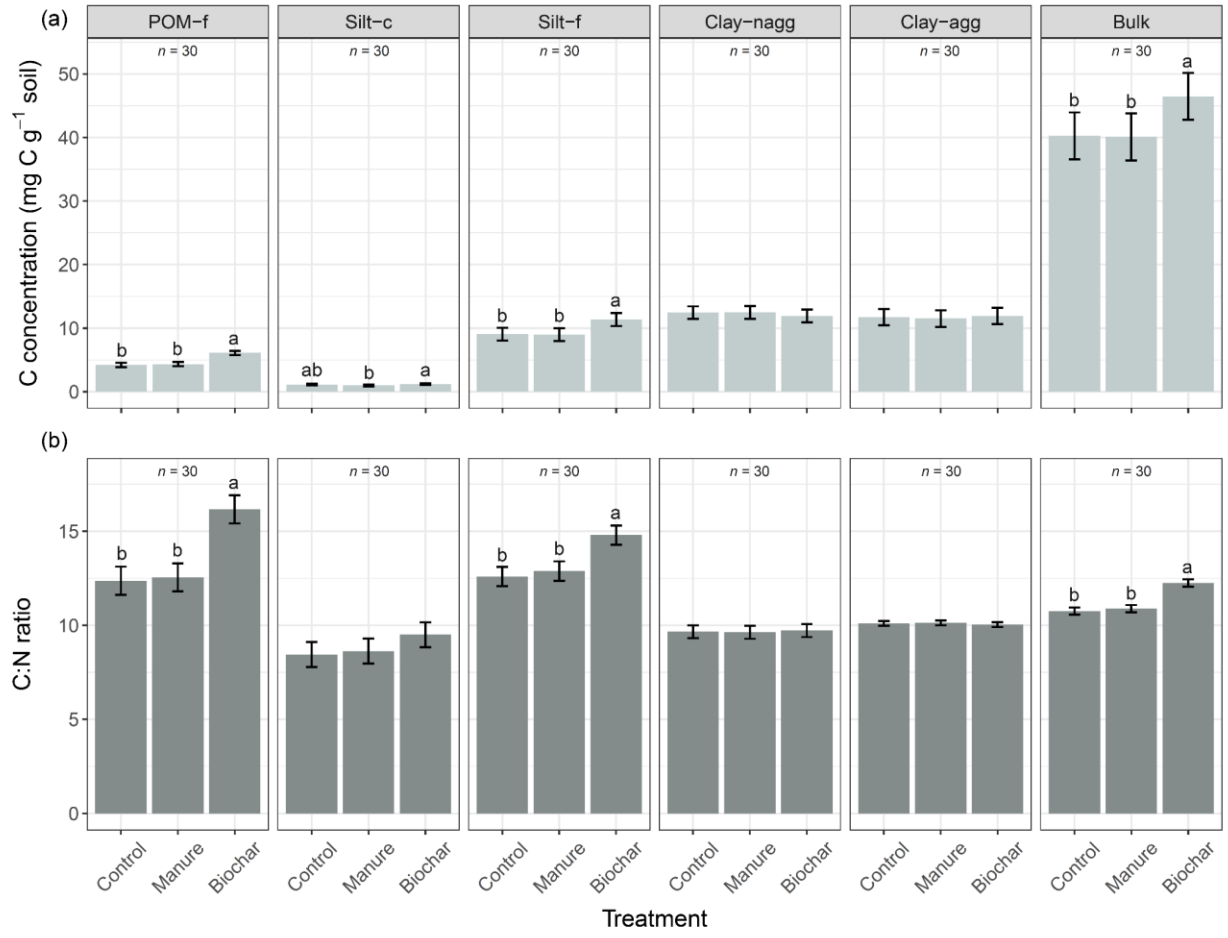

Figure 5.1. Agricultural treatment effects on (a) carbon (C) concentrations and (b) C to nitrogen (N) ratios of soil fractions in the non-planted treatment across ten agricultural sites in central Alberta, Canada. Error bars represent ± one standard error. Least-squares means within each soil fraction accompanied by different lowercase letters are significantly different (Tukey-adjusted, $\alpha = 0.05$) among the agricultural treatments. POM-f, fine particulate organic matter; silt-c, coarse silt; silt-f, fine silt; clay-nagg, non-aggregated clay; clay-agg, aggregated clay.

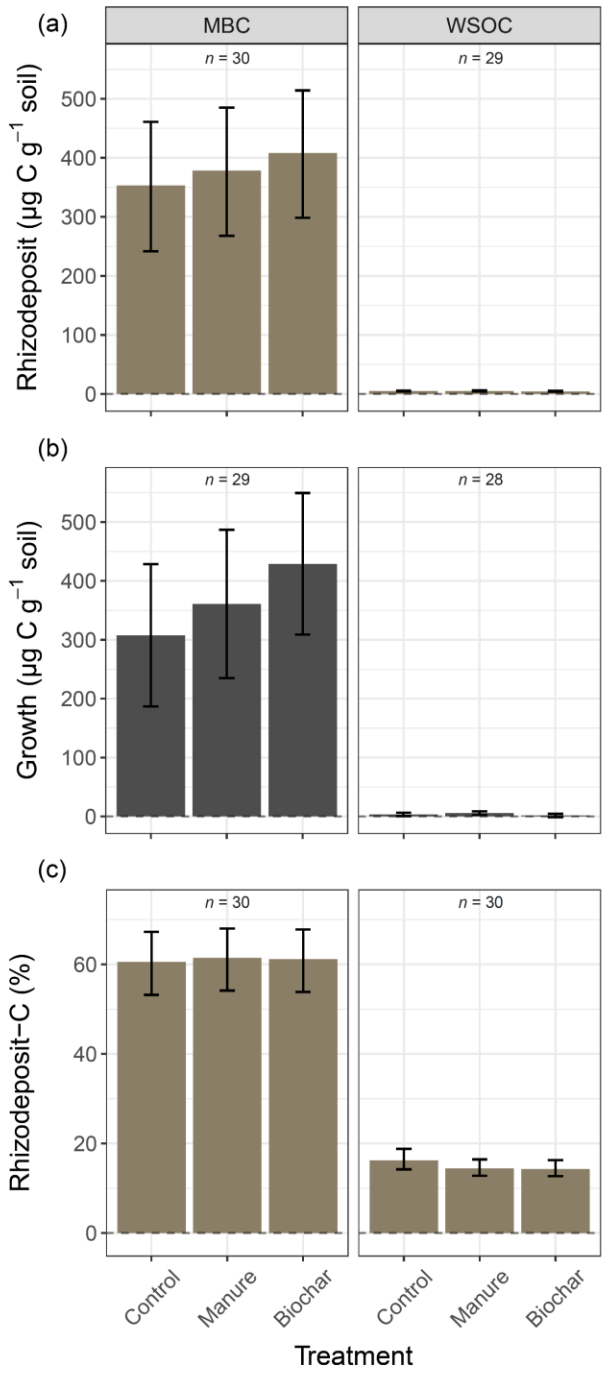

Figure 5.2. Agricultural treatment effects on (a) rhizodeposit carbon (C) incorporation, (b) growth (difference between planted and non-planted treatments), and (c) rhizodeposit-C proportions in microbial biomass C (MBC) and water-soluble organic C (WSOC) across ten agricultural sites in central Alberta, Canada. Error bars represent least-squares means ± 95% confidence intervals.

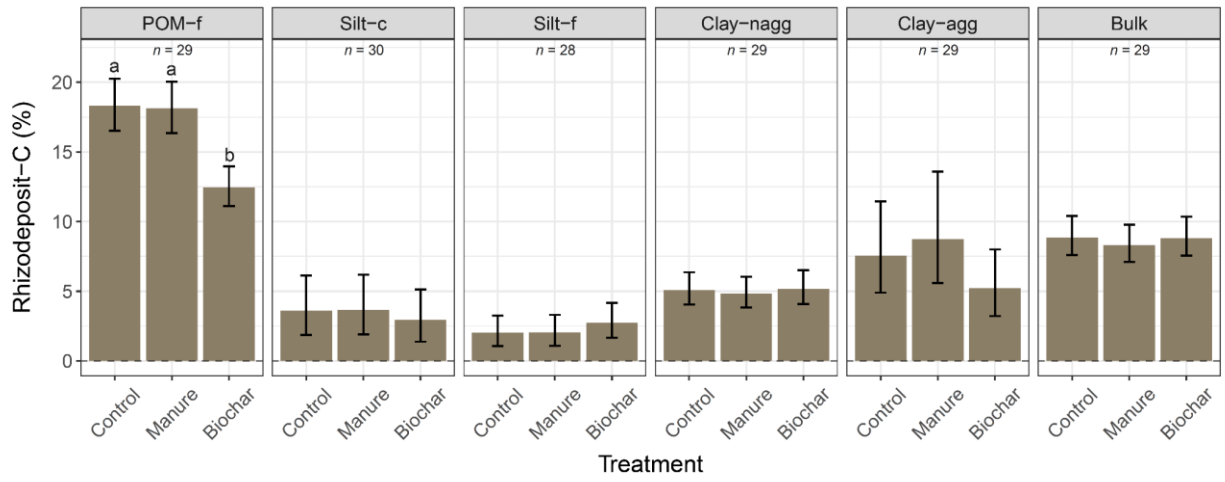

Figure 5.3. Agricultural treatment effects on rhizodeposit-carbon (C) proportions of soil fractions across ten agricultural sites in central Alberta, Canada. Error bars represent ± 95% confidence intervals. Least-squares means within each soil fraction accompanied by different lowercase letters are significantly different (Tukey-adjusted, $\alpha = 0.05$) among the agricultural treatments. POM-f, fine particulate organic matter; silt-c, coarse silt; silt-f, fine silt; clay-nagg, non-aggregated clay; clay-agg, aggregated clay.

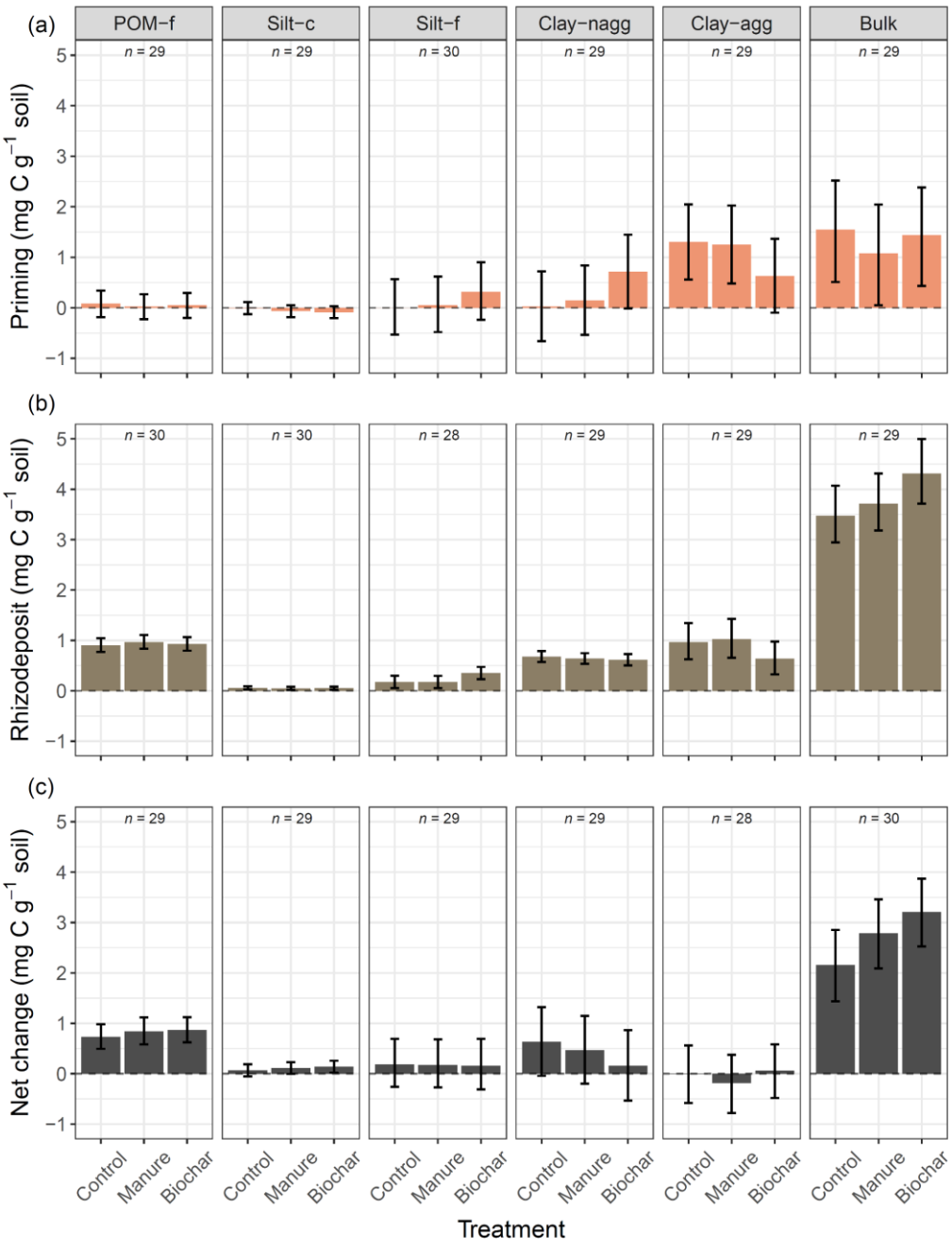

Figure 5.4. Agricultural treatment effects on (a) priming, i.e., the intensified loss of carbon (C), (b) rhizodeposit C incorporation, and (c) net C change (difference between planted and non-planted treatments) of soil fractions across ten agricultural sites in central Alberta, Canada. Error bars represent least-squares means ± 95% confidence intervals. POM-f, fine particulate organic matter; silt-c, coarse silt; silt-f, fine silt; clay-nagg, non-aggregated clay; clay-agg, aggregated clay.

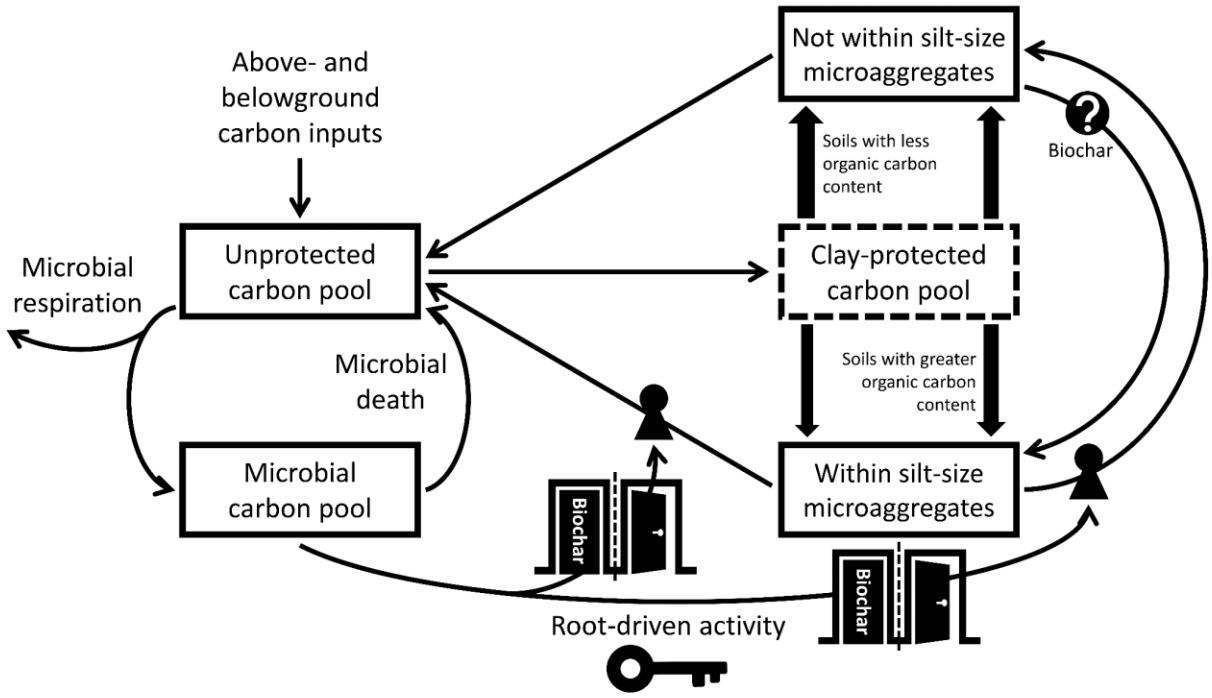

Figure 5.5. A soil carbon model structure that implements the interplay of physical (within silt-size microaggregates) and chemical (sorption) protection of clay-associated carbon and includes biochar-mediated stabilization of clay-protected carbon within silt-size microaggregates under the influence of living roots (after Chapter 4 and expanded from Yang *et al.,* 2021). Thicker arrows indicate greater rates of flow.

Chapter 6. Synthesis, conclusions, and recommendations

6.1. Synthesis and conclusions

My research aimed to find management practices that increase carbon (C) sequestration and reduce greenhouse gas (GHG) emissions from agroecosystems to help mitigate climate change. I conclude that agroforestry systems (AFS), which incorporate woody perennials into agricultural fields, are important for enhancing C sequestration and reducing GHG emissions. In particular, retaining hedgerows (naturally-occurring legacy woodland) and their associated deadwood across temperate agroecosystems is key to help mitigate climate change. Within the cropland, my results support the use of biochar (organic material pyrolyzed under low or no oxygen conditions) as a soil amendment for sequestering soil organic C (SOC) and mitigating GHG emissions. Finally, my findings demonstrate an interplay between physical and chemical protection of SOC from microbial decomposition that has important implications for our understanding of SOC persistence and the underlying processes used in soil C models.

Across two common AFS in the temperate climate zone, I found important differences between the woodland types, such as greater deadwood and SOC stocks, as well as increased heterotrophic respiration, within hedgerows relative to shelterbelts (planted trees on previously cleared land). Within the cropland, I found that manure compost application had none of the benefits of biochar, namely increasing SOC sequestration and reducing GHG emissions from agroecosystems across a range of soil types. My investigation of SOC dynamics revealed that clay-protected C within silt-size microaggregates (2–53 μm) is an important SOC pool across land uses and soil depths in a range of soils with varying properties. While most studies focus on soil aggregation at scales larger than silt-size, as well as combine silt- and clay-associated C into a single SOC pool, I show that clay-size particles within silt-size microaggregates are functionally different than other clay- and silt-size particles in terms of C storage and cycling. Critically, my study demonstrates that living roots can destabilize clay-protected C within silt-size microaggregates, leading to rapid and preferential decomposition of clay-protected C. However, my results also demonstrate that biochar can stabilize clay-protected C within silt-size microaggregates under the influence of living roots, which may foster long-term SOC sequestration and stabilization.

6.2. Recommendations for agroforestry: Retain, establish, and manage

With the urgent need to address climate change and governments globally committing resources to reduce GHG emissions and increase C sequestration, incentivizing the retention and establishment of AFS on agricultural lands would be an important step to help meet climate change mitigation goals. Given both the C sequestration and GHG emission mitigation potential of AFS, I recommend the adoption of frameworks that promote the retention and establishment of AFS on agricultural lands across Canada. For example, property tax reductions for retaining hedgerows on private agricultural lands would encourage landowners to protect natural woodlands, particularly if the tax rate reduction was directly based on the proportion of woodland to cropland. While a similar tax reduction system could be implemented for shelterbelt AFS, it is important to avoid incentivizing the establishment of shelterbelts over the retention of hedgerows. For instance, tax rate reductions for shelterbelt AFS could be based on the year of shelterbelt establishment, starting at a lower value than retained hedgerows and increasing over time to a comparable value. Providing grants and resources to landowners for the establishment or enhancement of shelterbelts would assist landowners in converting conventional agricultural lands into AFS.

While AFS establishment increases agroecosystem C storage on decadal timescales, removal of woody vegetation from AFS results in rapid and substantial losses in agroecosystem C storage (Amichev *et al.*, 2020; An *et al.*, 2022). I therefore stress retention of AFS foremost, in accordance with the decision-making framework proposed by Cook-Patton *et al.* (2021). Furthermore, where possible, landowners should be encouraged not to remove deadwood from the woodlands of AFS. As cleared trees and deadwood are usually burned rather than salvaged from agricultural lands (Rudd *et al.*, 2021), thereby releasing the C stored in tree biomass to the atmosphere, retaining deadwood within the woodlands of AFS is essential to avoid reductions in total ecosystem C stocks and help mitigate climate change. Moreover, deadwood enhances biodiversity (Blaser *et al.*, 2013; Vrška *et al.*, 2015; Sandström *et al.*, 2019) and supports healthy soil and ecosystem functions (Stokland *et al.*, 2012; Stutz *et al.*, 2017). Future research should further explore the relationships between deadwood and both SOC stocks and heterotrophic respiration in forests, including the woodlands of various AFS. For example, the effects of direct manipulations of deadwood within AFS, such as the creation of deadwood on-site from live trees (Sandström *et al.*, 2019), on SOC stocks and heterotrophic respiration would help inform management decisions. Moreover, the benefits of deadwood, such as enhanced biodiversity and

soil health, as well as other potential deadwood ecosystem effects, should be quantified in more detail to help inform decision-making and policy design concerning AFS.

6.3. Recommendations for biochar: Optimize, prioritize, and monitor

To fully realize the potential of biochar to mitigate climate change when used as an organic amendment in croplands, lifecycle assessments should be considered. Lifecycle assessments of biomass-pyrolysis systems, wherein the biochar was used as an agricultural soil amendment, have shown promise as far as avoiding net GHG emissions (Roberts *et al.*, 2010; Galinato *et al.*, 2011). However, optimizing biochar production-application systems is necessary to both reduce GHG emissions and support economic viability (Roberts *et al.*, 2010; Galinato *et al.*, 2011; Spokas *et al.*, 2012). The selection of appropriate feedstocks is one way in which to optimize biochar production-application systems. For example, biowaste feedstocks, including livestock manures, were identified as key resources for biochar production that have the potential for economic viability and renewable energy generation, as well as for increasing C sequestration and reducing GHG emissions (Roberts *et al.*, 2010), the latter of which my results have also shown. Indeed, further efforts should be made to assess and optimize biochar production-application systems, especially for processing biowaste feedstocks such as manure compost, the direct application of which only increased GHG emissions and did not increase SOC storage in my field study.

By using ten sites with different baseline soil properties, I was able to assess the performance of manure compost and its biochar on a broad scale as far as their differential abilities to mitigate climate change when amended into the soil of agroecosystems. My results, alongside decades of literature elucidating the benefits of biochar as a soil amendment, support that biochar application can act as a climate change mitigation strategy by enhancing surface SOC sequestration, thereby reducing GHG emissions resulting from agricultural practices. Future studies should investigate the performance of biochar across specific soil properties to help prioritize application. The effects of biochar application on surface soil properties (including increased SOC, total nitrogen, and pH in my field study) are expected to help foster sustainable agriculture. While changes in surface SOC due to organic amendments should not be viewed independently of potential effects on C-cycling processes occurring deeper in the soil, the latter effects may require longer-term assessments of treated soils, including across different amendment rates and frequencies. Therefore, ongoing and future biochar-amendment studies should sample

subsoil as well as surface soil to continue to monitor and determine treatment effects on deeper SOC-cycling processes over time.

6.4. Recommendations for soil carbon models: Integrate physical and chemical protection

I found that living roots can destabilize clay-protected C within silt-size microaggregates, leading to rapid and preferential decomposition of clay-protected C and further challenging the assumption that C associated with clay or silt-size microaggregates is stable (Keiluweit *et al.*, 2015; Yang *et al.*, 2021). While representative soil C models and most studies consider SOC protection within aggregates and on mineral surfaces as distinct processes (Lehmann & Kleber, 2015; Lavallee *et al.*, 2019), I suggest an integrated soil C model that considers the interplay of physical (within silt-size microaggregates) and chemical (sorption) protection of clay-associated C (Fig. 4.6). Net C gains found within the non-aggregated clay fraction due to living roots in my experiment may lead to a positive feedback loop, wherein dissolved organic C is more likely to be associated with the rough organo-mineral surfaces created (Vogel *et al.*, 2014). Under what conditions (or at what stage) the incorporation of recent C into the non-aggregated clay fraction will foster the formation of clay-size particles into silt-size microaggregates at a rate that surpasses any destabilization is an important question for future research.

The stabilizing effect of biochar on clay-protected C within silt-size microaggregates has important implications for the long-term stabilization and accumulation of SOC in agricultural soils. Therefore, I suggest that the integrated soil C model proposed above (Fig. 4.6) is expanded to consider the mitigating effect of biochar on root-driven SOC destabilization (Fig. 5.5). The ability of biochar to stabilize clay-protected C within silt-size microaggregates under the influence of living roots (e.g., through interactions with microorganisms and exoenzymes) may depend on a number of factors, such as its age (Lin *et al.*, 2012) and feedstock (Hernandez-Soriano *et al.*, 2016b), the effects of which are important questions for future research. Additionally, future studies should investigate if biochar at the fine-silt-size scale and associated root-derived C retention can directly foster the formation of clay-size particles into silt-size microaggregates, as this could lead to a positive feedback loop (Vogel *et al.*, 2014; Weng *et al.*, 2017). For example, a greater proportion of silt-size microaggregates may increase root-derived C retention in the long-

term (Weng *et al.*, 2017), including the retention of microbial products and necromass, which may, in turn, accelerate the formation of silt-size microaggregates.

6.5. Summary

In summary, to help meet climate change mitigation goals by fostering C sequestration and reducing GHG emissions, I recommend incentivizing the retention and establishment of AFS on agricultural lands, as well as optimizing biochar production-application systems to support biochar application in agriculture. Moreover, because root-driven stabilization or destabilization of clay-protected C within silt-size microaggregates may mediate SOC sequestration and SOC storage capacity, I suggest an integrated soil C model that considers the interplay of physical (within silt-size microaggregates) and chemical (sorption) protection of clay-associated C (Fig. 4.6), as well as the mitigating effect of biochar on root-driven SOC destabilization (Fig. 5.5).

6.6. References

Amichev BY, Laroque CP, Van Rees KCJ (2020) Shelterbelt removals in Saskatchewan, Canada: implications for long-term carbon sequestration. *Agroforestry Systems*, **94**, 1665–1680.

An Z, Bork EW, Duan X, Gross CD, Carlyle CN, Chang SX (2022) Quantifying past, current, and future forest carbon stocks within agroforestry systems in central Alberta, Canada. *GCB Bioenergy*, **14**, 669–680.

Blaser S, Prati D, Senn-Irlet B, Fischer M (2013) Effects of forest management on the diversity of deadwood-inhabiting fungi in Central European forests. *Forest Ecology and Management*, **304**, 42–48.

Cook-Patton SC, Drever CR, Griscom BW et al. (2021) Protect, manage and then restore lands for climate mitigation. *Nature Climate Change*, **11**, 1027–1034.

Galinato SP, Yoder JK, Granatstein D (2011) The economic value of biochar in crop production and carbon sequestration. *Energy Policy*, **39**, 6344–6350.

Hernandez-Soriano MC, Kerré B, Kopittke PM, Horemans B, Smolders E (2016) Biochar affects carbon composition and stability in soil: A combined spectroscopy-microscopy study. *Scientific Reports*, **6**, 1–13.

Keiluweit M, Bougoure JJ, Nico PS, Pett-Ridge J, Weber PK, Kleber M (2015) Mineral

protection of soil carbon counteracted by root exudates. *Nature Climate Change*, **5**, 588–595.

Lavallee JM, Soong JL, Cotrufo MF (2019) Conceptualizing soil organic matter into particulate and mineral-associated forms to address global change in the 21st century. *Global Change Biology*, 1–13.

Lehmann J, Kleber M (2015) The contentious nature of soil organic matter. *Nature*, **528**, 60–8.

Lin Y, Munroe P, Joseph S, Kimber S, Van Zwieten L (2012) Nanoscale organo-mineral reactions of biochars in ferrosol: An investigation using microscopy. *Plant and Soil*, **357**, 369–380.

Roberts KG, Gloy BA, Joseph S, Scott NR, Lehmann J (2010) Life cycle assessment of biochar systems: Estimating the energetic, economic, and climate change potential. *Environmental Science and Technology*, **44**, 827–833.

Rudd L, Kulshreshtha S, Belcher K, Amichev B (2021) Carbon life cycle assessment of shelterbelts in Saskatchewan, Canada. *Journal of Environmental Management*, **297**, 113400.

Sandström J, Bernes C, Junninen K, Lõhmus A, Macdonald E, Müller J, Jonsson BG (2019) Impacts of dead wood manipulation on the biodiversity of temperate and boreal forests. A systematic review. *Journal of Applied Ecology*, **56**, 1770–1781.

Spokas KA, Cantrell KB, Novak JM et al. (2012) Biochar: A synthesis of its agronomic impact beyond carbon sequestration. *Journal of Environmental Quality*, **41**, 973–989.

Stokland JN, Siitonen J, Jonsson BG (2012) *Biodiversity in Dead Wood*. Cambridge University Press, Cambridge.

Stutz KP, Dann D, Wambsganss J, Scherer-Lorenzen M, Lang F (2017) Phenolic matter from deadwood can impact forest soil properties. *Geoderma*, **288**, 204–212.

Vogel C, Mueller CW, Höschen C et al. (2014) Submicron structures provide preferential spots for carbon and nitrogen sequestration in soils. *Nature Communications*, **5**, 1–7.

Vrška T, Přívětivý T, Janík D, Unar P, Šamonil P, Král K (2015) Deadwood residence time in alluvial hardwood temperate forests - A key aspect of biodiversity conservation. *Forest Ecology and Management*, **357**, 33–41.

Weng Z (Han), Van Zwieten L, Singh BP et al. (2017) Biochar built soil carbon over a decade by stabilizing rhizodeposits. *Nature Climate Change*, **7**, 371–376.

Yang JQ, Zhang X, Bourg IC, Stone HA (2021) 4D imaging reveals mechanisms of clay-carbon protection and release. *Nature Communications*, **12**.

References

Alberta Climate Information Service (2021) Alberta Agriculture and Forestry.

Amichev BY, Bentham MJ, Kulshreshtha SN, Laroque CP, Piwowar JM, Van Rees KCJ (2016) Carbon sequestration and growth of six common tree and shrub shelterbelts in Saskatchewan, Canada. *Canadian Journal of Soil Science*, **97**, 368–381.

Amichev BY, Laroque CP, Van Rees KCJ (2020) Shelterbelt removals in Saskatchewan, Canada: implications for long-term carbon sequestration. *Agroforestry Systems*, **94**, 1665–1680.

Amundson R, Biardeau L (2018) Opinion: Soil carbon sequestration is an elusive climate mitigation tool. *Proceedings of the National Academy of Sciences*, **115**, 11652–11656.

An Z, Bork EW, Duan X, Gross CD, Carlyle CN, Chang SX (2022) Quantifying past, current, and future forest carbon stocks within agroforestry systems in central Alberta, Canada. *GCB Bioenergy*, **14**, 669–680.

Angst G, Messinger J, Greiner M et al. (2018) Soil organic carbon stocks in topsoil and subsoil controlled by parent material, carbon input in the rhizosphere, and microbial-derived compounds. *Soil Biology and Biochemistry*, **122**, 19–30.

Arevalo CBM, Bhatti JS, Chang SX, Sidders D (2011) Land use change effects on ecosystem carbon balance: From agricultural to hybrid poplar plantation. *Agriculture, Ecosystems and Environment*, **141**, 342–349.

Asano M, Wagai R, Yamaguchi N, Takeichi Y, Maeda M, Suga H, Takahashi Y (2018) In search of a binding agent: Nano-scale evidence of preferential carbon associations with poorly-crystalline mineral phases in physically-stable, clay-sized aggregates. *Soil Systems*, **2**, 32.

Ashton IW, Hyatt LA, Howe KM, Gurevitch J, Lerdau MT (2005) Invasive species accelerate decomposition and litter nitrogen loss in a mixed deciduous forest. *Ecological Applications*, **15**, 1263–1272.

Atkinson CJ, Fitzgerald JD, Hipps NA (2010) Potential mechanisms for achieving agricultural benefits from biochar application to temperate soils: A review. *Plant and Soil*, **337**, 1–18.

Baah-Acheamfour M, Chang SX, Carlyle CN, Bork EW (2015) Carbon pool size and stability are affected by trees and grassland cover types within agroforestry systems of western Canada. *Agriculture, Ecosystems and Environment*, **213**, 105–113.

Baah-Acheamfour M, Carlyle CN, Lim S, Bork EW, Chang SX (2016) Forest and grassland

cover types reduce net greenhouse gas emissions from agricultural soils. *Science of The Total Environment*, **571**, 1115–1127.

Baah-Acheamfour M, Carlyle CN, Bork EW, Chang SX (2020) Forest and perennial herbland cover reduce microbial respiration but increase root respiration in agroforestry systems. *Agricultural and Forest Meteorology*, **280**, 107790.

Beck T, Joergensen RG, Kandeler E, Makeshin E, Nuss E, Oberholzer HR, Scheu S (1997) An inter-laboratory comparison of ten different ways of measuring soil microbial biomass C. *Soil Biology & Biochemistry*, **29**, 1023–1032.

Benjamini Y, Hochberg Y (1995) Controlling the false discovery rate: A practical and powerful approach to multiple testing. *Journal of the Royal Statistical Society*, **57**, 289–300.

Le Bissonnais Y, Prieto I, Roumet C et al. (2018) Soil aggregate stability in Mediterranean and tropical agro-ecosystems: effect of plant roots and soil characteristics. *Plant and Soil*, **424**, 303–317.

Blaser S, Prati D, Senn-Irlet B, Fischer M (2013) Effects of forest management on the diversity of deadwood-inhabiting fungi in Central European forests. *Forest Ecology and Management*, **304**, 42–48.

Bolan NS, Kunhikrishnan A, Choppala GK, Thangarajan R, Chung JW (2012) Stabilization of carbon in composts and biochars in relation to carbon sequestration and soil fertility. *Science of the Total Environment*, **424**, 264–270.

Bradford MA, Maynard DS, Crowther TW et al. (2021) Belowground community turnover accelerates the decomposition of standing dead wood. *Ecology*, **102**, 1–13.

Butterbach-Bahl K, Baggs EM, Dannenmann M, Kiese R, Zechmeister-Boltenstern S (2013) Nitrous oxide emissions from soils: How well do we understand the processes and their controls? *Philosophical Transactions of the Royal Society B: Biological Sciences*, **368**.

Cambardella CA, Gajda AM, Doran JW, Wienhold BJ, Kettler TA (2001) Estimation of particulate and total organic matter by weight loss-on-ignition. In: *Assessment Methods for Soil Carbon* (eds Lal R, Kimble JM, Follett RJ, Stewart BA), pp. 349–359. Lewis Publishers/CRC Press, Boca Raton, FL.

Cardinael R, Guenet B, Chevallier T, Dupraz C, Cozzi T, Chenu C (2018) High organic inputs explain shallow and deep SOC storage in a long-term agroforestry system - Combining experimental and modeling approaches. *Biogeosciences*, **15**, 297–317.

Cayuela ML, van Zwieten L, Singh BP, Jeffery S, Roig A, Sánchez-Monedero MA (2014) Biochar's role in mitigating soil nitrous oxide emissions: A review and meta-analysis. *Agriculture, Ecosystems and Environment*, **191**, 5–16.

Chantigny MH, Angers DA, Kaiser K, Kalbitz K (2007) Extraction and characterization of dissolved organic matter. In: *Soil Sampling and Methods of Analysis*, 2nd edn (eds Carter MR, Gregorich EG), pp. 617–635. CRC Press, Boca Raton.

Chapman M, Walker WS, Cook-Patton SC, Ellis PW, Farina M, Griscom BW, Baccini A (2020) Large climate mitigation potential from adding trees to agricultural lands. *Global Change Biology*, **26**, 4357–4365.

Chenu C, Plante AT (2006) Clay-sized organo-mineral complexes in a cultivation chronosequence: Revisiting the concept of the "primary organo-mineral complex." *European Journal of Soil Science*, **57**, 596–607.

Christiansen JR, Korhonen JFJ, Juszczak R, Giebels M, Pihlatie M (2011) Assessing the effects of chamber placement, manual sampling and headspace mixing on CH4 fluxes in a laboratory experiment. *Plant and Soil*, **343**, 171–185.

Ciais P, Sabine C, Bala G et al. (2013) Carbon and other biogeochemical cycles. In: *Climate Change 2013: The Physical Science Basis. Contribution of Working Group I to the Fifth Assessment Report of the Intergovernmental Panel on Climate Change* (eds Stocker TF, Qin D, Plattner G-K, Tignor M, Allen SK, Boschung J, Nauels A, Xia Y, Bex V, Midgley PM), pp. 465–570. Cambridge University Press, Cambridge, United Kingdom and New York, NY, USA.

Clarholm M, Skyllberg U, Rosling A (2015) Organic acid induced release of nutrients from metal-stabilized soil organic matter - The unbutton model. *Soil Biology and Biochemistry*, **84**, 168–176.

Cook-Patton SC, Drever CR, Griscom BW et al. (2021) Protect, manage and then restore lands for climate mitigation. *Nature Climate Change*, **11**, 1027–1034.

Cooper RN, Wissel B (2012) Loss of trophic complexity in saline prairie lakes as indicated by stable-isotope based community-metrics. *Aquatic Biosystems*, **8**, 6.

Datta R, Vranová V, Pavelka M, Rejšek K, Formánek P (2014) Effect of soil sieving on respiration induced by low-molecular-weight substrates. *International Agrophysics*, **28**, 119–124.

Dhillon GS, Van Rees KCJ (2017) Soil organic carbon sequestration by shelterbelt agroforestry systems in Saskatchewan. *Canadian Journal of Soil Science*, **97**, 394–409.

Dierks J, Blaser-Hart WJ, Gamper HA, Nyoka IB, Barrios E, Six J (2021) Trees enhance abundance of arbuscular mycorrhizal fungi, soil structure, and nutrient retention in low-input maize cropping systems. *Agriculture, Ecosystems and Environment*, **318**, 107487.

Dijkstra FA, Cheng W (2007) Interactions between soil and tree roots accelerate long-term soil carbon decomposition. *Ecology Letters*, **10**, 1046–1053.

Dijkstra FA, Zhu B, Cheng W (2021) Root effects on soil organic carbon: A double-edged sword. *New Phytologist*, **230**, 60–65.

Drexler S, Gensior A, Don A (2021) Carbon sequestration in hedgerow biomass and soil in the temperate climate zone. *Regional Environmental Change*, **21**, 1–14.

Eisenhauer N, Lanoue A, Strecker T, Scheu S, Steinauer K, Thakur MP, Mommer L (2017) Root biomass and exudates link plant diversity with soil bacterial and fungal biomass. *Scientific Reports*, **7**, 1–8.

Ellert BH, Bettany JR (1995) Calculation of organic matter and nutrients stored in soils under contrasting management regimes. *Canadian Journal of Soil Science*, **75**, 529–538.

Feliciano D, Ledo A, Hillier J, Nayak DR (2018) Which agroforestry options give the greatest soil and above ground carbon benefits in different world regions? *Agriculture, Ecosystems and Environment*, **254**, 117–129.

Fontaine S, Barot S, Barré P, Bdioui N, Mary B, Rumpel C (2007) Stability of organic carbon in deep soil layers controlled by fresh carbon supply. *Nature*, **450**, 277–80.

Forster P, Storelvmo T, Armour K et al. (2021) The Earth's energy budget, climate feedbacks, and climate sensitivity. In: *Climate Change 2021: The Physical Science Basis. Contribution of Working Group I to the Sixth Assessment Report of the Intergovernmental Panel on Climate Change* (eds Masson-Delmotte V, Zhai P, Pirani A, Connors SL, Péan C, Berger S, Caud N, Chen Y, Goldfarb L, Gomis MI, Huang M, Leitzell K, Lonnoy E, Matthews JBR, Maycock KT, Waterfield T, Yelekçi O, Yu R, Zhou B), p. In Press. Cambridge University Press.

Galinato SP, Yoder JK, Granatstein D (2011) The economic value of biochar in crop production and carbon sequestration. *Energy Policy*, **39**, 6344–6350.

Gao Y, Cheng J, Ma Z, Zhao Y, Su J (2014) Carbon storage in biomass, litter, and soil of

different plantations in a semiarid temperate region of northwest China. *Annals of Forest Science*, **71**, 427–435.

Gross A, Glaser B (2021) Meta-analysis on how manure application changes soil organic carbon storage. *Scientific Reports*, **11**, 1–13.

Gross CD, Harrison RB (2019) The case for digging deeper: Soil organic carbon storage, dynamics, and controls in our changing world. *Soil Systems*, **3**, 28.

Gross CD, Bork EW, Carlyle CN, Chang SX (2022) Biochar and its manure-based feedstock have divergent effects on soil organic carbon and greenhouse gas emissions in croplands. *Science of The Total Environment*, **806**, 151337.

Gunina A, Kuzyakov Y (2022) From energy to (soil organic) matter. *Global Change Biology*, **28**, 2169–2182.

Guo LB, Gifford RM (2002) Soil carbon stocks and land use change: A meta analysis. *Global change biology*, **8**, 345–360.

Gurwick NP, Moore LA, Kelly C, Elias P (2013) A systematic review of biochar research, with a focus on its stability in situ and its promise as a climate mitigation strategy. *PLoS ONE*, **8**.

von Haden AC, Yang WH, DeLucia EH (2020) Soils' dirty little secret: Depth-based comparisons can be inadequate for quantifying changes in soil organic carbon and other mineral soil properties. *Global Change Biology*, **26**, 3759–3770.

Haney RL, Franzluebbers AJ, Hons FM, Hossner LR, Zuberer DA (2001) Molar concentration of K2SO4 and soil pH affect estimation of extractable C with chloroform fumigation-extraction. *Soil Biology and Biochemistry*, **33**, 1501–1507.

Hao X, Chang C, Larney FJ (2004) Carbon, nitrogen balances and greenhouse gas emission during cattle feedlot manure composting. *Journal of Environmental Quality*, **33**, 37–44.

Harmon ME, Woodall CW, Fasth B, Sexton J (2008) Woody detritus density and density reduction factors for tree species in the United States: A synthesis. *USDA General Technical Report NRS-29. USDA Forest Service Northern Research Station*, 84.

Harrison RB, Footen PW, Strahm BD (2011) Deep soil horizons: Contribution and importance to soil carbon pools and in assessing whole-ecosystem response to management and global change. *Forest Science*, **57**, 67–76.

He Y, Cheng W, Zhou L et al. (2020) Soil DOC release and aggregate disruption mediate rhizosphere priming effect on soil C decomposition. *Soil Biology and Biochemistry*, **144**,

107787.

Hedges J, Stern J (1984) Carbon and nitrogen determinations of carbonate-containing solids. *Limnology and Oceanography*, **29**, 657–663.

Hernandez-Soriano MC, Kerré B, Goos P, Hardy B, Dufey J, Smolders E (2016a) Long-term effect of biochar on the stabilization of recent carbon: Soils with historical inputs of charcoal. *GCB Bioenergy*, **8**, 371–381.

Hernandez-Soriano MC, Kerré B, Kopittke PM, Horemans B, Smolders E (2016b) Biochar affects carbon composition and stability in soil: A combined spectroscopy-microscopy study. *Scientific Reports*, **6**, 1–13.

Holz M, Zarebanadkouki M, Kuzyakov Y, Pausch J, Carminati A (2018) Root hairs increase rhizosphere extension and carbon input to soil. *Annals of Botany*, **121**, 61–69.

Horwath WR, Paul EA (1994) Microbial biomass. In: *Methods of Soil Analysis: Part 2—Microbiological and Biochemical Properties, SSSA Book Series no. 5* (eds Bottomley PS, Angle JS, Weaver RW), pp. 753–774. Soil Science Society of America, Madison.

Huo C, Luo Y, Cheng W (2017) Rhizosphere priming effect: A meta-analysis. *Soil Biology and Biochemistry*, **111**, 78–84.

Hüppi R, Felber R, Krauss M, Six J, Leifeld J, Fuß R (2018) Restricting the nonlinearity parameter in soil greenhouse gas flux calculation for more reliable flux estimates. *PLoS ONE*, **13**, 1–17.

IPCC (2014) *Climate Change 2014: Synthesis Report. Contribution of Working Groups I, II and III to the Fifth Assessment Report of the Intergovernmental Panel on Climate Change [Core Writing Team, R.K. Pachauri and L.A. Meyer (eds.)]*. Geneva, Switzerland, 151 pp.

IPCC (2019) *Climate Change and Land: An IPCC special report on climate change, desertification, land degradation, sustainable land management, food security, and greenhouse gas fluxes in terrestrial ecosystems [P.R. Shukla, J. Skea, E. Calvo Buendia, V. Masson-Delmot*. Geneva, Switzerland, 896 pp.

IPCC (2022) Summary for policymakers. In: *Climate Change 2022: Mitigation of Climate Change. Contribution of Working Group III to the Sixth Assessment Report of the Intergovernmental Panel on Climate Change* (eds Shukla PR, Skea J, Slade R, Khourdajie A Al, Diemen R van, McCollum D, Pathak M, Some S, Vyas P, Fradera R, Belkacemi M, Hasija A, Lisboa G, Luz S, Malley J), p. 63. Cambridge University Press, Cambridge, UK

and New York, NY, USA.

Jandl R, Rodeghiero M, Martinez C et al. (2014) Current status, uncertainty and future needs in soil organic carbon monitoring. *Science of the Total Environment*, **468**–**469**, 376–383.

Jeffery S, Verheijen FGA, Kammann C, Abalos D (2016) Biochar effects on methane emissions from soils: A meta-analysis. *Soil Biology and Biochemistry*, **101**, 251–258.

Jenkinson DS, Brookes PC, Powlson DS (2004) Measuring soil microbial biomass. *Soil Biology and Biochemistry*, **36**, 5–7.

Joly FX, Milcu A, Scherer-Lorenzen M et al. (2017) Tree species diversity affects decomposition through modified micro-environmental conditions across European forests. *New Phytologist*, **214**, 1281–1293.

Jones C, McConnell C, Coleman K, Cox P, Falloon P, Jenkinson D, Powlson D (2005) Global climate change and soil carbon stocks; predictions from two contrasting models for the turnover of organic carbon in soil. *Global Change Biology*, **11**, 154–166.

Jonsson BG, Stokland JN (2012) The surrounding environment. In: *Biodiversity in Dead Wood*, pp. 194–217. Cambridge University Press, Cambridge.

Kaiser M, Berhe AA (2014) How does sonication affect the mineral and organic constituents of soil aggregates? - A review. *Journal of Plant Nutrition and Soil Science*, **177**, 479–495.

Kaiser K, Kalbitz K (2012) Cycling downwards - dissolved organic matter in soils. *Soil Biology and Biochemistry*, **52**, 29–32.

Kaiser M, Kleber M, Berhe AA (2015) How air-drying and rewetting modify soil organic matter characteristics: An assessment to improve data interpretation and inference. *Soil Biology and Biochemistry*, **80**, 324–340.

Keiluweit M, Bougoure JJ, Nico PS, Pett-Ridge J, Weber PK, Kleber M (2015) Mineral protection of soil carbon counteracted by root exudates. *Nature Climate Change*, **5**, 588–595.

Kelting DL, Burger JA, Edwards GS (1998) Estimating root respiration, microbial respiration in the rhizosphere, and root-free soil respiration in forest soils. *Soil Biology and Biochemistry*, **30**, 961–968.

Kettler TA, Doran JW, Gilbert TL (2001) Simplified method for soil particle-size determination to accompany soil-quality analyses. *Soil Science Society of America Journal*, **65**, 849–852.

Kim DG, Kirschbaum MUF, Beedy TL (2016) Carbon sequestration and net emissions of CH4

and N2O under agroforestry: Synthesizing available data and suggestions for future studies. *Agriculture, Ecosystems and Environment*, **226**, 65–78.

Kleber M, Sollins P, Sutton R (2007) A conceptual model of organo-mineral interactions in soils: Self-assembly of organic molecular fragments into zonal structures on mineral surfaces. *Biogeochemistry*, **85**, 9–24.

Kort J, Turnock R (1998) Carbon reservoir and biomass in Canadian prairie shelterbelts. *Agroforestry Systems*, **44**, 175–186.

Kravchenko AN, Guber AK, Razavi BS, Koestel J, Quigley MY, Robertson GP, Kuzyakov Y (2019) Microbial spatial footprint as a driver of soil carbon stabilization. *Nature Communications*, **10**, 1–10.

Kreitzman M, Eyster H, Mitchell M et al. (2022) Woody perennial polycultures in the U.S. Midwest enhance biodiversity and ecosystem functions. *Ecosphere*, **13**, 1–35.

Kuzyakov Y, Friedelb JK, Stahra K (2000) Review of mechanisms and quantification of priming effects. *Soil Biology & Biochemistry*, **32**, 1485–1498.

Lal R (2004) Soil carbon sequestration impacts on global climate change and food security. *Science*, **304**, 1623–1627.

Lavallee JM, Soong JL, Cotrufo MF (2019) Conceptualizing soil organic matter into particulate and mineral-associated forms to address global change in the 21st century. *Global Change Biology*, 1–13.

Lee J, Hopmans JW, Rolston DE, Baer SG, Six J (2009) Determining soil carbon stock changes: Simple bulk density corrections fail. *Agriculture, Ecosystems and Environment*, **134**, 251–256.

Lehmann J, Kleber M (2015) The contentious nature of soil organic matter. *Nature*, **528**, 60–8.

Lehmann J, Gaunt J, Rondon M (2006) Bio-char sequestration in terrestrial ecosystems - A review. *Mitigation and Adaptation Strategies for Global Change*, **11**, 403–427.

Lehmann J, Kinyangi J, Solomon D (2007) Organic matter stabilization in soil microaggregates: Implications from spatial heterogeneity of organic carbon contents and carbon forms. *Biogeochemistry*, **85**, 45–57.

Lehmann J, Rillig MC, Thies J, Masiello CA, Hockaday WC, Crowley D (2011) Biochar effects on soil biota - A review. *Soil Biology and Biochemistry*, **43**, 1812–1836.

Li Z, Kurz WA, Apps MJ, Beukema SJ (2003) Belowground biomass dynamics in the Carbon

Budget Model of the Canadian Forest Sector: Recent improvements and implications for the estimation of NPP and NEP. *Canadian Journal of Forest Research*, **33**, 126–136.

Li Y, Li Y, Chang SX, Yang Y, Fu S, Jiang P (2018) Biochar reduces soil heterotrophic respiration in a subtropical plantation through increasing soil organic carbon recalcitrancy and decreasing carbon-degrading microbial activity. *Soil Biology and Biochemistry*, **122**, 173–185.

Liang BC, Wang XL, Ma BL (2002) Maize root-induced change in soil organic carbon pools. *Soil Science Society of America Journal*, **66**, 845–847.

Liang C, Schimel JP, Jastrow JD (2017) The importance of anabolism in microbial control over soil carbon storage. *Nature Microbiology*, **2**, 1–6.

Liang C, Amelung W, Lehmann J, Kästner M (2019) Quantitative assessment of microbial necromass contribution to soil organic matter. *Global Change Biology*, **25**, 3578–3590.

Lin Y, Munroe P, Joseph S, Kimber S, Van Zwieten L (2012) Nanoscale organo-mineral reactions of biochars in ferrosol: An investigation using microscopy. *Plant and Soil*, **357**, 369–380.

Lin HC, Huber JA, Gerl G, Hülsbergen KJ (2016) Nitrogen balances and nitrogen-use efficiency of different organic and conventional farming systems. *Nutrient Cycling in Agroecosystems*, **105**, 1–23.

Lorenz K, Lal R (2014) Soil organic carbon sequestration in agroforestry systems. A review. *Agronomy for Sustainable Development*, **34**, 443–454.

Lorenz K, Lal R (2022) *Soil Organic Carbon Sequestration in Terrestrial Biomes of the United States*, 1st edn. Springer, Cham, Switzerland, 201 pp.

Lustenhouwer N, Maynard DS, Bradford MA, Lindner DL, Oberle B, Zanne AE, Crowther TW (2020) A trait-based understanding of wood decomposition by fungi. *Proceedings of the National Academy of Sciences of the United States of America*, **117**, 11551–11558.

Ma S, He F, Tian D et al. (2018) Variations and determinants of carbon content in plants: A global synthesis. *Biogeosciences*, **15**, 693–702.

Ma Z, Chen HYH, Bork EW, Carlyle CN, Chang SX (2020) Carbon accumulation in agroforestry systems is affected by tree species diversity, age and regional climate: A global meta-analysis. *Global Ecology and Biogeography*, **29**, 1817–1828.

Ma Z, Bork EW, Carlyle CN, Tieu J, Gross CD, Chang SX (2022) Carbon stocks differ among

land-uses in agroforestry systems in western Canada. *Agricultural and Forest Meteorology*, **313**, 108756.

Major J, Rondon M, Molina D, Riha SJ, Lehmann J (2010) Maize yield and nutrition during 4 years after biochar application to a Colombian savanna oxisol. *Plant and Soil*, **333**, 117–128.

Mao J, Zhang K, Chen B (2019) Linking hydrophobicity of biochar to the water repellency and water holding capacity of biochar-amended soil. *Environmental Pollution*, **253**, 779–789.

Martínez-Blanco J, Lazcano C, Christensen TH et al. (2013) Compost benefits for agriculture evaluated by life cycle assessment. A review. *Agronomy for Sustainable Development*, **33**, 721–732.

Marx M, Buegger F, Gattinger A, Marschner B, Zsolnay Á, Munch JC (2007) Determination of the fate of 13C labelled maize and wheat rhizodeposit-C in two agricultural soils in a greenhouse experiment under 13C-CO2-enriched atmosphere. *Soil Biology and Biochemistry*, **39**, 3043–3055.

Mayer S, Wiesmeier M, Sakamoto E, Hübner R, Cardinael R, Kühnel A, Kögel-Knabner I (2022) Soil organic carbon sequestration in temperate agroforestry systems – A meta-analysis. *Agriculture, Ecosystems and Environment*, **323**.

Mayrinck RC, Laroque CP, Amichev BY, Van Rees K (2019) Above- and below-ground carbon sequestration in shelterbelt trees in Canada: A review. *Forests*, **10**, 1–17.

Meinshausen M, Meinshausen N, Hare W et al. (2009) Greenhouse-gas emission targets for limiting global warming to 2°C. *Nature*, **458**, 1158–1162.

Michel FC, Pecchia JA, Rigot J, Keener HM (2004) Mass and nutrient losses during the composting of dairy manure amended with sawdust or straw. *Compost Science and Utilization*, **12**, 323–334.

Mildrexler DJ, Berner LT, Law BE, Birdsey RA, Moomaw WR (2020) Large trees dominate carbon storage in forests east of the Cascade Crest in the United States Pacific Northwest. *Frontiers in Forests and Global Change*, **3**, 1–15.

Minasny B, Malone BP, McBratney AB et al. (2017) Soil carbon 4 per mille. *Geoderma*, **292**, 59–86.

Mobley ML, Lajtha K, Kramer MG, Bacon AR, Heine PR, Richter DD (2015) Surficial gains and subsoil losses of soil carbon and nitrogen during secondary forest development. *Global*

Change Biology, **21**, 986–996.

Moni C, Rumpel C, Virto I, Chabbi A, Chenu C (2010) Relative importance of sorption versus aggregation for organic matter storage in subsoil horizons of two contrasting soils. *European Journal of Soil Science*, **61**, 958–969.

Nair PKR (2012) Carbon sequestration studies in agroforestry systems: A reality-check. *Agroforestry Systems*, **86**, 243–253.

Nannipieri P, Trasar-Cepeda C, Dick RP (2018) Soil enzyme activity: a brief history and biochemistry as a basis for appropriate interpretations and meta-analysis. *Biology and Fertility of Soils*, **54**, 11–19.

Neff JC, Asner GP (2001) Dissolved organic carbon in terrestrial ecosystems: Synthesis and a model. *Ecosystems*, **4**, 29–48.

Nyborg M, Laidlaw JW, Solberg ED, Malhi SS (1997) Denitrification and nitrous oxide emissions from a black chernozemic soil during spring thaw in Alberta. *Canadian Journal of Soil Science*, **77**, 153–160.

Oertel C, Matschullat J, Zurba K, Zimmermann F, Erasmi S (2016) Greenhouse gas emissions from soils—A review. *Chemie der Erde*, **76**, 327–352.

Ojeda G, Mattana S, Àvila A, Alcañiz JM, Volkmann M, Bachmann J (2015) Are soil-water functions affected by biochar application? *Geoderma*, **249**–**250**, 1–11.

Olfs HW, Westerschulte M, Ruoss N et al. (2018) A new chamber design for measuring nitrous oxide emissions in maize crops. *Journal of Plant Nutrition and Soil Science*, **181**, 69–77.

Pan Y, Birdsey RA, Fang J et al. (2011) A large and persistent carbon sink in the world's forests. *Science*, **333**, 988–993.

Paustian K, Lehmann J, Ogle S, Reay D, Robertson GP, Smith P (2016) Climate-smart soils. *Nature*, **532**, 49–57.

Pedersen AR, Petersen S. O., Schelde K. (2010) A comprehensive approach to soil-atmosphere trace-gas flux estimation with static chambers. *European Journal of Soil Science*, **61**, 888–902.

Pierson D, Evans L, Kayhani K, Bowden RD, Nadelhoffer K, Simpson M, Lajtha K (2021) Mineral stabilization of soil carbon is suppressed by live roots, outweighing influences from litter quality or quantity. *Biogeochemistry*, **154**, 433–449.

Poeplau C, Don A, Vesterdal L, Leifeld J, Van Wesemael B, Schumacher J, Gensior A (2011)

Temporal dynamics of soil organic carbon after land-use change in the temperate zone - carbon response functions as a model approach. *Global Change Biology*, **17**, 2415–2427.

Pokharel P, Kwak JH, Ok YS, Chang SX (2018) Pine sawdust biochar reduces GHG emission by decreasing microbial and enzyme activities in forest and grassland soils in a laboratory experiment. *Science of the Total Environment*, **625**, 1247–1256.

Le Quéré C, Andrew RM, Friedlingstein P et al. (2018) Global carbon budget 2017. *Earth System Science Data*, **10**, 405–448.

Ramnarine R, Voroney RP, Wagner-Riddle C, Dunfield KE (2011) Carbonate removal by acid fumigation for measuring the δ13C of soil organic carbon. *Canadian Journal of Soil Science*, **91**, 247–250.

Rasmussen C, Heckman K, Wieder WR et al. (2018) Beyond clay: towards an improved set of variables for predicting soil organic matter content. *Biogeochemistry*, **137**, 297–306.

Rasse DP, Rumpel C, Dignac MF (2005) Is soil carbon mostly root carbon? Mechanisms for a specific stabilisation. *Plant and Soil*, **269**, 341–356.

Roberts KG, Gloy BA, Joseph S, Scott NR, Lehmann J (2010) Life cycle assessment of biochar systems: Estimating the energetic, economic, and climate change potential. *Environmental Science and Technology*, **44**, 827–833.

RStudio Team (2021) *RStudio: Integrated Development Environment for R*. Boston, MA.

Rudd L, Kulshreshtha S, Belcher K, Amichev B (2021) Carbon life cycle assessment of shelterbelts in Saskatchewan, Canada. *Journal of Environmental Management*, **297**, 113400.

Ryals R, Hartman MD, Parton WJ, Delonge MS, Silver WL (2015) Long-term climate change mitigation potential with organic matter management on grasslands. *Ecological Applications*, **25**, 531–545.

Sanderman J, Baldock JA, Amundson R, Baldock JA (2008) Dissolved organic carbon chemistry and dynamics in contrasting forest and grassland soils. *Biogeochemistry*, **89**, 181–198.

Sandström J, Bernes C, Junninen K, Lõhmus A, Macdonald E, Müller J, Jonsson BG (2019) Impacts of dead wood manipulation on the biodiversity of temperate and boreal forests. A systematic review. *Journal of Applied Ecology*, **56**, 1770–1781.

Schlautman B, Bartel C, Diaz-Garcia L et al. (2021) Perennial groundcovers: An emerging technology for soil conservation and the sustainable intensification of agriculture. *Emerging*

Topics in Life Sciences, **5**, 337–347.

Schmidt MWI, Rumpel C, Kögel-Knabner I (1999) Evaluation of an ultrasonic dispersion procedure to isolate primary organomineral complexes from soils. *European Journal of Soil Science*, **50**, 87–94.

Schmidt MWI, Torn MS, Abiven S et al. (2011) Persistence of soil organic matter as an ecosystem property. *Nature*, **478**, 49–56.

Seibold S, Rammer W, Hothorn T et al. (2021) The contribution of insects to global forest deadwood decomposition. *Nature*, **597**, 77–81.

Shahzad T, Chenu C, Genet P, Barot S, Perveen N, Mougin C, Fontaine S (2015) Contribution of exudates, arbuscular mycorrhizal fungi and litter depositions to the rhizosphere priming effect induced by grassland species. *Soil Biology and Biochemistry*, **80**, 146–155.

Shahzad T, Rashid MI, Maire V et al. (2018) Root penetration in deep soil layers stimulates mineralization of millennia-old organic carbon. *Soil Biology and Biochemistry*, **124**, 150–160.

Shakoor A, Shahzad SM, Chatterjee N et al. (2021) Nitrous oxide emission from agricultural soils: Application of animal manure or biochar? A global meta-analysis. *Journal of Environmental Management*, **285**, 112170.

Shi L, Feng W, Xu J, Kuzyakov Y (2018) Agroforestry systems: Meta-analysis of soil carbon stocks, sequestration processes, and future potentials. *Land Degradation & Development*, **29**, 1–12.

Shrestha BM, Chang SX, Bork EW, Carlyle CN (2018) Enrichment planting and soil amendments enhance carbon sequestration and reduce greenhouse gas emissions in agroforestry systems: A review. *Forests*, **9**, 1–18.

Six J, Conant RT, Paul E a, Paustian K (2002) Stabilization mechanisms of soil organic matter: Implications for C-saturatin of soils. *Plant and Soil*, **241**, 155–176.

Sleutel S, De Neve S, Németh T, Tóth T, Hofman G (2006) Effect of manure and fertilizer application on the distribution of organic carbon in different soil fractions in long-term field experiments. *European Journal of Agronomy*, **25**, 280–288.

Sohi SP, Krull E, Lopez-Capel E, Bol R (2010) A review of biochar and its use and function in soil. *Advances in Agronomy*, **105**, 47–82.

Sokol NW, Bradford MA (2019) Microbial formation of stable soil carbon is more efficient from

belowground than aboveground input. *Nature Geoscience*, **12**, 46–53.

Sokol NW, Sanderman J, Bradford MA (2018) Pathways of mineral-associated soil organic matter formation: Integrating the role of plant carbon source, chemistry, and point of entry. *Global Change Biology*, 12–24.

Sokol NW, Kuebbing SE, Karlsen-Ayala E, Bradford MA (2019) Evidence for the primacy of living root inputs, not root or shoot litter, in forming soil organic carbon. *New Phytologist*, **221**, 233–246.

Sokol NW, Slessarev E, Marschmann GL et al. (2022) Life and death in the soil microbiome: How ecological processes influence biogeochemistry. *Nature Reviews Microbiology*, **0123456789**.

Sollins P, Swanston C, Kleber M et al. (2006) Organic C and N stabilization in a forest soil: Evidence from sequential density fractionation. *Soil Biology and Biochemistry*, **38**, 3313–3324.

Sothe C, Gonsamo A, Arabian J, Kurz WA, Finkelstein SA, Snider J (2022) Large soil carbon storage in terrestrial ecosystems of Canada. *Global Biogeochemical Cycles*, 1–18.

Spokas KA, Cantrell KB, Novak JM et al. (2012) Biochar: A synthesis of its agronomic impact beyond carbon sequestration. *Journal of Environmental Quality*, **41**, 973–989.

Statistics Canada Census of Agriculture (2008) *Census of Agriculture for Alberta, 2006*. 1–13 pp.

Stavi I, Lal R (2013) Agroforestry and biochar to offset climate change: A review. *Agronomy for Sustainable Development*, **33**, 81–96.

Stockmann U, Adams MA, Crawford JW et al. (2013) The knowns, known unknowns and unknowns of sequestration of soil organic carbon. *Agriculture, Ecosystems and Environment*, **164**, 80–99.

Stokland JN, Siitonen J, Jonsson BG (2012) *Biodiversity in Dead Wood*. Cambridge University Press, Cambridge.

Stutz KP, Dann D, Wambsganss J, Scherer-Lorenzen M, Lang F (2017) Phenolic matter from deadwood can impact forest soil properties. *Geoderma*, **288**, 204–212.

Sulman BN, Phillips RP, Oishi AC, Shevliakova E, Pacala SW (2014) Microbe-driven turnover offsets mineral-mediated storage of soil carbon under elevated CO2. *Nature Climate Change*, **4**, 1099–1102.

Tautges NE, Chiartas JL, Gaudin ACM, O'Geen AT, Herrera I, Scow KM (2019) Deep soil inventories reveal that impacts of cover crops and compost on soil carbon sequestration differ in surface and subsurface soils. *Global Change Biology*, **25**, 3753–3766.

Teissier Du Cros R, Lopez S (2009) Preliminary study on the assessment of deadwood volume by the French national forest inventory. *Annals of Forest Science*, **66**, 1–10.

Thiagarajan A, Fan J, McConkey BG, Janzen HH, Campbell CA (2018) Dry matter partitioning and residue N content for 11 major field crops in Canada adjusted for rooting depth and yield. *Canadian Journal of Soil Science*, **98**, 574–579.

Tian Q, Yang X, Wang X et al. (2016) Microbial community mediated response of organic carbon mineralization to labile carbon and nitrogen addition in topsoil and subsoil. *Biogeochemistry*, **128**, 125–139.

Totsche KU, Amelung W, Gerzabek MH et al. (2018) Microaggregates in soils. *Journal of Plant Nutrition and Soil Science*, **181**, 104–136.

UNFCCC (2015) *Measurements for Estimation of Carbon Stocks in Afforestation and Reforestation Project Activities under the Clean Development Mechanism: A Field Manual*. 72 pp.

Vance ED, Brookes PC, Jenkinson DS (1987) An extraction method for measuring soil microbial biomass C. *Soil Biology and Biochemistry*, **19**, 703–707.

Venterea RT, Burger M, Spokas KA (2005) Nitrogen oxide and methane emissions under varying tillage and fertilizer management. *Journal of Environment Quality*, **34**, 1467.

Virto I, Barré P, Chenu C (2008) Microaggregation and organic matter storage at the silt-size scale. *Geoderma*, **146**, 326–335.

Virto I, Moni C, Swanston C, Chenu C (2010) Turnover of intra- and extra-aggregate organic matter at the silt-size scale. *Geoderma*, **156**, 1–10.

Vogel C, Mueller CW, Höschen C et al. (2014) Submicron structures provide preferential spots for carbon and nitrogen sequestration in soils. *Nature Communications*, **5**, 1–7.

Vrška T, Přívětivý T, Janík D, Unar P, Šamonil P, Král K (2015) Deadwood residence time in alluvial hardwood temperate forests - A key aspect of biodiversity conservation. *Forest Ecology and Management*, **357**, 33–41.

Walthert L, Graf U, Kammer A, Luster J, Pezzotta D, Zimmermann S, Hagedorn F (2010) Determination of organic and inorganic carbon, δ13C, and nitrogen in soils containing

carbonates after acid fumigation with HCl. *Journal of Plant Nutrition and Soil Science*, **173**, 207–216.

Wang Y, Zhang B, Lin L, Zepp H (2011) Agroforestry system reduces subsurface lateral flow and nitrate loss in Jiangxi Province, China. *Agriculture, Ecosystems and Environment*, **140**, 441–453.

Wang X, Yin L, Dijkstra FA, Lu J, Wang P, Cheng W (2020) Rhizosphere priming is tightly associated with root-driven aggregate turnover. *Soil Biology and Biochemistry*, **149**, 107964.

Wang B, An S, Liang C, Liu Y, Kuzyakov Y (2021) Microbial necromass as the source of soil organic carbon in global ecosystems. *Soil Biology and Biochemistry*, **162**, 108422.

Wendt JW (2013) ESM sample spreadsheets.

Wendt JW, Hauser S (2013) An equivalent soil mass procedure for monitoring soil organic carbon in multiple soil layers. *European Journal of Soil Science*, **64**, 58–65.

Weng Z (Han), Van Zwieten L, Singh BP et al. (2017) Biochar built soil carbon over a decade by stabilizing rhizodeposits. *Nature Climate Change*, **7**, 371–376.

Werth M, Kuzyakov Y (2008) Root-derived carbon in soil respiration and microbial biomass determined by 14C and 13C. *Soil Biology and Biochemistry*, **40**, 625–637.

Werth M, Kuzyakov Y (2010) 13C fractionation at the root-microorganisms-soil interface: A review and outlook for partitioning studies. *Soil Biology and Biochemistry*, **42**, 1372–1384.

Xing D, Bergeron JAC, Solarik KA, Tomm B, Macdonald SE, Spence JR, He F (2019) Challenges in estimating forest biomass: Use of allometric equations for three boreal tree species. *Canadian Journal of Forest Research*, **49**, 1613–1622.

Yang XM, Drury CF, Reynolds WD, MacTavish DC (2009) Use of sonication to determine the size distributions of soil particles and organic matter. *Canadian Journal of Soil Science*, **89**, 413–419.

Yang JQ, Zhang X, Bourg IC, Stone HA (2021) 4D imaging reveals mechanisms of clay-carbon protection and release. *Nature Communications*, **12**.

Yousaf B, Liu G, Wang R, Abbas Q, Imtiaz M, Liu R (2017) Investigating the biochar effects on C-mineralization and sequestration of carbon in soil compared with conventional amendments using the stable isotope (δ13C) approach. *GCB Bioenergy*, **9**, 1085–1099.

Yu H, Ding W, Luo J, Geng R, Cai Z (2012) Long-term application of organic manure and

mineral fertilizers on aggregation and aggregate-associated carbon in a sandy loam soil. *Soil and Tillage Research*, **124**, 170–177.

Zhu X, Jackson RD, DeLucia EH, Tiedje JM, Liang C (2020) The soil microbial carbon pump: From conceptual insights to empirical assessments. *Global Change Biology*, **26**, 6032–6039.

Zomer RJ, Bossio DA, Sommer R, Verchot L V. (2017) Global sequestration potential of increased organic carbon in cropland soils. *Scientific Reports*, **7**, 1–8.

Zsolnay Á (2003) Dissolved organic matter: Artefacts, definitions, and functions. *Geoderma*, **113**, 187–209.

Appendix A. Supplementary data

Table A.S1. Classifications and properties of soils among the different land uses of two agroforestry systems in central Alberta, Canada (n = 10). Least-squares means (one standard error) are reported. OC, organic carbon; N, total nitrogen; Conc., concentration.

Agroforestry system	Land-use type	Classification*	Depth (cm)	%Sand	%Silt	%Clay	OC conc. (mg g^{-1} soil)	N conc. (mg g^{-1} soil)	OC:N
Hedgerow	Cropland	CA.BC, CA.BLC, CA.BLC, CA.DGC, O.DBC	0–10	33.27 (8.58)	38.07 (5.75)	28.65 (3.21)	39.13 (14.10)	3.56 (1.14)	10.87 (0.38)
			10–30	35.04 (8.97)	35.86 (6.04)	29.10 (3.36)	21.07 (13.93)	2.02 (1.16)	10.30 (0.55)
			30–50	39.58 (7.93)	31.72 (5.28)	28.70 (3.90)	9.22 (21.31)	0.94 (1.61)	9.75 (0.71)
			50–100	43.25 (8.18)	22.31 (5.19)	34.44 (4.42)	6.67 (2.04)	0.58 (0.17)	11.47 (1.23)
	Grassland	CA.DBC, CA.DGC, O.BLC, O.BLC, O.DGC	Litter	na†	na	na	272.26 (22.00)	13.98 (1.82)	20.78 (2.23)
			0–10	32.10 (8.58)	39.14 (5.75)	28.77 (3.21)	64.66 (14.10)	5.68 (1.14)	11.33 (0.38)
			10–30	30.83 (8.97)	38.29 (6.04)	30.88 (3.36)	53.63 (13.93)	4.74 (1.16)	10.67 (0.55)
			30–50	31.07 (7.93)	33.78 (5.28)	35.16 (3.90)	55.90 (21.31)	4.90 (1.61)	10.52 (0.71)
			50–100	40.31 (8.18)	30.93 (5.19)	28.76 (4.42)	11.32 (2.04)	1.12 (0.17)	10.57 (1.23)
	Saplings‡	CA.DBC, CA.DGC, O.BLC, O.BLC, O.DGC	Litter	na	na	na	286.18 (22.00)	15.58 (1.82)	19.81 (2.23)
			0–10	32.10 (8.58)	39.14 (5.75)	28.77 (3.21)	62.04 (14.10)	5.30 (1.14)	11.63 (0.38)
			10–30	30.83 (8.97)	38.29 (6.04)	30.88 (3.36)	46.18 (13.93)	4.04 (1.16)	10.93 (0.55)
			30–50	31.07 (7.93)	33.78 (5.28)	35.16 (3.90)	42.90 (21.31)	3.74 (1.61)	9.95 (0.71)
			50–100	40.31 (8.18)	30.93 (5.19)	28.76 (4.42)	8.64 (2.04)	0.90 (0.17)	9.60 (1.23)
	Woodland	CA.DGC, E.DBC, O.BLC, O.DGC, O.EB	Litter	na	na	na	270.74 (22.00)	18.78 (1.82)	14.59 (2.23)
			0–10	26.46 (8.58)	43.91 (5.75)	29.63 (3.21)	106.05 (14.10)	7.62 (1.14)	13.58 (0.38)
			10–30	29.57 (8.97)	40.85 (6.04)	29.58 (3.36)	45.03 (13.93)	3.64 (1.16)	12.05 (0.55)
			30–50	23.21 (7.93)	42.30 (5.28)	34.49 (3.90)	56.34 (21.31)	4.10 (1.61)	11.13 (0.71)
			50–100	29.78 (8.18)	36.19 (5.19)	34.03 (4.42)	11.99 (2.04)	1.10 (0.17)	10.57 (1.23)
Shelterbelt	Cropland	CA.BC,	0–10	29.97 (8.58)	43.16 (5.75)	26.87 (3.21)	42.60 (14.10)	3.82 (1.14)	11.12 (0.38)

	CA.BLC, CA.DBC, CA.DBC, O.BC	10–30	29.88 (8.97)	41.04 (6.04)	29.08 (3.36)	19.19 (13.93)	1.82 (1.16)	10.46 (0.55)
		30–50	31.11 (7.93)	37.65 (5.28)	31.24 (3.90)	10.44 (21.31)	1.00 (1.61)	10.55 (0.71)
		50–100	38.86 (8.18)	32.88 (5.19)	28.25 (4.42)	7.31 (2.04)	0.58 (0.17)	12.14 (1.23)
Grassland	CA.BC, CA.BC, CA.DGC, E.BLC, O.BLC	Litter	na	na	na	257.50 (22.00)	13.46 (1.82)	19.36 (2.23)
		0–10	29.19 (8.58)	43.89 (5.75)	26.92 (3.21)	50.67 (14.10)	4.56 (1.14)	11.18 (0.38)
		10–30	31.20 (8.97)	41.87 (6.04)	26.93 (3.36)	23.45 (13.93)	2.26 (1.16)	10.35 (0.55)
		30–50	29.72 (7.93)	40.16 (5.28)	30.13 (3.90)	11.34 (21.31)	1.22 (1.61)	9.31 (0.71)
		50–100	36.95 (8.18)	33.10 (5.19)	29.95 (4.42)	7.90 (2.04)	0.70 (0.17)	10.95 (1.23)
Saplings‡	CA.BC, CA.BC, CA.DGC, E.BLC, O.BLC	Litter	na	na	na	245.70 (22.00)	13.48 (1.82)	19.25 (2.23)
		0–10	29.19 (8.58)	43.89 (5.75)	26.92 (3.21)	42.06 (14.10)	3.70 (1.14)	11.38 (0.38)
		10–30	31.20 (8.97)	41.87 (6.04)	26.93 (3.36)	25.94 (13.93)	2.42 (1.16)	10.68 (0.55)
		30–50	29.72 (7.93)	40.16 (5.28)	30.13 (3.90)	13.36 (21.31)	1.38 (1.61)	9.46 (0.71)
		50–100	36.95 (8.18)	33.10 (5.19)	29.95 (4.42)	8.66 (2.04)	0.74 (0.17)	11.27 (1.23)
Woodland	CA.BLC, CA.DBC, E.BC, E.DBC, O.BLC	Litter	na	na	na	282.22 (22.00)	17.02 (1.82)	17.15 (2.23)
		0–10	29.07 (8.58)	44.95 (5.75)	25.98 (3.21)	53.01 (14.10)	4.44 (1.14)	12.19 (0.38)
		10–30	27.98 (8.97)	44.30 (6.04)	27.72 (3.36)	29.16 (13.93)	2.66 (1.16)	10.84 (0.55)
		30–50	27.96 (7.93)	42.76 (5.28)	29.29 (3.90)	18.73 (21.31)	1.82 (1.61)	9.92 (0.71)
		50–100	31.10 (8.18)	36.79 (5.19)	32.11 (4.42)	7.86 (2.04)	0.80 (0.17)	9.92 (1.23)

* Soil was classified using the Canadian System of Soil Classification. CA.BC, Calcareous Brown Chernozem; CA.BLC, Calcareous Black Chernozem; CA.DBC, Calcareous Dark Brown Chernozem; CA.DGC, Calcareous Dark Gray Chernozem; E.BC, Eluviated Brown Chernozem; E.BLC, Eluviated Black Chernozem; E.DBC, Eluviated Dark Brown Chernozem; O.BC, Orthic Brown Chernozem; O.BLC, Orthic Black Chernozem; O.DBC, Orthic Dark Brown Chernozem; O.DGC, Orthic Dark Gray Chernozem; O.EB, Orthic Eutric Brunisol.

† na indicates that the property was not applicable within the given depth.

‡ Soil classification and texture determination in the saplings land-use type were based on grassland soils and not repeated after the saplings were planted in grassland.

Table A.S2. Basic soil properties among the grassland and saplings treatment (prior to planting the saplings) land uses of two agroforestry systems in central Alberta, Canada (n = 10). Least-squares means (one standard error) within each soil depth accompanied by different lowercase letters are significantly different (Tukey-adjusted, $\alpha = 0.05$) between the land-use types. BD, bulk density; OC, organic carbon; N, total nitrogen; Conc., concentration.

Land-use type	Soil depth (cm)	BD (g cm^{-3})	OC conc. (mg g^{-1} soil)	N conc. (mg g^{-1} soil)	OC:N
Grassland	0–10	0.80 (0.08)	56.96 (11.01)	4.93 (0.90)	11.42 (0.13)
Saplings	0–10	0.82 (0.08)	46.39 (11.01)	4.04 (0.90)	11.40 (0.13)
Grassland	10–30	1.05 (0.10)	39.47 (12.41)	3.48 (1.02)	10.95 (0.20)
Saplings	10–30	1.09 (0.10)	34.35 (12.41)	3.06 (1.02)	10.99 (0.20)
Grassland	30–50	1.23 (0.09)	26.72 (10.84)	2.57 (0.97)	9.99 (0.24) b
Saplings	30–50	1.20 (0.09)	24.75 (10.84)	2.27 (0.97)	10.49 (0.24) a
Grassland	50–100	1.47 (0.07)	8.25 (1.79)	0.82 (0.17)	10.16 (0.59)
Saplings	50–100	1.40 (0.07)	9.77 (1.79)	0.95 (0.17)	10.36 (0.59)

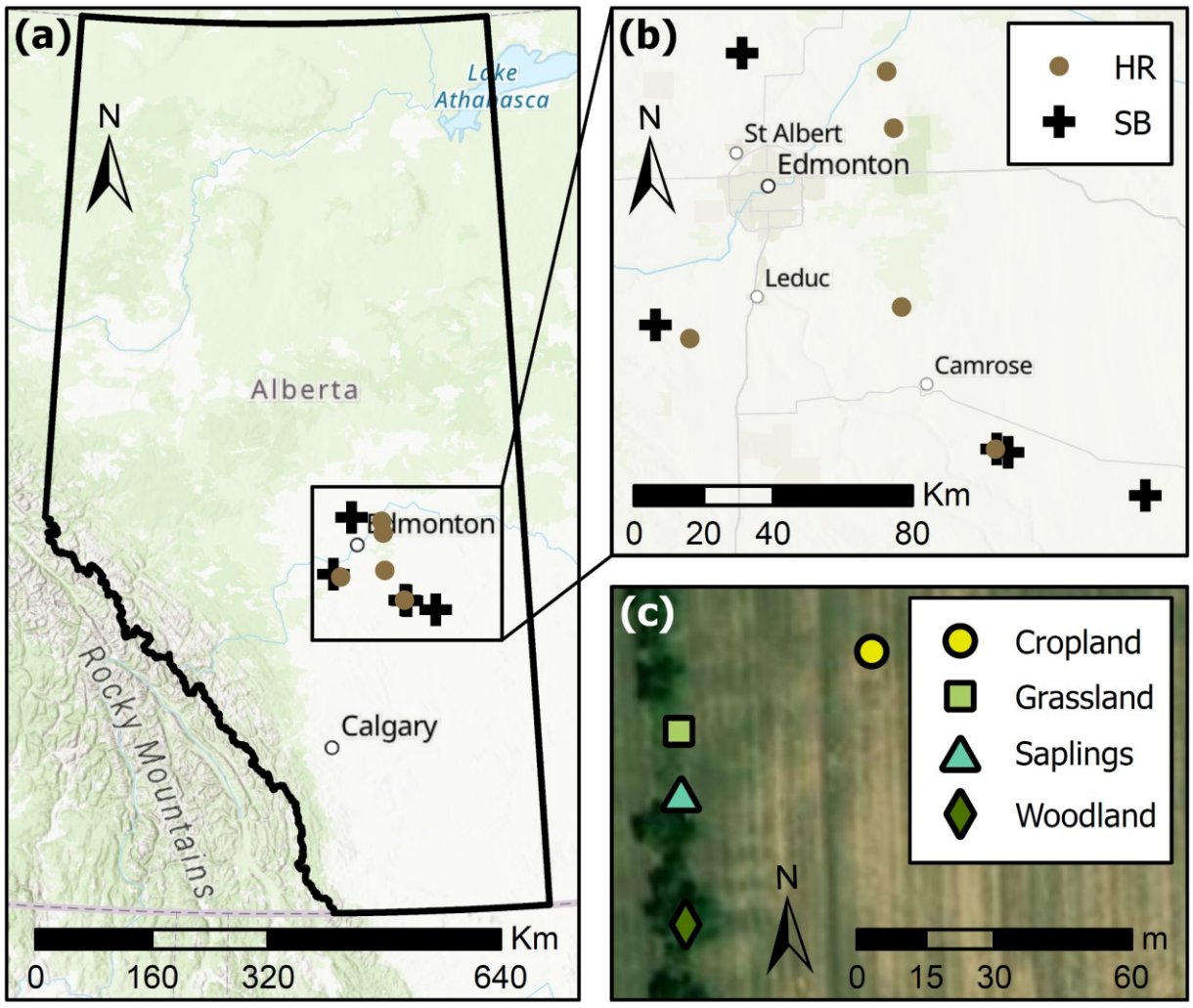

Figure A.S1. (a) Location of the ten agroforestry sites in central Alberta, Canada, (b) location of the ten study sites relative to nearby cities, and (c) an example of a plot layout within a site. HR, hedgerow; SB, shelterbelt. Source: Esri, Maxar, GeoEye, Earthstar Geographics, CNES/Airbus DS, USDA, USGS, AeroGRID, IGN, Esri Canada, HERE, Garmin, FAO, NOAA, EPA, NRCan, Parks Canada, and the GIS User Community.

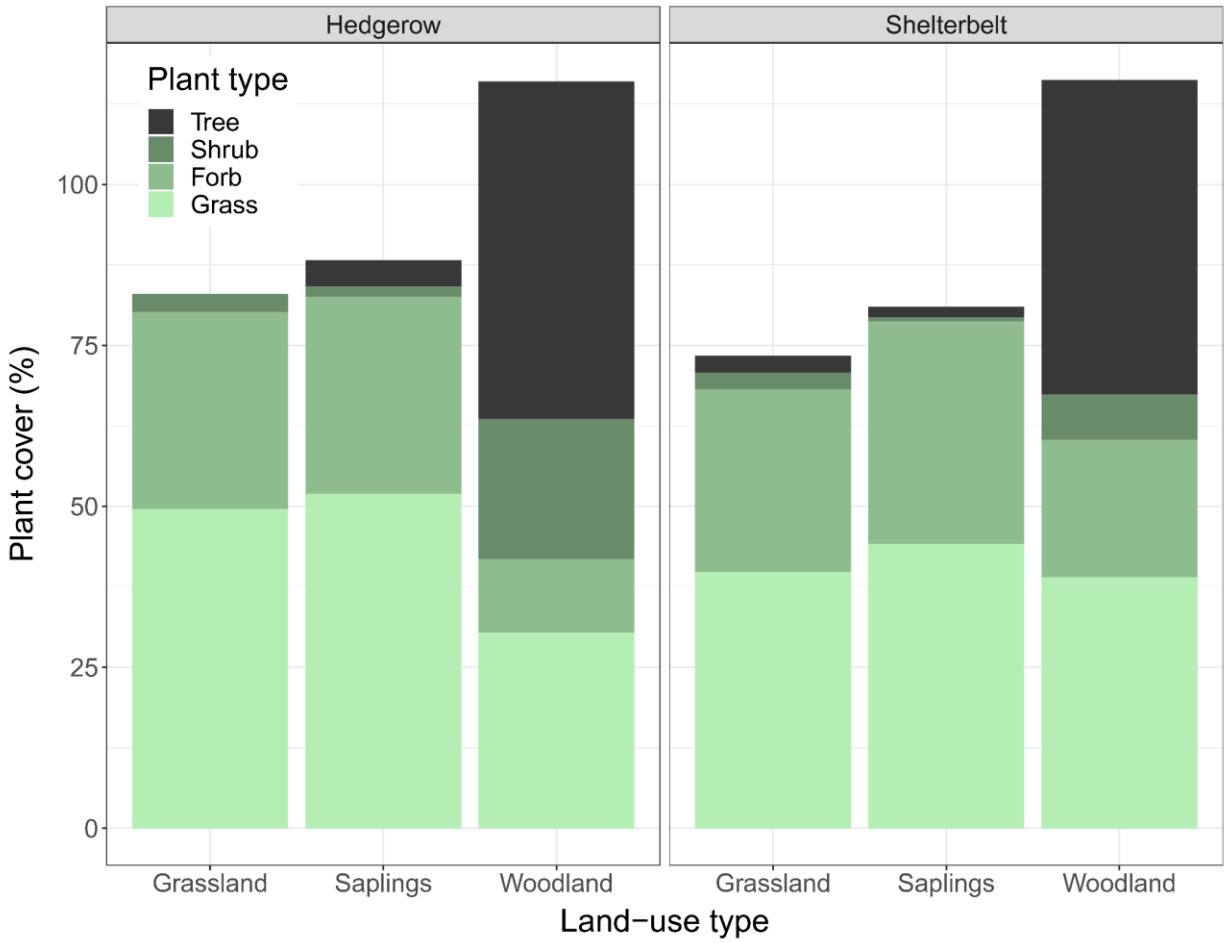

Figure A.S2. Plant type and cover among the different perennial vegetated land uses of two agroforestry systems in central Alberta, Canada (n = 10).

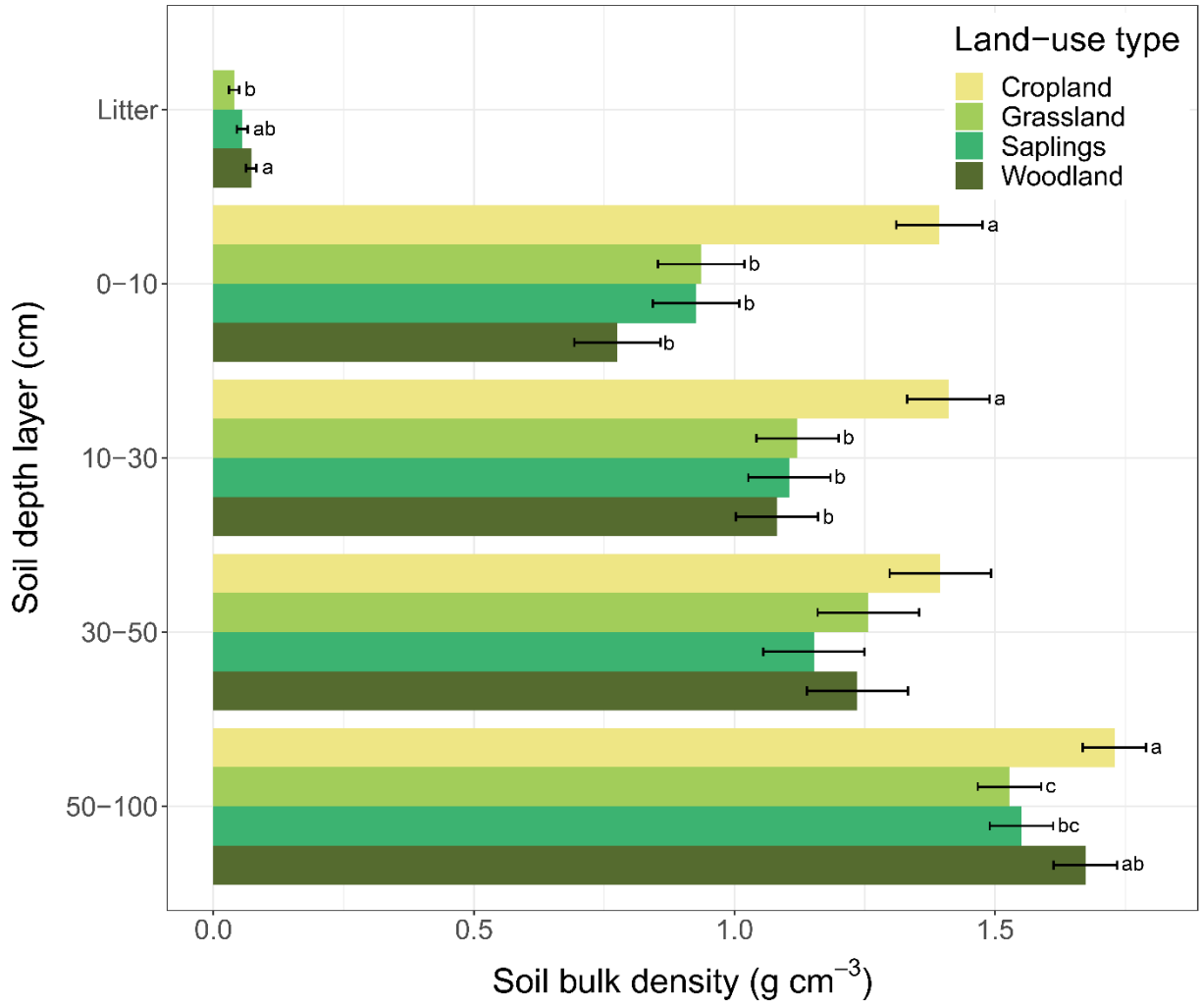

Figure A.S3. Soil bulk density among the different land uses of two agroforestry systems in central Alberta, Canada (n = 10). Error bars represent ± one standard error. Least-squares means within each depth layer accompanied by different lowercase letters are significantly different (Tukey-adjusted, $\alpha = 0.05$) among the land-use types.

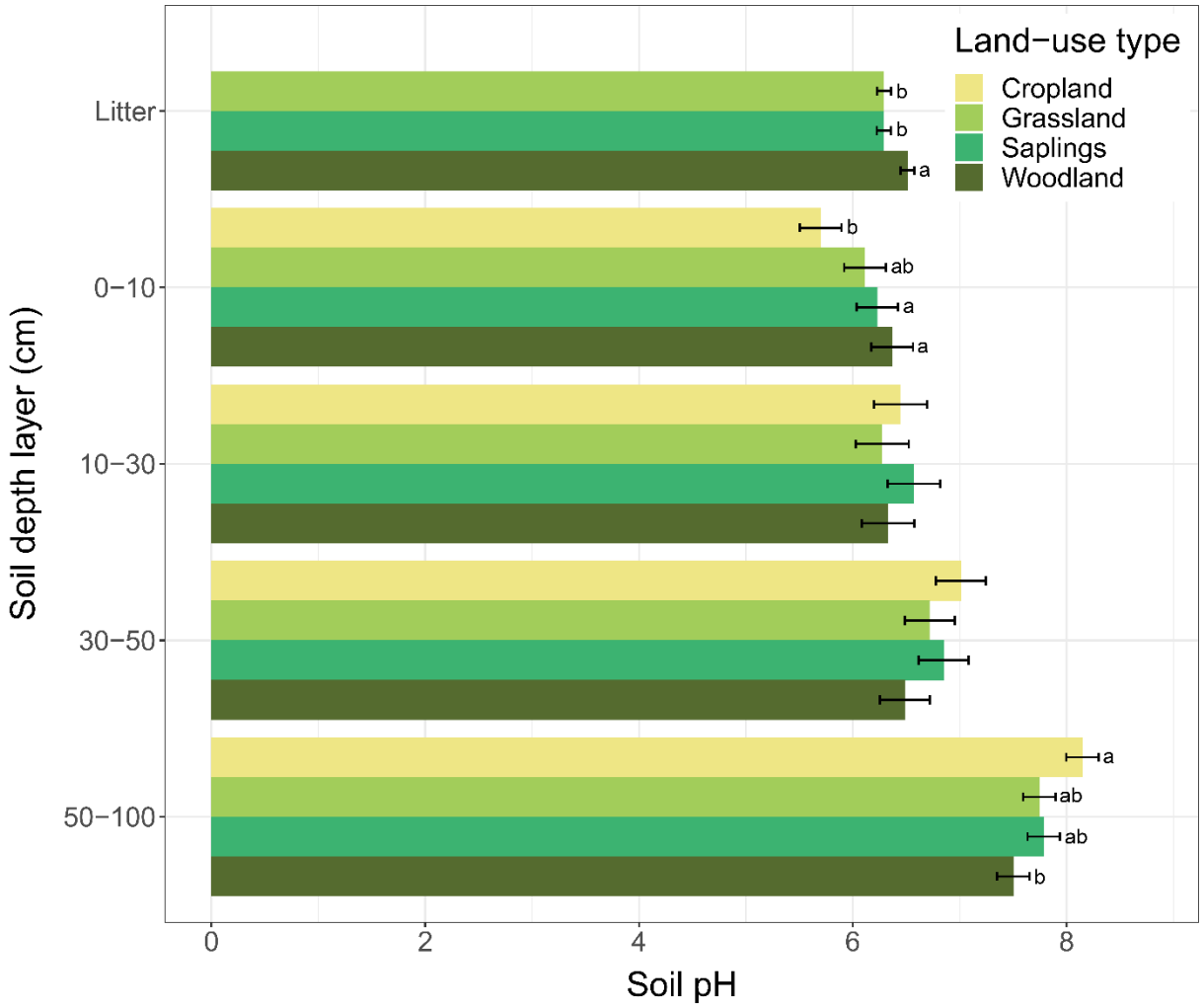

Figure A.S4. Soil pH among the different land uses of two agroforestry systems in central Alberta, Canada (n = 10). Error bars represent ± one standard error. Least-squares means within each depth layer accompanied by different lowercase letters are significantly different (Tukey-adjusted, α = 0.05) among the land-use types.

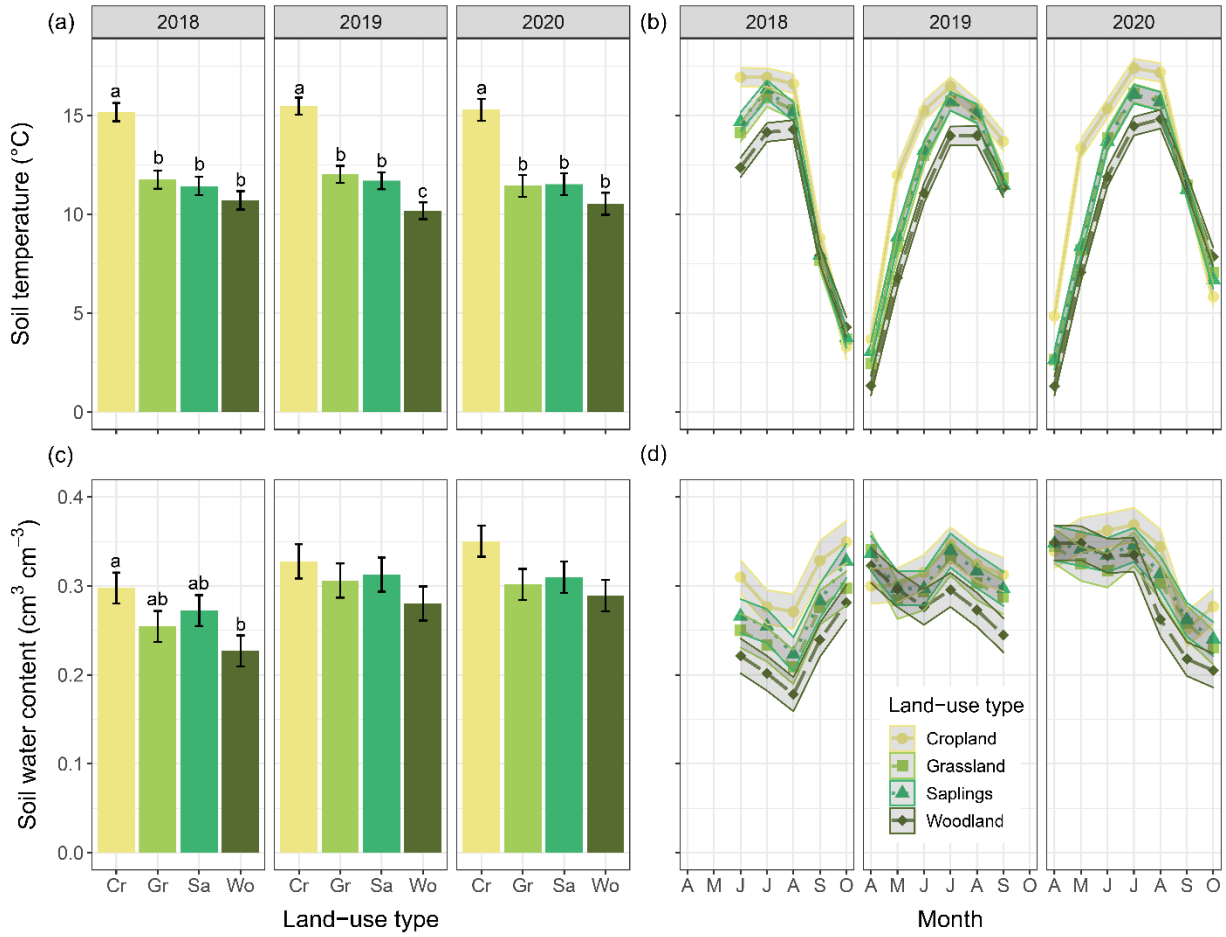

Figure A.S5. Soil temperature by (a) year and (b) month and soil water content by (c) year and (d) month at 10 cm depth among the different land uses of two agroforestry systems in central Alberta, Canada (n = 10). Error bars and ribbons represent ± one standard error. Least-squares means within each year accompanied by different lowercase letters are significantly different (Tukey-adjusted, $\alpha = 0.05$) among the land-use types. Cr, cropland; Gr, grassland; Sa, saplings; Wo, woodland.

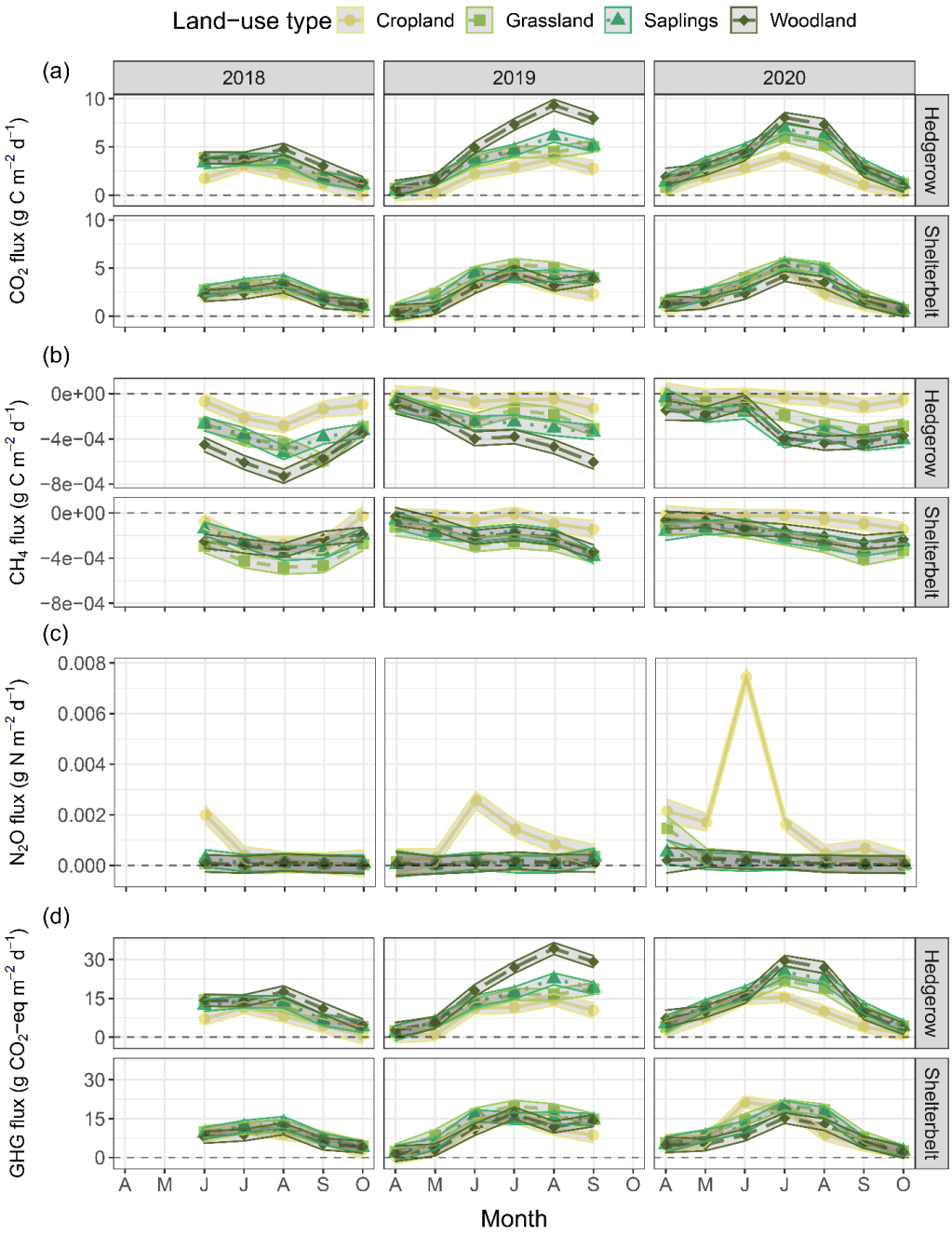

Figure A.S6. Soil (a) carbon dioxide (CO_2), (b) methane (CH_4), (c) nitrous oxide (N_2O), and (d) total greenhouse gas (GHG; sum of CO_2, CH_4, and N_2O) fluxes by month and year among the different land uses of two agroforestry systems in central Alberta, Canada (n = 10). Error ribbons represent least-squares means ± one standard error. Note that CO_2 (and GHG) flux includes autotrophic respiration.

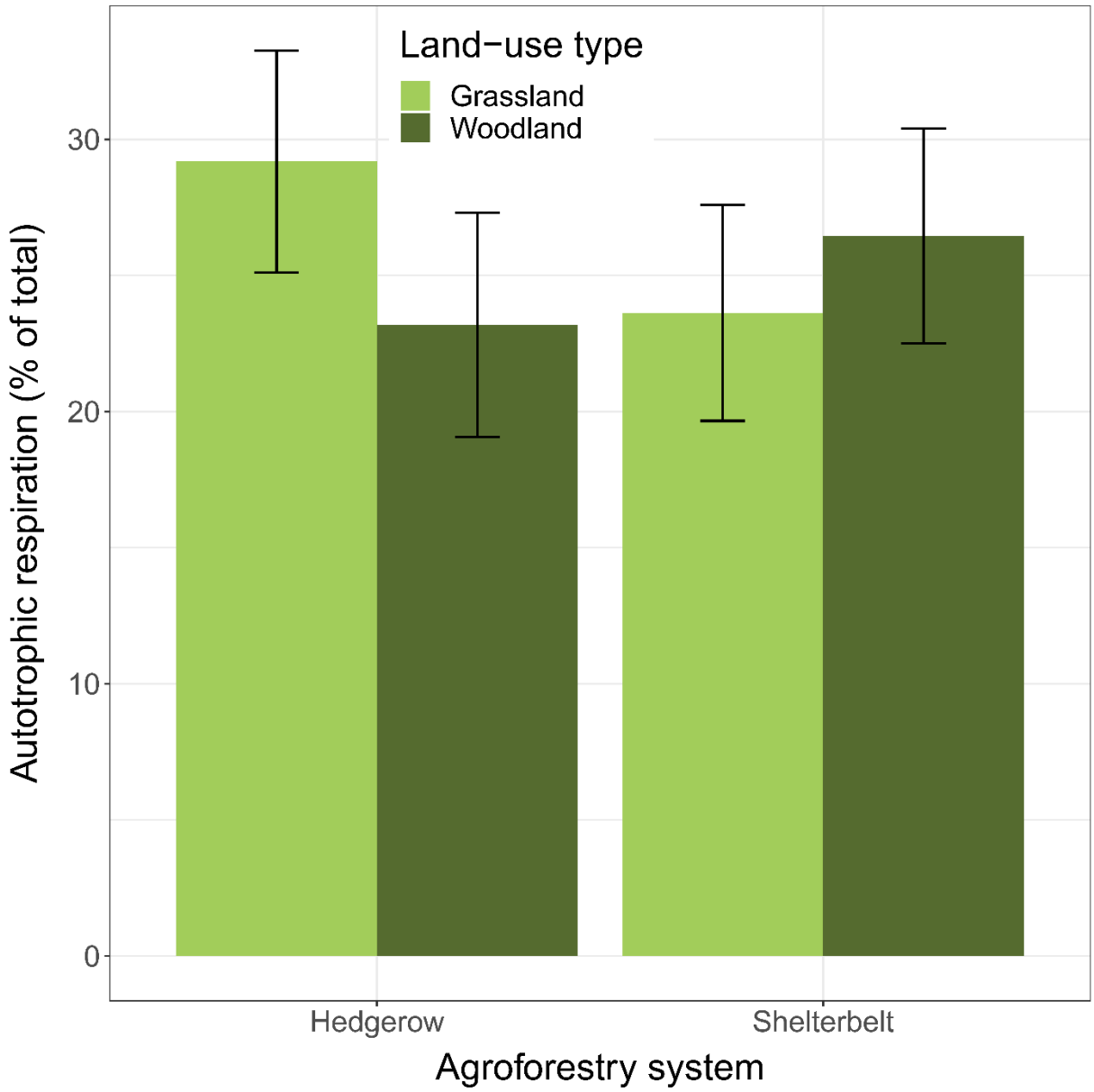

Figure A.S7. Soil autotrophic respiration measured in 2020 (~April–October) among the grassland and woodland land uses of two agroforestry systems in central Alberta, Canada (n = 10). Error bars represent least-squares means ± one standard error.

Appendix B. Supplementary data

Table B.S1. Soil classifications and properties of ten agricultural sites in central Alberta, Canada. HR, hedgerow; SB, shelterbelt. BD, bulk density; OC, organic carbon; N, total nitrogen; Conc., concentration.

Site	Classification[†]	Depth (cm)	%Sand[‡]	%Silt	%Clay	BD (g cm^{-3})	pH	OC Conc. (mg g^{-1} soil)	N Conc. (mg g^{-1} soil)	OC:N
HR1	CA.DGC	10	26.44	43.68	29.88	0.82	5.36	52.20	52.20	11.35
		30	21.99	48.07	29.93	1.31	6.04	31.70	31.70	10.93
		50	27.35	41.98	30.67	1.29	6.55	11.70	11.70	9.75
		100	31.31	26.45	42.24	1.66	7.89	6.70	9.50	9.57
HR2	CA.BLC	10	62.41	14.38	23.21	1.09	8.04	40.35	48.70	11.87
		30	67.33	11.82	20.84	1.03	8.09	22.20	28.40	12.33
		50	74.32	8.67	17.01	1.49	8.18	8.00	15.50	11.43
		100	81.56	4.83	13.61	1.19	8.20	3.40	16.10	11.33
HR3	CA.BLC	10	10.05	54.09	35.86	1.11	7.06	49.75	49.75	12.13
		30	11.64	52.94	35.42	0.97	7.69	33.13	33.13	11.62
		50	17.51	48.95	33.54	1.18	7.95	14.50	16.40	10.36
		100	32.79	33.37	33.84	1.46	8.07	6.70	9.70	9.57
HR4	CA.BC	10	34.38	35.55	30.07	1.24	5.39	22.20	22.20	10.57
		30	38.35	27.54	34.12	1.58	5.56	7.10	7.10	10.14
		50	36.94	29.08	33.98	1.41	5.63	5.60	5.60	11.20
		100	32.98	17.98	49.04	1.31	7.82	5.00	10.20	10.00
HR5	O.DBC	10	33.09	42.66	24.24	1.06	5.51	29.40	29.40	10.14
		30	35.90	38.92	25.18	1.53	5.85	18.50	18.50	10.28
		50	41.78	29.94	28.28	1.36	7.07	5.90	5.90	9.83
		100	37.59	28.92	33.49	1.81	7.93	5.70	7.30	11.40
SB1	O.BC	10	13.56	51.98	34.47	1.24	5.79	53.50	53.50	11.89
		30	13.60	51.47	34.93	1.27	7.01	24.45	24.45	12.23
		50	10.56	51.07	38.37	1.32	7.71	14.65	14.65	11.27
		100	25.88	36.08	38.04	1.69	8.05	10.80	11.90	15.43
SB2	CA.DBC	10	29.72	44.39	25.89	1.12	6.08	27.80	27.80	11.12
		30	29.68	40.09	30.23	1.49	6.62	16.15	16.15	10.77
		50	37.11	32.39	30.50	1.23	7.16	5.10	5.10	6.38
		100	40.80	29.93	29.26	1.82	8.20	3.90	8.20	9.75
SB3	CA.BLC	10	36.45	39.58	23.97	1.07	5.12	43.90	43.90	11.26
		30	33.43	36.90	29.67	1.01	5.67	28.45	28.45	10.74
		50	35.69	32.93	31.38	2.14	6.11	15.80	15.80	9.88
		100	42.46	34.80	22.75	1.90	8.05	6.10	10.90	10.17
SB4	CA.DBC	10	33.37	40.39	26.24	1.07	5.06	44.90	44.90	10.95
		30	38.98	36.86	24.16	1.07	5.85	34.70	34.70	10.52

		50	36.86	34.44	28.70	1.27	6.77	18.45	18.45	10.25
		100	51.54	26.18	22.29	1.56	8.08	10.40	15.20	10.40
SB5	CA.BC	10	36.74	39.46	23.80	1.02	5.32	28.90	28.90	9.97
		30	33.69	39.89	26.43	1.43	5.59	14.70	14.70	9.80
		50	35.31	37.42	27.27	1.20	6.71	6.75	6.75	9.64
		100	33.63	37.43	28.93	1.15	8.16	6.00	11.00	8.57

† Soil was classified using the Canadian System of Soil Classification. ‡ Soil properties are for the control plot.

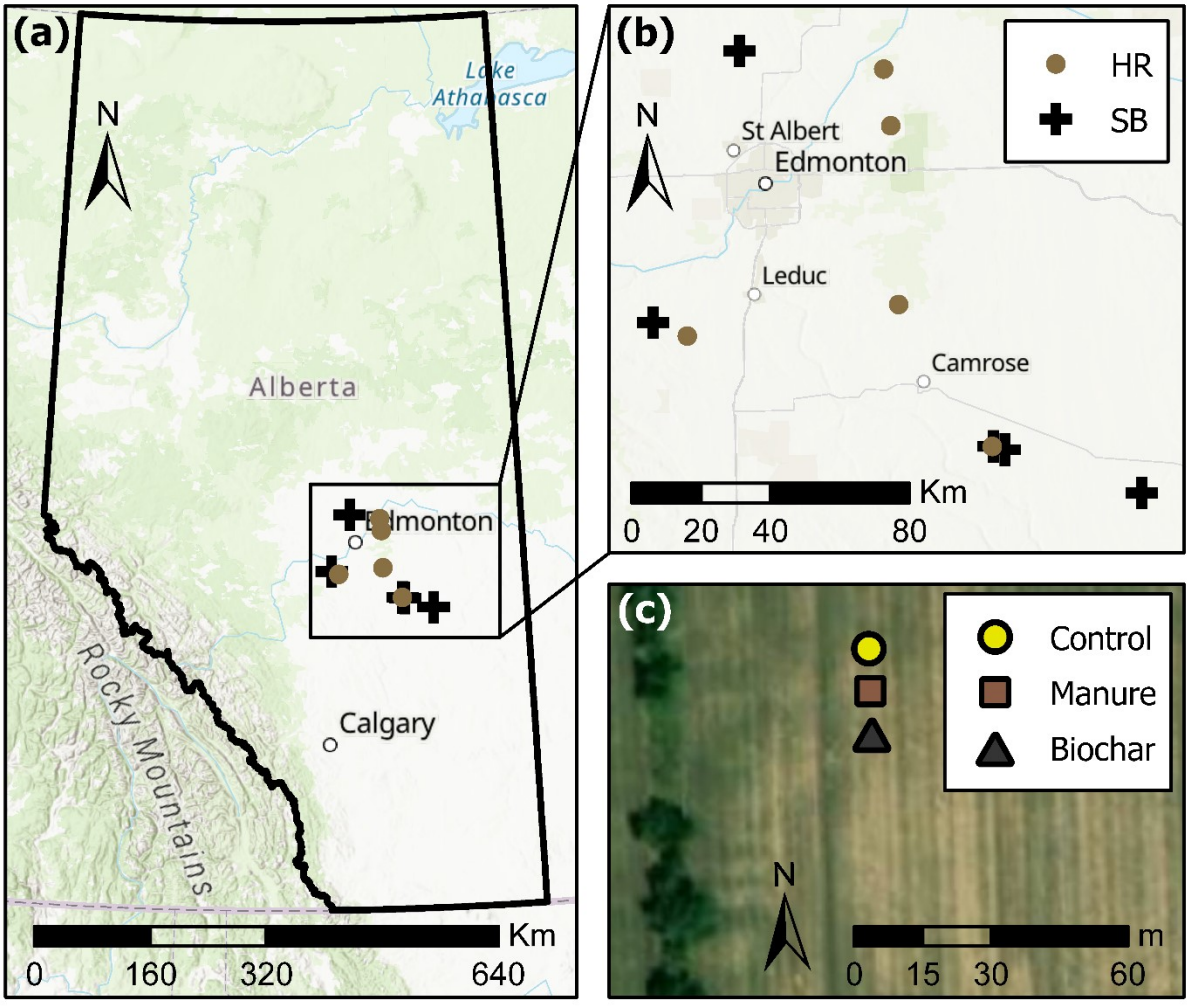

Figure B.S1. (a) Location of the ten agricultural sites in central Alberta, Canada, (b) location of the ten study sites relative to nearby cities, and (c) an example of a plot layout within a site. HR, hedgerow; SB, shelterbelt; CT, control treatment; MT, manure compost treatment; BT, biochar treatment. Source: Esri, Maxar, GeoEye, Earthstar Geographics, CNES/Airbus DS, USDA, USGS, AeroGRID, IGN, Esri Canada, HERE, Garmin, FAO, NOAA, EPA, NRCan, Parks Canada, and the GIS User Community.

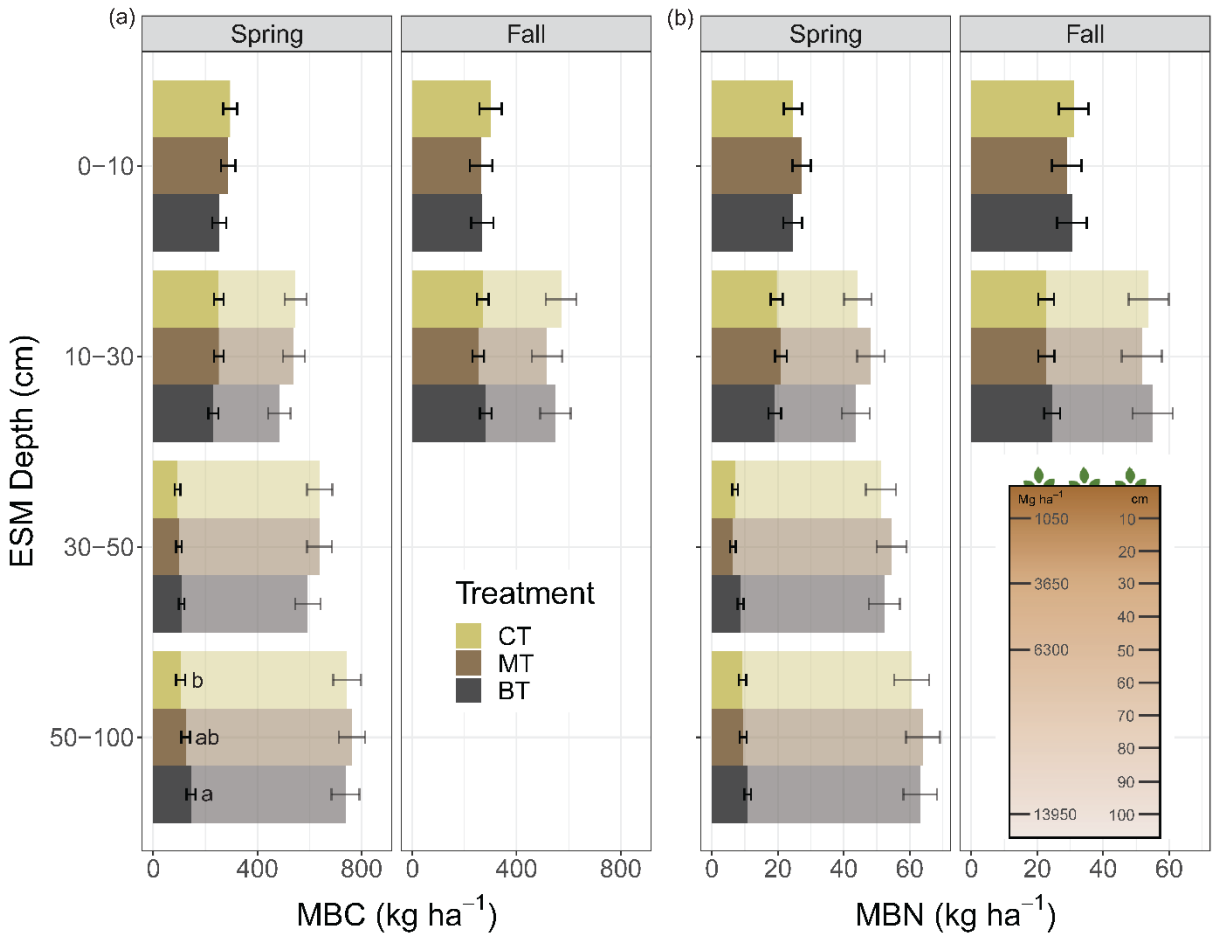

Figure B.S2. (a) Soil microbial biomass carbon (MBC) and (b) nitrogen (MBN) stocks among three soil amendment treatments sampled across ten agricultural sites in central Alberta, Canada, as measured in spring 2020 (spring 2018 pretreatment values were used as a covariate for statistical analysis) and fall 2020. Transparent columns are cumulative stocks based on equivalent soil mass (ESM). Error bars represent ± one standard error. Least-squares means within each ESM depth layer or total cumulative mass accompanied by different lowercase letters are significantly different (Tukey-adjusted, $\alpha = 0.05$) among the treatments. The soil profile illustrates the relationship between soil mass and approximate sampling depth. CT, control treatment; MT, manure compost treatment; BT, biochar treatment.

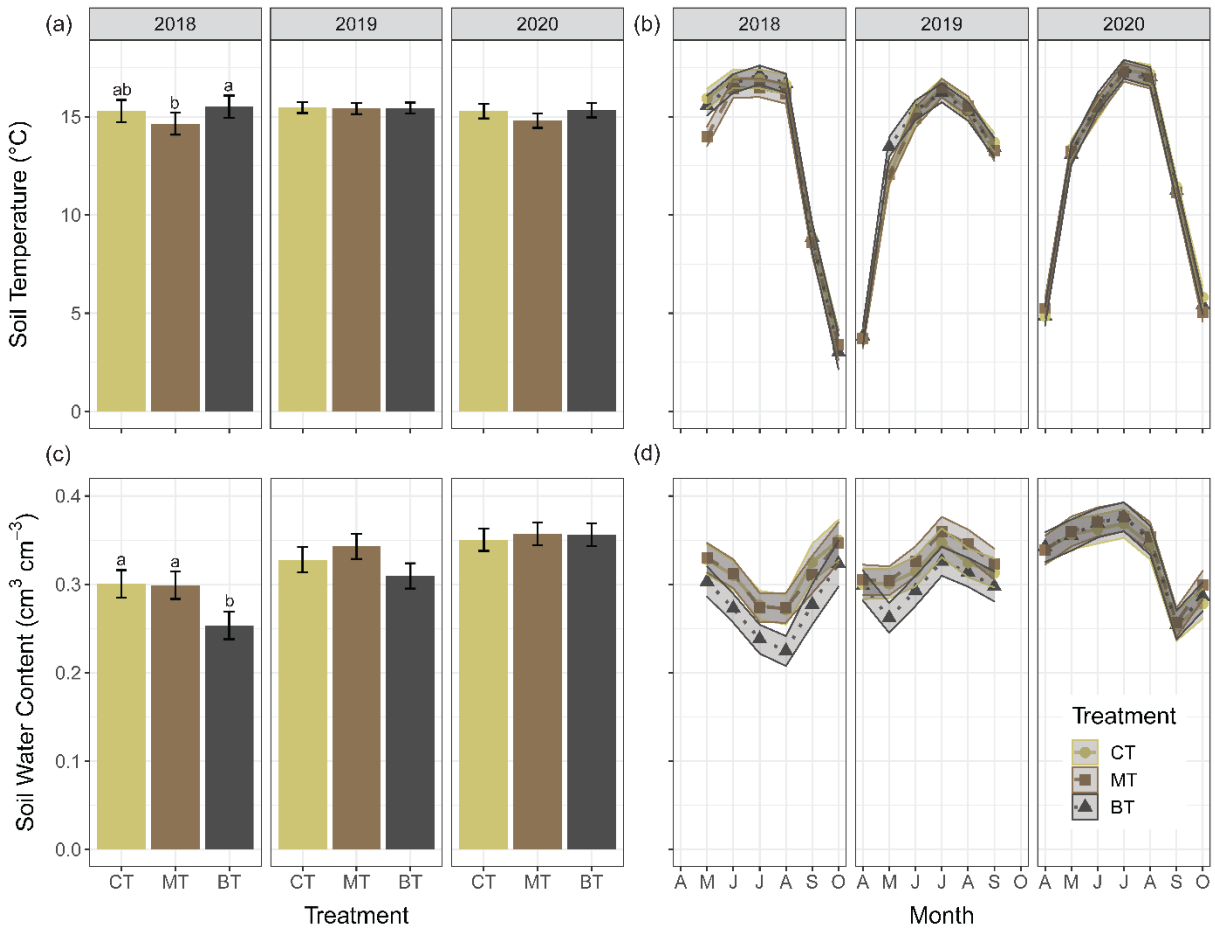

Figure B.S3. Soil temperature by (a) year and (b) month and soil water content by (c) year and (d) month at 10 cm depth among three soil amendment treatments sampled across ten agricultural sites in central Alberta, Canada. Error bars and ribbons represent ± one standard error. Least-squares means within each year accompanied by different lowercase letters are significantly different (Tukey-adjusted, $\alpha = 0.05$) among the treatments. CT, control treatment; MT, manure compost treatment; BT, biochar treatment.

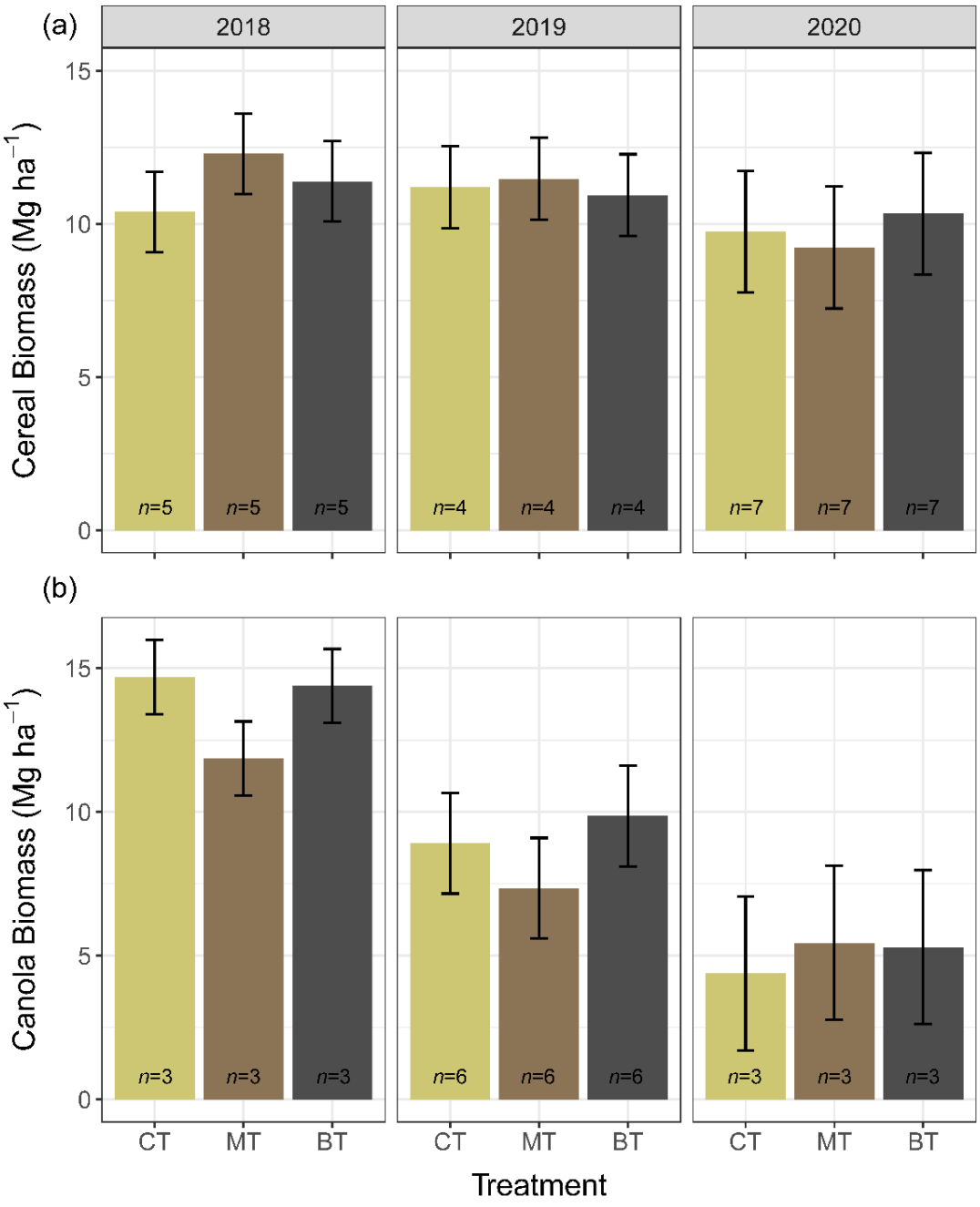

Figure B.S4. (a) Total aboveground biomass for cereal crops (wheat (*Triticum aestivum*) and barley (*Hordeum vulgare*)) and (b) canola (*Brassica rapa*) among three soil amendment treatments sampled across ten agricultural sites in central Alberta, Canada. Error bars represent least-squares means ± one standard error. CT, control treatment; MT, manure compost treatment; BT, biochar treatment.

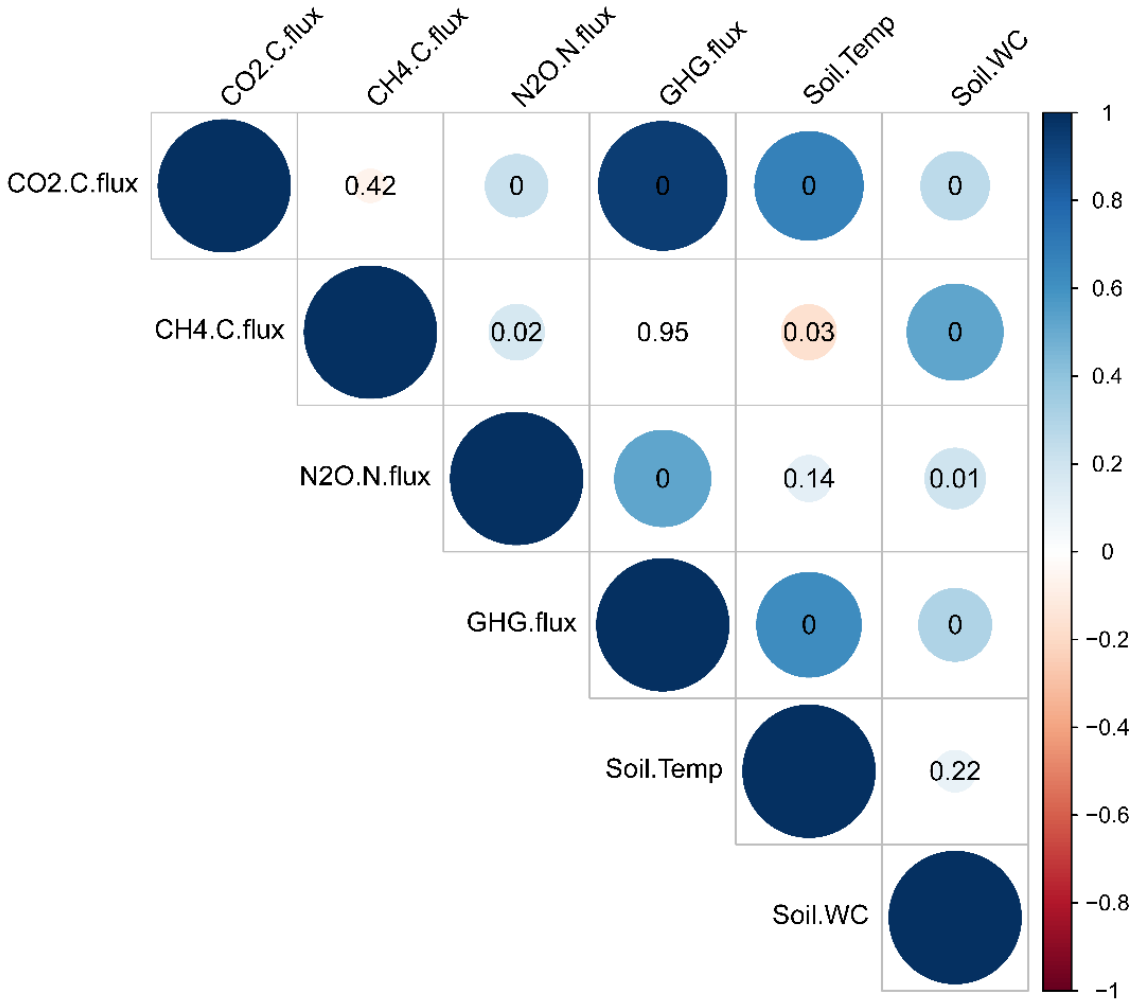

Figure B.S5. Pearson correlations (with *p* values reported) between monthly soil temperature, water content, and greenhouse gas (GHG) emissions over three years and averaged among three soil amendment treatments sampled across ten agricultural sites in central Alberta, Canada. CO2.C.flux, carbon dioxide flux (g C m^{-2} d^{-1}); CH4.C.flux, methane flux (g C m^{-2} d^{-1}); N2O.N.flux, nitrous oxide flux (g N m^{-2} d^{-1}); GHG.flux, GHG flux (sum of CO_2, CH_4, and N_2O, with the latter two GHGs assessed as CO_2-equivalents); Soil.Temp, soil temperature at 10 cm in depth; Soil.WC, soil water content at 10 cm in depth.

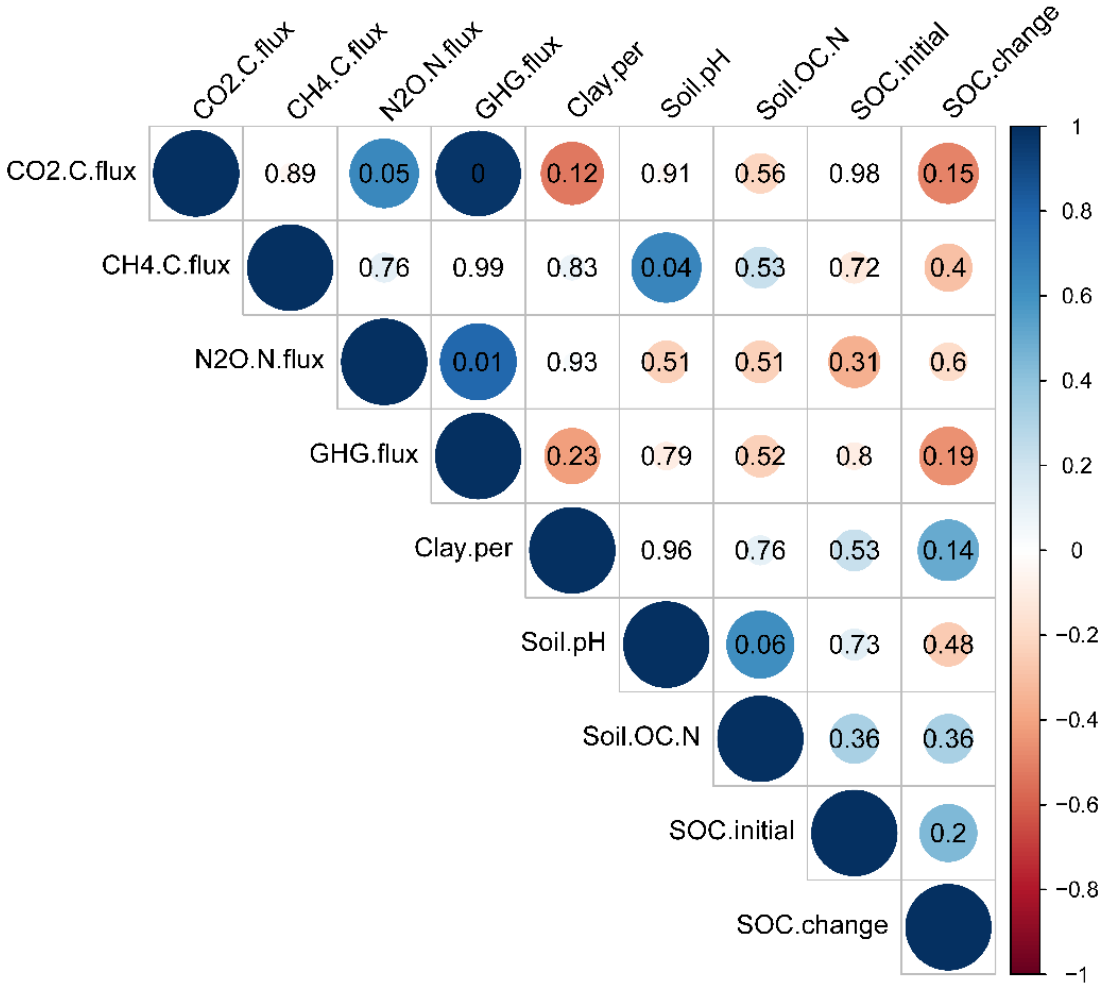

Figure B.S6. Pearson correlations (with *p* values reported) between surface soil (~0–10 cm) properties and average cumulative greenhouse gas (GHG) emissions over three years for biochar-amended soil sampled across ten agricultural sites in central Alberta, Canada. CO2.C.flux, carbon dioxide flux (g C m^{-2} y^{-1}); CH4.C.flux, methane flux (g C m^{-2} y^{-1}); N2O.N.flux, nitrous oxide flux (g N m^{-2} y^{-1}); GHG.flux, GHG flux (sum of CO_2, CH_4, and N_2O, with the latter two GHGs assessed as CO_2-equivalents); Clay.per, percentage of clay; Soil.pH, pretreatment soil pH; Soil.OC.N, pretreatment soil organic carbon to total nitrogen ratio; SOC.initial, pretreatment soil organic carbon (SOC) mass (Mg ha^{-1}); SOC.change, change in SOC mass (two years post-treatment minus pretreatment).

Appendix C. Supplementary data

Table C.S1. Classification of soils and basic soil properties among the different depths and land uses of ten agroforestry sites in central Alberta, Canada. Least-squares means (one standard error) are reported. OC, organic carbon; N, total nitrogen; Conc., concentration.

Land-use type	Classification*	Soil depth (cm)	%Sand	%Silt	%Clay	pH	OC conc. (mg g^{-1} soil)	N conc. (mg g^{-1} soil)	OC:N
Cropland	CA.BC, CA.BC, CA.BLC, CA.BLC, CA.BLC, CA.DBC, CA.DBC, CA.DGC, O.BC, O.DBC	0–10	31.62 (5.63)	40.62 (3.87)	27.76 (2.07)	5.70 (0.20)	40.87 (9.77)	3.69 (0.78)	11.00 (0.30)
		10–30	32.46 (6.18)	38.45 (4.19)	29.09 (2.29)	6.45 (0.26)	20.13 (9.37)	1.92 (0.78)	10.38 (0.42)
		30–50	35.34 (5.27)	34.69 (3.64)	29.97 (2.48)	7.01 (0.25)	9.83 (15.12)	0.97 (1.12)	10.15 (0.53)
Grassland	CA.BC, CA.BC, CA.DBC, CA.DGC, CA.DGC, E.BLC, O.BLC, O.BLC, O.BLC, O.DGC	0–10	30.65 (5.63)	41.51 (3.87)	27.84 (2.07)	6.11 (0.20)	57.67 (9.77)	5.12 (0.78)	11.26 (0.30)
		10–30	31.01 (6.18)	40.08 (4.19)	28.90 (2.29)	6.28 (0.26)	38.54 (9.37)	3.50 (0.78)	10.51 (0.42)
		30–50	30.39 (5.27)	36.97 (3.64)	32.64 (2.48)	6.72 (0.25)	33.62 (15.12)	3.06 (1.12)	9.91 (0.53)
Woodland	CA.BLC, CA.DBC, CA.DGC, E.BC, E.DBC, E.DGC, O.BLC, O.BLC, O.DGC, O.EB	0–10	27.77 (5.63)	44.43 (3.87)	27.81 (2.07)	6.37 (0.20)	79.53 (9.77)	6.03 (0.78)	12.88 (0.30)
		10–30	28.78 (6.18)	42.57 (4.19)	28.65 (2.29)	6.33 (0.26)	37.10 (9.37)	3.15 (0.78)	11.45 (0.42)
		30–50	25.58 (5.27)	42.53 (3.64)	31.89 (2.48)	6.49 (0.25)	37.54 (15.12)	2.96 (1.12)	10.53 (0.53)

* Soil was classified using the Canadian System of Soil Classification.

Table C.S2. Non-planted treatment $\delta^{13}C$ values of soil fractions by soil depth and land-use type across ten agroforestry sites in central Alberta, Canada. Least-squares means (one standard error) are reported. POM, particulate organic matter; MBC, microbial biomass carbon; WSOC, water-soluble organic carbon.

Soil depth (cm)	0–10	10–30	30–50
Fine POM (*n* = 81)	-28.08 (0.42)	-27.22 (0.42)	-26.89 (0.43)
Coarse silt (*n* = 81)	-27.15 (0.27)	-26.40 (0.27)	-25.91 (0.27)
Fine silt (*n* = 85)	-26.93 (0.28)	-26.27 (0.28)	-25.91 (0.28)
Non-aggregated clay (*n* = 84)	-26.11 (0.16)	-25.58 (0.16)	-25.63 (0.16)
Aggregated clay (*n* = 85)	-26.83 (0.22)	-25.90 (0.22)	-25.80 (0.22)
Bulk soil (*n* = 86)	-26.73 (0.23)	-25.92 (0.23)	-25.65 (0.23)
MBC (*n* = 87)	-25.61 (0.37)	-25.22 (0.37)	-25.17 (0.37)
WSOC (*n* = 87)	-27.17 (0.20)	-26.30 (0.20)	-26.67 (0.21)
Land-use type	Cropland	Grassland	Woodland
Fine POM (*n* = 81)	-26.98 (0.32)	-27.51 (0.32)	-27.56 (0.32)
Coarse silt (*n* = 81)	-26.09 (0.24)	-26.69 (0.24)	-26.65 (0.23)
Fine silt (*n* = 85)	-26.21 (0.27)	-26.40 (0.27)	-26.49 (0.27)
Non-aggregated clay (*n* = 84)	-25.75 (0.18)	-25.69 (0.18)	-25.87 (0.18)
Aggregated clay (*n* = 85)	-26.33 (0.24)	-26.03 (0.25)	-26.14 (0.24)
Bulk soil (*n* = 86)	-25.76 (0.21)	-26.27 (0.21)	-26.29 (0.21)
MBC (*n* = 87)	-25.42 (0.31)	-25.36 (0.31)	-25.24 (0.31)
WSOC (*n* = 87)	-26.77 (0.21)	-26.57 (0.21)	-26.80 (0.21)

Table C.S3. Planted treatment total root mass (mg) by soil depth and land-use type across ten agroforestry sites in central Alberta, Canada. Least-squares means (one standard error) accompanied by different lowercase letters are significantly different (Tukey-adjusted, $\alpha = 0.05$) among the soil depths or land-use types.

Soil depth (cm)	0–10	10–30	30–50
Root mass (n = 88)	424.59 (27.50) a	305.16 (26.55) b	327.19 (26.55) b
Land-use type	Cropland	Grassland	Woodland
Root mass (n = 88)	317.35 (26.55)	364.30 (26.55)	375.29 (27.50)

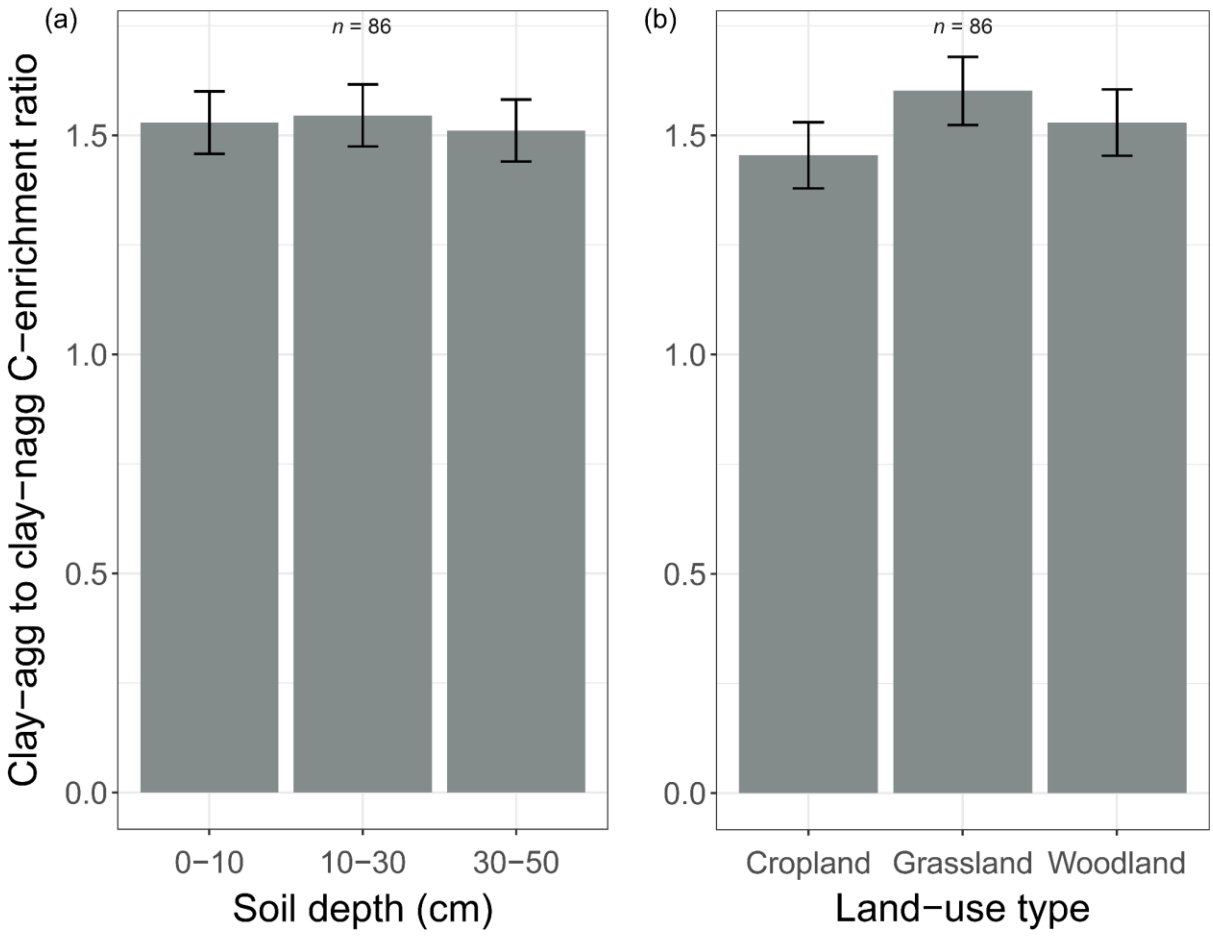

Figure C.S1. Non-planted treatment aggregated clay fraction (clay-agg) to non-aggregated clay fraction (clay-nagg) ratio of carbon (C) enrichment (mg C g^{-1} fraction) by (a) soil depth and (b) land-use type across ten agroforestry sites in central Alberta, Canada. Error bars represent least-squares means ± one standard error.

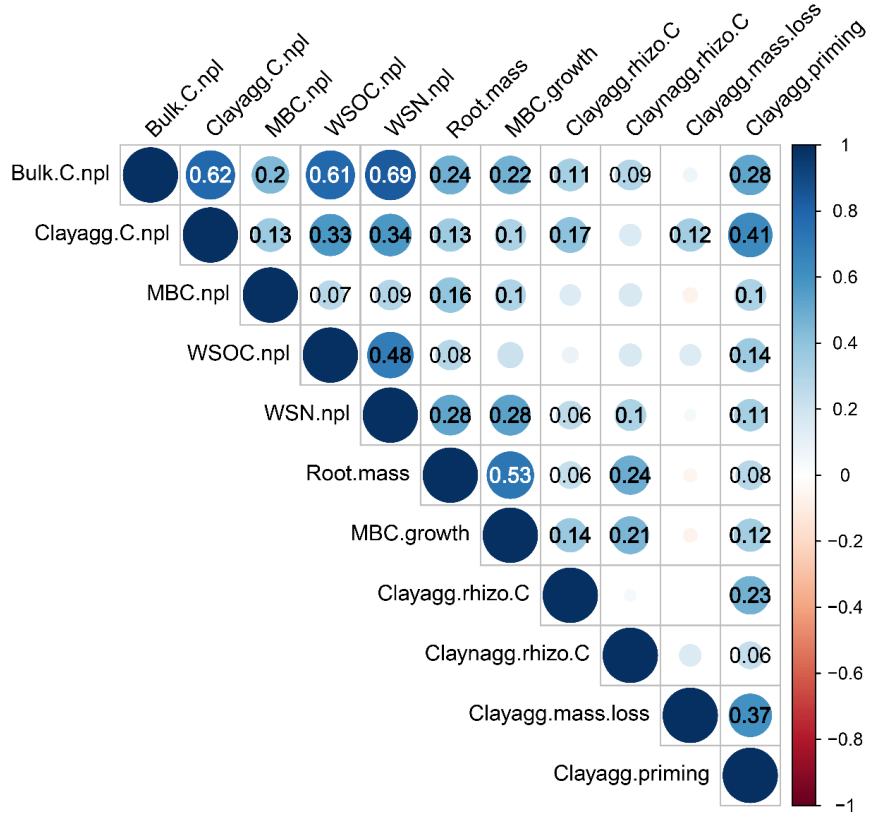

Figure C.S2. Pearson correlations (with R^2 values reported) between soil properties in the non-planted treatment and root-driven soil effects across the different soil depths (0–10, 10–30, 30–50 cm) and land uses (cropland, grassland, and woodland) of ten agroforestry sites in central Alberta, Canada ($n = 86$). Only statistically significant ($\alpha = 0.05$) correlations are reported. Bulk.C.npl, bulk soil carbon (C) in the non-planted treatment; clayagg.C.npl, aggregated clay fraction to total clay C proportion in the non-planted treatment; MBC.npl, microbial biomass C in the non-planted treatment; WSOC.npl, water-soluble organic C in the non-planted treatment; WSN.npl, water-soluble total nitrogen in the non-planted treatment; root.mass, total root mass in the planted treatment; MBC.growth, MBC difference between the planted and non-planted treatments; clayagg.rhizo.C and claynagg.rhizo.C, amount of root-derived C incorporated into the aggregated and non-aggregated clay fractions, respectively, in the planted treatment; clayagg.mass.loss, difference in aggregated clay fraction to total clay mass proportions between the non-planted and planted treatments; clayagg.priming, intensified loss of soil-derived C within the aggregated clay fraction in the planted treatment.

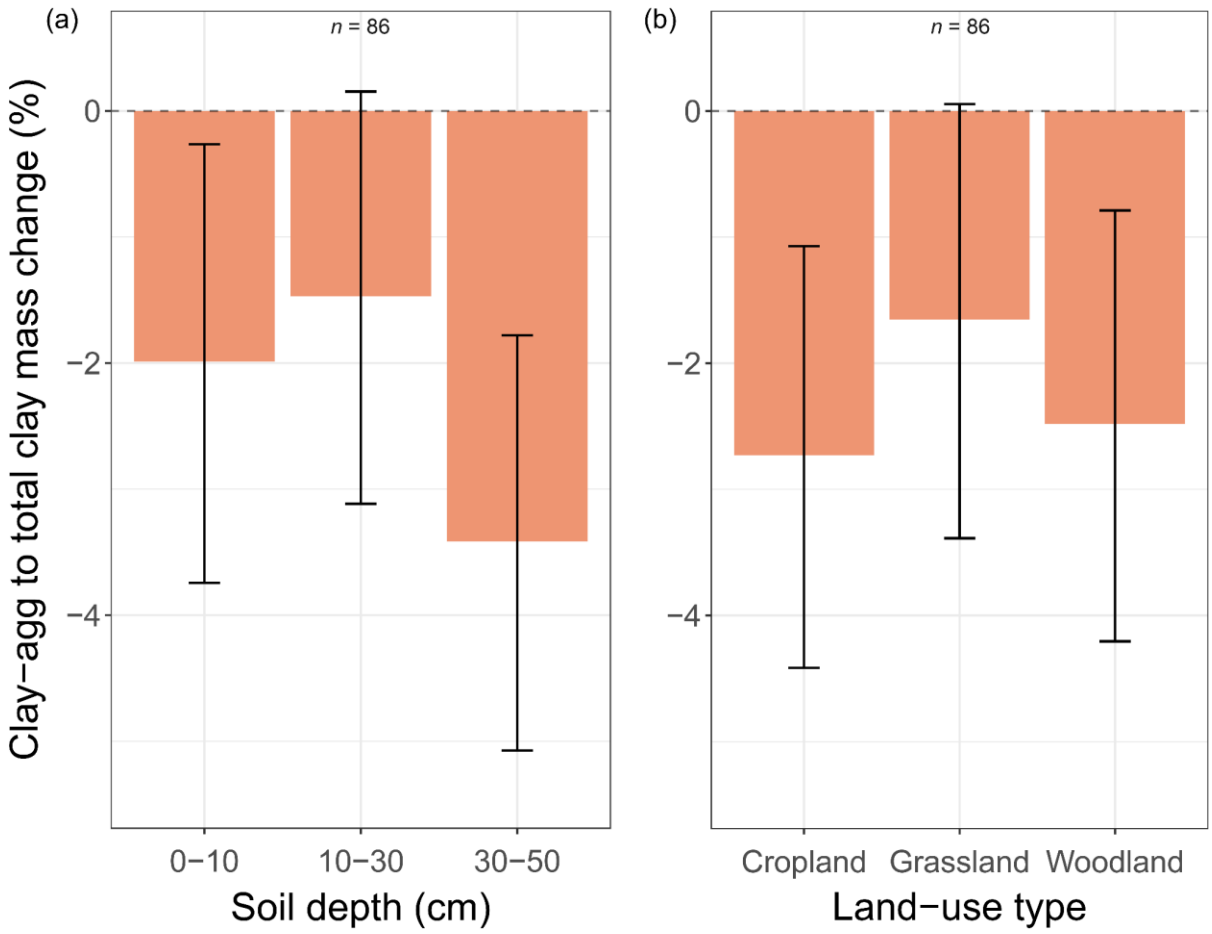

Figure C.S3. Change (difference between planted and non-planted treatments) in aggregated clay fraction (clay-agg) to total clay mass proportion by (a) soil depth and (b) land-use type across ten agroforestry sites in central Alberta, Canada. Error bars represent least-squares means ± 95% confidence intervals.

Appendix D. Supplementary data

Table D.S1. Agricultural treatment effects on $\delta^{13}C$ values of soil fractions in the non-planted treatment across ten agricultural sites in central Alberta, Canada. Least-squares means (one standard error) are reported. POM, particulate organic matter; MBC, microbial biomass carbon; WSOC, water-soluble organic carbon.

Treatment	Control	Manure	Biochar
Fine POM (*n* = 27)	-27.80 (0.13)	-27.71 (0.13)	-27.50 (0.13)
Coarse silt (*n* = 27)	-26.78 (0.12)	-26.74 (0.12)	-26.97 (0.12)
Fine silt (*n* = 29)	-26.68 (0.17)	-26.76 (0.17)	-26.75 (0.17)
Non-aggregated clay (*n* = 30)	-25.96 (0.16)	-26.03 (0.16)	-26.00 (0.16)
Aggregated clay (*n* = 28)	-26.75 (0.33)	-26.99 (0.33)	-26.27 (0.31)
Bulk soil (*n* = 30)	-26.34 (0.13)	-26.38 (0.13)	-26.40 (0.13)
MBC (*n* = 27)	-25.08 (0.21)	-25.02 (0.21)	-25.64 (0.21)
WSOC (*n* = 30)	-26.96 (0.23)	-26.83 (0.23)	-26.61 (0.23)

Table D.S2. Agricultural treatment effects on total root mass (mg) in the planted treatment across ten agricultural sites in central Alberta, Canada. Least-squares means (one standard error) are reported.

Treatment	Control	Manure	Biochar
Root mass (n = 30)	409.27 (44.94)	384.34 (44.94)	385.69 (44.94)

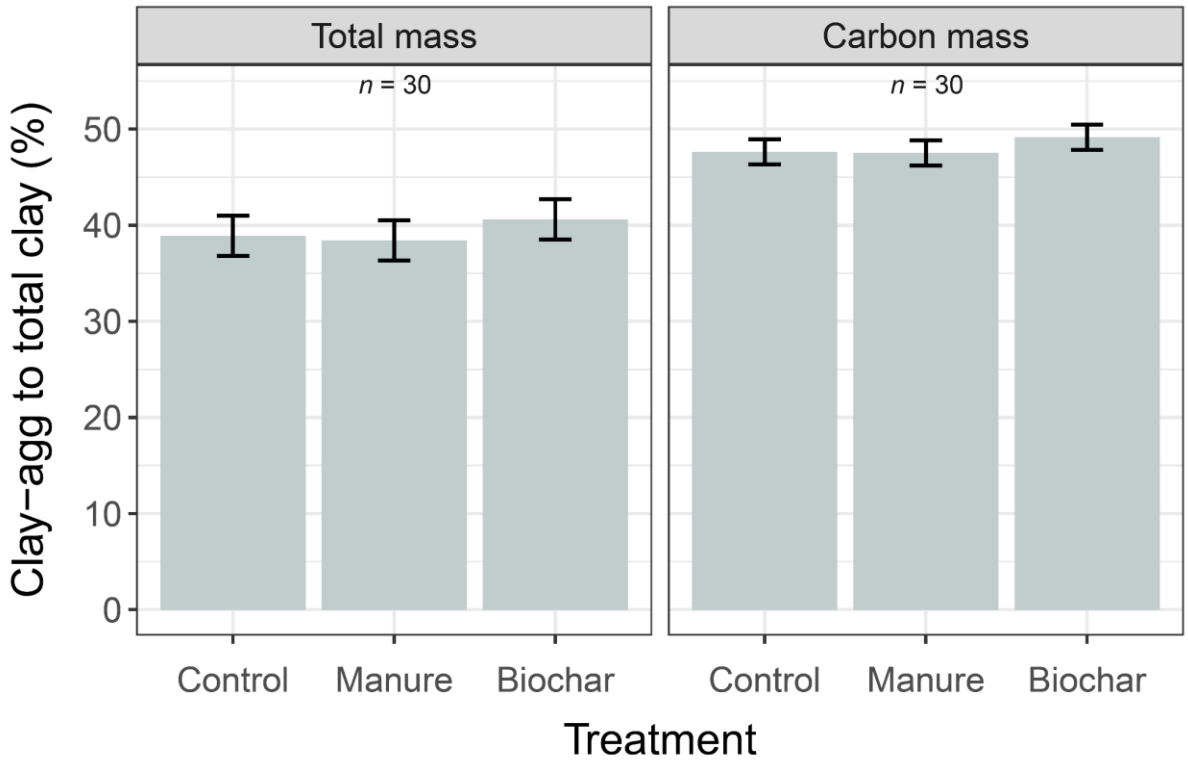

Figure D.S1. Agricultural treatment effects on the aggregated clay fraction (clay-agg) to total clay (total mass or carbon mass) proportion in the non-planted treatment across ten agricultural sites in central Alberta, Canada. Error bars represent least-squares means ± one standard error.

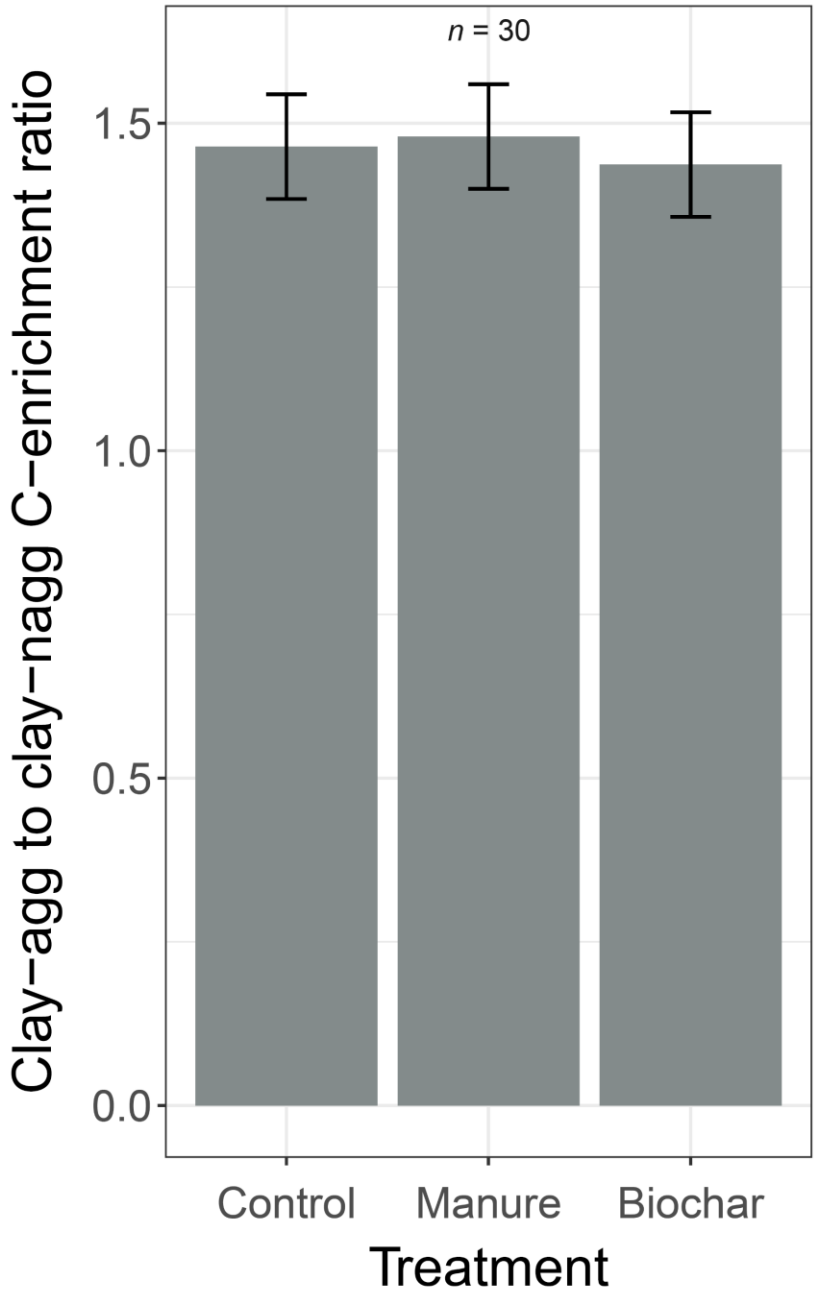

Figure D.S2. Agricultural treatment effects on the aggregated clay fraction (clay-agg) to non-aggregated clay fraction (clay-nagg) ratio of carbon (C) enrichment (mg C g^{-1} fraction) in the non-planted treatment across ten agricultural sites in central Alberta, Canada. Error bars represent least-squares means ± one standard error.

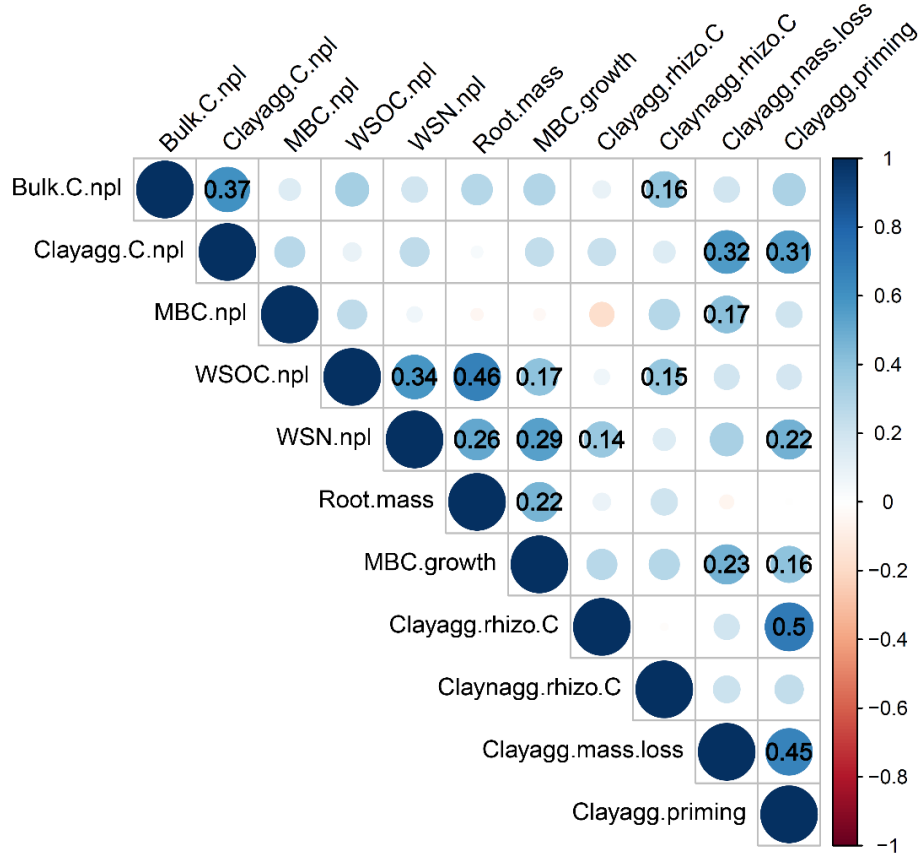

Figure D.S3. Pearson correlations (with R^2 values reported) between soil properties in the non-planted treatment and root-driven soil effects across the different agricultural treatments (control, manure, and biochar) of ten agricultural sites in central Alberta, Canada ($n = 30$). Only statistically significant ($\alpha = 0.05$) correlations are reported. Bulk.C.npl, bulk soil carbon (C) in the non-planted treatment; clayagg.C.npl, aggregated clay fraction to total clay C proportion in the non-planted treatment; MBC.npl, microbial biomass C in the non-planted treatment; WSOC.npl, water-soluble organic C in the non-planted treatment; WSN.npl, water-soluble total nitrogen in the non-planted treatment; root.mass, total root mass in the planted treatment; MBC.growth, MBC difference between the planted and non-planted treatments; clayagg.rhizo.C and claynagg.rhizo.C, amount of root-derived C incorporated into the aggregated and non-aggregated clay fractions, respectively, in the planted treatment; clayagg.mass.loss, difference in aggregated clay fraction to total clay mass proportions between the non-planted and planted treatments; clayagg.priming, intensified loss of soil-derived C within the aggregated clay fraction in the planted treatment.

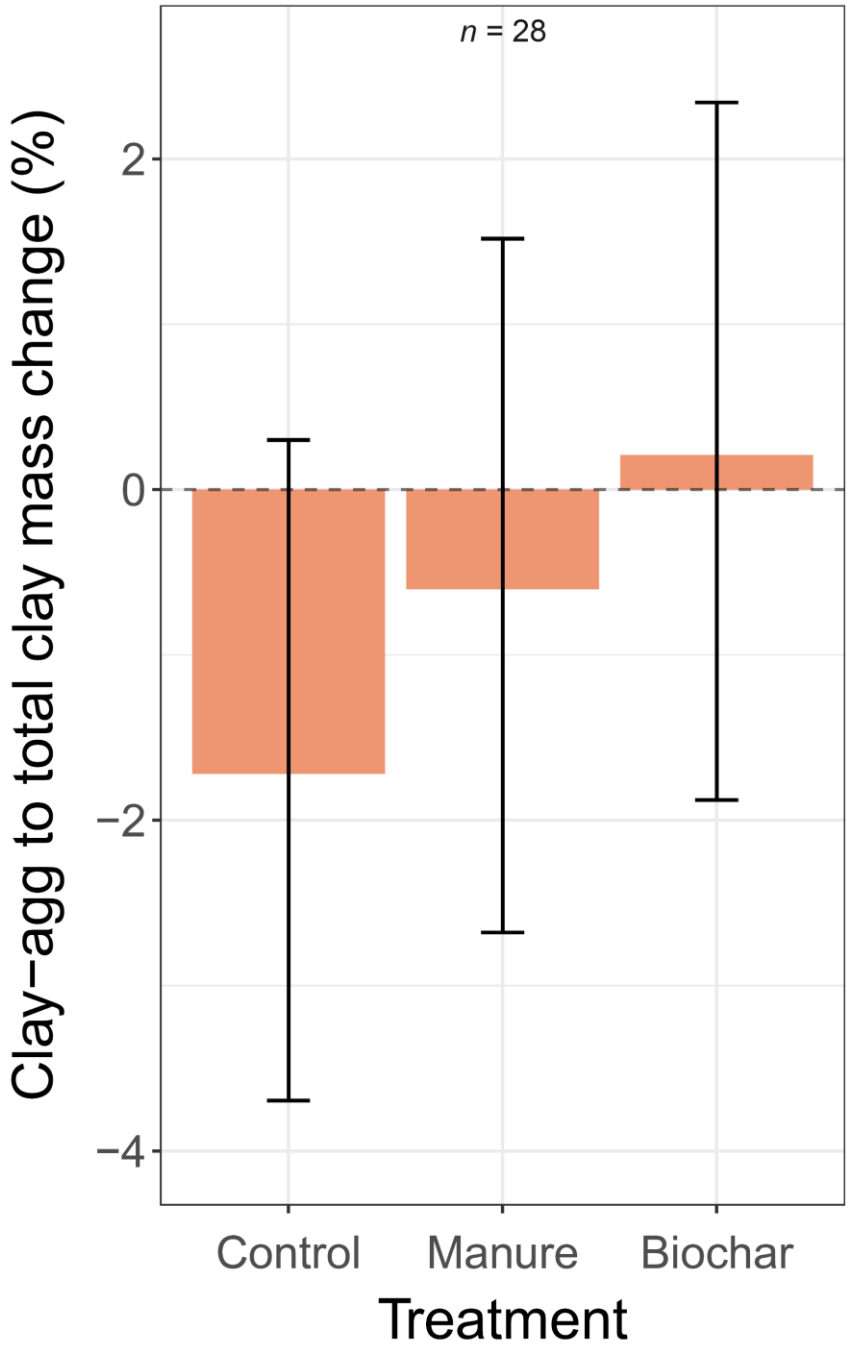

Figure D.S4. Agricultural treatment effects on the change (difference between planted and non-planted treatments) in the aggregated clay fraction (clay-agg) to total clay mass proportion across ten agricultural sites in central Alberta, Canada. Error bars represent least-squares means ± 95% confidence intervals.